Edward E. O'Brien's Seminal Contributions to Turbulence Theory

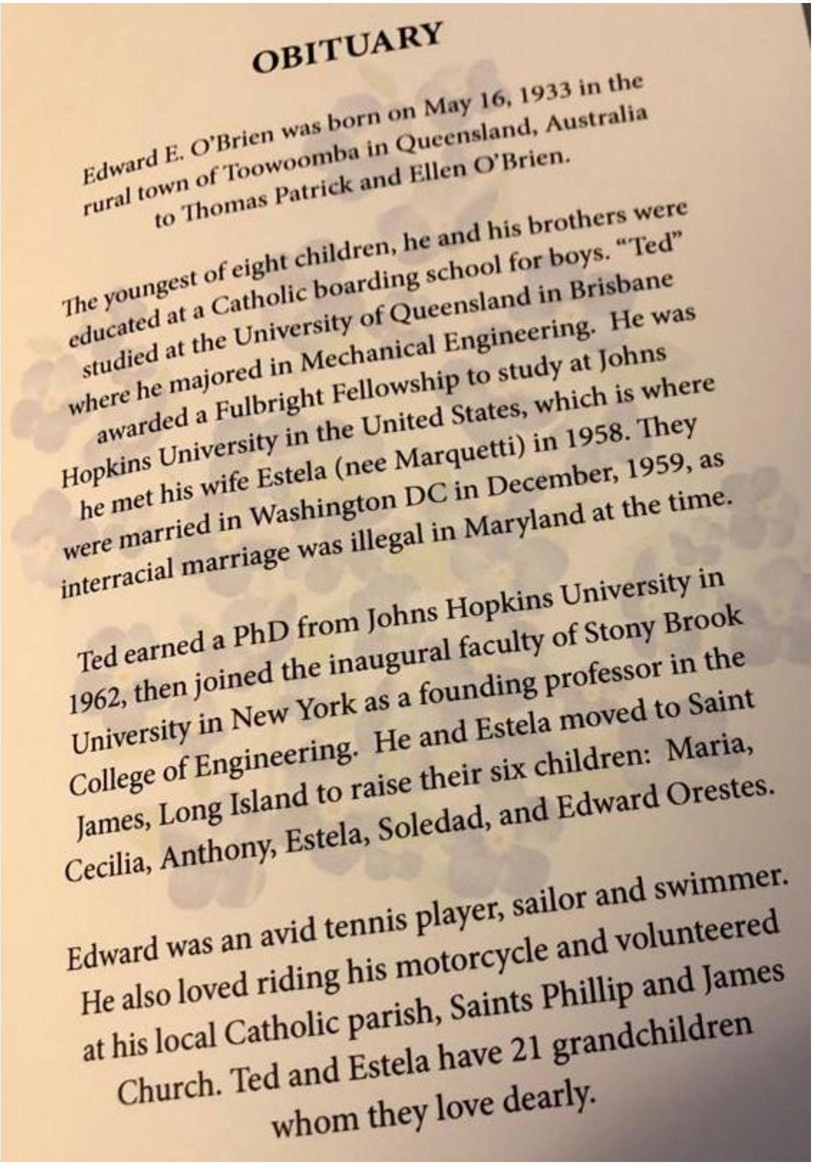
OBITUARY

Edward E. O'Brien was born on May 16, 1933 in the rural town of Toowoomba in Queensland, Australia to Thomas Patrick and Ellen O'Brien.

The youngest of eight children, he and his brothers were educated at a Catholic boarding school for boys. "Ted" studied at the University of Queensland in Brisbane where he majored in Mechanical Engineering. He was awarded a Fulbright Fellowship to study at Johns Hopkins University in the United States, which is where he met his wife Estela (nee Marquetti) in 1958. They were married in Washington DC in December, 1959, as interracial marriage was illegal in Maryland at the time.

Ted earned a PhD from Johns Hopkins University in 1962, then joined the inaugural faculty of Stony Brook University in New York as a founding professor in the College of Engineering. He and Estela moved to Saint James, Long Island to raise their six children: Maria, Cecilia, Anthony, Estela, Soledad, and Edward Orestes.

Edward was an avid tennis player, sailor and swimmer. He also loved riding his motorcycle and volunteered at his local Catholic parish, Saints Phillip and James Church. Ted and Estela have 21 grandchildren whom they love dearly.

F. Ladeinde, C. Dopazo, P. Givi

APS/DFD 2019, Seattle, WA
November 23-26, 2019

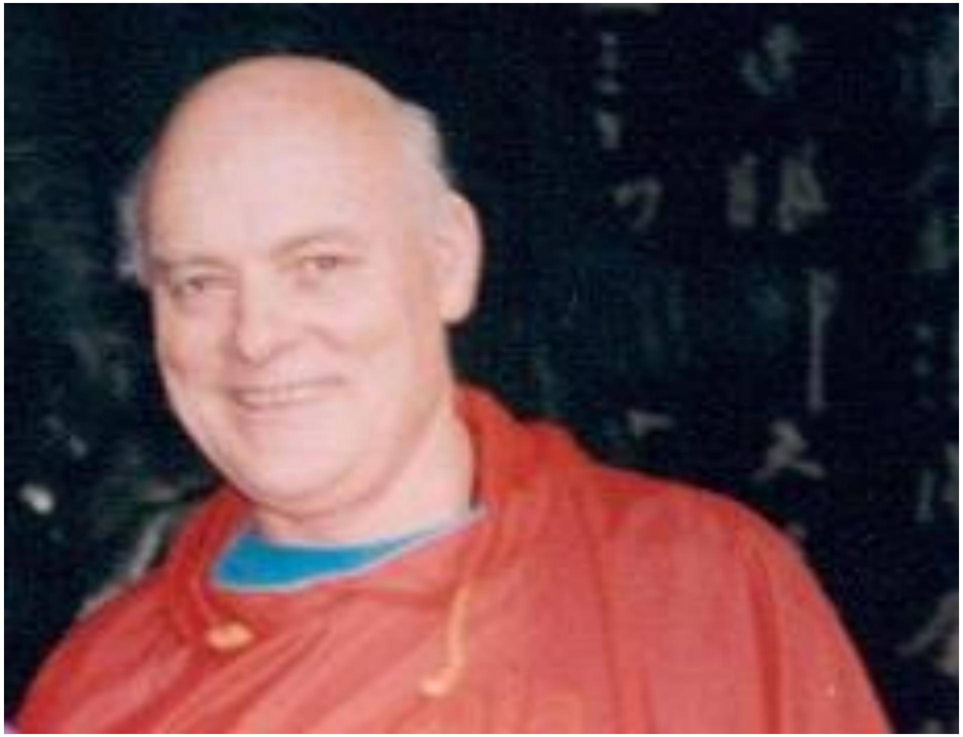

1933-2019

Edward Ephrem O'Brien

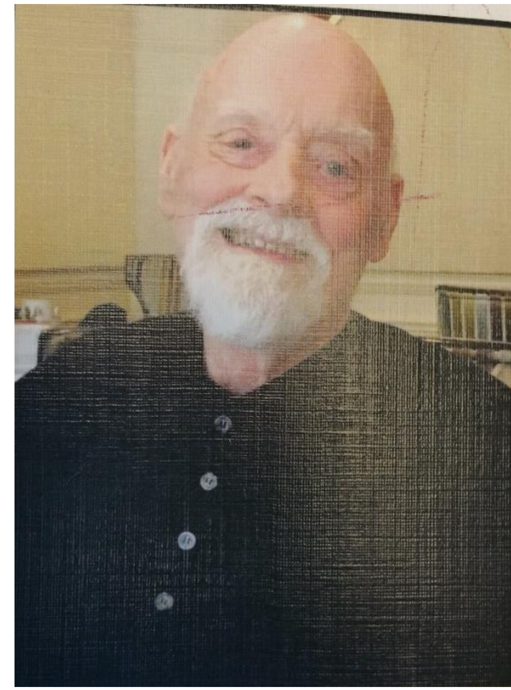

Academic Ancestry of Edward E. O'Brien

,

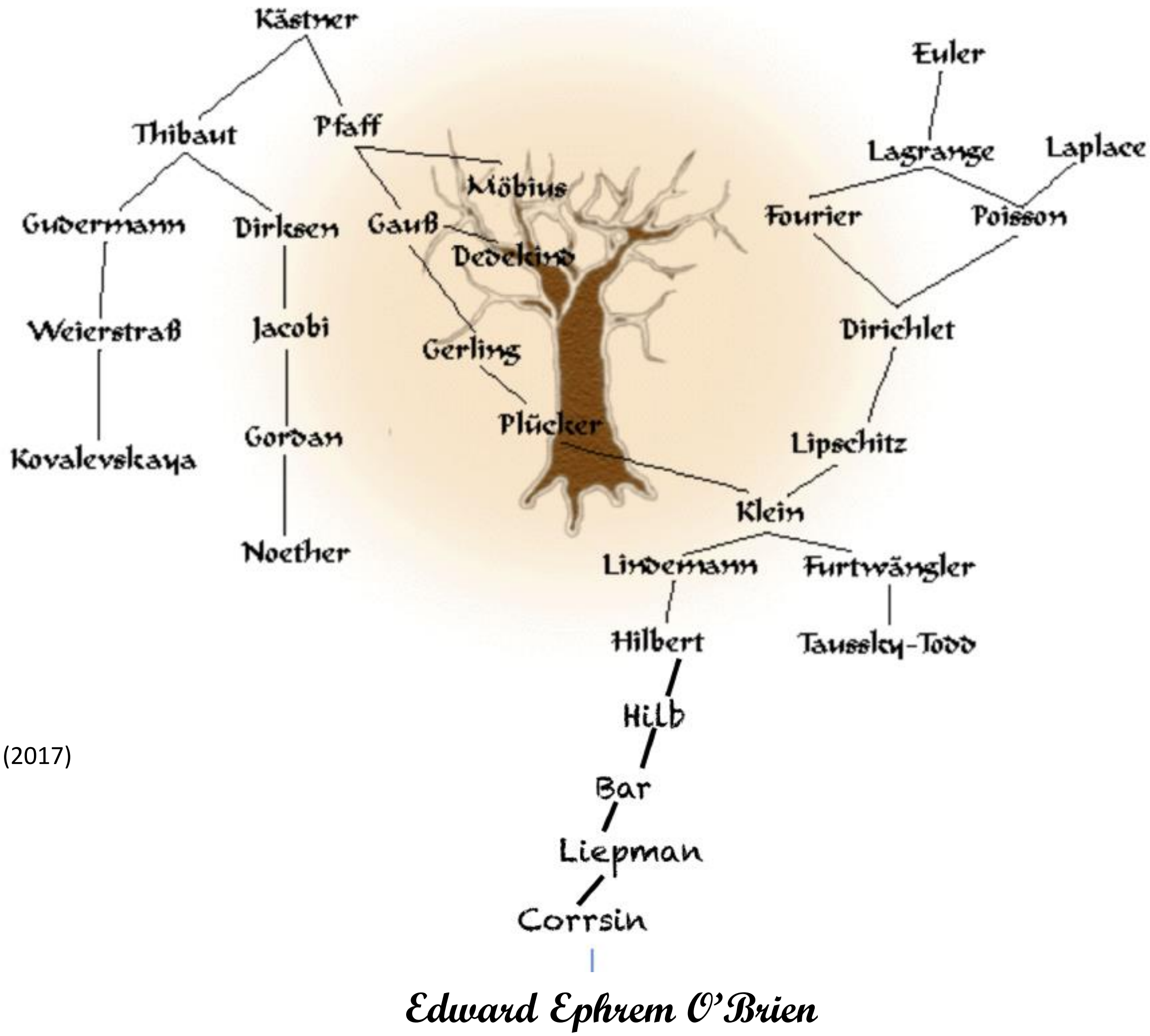

Adapted from Bhaganagar & Gatski (2017)

“Models of the Day” c. 1950/60s

,

Closing the infinite set of correlation equations

- Mostly spectral space theories

- Heisenberg’s eddy diffusivity type of transfer function (Heisenberg, 1948)
- Quasi-Normal (QN) Approximations (Millionshtchikov, 1941; Chou, 1940): Fourth-order cumulants are zero.
  - ✓ O’Brien and Francis (1961): The scalar spectrum develops negative values for some specific initial conditions for a first-order reaction
- Direct Interaction Approximation: Not Galilean Invariant, $k^{-2/3}$ (Kraichnan, 1962)
  - ✓ O’Brien (1968): Does not satisfy an important invariant for reacting flows under homogeneous turbulence assumption: Central moments of the scalar fluctuating field is independent of the turbulence
- Long history DIA (Kraichnan, 1965): Heuristic Lagrangian modification of DIA (LHDI); Restores Galilean Invariance, $k^{-5/3}$
  - ✓ O’Brien (1968) – Developed the LHDI equations for isotropic turbulent mixing of a second-order chemical reaction
  - ✓ O’Brien (1968) - Preserves an important property: In the absence of molecular diffusion the decay of single point statistical functions of the concentration field in independent of turbulence (Corrsin, 1952)
- Eddy-Damped Quasi-Normal (EQDN) Models (Orszag, 1970;1972): Added an “eddy-damping rate” to the QN equations
- Test-Field Model (TFM) (Kriachnan, 1971): Markovian model of the EDQNM type

Direct Interaction Approximation for Scalars

Fluctuating scalar equation

$$(\partial/\partial t - D\nabla^2)s(\mathbf{x}, t) = -\partial s(\mathbf{x}, t)u_i(\mathbf{x}, t)/\partial x_i,$$

$$\mathcal{S}(\mathbf{x}, t; \mathbf{x}', t') = \langle s(\mathbf{x}, t)s(\mathbf{x}', t')\rangle,$$

$$\mathcal{U}_{ij}(\mathbf{x}, t; \mathbf{x}', t') = \langle u_i(\mathbf{x}, t)u_j(\mathbf{x}', t')\rangle$$

s = Fluctuating scalar field
u_i = Fluctuating velocity field
$\mathfrak{s}$ = Covariance of the the scalar field
$\mathcal{U}_{ij}$ = Covariance of the velocity field

Scalar DIA for Gaussian Initial Conditions

$$(\partial/\partial t - D\nabla^2)\mathcal{S}(\mathbf{x}, t; \mathbf{x}', t')$$

$$= \frac{\partial}{\partial x_i}\int_{t_0}^{t'} ds \int d\mathbf{y}\, \mathcal{U}_{ij}(\mathbf{x}, t; \mathbf{y}, s)$$

$$\cdot \mathcal{G}(\mathbf{x}', t'; \mathbf{y}, s)\frac{\partial}{\partial y_i}\mathcal{S}(\mathbf{x}, t,; \mathbf{y}, s)$$

$$+ \frac{\partial}{\partial x_i}\int_{t_0}^{t} ds \int d\mathbf{y}\, \mathcal{U}_{ij}(\mathbf{x}, t; \mathbf{y}, s)$$

$$\cdot \mathcal{G}(\mathbf{x}, t; \mathbf{y}, s)\frac{\partial}{\partial y_i}\mathcal{S}(\mathbf{x}', t'; \mathbf{y}, s),$$

$$(\partial/\partial t - D\nabla^2)\mathcal{G}(\mathbf{x}, t; \mathbf{x}', t')$$

$$= \int_{t'}^{t} ds \int d\mathbf{y}\, \mathcal{U}_{ij}(\mathbf{x}, t; \mathbf{y}, s)\frac{\partial}{\partial x_i}\mathcal{G}(\mathbf{x}, t; \mathbf{y}, s)$$

$$\cdot \frac{\partial}{\partial y_i}\mathcal{G}(\mathbf{y}, s; \mathbf{x}', t'),$$

$\mathcal{G}$ = Mean Green's function for the scalar field
= The probability density that the scalar quantity introduced at $\boldsymbol{x}'$ and t' will be found in d$\mathbf{x}$ at ($\mathbf{x}$, t)

Direct Interaction Approximation for Scalars

Introduce homogeneity and take Fourier Transform:

$$\mathcal{S}(\mathbf{x},\, t;\, \mathbf{x}',\, t') = \mathcal{S}(\mathbf{x} - \mathbf{x}';\, t,\, t')$$
$$= \int \tilde{S}(\mathbf{k};\, t,\, t') e^{i\mathbf{k}\cdot(\mathbf{x}-\mathbf{x}')}\, d\mathbf{k},$$

Similar Fourier transforms exist for ly for $\mathcal{G}(\mathbf{x}-\mathbf{x}';\mathbf{t},\mathbf{t}')$and $\mathcal{U}_{\mathrm{ij}}(\mathbf{x}-\mathbf{x}';\mathbf{t},\mathbf{t}')$

Introduce wave space: $\mathbf{k} = \mathbf{p} + \mathbf{q}$

$$(\partial/\partial t + Dk^2)\tilde{S}(\mathbf{k};\, t,\, t') = (2\pi)^3 q_i q_j \int_{t_0}^{t'} ds \int d\mathbf{p}\, \tilde{U}_{ij}(\mathbf{p};\, t,\, s)\tilde{G}(\mathbf{k};\, t',\, s)\tilde{S}(\mathbf{q};\, t,\, s)$$
$$- (2\pi)^3 q_i k_j \int_{t_0}^{t} ds \int d\mathbf{p}\, \tilde{U}_{ij}(\mathbf{p};\, t,\, s)\tilde{G}(\mathbf{q};\, t,\, s)\tilde{S}(\mathbf{k};\, t',\, s),$$

$$(\partial/\partial t + Dk^2)\tilde{G}(\mathbf{k};\, t,\, t') = -(2\pi)^3 q_i k_j \int_{t'}^{t} ds \int d\mathbf{p}\, \tilde{U}_{ij}(\mathbf{p};\, t,\, s)\tilde{G}(\mathbf{q};\, t,\, s)\tilde{G}(\mathbf{k};\, t',\, s),$$

Introduce isotropy:

$$\tilde{U}_{ij}(\mathbf{k};\, t,\, s) = \tfrac{1}{2}P_{ij}(\mathbf{k})U(k,\, t,\, s)$$
$$\tilde{S}(\mathbf{k};\, t,\, s) = S(k,\, t,\, s),$$
$$(2\pi)^3\tilde{G}(\mathbf{k};t,\, s) = g_s(k,\, t,\, s),$$

g_s is response function for a Fourier mode of wavenumber k

Direct Interaction Approximation for Scalars

Scalar DIA

$$(\partial/\partial t + Dk^2)S(k, t, t')$$

$$= \pi k \int_{t_0}^{t'} ds \iint_\Delta dp\, dq\, pq(1 - \omega^2)$$

$$\cdot U(p, t, s) g_s(k, t', s) S(q, t, s)$$

$$g_s(k, t', t') = 1$$

$$- \pi k \int_{t_0}^{t} ds \iint_\Delta dp\, dq\, pq(1 - \omega^2)$$

$$\cdot U(p, t, s) g_s(q, t, s) S(k, t', s),$$

$$(\partial/\partial t + Dk^2) g_s(k, t, t')$$

$$= -\pi k \int_{t'}^{t} ds \iint_\Delta dp\, dq\, pq(1 - \omega^2) \cdot U(p, t, s) g_s(q, t, s) g_s(k, t', s)$$

Relating covariances to phase-correlation functions

$$\int_0^\infty E(k, t)\, dk = \tfrac{3}{2} u_0(t)^2$$

$$\int_0^\infty E_s(k, t)\, dk = s_0(t)^2$$

$$r_s(k, t, t') = S(k, t, t')/[S(k, t, t) S(k, t', t')]^{\frac{1}{2}}$$

$$= 4\pi k^2 S(k, t, t')/[E_s(k, t) E_s(k, t')]^{\frac{1}{2}},$$

$$r(k, t, t') = 2\pi k^2 U(k, t, t')/[E(k, t) E(k, t')]^{\frac{1}{2}},$$

Direct Interaction Approximation for Scalars

$$(\partial/\partial t + 2Dk^2)E_s(k, t) = T_s(k, t) = 4\pi^2 k^3 \iint_\Delta dp\, dq\, pq(1 - \omega^2) \cdot \int_{t_0}^{t} U(p, t, s)\{g_s(k, t, s)S(q, t, s) - g_s(q, t, s)S(k, t, s)\}\, ds.$$

Invariance of the Transfer Function

$$\int_0^\infty T_s(k, t)\, dk = 0.$$

$$\begin{aligned} I(t) &= \int_0^\infty T_s(k, t)\, dk \\ &= 4\pi^2 \int_0^\infty \int_0^\infty \int_{-1}^{1} dk\, dq\, d\omega'\, k^4 q^4 p^{-2}(1 - \omega'^2) \int_{t_0}^{t} ds \\ &\quad \cdot U(p, t, s)\{g_s(k, t, s)S(q, t, s) - g_s(q, t, s)S(k, t, s)\} \\ &= 4\pi^2 \int_0^\infty \int_0^\infty Q(t, k, q)\, dk\, dq. \end{aligned} \tag{14}$$

With chemical reaction (O'Brien, 1968)

$$\frac{\partial \Gamma}{\partial t} + \frac{\partial}{\partial x_i}(u_i \Gamma) = D\, \nabla^2 \Gamma - C\Gamma^2$$

C= reaction rate, $\Gamma =$ Random concentration field, $\gamma =$ Fluctuating scalar field,

Direct Interaction Approximation for Scalars

Dimensional Groupings

$$\hat{k} = \frac{k}{k_o}, \qquad \hat{t} = \langle\Gamma\rangle_{av}(0)Ct,$$

$$N_{da} = \frac{C\langle\Gamma\rangle_{av}(0)}{Dk_0^2}, \qquad N = \frac{uk_0}{C\langle\Gamma\rangle_{av}(0)},$$

$$\hat{\psi}(k, t, t) = \frac{k_0^3}{\langle\gamma^2\rangle_{av}(0)}\psi(k, t, t),$$

$$\langle\Gamma\rangle_{av}(t) = \frac{\langle\Gamma\rangle_{av}(t)}{\langle\Gamma\rangle_{av}(0)}, \qquad \alpha = \frac{\langle\Gamma\rangle_{av}(0)}{\langle\gamma^2\rangle_{av}(0)^{\frac{1}{2}}},$$

$$U(k, t, s) = \frac{2u^2}{\pi^{\frac{3}{2}}k_0^5}k^2 \exp\left[-\left(\frac{k}{k_0}\right)^2 - \tfrac{1}{2}u^2k^2(t-s)^2\right]$$

$$\psi(k, 0, 0) = (2\pi)^{-\frac{3}{2}} \exp\left[-\frac{1}{2}\left(\frac{k}{k_0}\right)^2\right], \quad \langle\Gamma\rangle_{av}(0) = 1$$

$U(k,t,t')$, $\psi(k,t,t')$ = velocity, concentration spectrum, k_0 = peak wave number, $\langle\gamma^n\rangle$ = central moments of concentration.

$$R = 2N^2\pi^{-\frac{1}{2}}q^2\left(\frac{\exp(-2kq\rho) + \exp(2kq\rho)}{2\rho^2} + \frac{\exp(-2kq\rho) - \exp(2kq\rho)}{4kq\rho^3}\right)$$

$$\rho = 1 + \tfrac{1}{2}N^2(t-s)^2,$$

$$\psi(k, 0, 0) = (2\pi)^{-\frac{3}{2}} \exp\left(-\frac{k^2}{2}\right),$$

$$\langle\Gamma\rangle_{av}(0) = 1,$$

DIA Equations for the Reacting Case

$$\frac{d\langle\Gamma\rangle_{av}}{dt} = -\langle\Gamma\rangle_{av}^2(t) - \frac{4\pi}{\alpha^2}\int_0^\infty k^2\psi(k, t, t)\,dk, \qquad (\text{:}$$

$$\left[\frac{\partial}{\partial t} + \frac{k^2}{N_{da}} + 2\langle\Gamma\rangle_{av}(t)\right]g(k, t, t')$$
$$= -\int_{t'}^{t} ds \int_0^\infty R\; g(q, t, s)g(k, s, t')$$
$$+ \frac{8\pi}{\alpha^2 k}\int_{t'}^{t} ds\left[\int_0^\infty \int_{|k-p|}^{k+p} dp\,dp\; q\; g(q, t, s)\cdot\psi(p, t, s)g(k, s, t')\right], \qquad (\text{:}$$

$$\left[\frac{\partial}{\partial t} + \frac{k^2}{N_{da}} + 2\langle\Gamma\rangle_{av}(t)\right]\psi(k, t, t')$$
$$= \int_0^{t'} ds\left[\int_0^\infty R\;\psi(q, t, s)\right]g(k, t', s)$$
$$- \int_0^{t} ds\left[\int_0^\infty R\; g(q, t, s)\psi(k, t', s)\right]$$
$$+ \frac{4\pi}{\alpha^2 k}\int_0^{t'} ds\left[\int_0^\infty \int_{|k-p|}^{k+p} dp\; qpq\;\psi(p, t, s)\cdot\psi(q, t, s)\right]g(k, t', s)$$
$$+ \frac{8\pi}{\alpha^2 k}\int_0^{t} ds\left[\int_0^\infty \int_{|k-p|}^{k+p} dp\,dq\; pq\;\psi(p, t, s)\cdot g(q, t, s)\right]\psi(k, t', s),$$

Direct Interaction Approximation for Scalars

Invariance (cf Corrsin, 1952):

In homogeneous turbulence, $\langle \gamma^n \rangle(t)$, n=2, 3,… should be independent of N

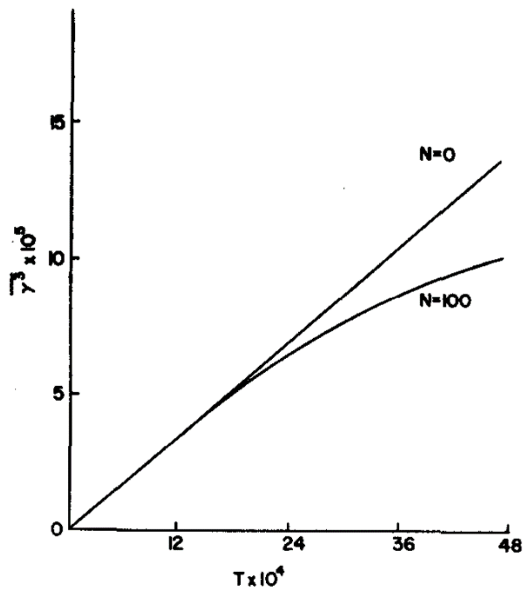

O’Brien (1968)

It is shown that the direct interaction hypothesis, when applied to the problem of isotropic mixing of a reactant undergoing an isothermal second-order reaction, fails to preserve, even approximately, an important invariance. Namely, in the absence of molecular diffusion the decay of single-point statistical functions of the concentration field should be independent of the turbulence.

With Cesar Dopazo in Spain

Scalar Probability Density Function (PDF) transport equation (1970-1980)

Motivation

- Statistical Mechanics non-linear terms in physical space become linear with variable coefficients in PDF formulation.
- Lundgren (1967, 1969): Velocity PDF transport equation.
- PD Functional: Projection leads to PDF transport equation (Kollmann).

Original form of single point scalar PDF transport equ. (projection from PD Functional)

$$\frac{\partial P(\phi;\mathbf{x},t)}{\partial t}+\underbrace{C\frac{\partial}{\partial\phi}\left[e^{\phi}P(\phi;\mathbf{x},t)\right]}_{Reaction}=\underbrace{-Da_2^{-1}\lim_{\boldsymbol{\xi}\to\mathbf{x}}\nabla_{\boldsymbol{\xi}}^2\frac{\partial}{\partial\phi}\int d\phi'\phi' P(\phi,\phi';\mathbf{x},\boldsymbol{\xi},t)}_{Molecular\ diffusion}\underbrace{-Da_1^{-1}\int d\mathbf{u}\mathbf{u}\cdot\nabla_{\mathbf{x}}P(\phi,\mathbf{u};\mathbf{x},t)}_{Convection}$$

Also transport equ. for two-point PDF: $P(\phi,\phi';\mathbf{x},\boldsymbol{\xi},t)$

For statistically homogeneous turbulence and scalar fields: dependence on $\boldsymbol{r}=\boldsymbol{\xi}-\boldsymbol{x}$

$$\frac{\partial P(\phi;t)}{\partial t}+C\frac{\partial}{\partial\phi}\left[e^{\phi}P(\phi;t)\right]=-Da_2^{-1}\lim_{\mathbf{r}\to 0}\nabla_{\mathbf{r}}^2\frac{\partial}{\partial\phi}\int d\phi'^{\phi'}P(\phi,\phi';\mathbf{r},t)=-Da_2^{-1}\frac{\partial}{\partial\phi}\left\{\underbrace{\left[\lim_{\mathbf{r}\to 0}\nabla_{\mathbf{r}}^2\langle\phi'|\phi;r,t\rangle\right]}_{\textbf{Closure needed}}P(\phi;t)\right\}$$

Modeling: Linear Mean Square Estimation

LMSE: Dopazo and O'Brien (1976)

Closure needed for the conditional expected value $\left[\lim_{\mathbf{r}\to 0} \nabla_{\mathbf{r}}^2 \langle \phi' | \phi; \mathbf{r}, t \rangle\right]$.

Initially termed conditionally Gaussian closure. Same results with linear estimation.

$$\langle \phi' | \phi; \mathbf{r}, t \rangle = \underbrace{\langle \phi \rangle (t)}_{Mean} + \underbrace{\rho(\mathbf{r}, t)}_{\substack{Autocorrelation \\ coefficient}} [\phi - \langle \phi \rangle (t)]$$

$$\rho(\mathbf{r}, t) = \frac{\langle [\phi - \langle \phi \rangle (t)][\phi' - \langle \phi \rangle (t)] \rangle}{\sigma^2(t)}$$

Scalar variance: $\sigma^2(t) = \langle [\phi - \langle \phi \rangle (t)]^2 \rangle$

For isotropic scalar field: $\rho(\mathbf{r}, t) = \rho(r, t)$

$$-\lim_{r\to 0} \nabla_{\mathbf{r}}^2 \langle \phi' | \phi; \mathbf{r}, t \rangle = 3[\phi - \langle \phi \rangle (t)] \left[-\left(\frac{\partial^2 \rho(r, t)}{\partial r^2} \right)_{r=0} \right] = \frac{6[\phi - \langle \phi \rangle (t)]}{\lambda_\phi^2(t)} = \mathrm{Sc} \frac{3[\phi - \langle \phi \rangle (t)]}{\lambda^2(t)}$$

$$\frac{\partial P(\phi; t)}{\partial t} + C \frac{\partial}{\partial \phi} \left[e^{\phi} P(\phi; t)) \right] = 3 \frac{\nu \tau_{ch}}{\lambda^2} \frac{\partial}{\partial \phi} \{ [\phi - \langle \phi \rangle (t)] P(\phi; t) \}$$

A Few Results

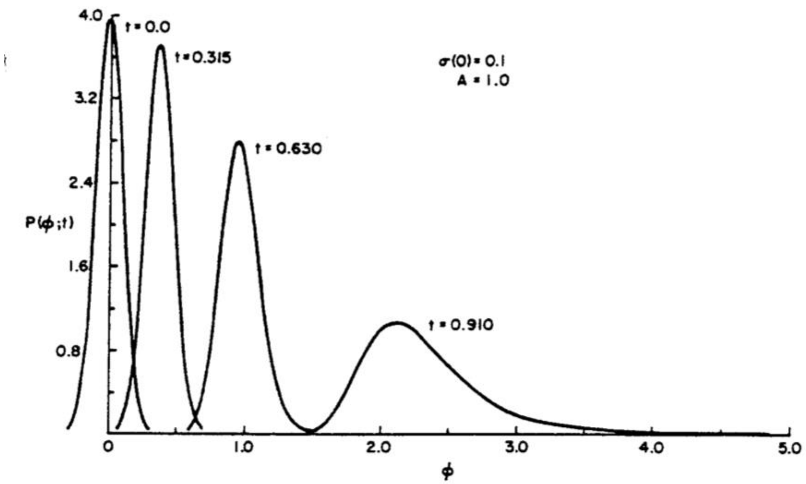

Fig. 2. Probability density function vs. dimensionless temperature for several times.

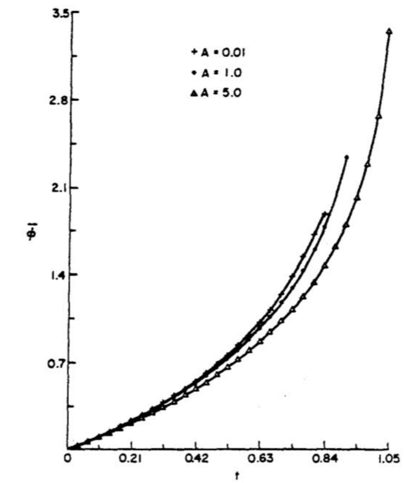

Fig. 13. Mean dimensionless temperature vs. time for $\sigma(0) = 0.1$.

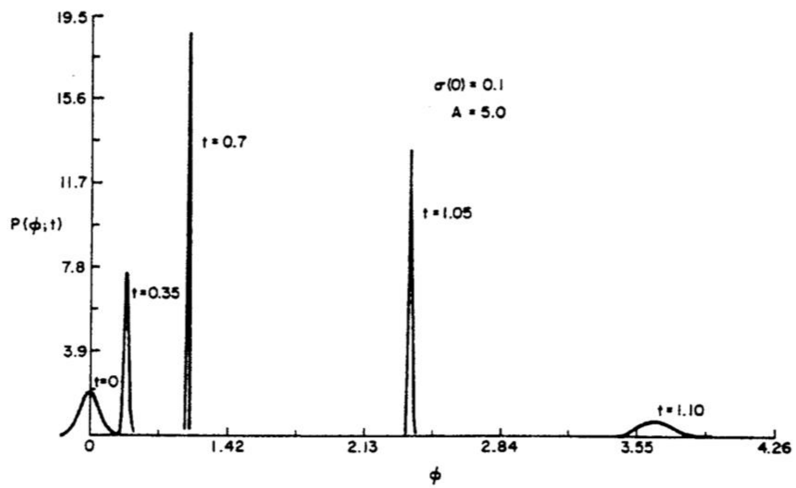

Fig. 3. Probability density function vs. dimensionless temperature for several times.

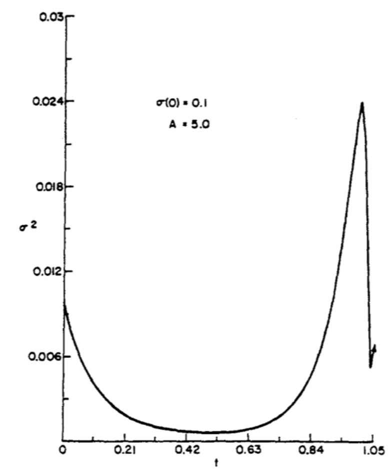

Fig. 18. Variance vs. time.

Scalar-Gradient PDF Transport Equation

Meyers and O'Brien (1981)

Scalar conservation model equ. $$\frac{\partial \phi}{\partial t} + \mathbf{u} \cdot \nabla \phi = -\beta(t)[\phi - \langle \phi(\mathbf{x}, t) \rangle] + \dot{w}(\phi)$$ $$\beta(t) = \frac{12D\langle (\nabla\phi)^2 \rangle}{(\langle \phi^2 \rangle - \langle \phi \rangle^2)}$$

Scalar-gradient conservation equ. $$\frac{\partial \psi_i}{\partial t} + \frac{\partial u_j}{\partial x_i}\psi_j + u_j \frac{\partial \psi_i}{\partial x_j} + \beta(t)[\psi_i - \langle \psi_i \rangle] = \frac{d\dot{w}}{d\phi}\psi_i$$ $$\psi_i = \frac{\partial \phi}{\partial x_i}$$

Joint PDF, $P(\phi, \psi_i)$, transport equ.

$$\frac{\partial P}{\partial t} + \langle u \rangle \cdot \nabla P - \frac{\partial \langle u_i \rangle}{\partial x_j}\frac{\partial \psi_i P}{\partial \psi_j} - \beta \frac{\partial}{\partial \phi}[(\phi - \langle \phi \rangle)P] - \beta \frac{\partial}{\partial \psi_i}[(\psi_i - \langle \psi_i \rangle)P] + \frac{\partial}{\partial \phi}[\dot{w}(\phi)P] + \frac{\partial}{\partial \psi_i}\left[\frac{d\dot{w}}{d\phi}\psi_i P\right] =$$
$$\frac{\partial D_{ij}}{\partial x_i}\frac{\partial P}{\partial x_j} + D_{ijpq}\frac{\partial}{\partial \psi_j}\left[\psi_i \frac{\partial}{\partial \psi_q}(\psi_p P)\right] - D_{ipq}\frac{\partial}{\partial \psi_q}\left(\psi_p \frac{\partial P}{\partial x_i}\right) - D_{ijp}\frac{\partial}{\partial \psi_j}\left(\psi_i \frac{\partial P}{\partial x_q}\right)$$

$$D_{ij}(t) = \int_0^t dt^* \langle u_i(t) u_j(t^*) \rangle$$

$$D_{ijpq}(t) = \int_0^t dt^* \left\langle \frac{\partial u_i}{\partial x_j}(t) \frac{\partial u_p}{\partial x_q}(t^*) \right\rangle$$

$$D_{ipq}(t) = \int_0^t dt^* \left\langle u_i(t) \frac{\partial u_p}{\partial x_q}(t^*) \right\rangle$$

$$D_{ijp}(t) = \int_0^t dt^* \left\langle \frac{\partial u_i}{\partial x_j}(t) u_p(t^*) \right\rangle$$

Turbulent/Non-Turbulent and Scalar Interfaces

Vorticity interface

Intermittency function: I(**x**,t)

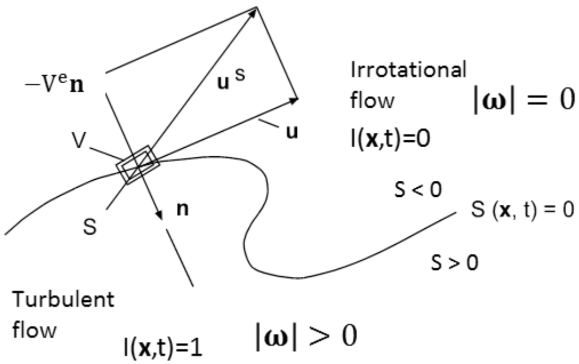

$$\underbrace{\mathbf{u}^S(\mathbf{x},t)}_{\substack{\textit{Interface}\\ \textit{velocity}}} = \underbrace{\mathbf{u}(\mathbf{x},t)}_{\substack{\textit{Fluid}\\ \textit{velocity}}} - \underbrace{V^e(\mathbf{x},t)}_{\substack{\textit{Entrainment}\\ \textit{velocity}}} \; \mathbf{n}$$

$$\frac{\partial I}{\partial t} + u_j \frac{\partial I}{\partial x_J} = \lim_{V\to 0} \frac{1}{V} \iint V^e dS = V^e \delta(S)$$

Conditioned variables

$$\langle IQ \rangle = \langle I \rangle \langle Q \rangle_T = \underbrace{\gamma}_{\substack{\textit{Inter-}\\ \textit{mittency}}} \langle Q \rangle^1$$

Scalar inteface

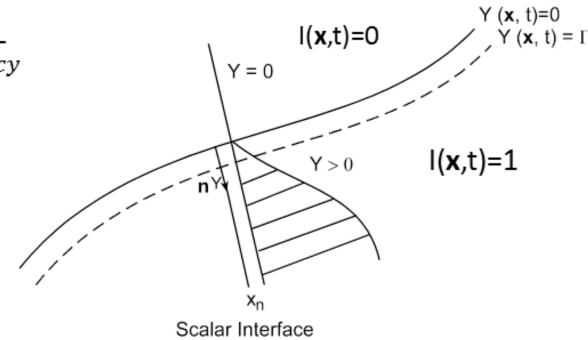

Let $\wp = \delta[Y(\mathbf{x},t) - \Gamma]$ be the fine-grained PDF of mass-fraction Y(**x**,t). Then:

$$\langle I\wp \rangle = \gamma P^1$$

$$\frac{\partial \gamma P^1}{\partial t} + \nabla \cdot (\gamma \langle \mathbf{u}^1 \wp^1 \rangle) = \underbrace{\langle V^e \wp \delta(S) \rangle}_{\substack{\textit{PDF}\\ \textit{entrainment}}} \underbrace{-D \frac{\partial}{\partial \Gamma}[\gamma F^1(\Gamma)]}_{\substack{\textit{Molecular}\\ \textit{diffusion}}}$$

Corrsin (1943): A "superlayer" separates turbulent zone of a jet from surrounding irrorational flow
Roshko (1973): Re-discovered "coherent" structures, driving interests in engulfment by large-scale organized structures. Ways to predict measured bimodal PDFs sought
Libby (1975, 1976): Proposed a transport model for the associated intermittency function
Dopazo and O'Brien (1976): Derived the exact form of the source of intermittency in terms of an entrainment velocity and a generalized delta function.
O'Brien (1977): Derived the relevant transport equation for the conditioned scalar PDF

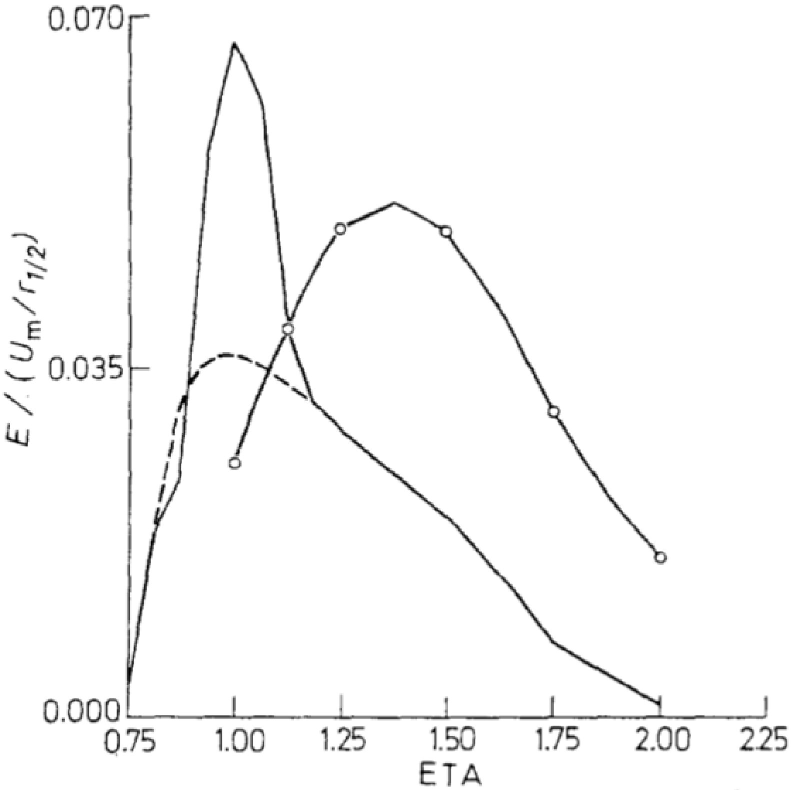

Fig. 3. Mass entrainment per unit mass for the heated jet. The dashed line is the result of taking for $\overline{v}_1/U_m$ the smooth curve in [12]. —o— *Tutu*'s modeling, i.e.,

$$\frac{2f\gamma}{(U_m/r_{1/2})}$$

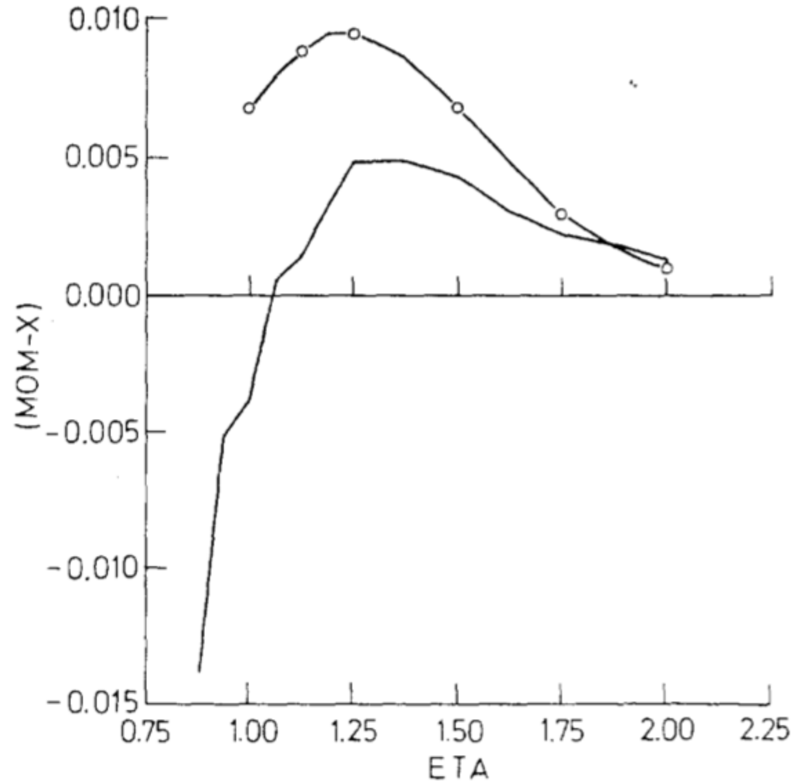

Fig. 4. Average entrainment of x-momentum for the heated jet. —o— *Tutu*'s modeling, i.e.,

$$\frac{f\gamma\overline{u}_1}{(U_m^2/r_{1/2})}$$

Co-Authored Publications (Dopazo)

1. C. Dopazo and E.E. O'Brien, *"Isochoric turbulent mixing of two rapidly reacting chemical species with chemical heat release"*, Physics of Fluids **16**, 12, 2075-2081 (1973). PDF
2. C. Dopazo and E.E. O'Brien, *"An approach to the autoignition of a turbulent mixture"*, Acta Astronautica **1**, 1239-1266 (1974). PDF
3. C. Dopazo and E.E. O'Brien, *"Functional formulation of nonisothermal turbulent reactive flows"*, Physics of Fluids **17**, 1968-1975 (1974). PDF
4. C. Dopazo and E. E. O'Brien (invited contribution), *"Statistical treatment of nonisothermal chemical reactions in turbulence"*, Combustion Science and Technology **13**, 99-122 (1976). PDF
5. C. Dopazo and E.E. O'Brien, *"Intermittency in free turbulent shear flow"*, Lecture Notes in Physics Turbulent Shear Flow I, 6-23, Ed. F. Durst et al., Springer Verlag, Berlin (1978).PDF
6. E.E O'Brien and C. Dopazo, *"Behavior of conditioned variables in free turbulent shear flows"*, H. Fiedler Ed., Structure and Mechanisms of Turbulence II., Lecture Notes in Physics, **76**, 124-137, Springer-Verlag, New York (1979). PDF
7. R. E. Meyers, C. Dopazo, E.E. O'Brien and R. Scott (invited contribution), *"Application of probability density and intermittency to random processes in environmental chemistry and hydrodynamics"*, Advances in Environmental Science & Engineering. Vol. 1, Gordon & Breach (1979). PDF

Co-Authored Publications (Ladeinde)

1 Ladeinde, F., O'Brien, E. E. & Liu, W. 2000. The effects of combustion on turbulence in high speed mixing layers. In "Advances in Turbulence VIII ", Edit C. Dopazo, CIMNE, Publ., Barcelona, Spain, pp. 433-436.

2 Ladeinde, F., O'Brien, E.E., W. Liu, & Nearon, M. 1999. The Effects of Kinetics Modeling on Mass Fraction PDF in Reacting Compressible Mixing Layers, In "Turbulence and Shear Flow - I", Begell House, Inc., Publishers, Edit. S. Banerjee & J. Eaton, pp. 321-326.

3 Cai, X., Ladeinde, F. & O'Brien, E. E. 1997. DNS on SP2 with MPI. In "Advances in DNS/LES", Greyden Publishing Co., Columbus Ohio., Edit. C. Liu & Z. Liu., pp. 491-495.

4 Cai, X., O'Brien, E. E. & Ladeinde, F. 1998. Advection of Mass Fraction in Forced, Homogeneous, Compressible Turbulence. *Physics of Fluids*, Vol. **10** (9), pp. 2249-2259 https://doi.org/10.1063/1.869746,

5 Ladeinde, F. Liu, W., & O'Brien, E. E., "Turbulence in Compressible Mixing Layers. ASME Journal of Fluids Engineering," Vol. 120, No. 1, 1998, pp. 48-53 doi:10.1115/1.2819659

6 Cai, X., O'Brien, E. E. & Ladeinde, F. 1997. Thermodynamic Behavior in Decaying, Compressible Turbulence with Initially Dominant Temperature Fluctuations. *Physics of Fluids*, Vol. **9** (6), pp. 1754, doi10.1063/1.869292

7 Ladeinde, F., O'Brien, E. E. & Cai 1996. An Efficient Parallelized ENO Procedure for Direct Numerical Simulation of Turbulence. *The Journal of Scientific Computing*, Vol. **38** (11), pp. 215-242, doi10.1007/bf02088815

8 Cai, X., O'Brien, E. E. & Ladeinde, F. 1996. Uniform Mean Scalar Gradient in Grid Turbulence: Asymptotic Probability Distribution of a Passive Scalar, *Physics of Fluids*, Vol. **8** (9), pp.2555-2558, doi10.1063/1.869038

9 Ladeinde, F., O'Brien, E. E., Cai, X., & Liu, W. 1995. Advection by Polytropic Compressible Turbulence. *Physics of Fluids*, Vol. **48** (11), pp. 2848-2857, https://doi.org/10.1063/1.868661

10 Ladeinde, F., O'Brien, E. E., & Liu, W. 2000. The Effects of Combustion on Turbulence in High-Speed Mixing Layers. Advances in Turbulence VIII, (Edit. C. Dopazo, Kluwer Publ.), pp. 433-436.

11 Wu, J., Ladeinde, F., & O'Brien, E. E. 2000. Second-Order Non-Linear Spatial Stability Analysis of Compressible Reacting Mixing Layers. AIAA Paper 2000-0146, Reno, Nevada.

12 Ladeinde, F., O'Brien, E.E., W. Liu, & Nearon, M. 1999. The Effects of Kinetics Modeling on Mass Fraction PDF in reacting Compressible Mixing Layers, Proc. First International Symposium on Turbulence and Shear Flow Phenomenon. Santa Barbara, CA., Sept. 12-15.

13 Nearon, M., Ladeinde, F. & O'Brien, E.E. 1999. Single-Point Concentration PDFs in Turbulent, Compressible, Mixing Layers. AIAA Paper 99-0929.

Co-Authored Publications (Ladeinde)

14 Ladeinde, F., Liu, W. & O'Brien, E. E. 1999. DNS Evaluation of Chemistry Models for Compressible Non-Premixed Flames. AIAA Paper 99-0143. January 1999.

15 Cai, X., Ladeinde, F. & O'Brien, E. E. 1997. Parallel DNS With MPI on SP/2. First Air Force Office of Scientific Research (AFOSR) Conference on DNS and LES. Louisiana State University, August 19-24, 1997.

16 Ladeinde, F., O'Brien, E. E., Liu, W. & Cai, X. D. 1997. Fundamental Studies of Three-Dimensional, Chemically-Reacting Compressible Turbulence. Presented at the May 1997 International Colloquium on Advanced Computation & Analysis of Combustion, Russian Academy of Sciences, Moscow, Russia.

17 Ladeinde, F., Liu, W. & O'Brien, E. E. 1997. DNS Studies of Turbulence in Compressible Mixing Layers. Presented at 1997 ASME Fluid Engineering Conference, Vancouver, Canada (June 24, 1997).

18 Cai, X., Ladeinde, F. & O'Brien, E. E. 1995. Mixing By Compressible Turbulence. 1995 International Conference on Turbulent Mixing. Hosted by Department of Applied Mathematics and Statistics, SBU Stony Brook, July 19th, 1995.

19 Wu, J., Ladeinde, F., O'Brien, E. E., & Cai, X. 2000. Non-linear Spatial Instability of Mixing Layers. Presented at 53rd Annual Fluid Dynamics Meeting of the American Physical Society. Washington, DC

20 Wu, J., Ladeinde, F., O'Brien, E.E., & Cai, X. 1999. Second order Non-linear Spatial Analysis of Compressible Mixing Layers. Presented at 52nd Annual Fluid Dynamics Meeting of the American Physical Society. New Orleans, USA

21 Ladeinde, F., W. Liu, & O'Brien, E.E. 1998. The Effect of Chemistry Modeling on Turbulence in Compressible Mixing Layers, Bulletin of the American Physical Society, Vol. 43, No.9. pp. 2115.

22 Nearon, M. D., Ladeinde, F., O'Brien, E. E., Raghu, S., & Pitts, W. M. 1996. Joint Velocity and Concentration Measurements in a Buoyant Helium Plume. Bulletin of the American Physical Society, Vol. 41, No. 12., pp. 1696.

23 Ladeinde, F., Liu, W., & O'Brien, E. E. 1996. The Intensity of the Second Moments of Turbulence in Compressible Mixing Layers. Bulletin of the American Physical Society, Vol. 41, No. 12, pp. 1741.

24 Cai, X. D., O'Brien, E. E., & Ladeinde, F. 1996. Thermodynamics Relations in Compressible Turbulence. Bulletin of the American Physical Society, Vol. 41, No. 12, pp. 1755

25 Ladeinde, F., O'Brien, E. E., & Cai, X. 1995. A Simple and Efficient Parallel Procedure for Direct Numerical Simulation of Compressible Turbulence. Bulletin of the American Physical Society, Vol. 40, No. 12, Page 1917.

26 O'Brien, E. E., Ladeinde, F., Cai, X., & W. Liu. 1995. DNS Evaluation of Statistics of Scalars in Two-Dimensional Compressible Turbulence. Bulletin of the American Physical Society, Vol. 40, No. 12.

27 Ladeinde, F. & O'Brien, E. E. 1994. Advection By Compressible Turbulence. Bulletin of the American Physical Society, Vol. 39, No. 9, Page 1851.

CONCLUDING REMARKS

- Briefly presented Ted's seminal contribution to Turbulence Theory, with a focus on passive and reacting scalars
- His early work focused on spectral theories for closing the infinite set of correlation equations
- His later work were on PDF-based closures, LMSE, Mapping Closures, LES, and DNS.

THE END

THANK YOU!

Foluso.Ladeinde@stonybrook.edu

LES/FMDF of Colorless Distributed Combustion

Husam Abdulrahman[1] , Farhad Jaberi [1] , Ashwani Gupta[2] , Ahad Validi [3]

[1] Mechanical Engineering Department, Michigan State University

[2] Mechanical Engineering Department, University of Maryland

[3] Ansys-Fluent

APS-DFD November 2019 Meeting - Special Session in Honor of Professor Edward O'Brien

- Supported by: DOE

- Computations are Conducted at: MSU's HPCC

CFD LAB MICHIGAN STATE UNIVERSITY

Outlines

- Why LES/FMDF methodology?
- Problem setup
- Results
  - Non-reacting flow
  - Reacting flow
    - Non-premixed reaction
    - Premixed reaction
- Conclusions

Colorless Distributed Combustion (CDC)

- The name **Colorless** is due to negligible visible flame compared to conventional flames.
- The ***Distributed Combustion*** is from the distributed reaction zone in the entire combustor.

How it works?

Three-stream mixture; reactants are diluted with large amounts of hot reaction products prior to combustion and mixed with air inlet.

- Lean combustion (Low CO and carbon emissions),
- Lower flame temperature & uniform temperature distribution (Low Nox emissions),
- This small temperature rise across the flame produces non visible and uniform combustion,
- Stable combustion ($P_{rms} < 1.5\%$),
- Low noise,
- Fuel flexibility (gas , liquid and biofuels) & reduced volume.

Ordinary combustion

Colorless Distributed Combustion

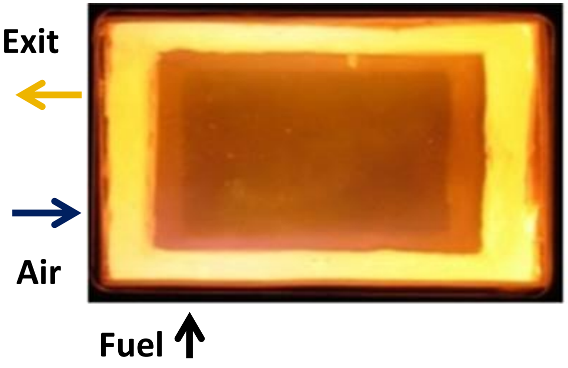

Modeling

- **Challenges:** a combination of highly unsteady turbulent flow, complex temperature field, mixing, ***<u>distributed combustion</u>***.
  - Jet-in-Jet interaction and reverse flows,
  - Mixing timescales are reduced,
  - Thicker and distributed flame *(**not thin flame fronts**)*,
  - Chemical timescales are increased due to dilution and ***Reaction rates*** could be ***low***.
- **Reliable CFD Model:** The solver should be able to handle the complexity of cross jet flow interactions with the main flow. High order numerical methods and accurate SGS models are needed for LES. Models for ***<u>distributed turbulent combustion</u>*** are also needed.
- **Previous Works:** Mostly based on ***RANS*** and ***Flamelet*** reaction models.

Computational Modeling of CDC with LES/FMDF

Gasdynamics Field

Filtered continuity and momentum equations via a multi-block high-order finite difference Eulerian scheme for turbulent flows. Dynamic closures for subgrid stresses and scalar Fluxes

Scalar Field (mass fractions and temperature)

Filtered Mass Density Function (FMDF) equation via Lagrangian Monte Carlo method - Ito Eq. for convection, diffusion & reaction

Chemistry

Kinetics: (I) global or reduced kinetics models with direct ODE or ISAT solvers, and (II) flamelet library with detailed mechanisms
Fuels: hydrogen, ethylene, methane & biofuels

In LES ,the "resolved" field is obtained by solving the filtered compressible N-S , energy and scalar equations.

MC particle moves in physical space due to filtered velocity and molecular and subgrid diffusivities.

The change in scalar space is due to mixing, reaction, viscous dissipation and Pressure variations.

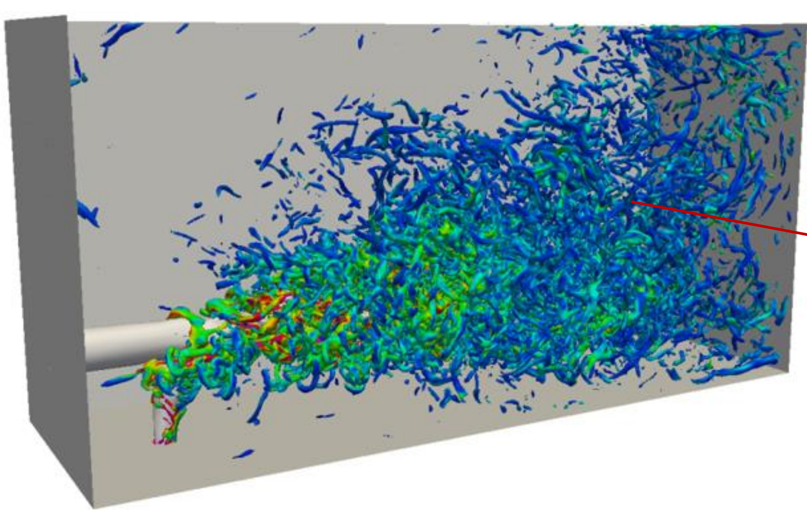

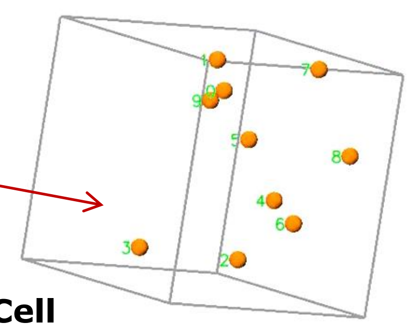

- Eulerian Cell
- Monte Carlo Particles

Problem Setup

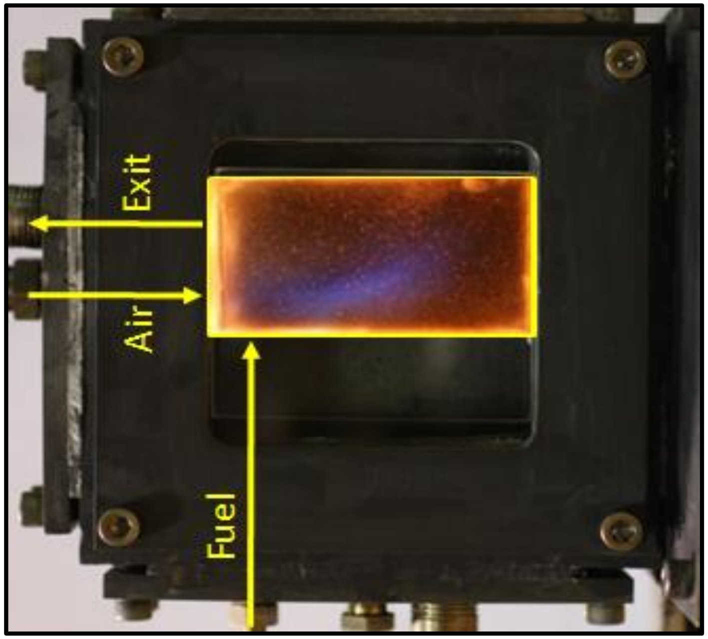

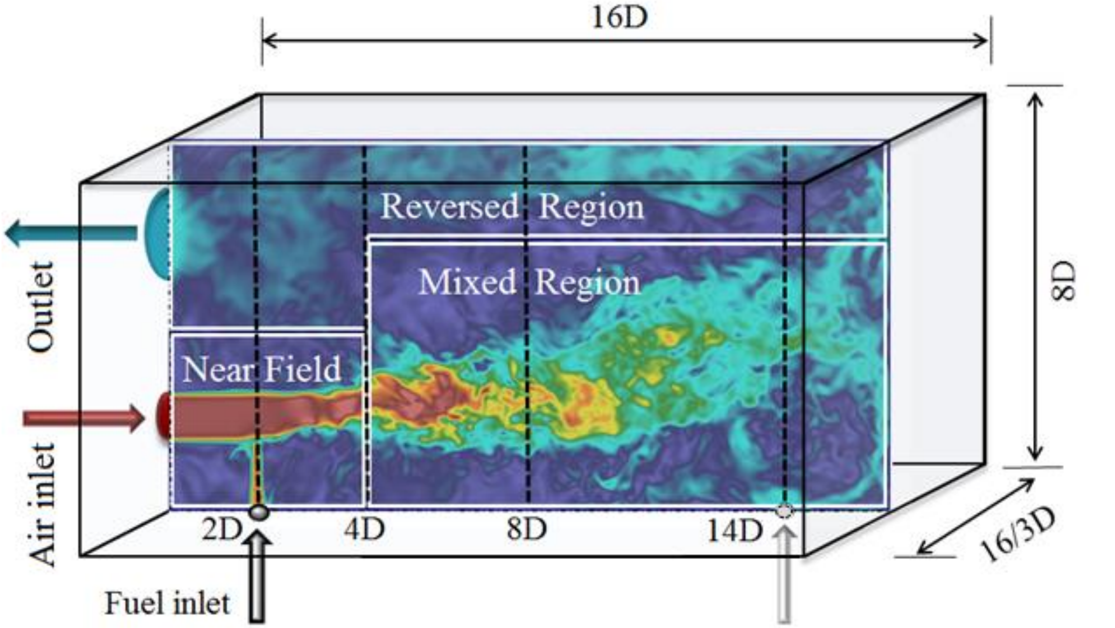

Schematic diagram of Reversed-Cross flow RC-CDC Combustor

Non-Reacting - LES model validation

The flow variables were averaged over 9 pass-over times.

$t_{pass-over} = x_{max}/U$

Comparison of mean and RMS vertical velocity at the *xz* mid-plan

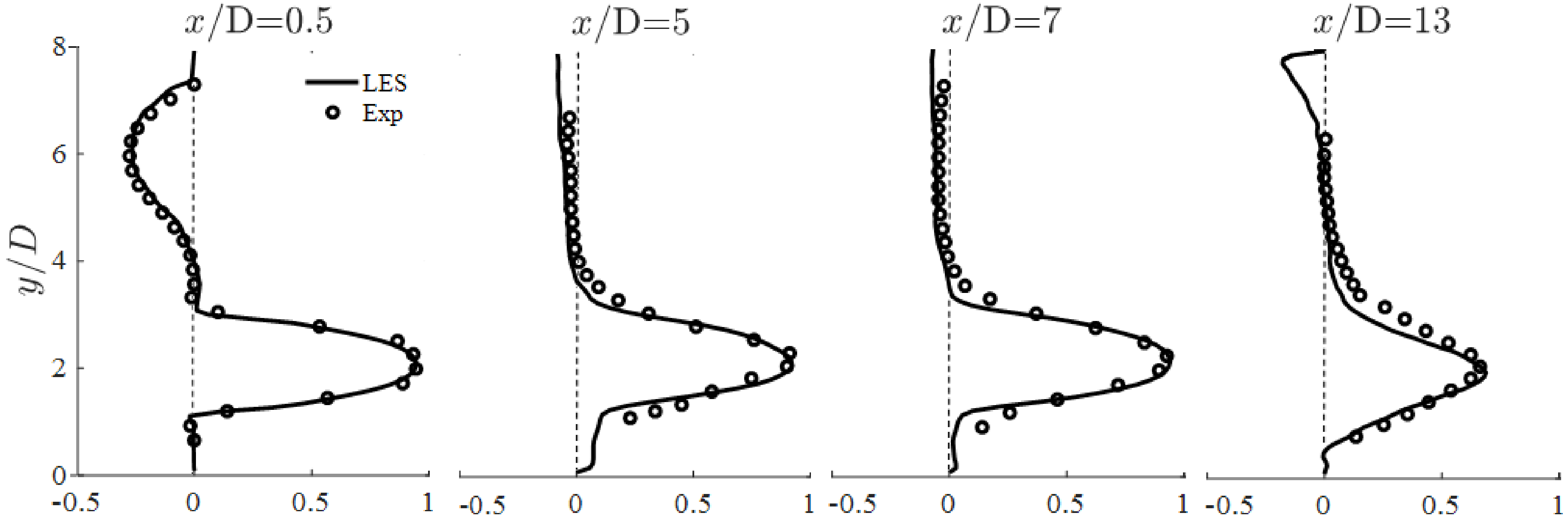

Experimental and numerical mean axial velocity profiles at different locations.

Non-Reacting: Flow structure and scalar field

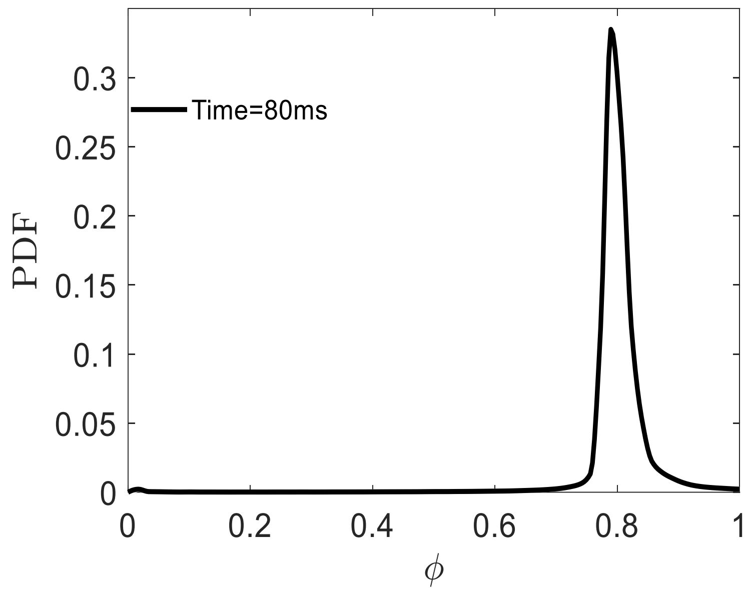

Temporal evolution of PDF of equivalence ratio

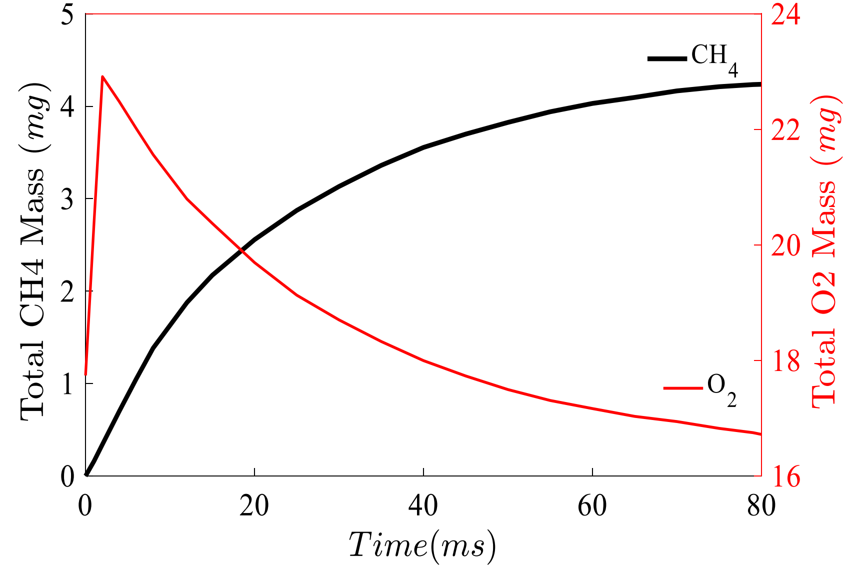

Temporal variation of total mass of CH_4 and O_2

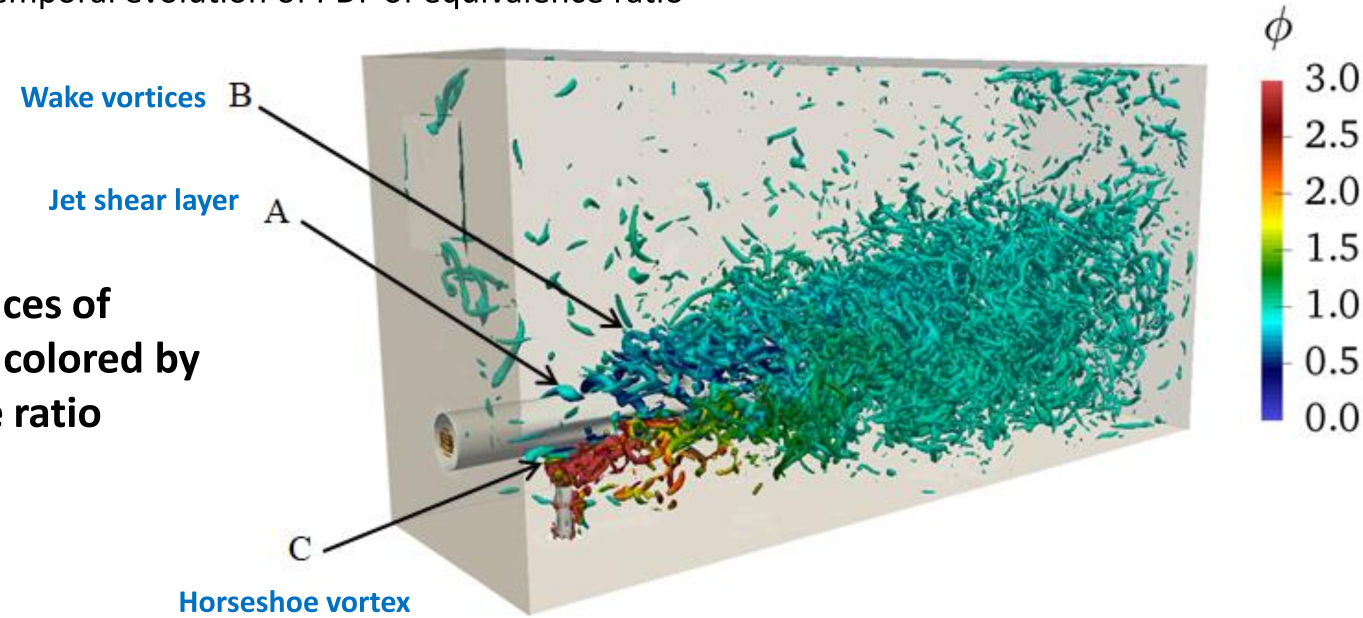

3D iso-surfaces of Q-criterion colored by equivalence ratio

LES/FMDF of non-premixed Colorless Distributed Combustion (CDC) System – Isothermal Case

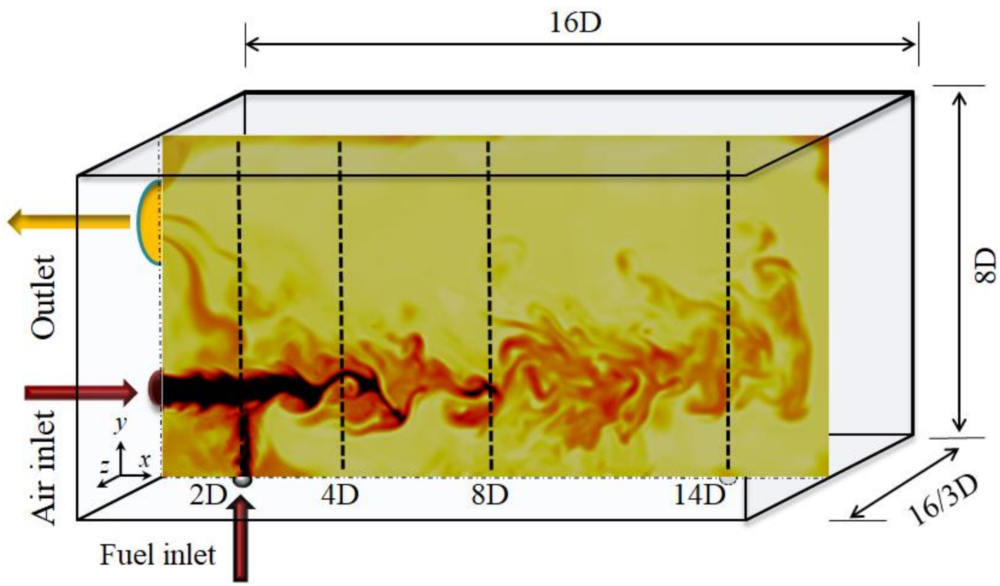

Case	Air jet inlet temperature (K)	Air jet velocity (m/s)	Fuel jet velocity (m/s)	Equivalene ratio
NP1	300	128	97	0.8
NP2	600	128	97	0.8

Consistency of LES-FD and FMDF-MC

Mathematically, the LES-FD and FMDF-MC parts of the hybrid LES/FMDF model should predict similar values for the filtered variables like temperature and scalar.

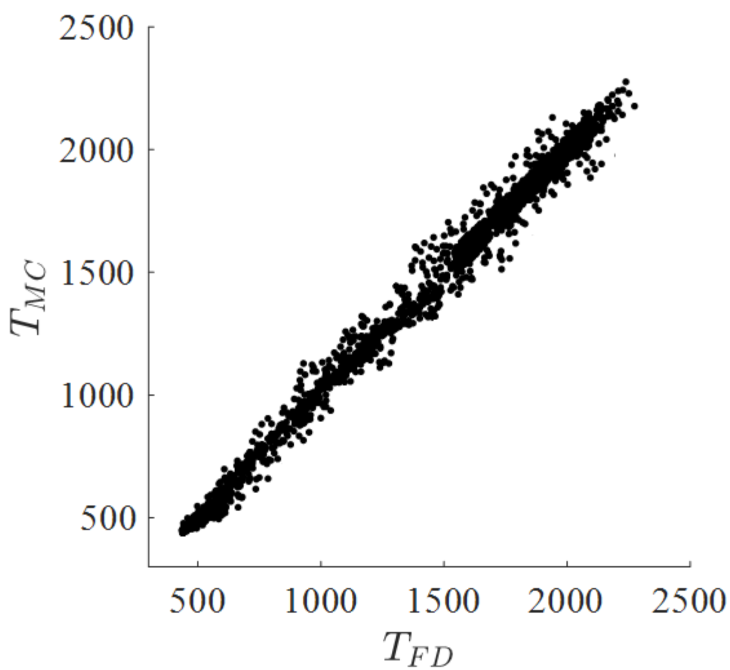

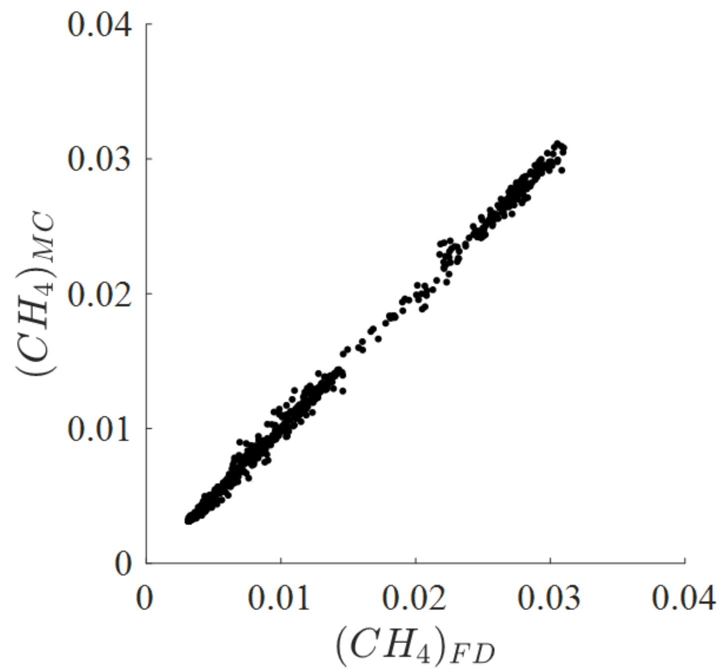

Scatter plots of instantaneous temperature and methane mass fraction obtained by LES-FD and FMDF-MC solvers.

Non-premixed Reacting vs Non-Reacting CDC

Flow and Turbulence Structure

(Air and fuel temperature inlets = 300K)

Qualitative comparison of the reacting and non-recating vorticity fields

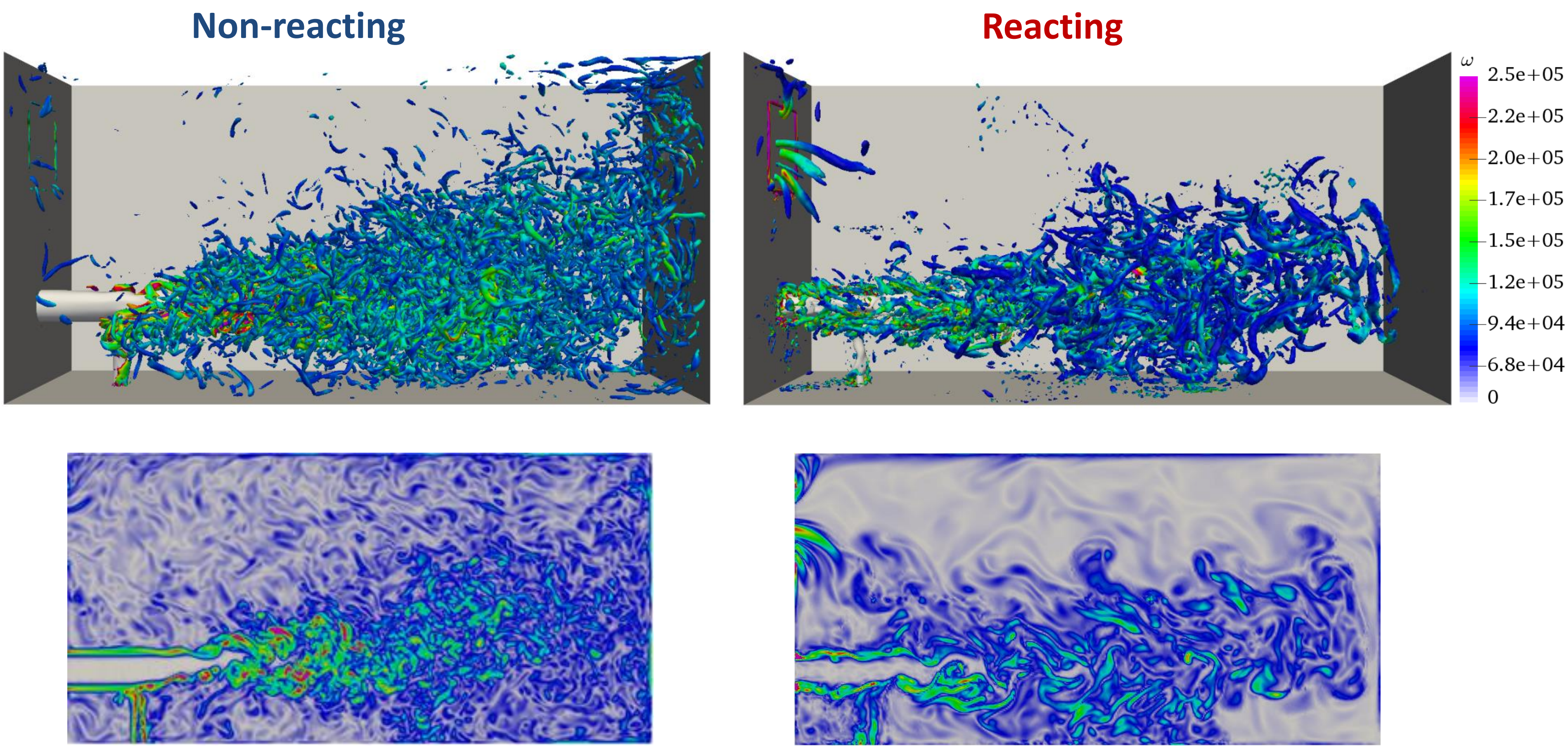

3D iso-surfaces of Q-criterion variable colored by vorticity magnitude, and contours of instantaneous vorticity magnitude at the mid-xy-plane

Non-premixed CDC: Isothermal Case

Quantitative comparison of the reacting and nonrecating velocity fields

x/D=0

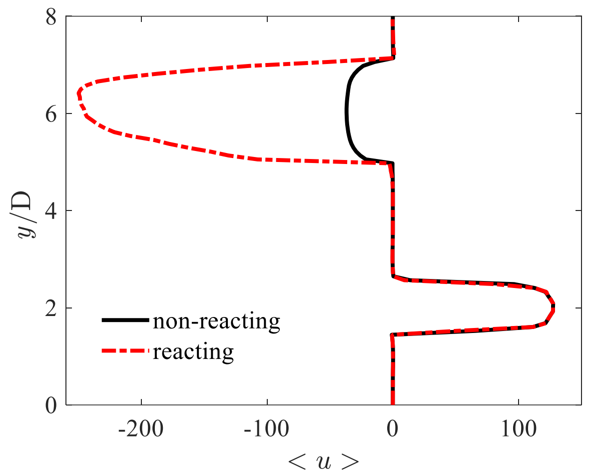

x/D=4

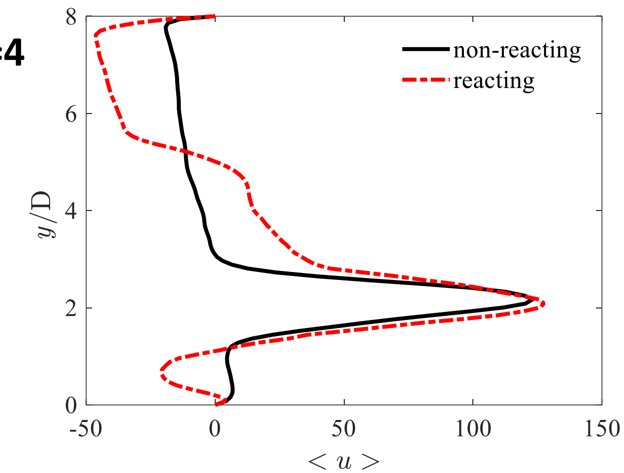

x/D=8

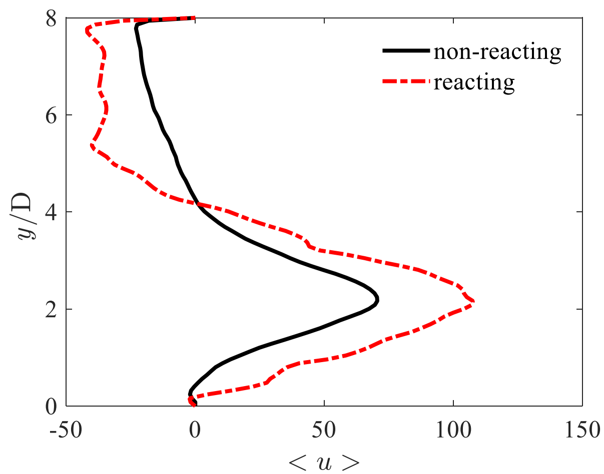

x/D=14

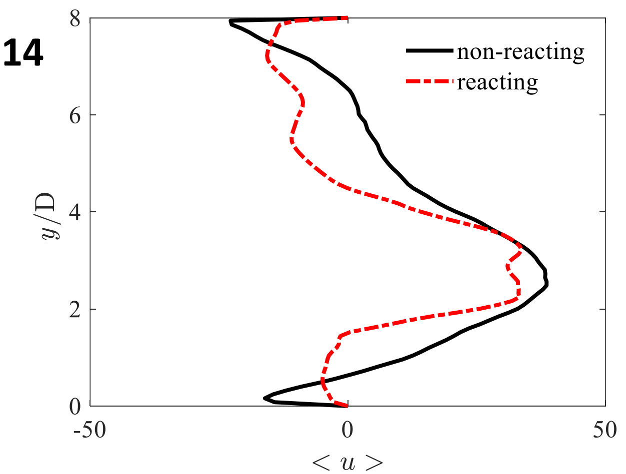

Mean Axial velocity profiles at mid z and different axial locations for non-reacting and reacting cases

Nonpremixed CDC

Scalar field Conditional Statistics

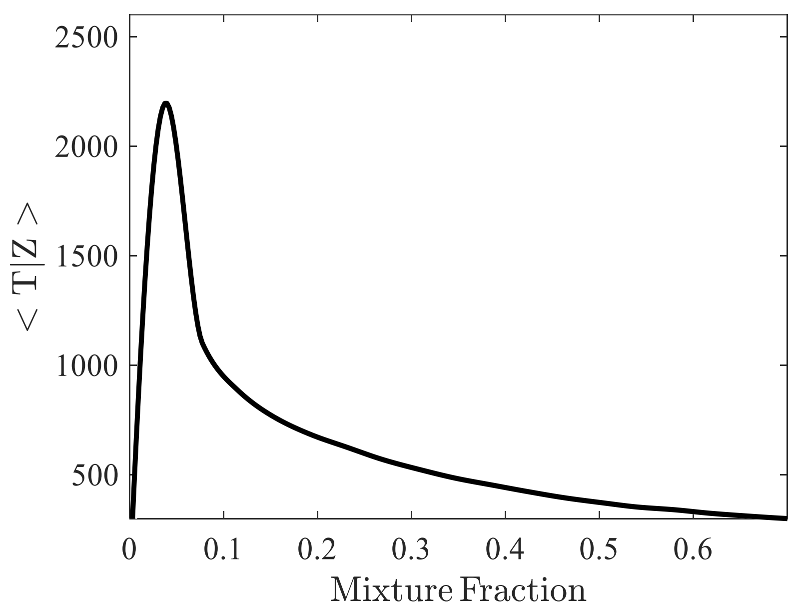

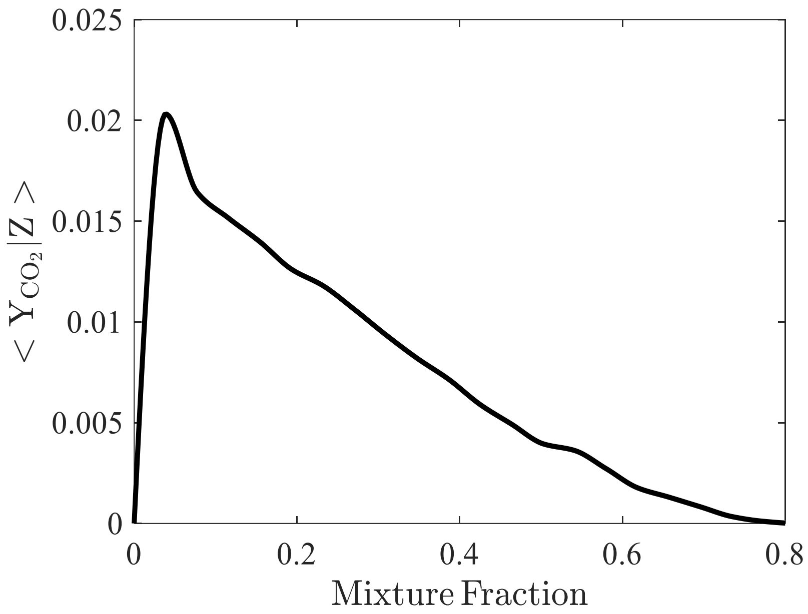

Conditional PDF of temperature, conditioned on the mixture fraction (left), and Conditional PDF of carbon dioxide, conditioned on the mixture fraction (right) for case NP1.

Conclusions

- Turbulent flow, mixing and combustion in isothermal and non-isothermal colorless distributed combustion (CDC) are computationally investigated for different flow configurations and parameters under non-reacting and reacting (non-premixed and premixed methane-air combustion) conditions with the LES/FMDF model and efficient high-order Finite Difference/Monte Carlo methods.

- Numerical results are shown to compare well with available experimental data and LES-FD and FMDF-MC results are fully consistent in all cases.

- Temporal and spatial variations of velocity, pressure and scalar fields indicate the unique structure of the flow in the simulated CDC. Air jet preheating (or JIJ momentum flux ratio) and fuel jet location have a substantial effect on the flow, mixing and combustion.

- The LES/FMDF model successfully handle the complex turbulent flow, mixing and combustion in CDC for various reacting conditions even at low DamKohler number range with substantial "non-flamelet combustion."

- The extension of LES/FMDF to multiphase flows allows the simulations of CDC with liquid fuel sprays.

Filtered Mass Density Function for Large-Eddy Simulations of Multiphase Turbulent Reacting Flows

Farhad Jaberi [1], Zhaorui Li [2], Araz Banaeizadeh [3], Abolfazl Irannejad [4]

[1] Mechanical Engineering Department, Michigan State University

[2] Mechanical Engineering Department, Texas A&M – CP Campus

[3] Altair Engineering Inc.

[4] Alcon-Novartis Inc.

APS-DFD November 2019 Meeting - Special Session in Honor of Professor Edward O'Brien

- Supported by: DOE, NSF, ONR, NASA, AFOSR and AFRL

- Computations are Conducted at: MSU's HPCC and XSEDE UT's ACC

CFD LAB

MICHIGAN STATE UNIVERSITY

Application of LES/FMDF to Complex Flows

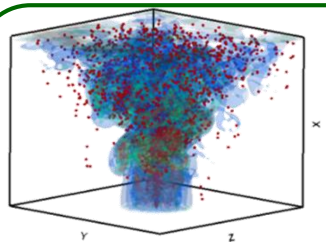

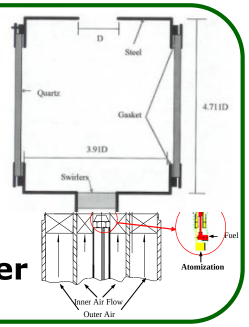

Double Swirl Spray Burner

IC Engines with Moving Valves/Piston, spray and combustion

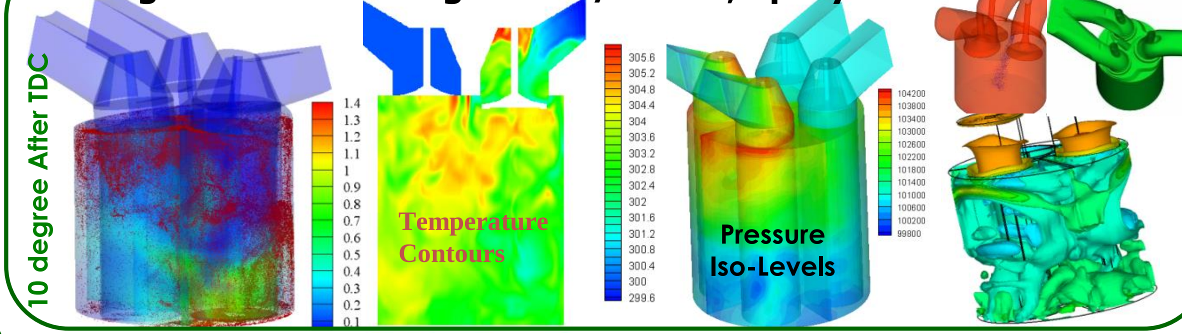

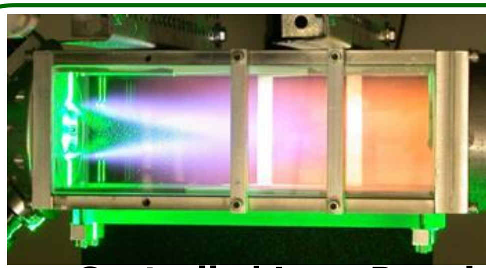

Spray Controlled Lean Premixed Dump Combustor

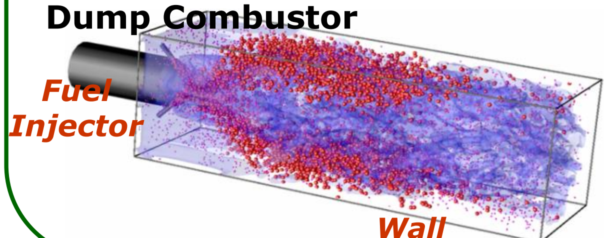

Turbulent Jet Ignition Assisted Combustion in a RCM

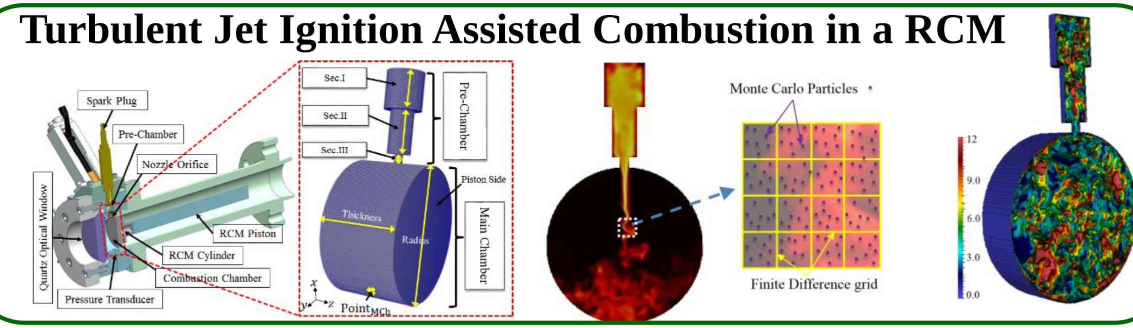

Supersonic H_2-Air Shear Combustion

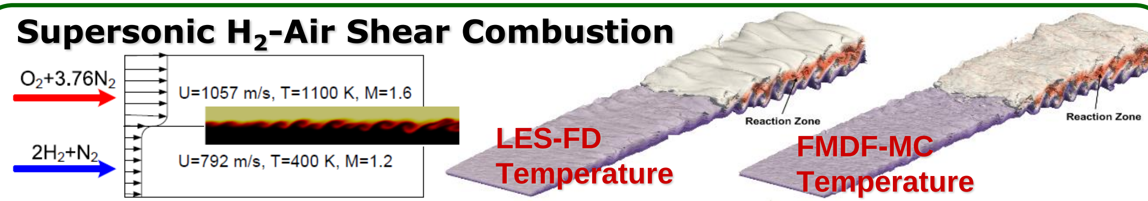

Turbulent Spray Combustion

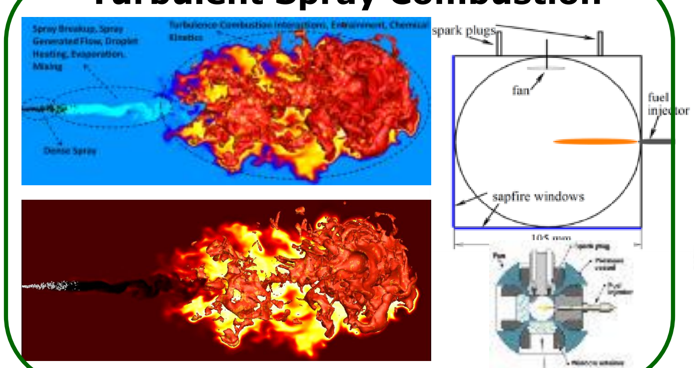

Supersonic Cavity Combustor

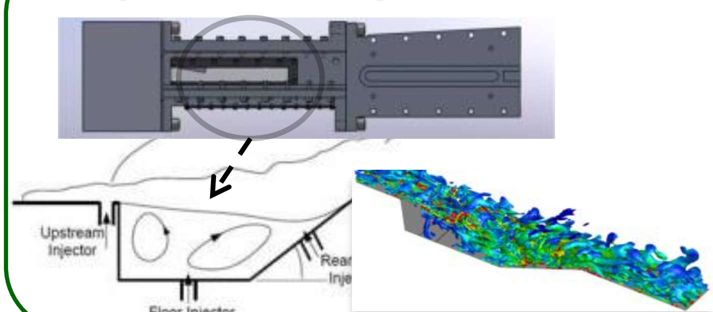

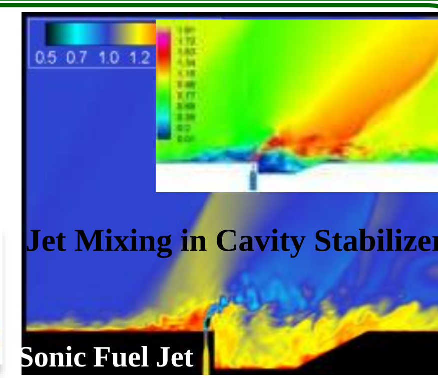

Mathematical/Computational LES/FMDF Methodology

Gasdynamics Field → Filtered continuity and momentum equations via a generalized multi-block high-order finite difference Eulerian scheme for high Reynolds number turbulent flows in complex geometries

Various closures for subgrid stresses

Scalar Field (mass fractions and temperature) → Filtered Mass Density Function (FMDF) equation via Lagrangian Monte Carlo method - Ito Eq. for convection, diffusion & reaction

Droplet Field (spray) → Lagrangian model for droplet equations with full mass, momentum and energy couplings between phases and a stochastic subgrid velocity model

Chemistry → Kinetics: (I) reduced kinetics schemes with direct ODE or ISAT solvers, and (II) flamelet library with detailed mechanisms or complex reduced schemes.
Fuels: methane, propane, decane, kerosene, heptane, JP-10, Hydrogen, Biofuel blends,………

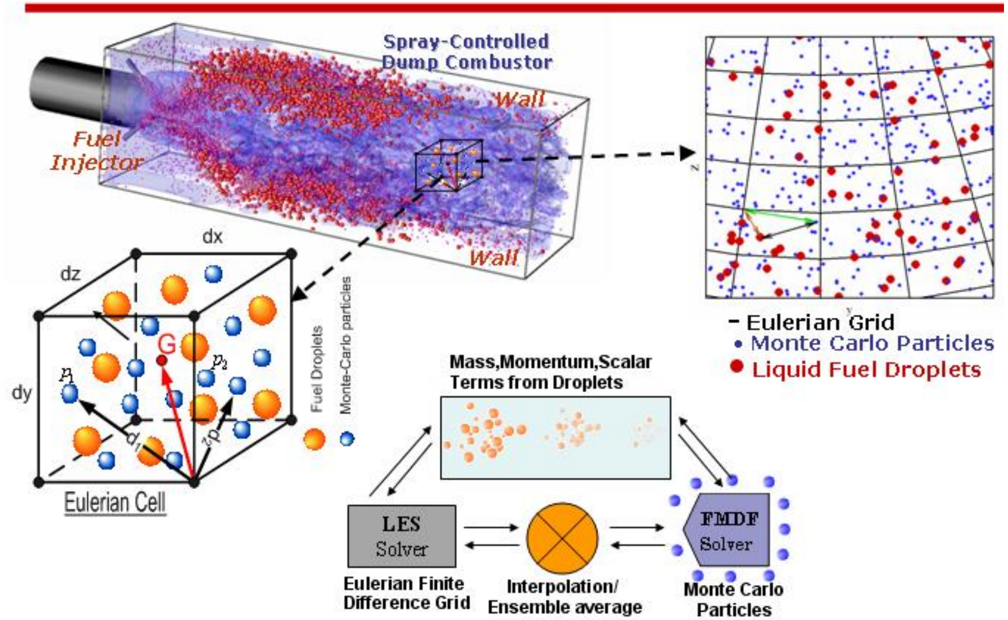

- **Eulerian:** Compressible filtered LES equations are solved with
  - High order finite difference method
  - Various SGS closures
- **Lagrangian:** Transport equation for FMDF is solved with
  - Monte Carlo simulations
  - Compressible and Multi-Phase terms are included
- **Lagrangian:** Transport equations for Spray (droplets) are solved with
  - Point particle simulations
  - Stochastic breakup models
  - Finite rate heat and mass transfer with two-way coupling
- **Eulerian & Lagrangian** fields are coupled through several gas and liquid source/sink terms
- **Consistency:** “Redundant” variables are used for testing and control of numerical accuracy of FD and MC solvers

3D Simulations of Premixed Hydrogen Combustion in a Mach 2 Cavity Burner

Computed by a Detailed 9 Species, 37 Step Detailed H_2-Air Mechanism

Consistency and Numerical Accuracy of LES/FMDF Solver

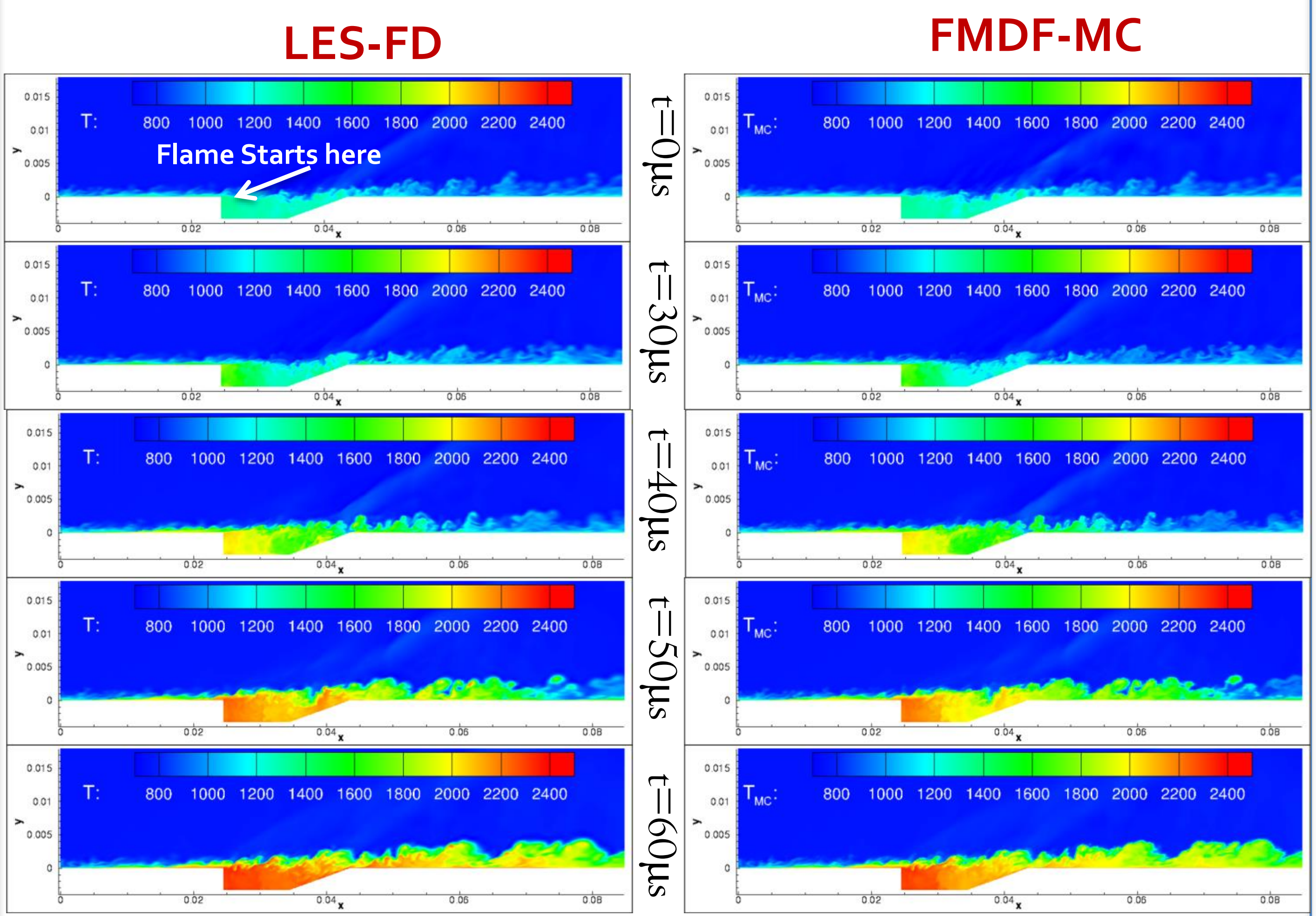

Temperatures Contours at Midplane at Different Times after Flame Ignition

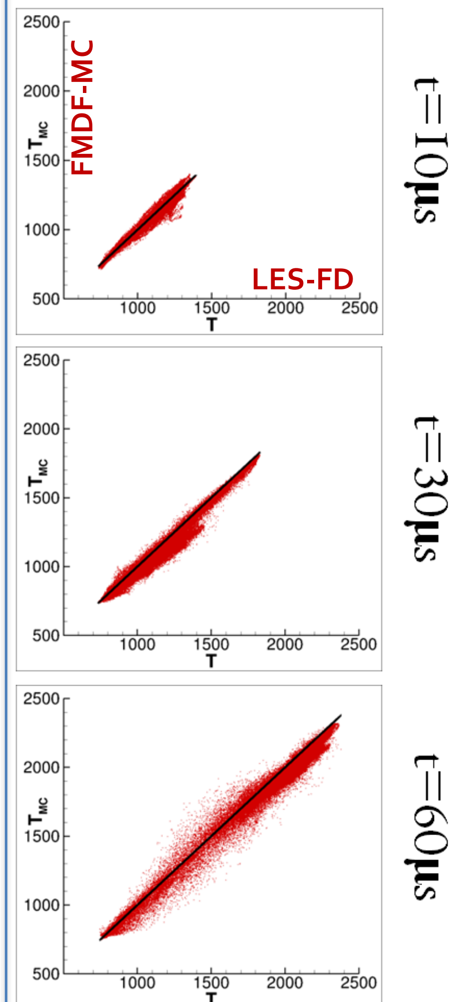

Temperature

LES with Compressible Scalar FMDF- Square Shock "Tube"

3D Shock "Tube" with Turbulence

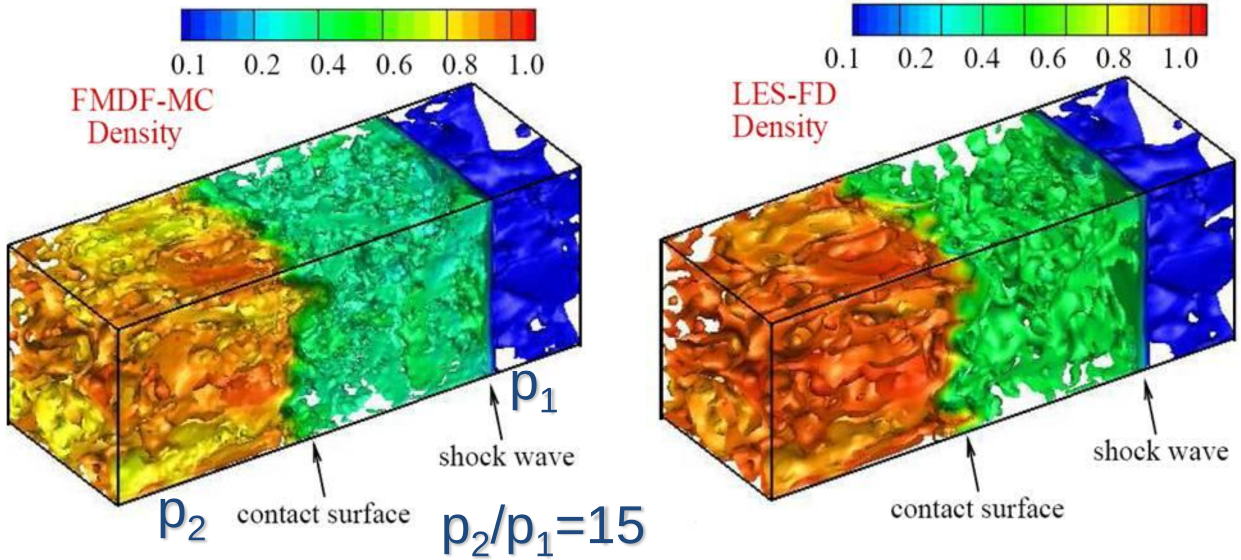

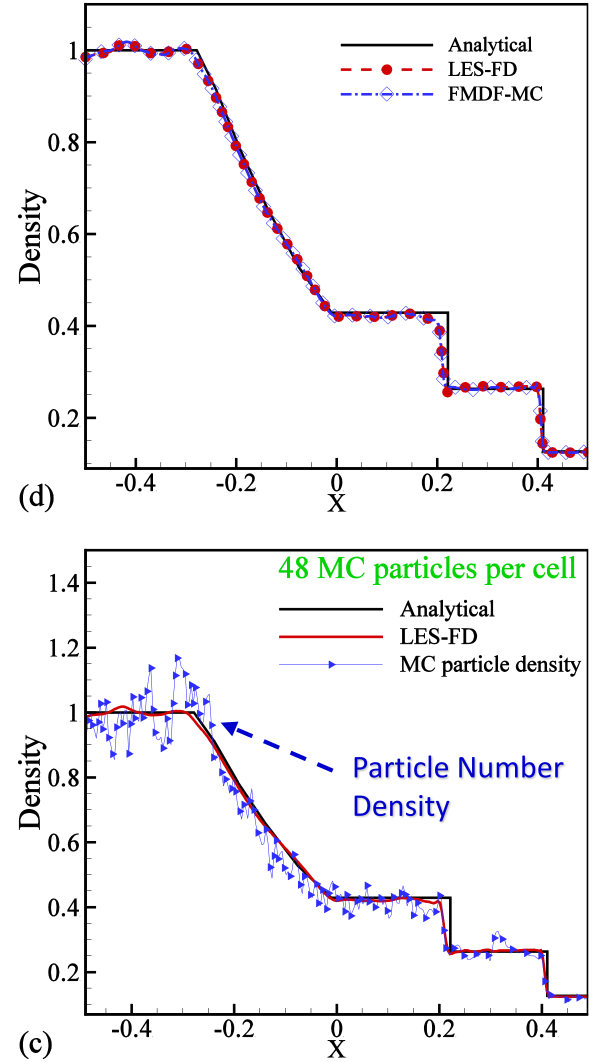

Plane-averaged Mean Density

- Compressibility effects are included in FMDF-MC; without compressible term FMDF-MC results are very erroneous.
- By varying the initial number of MC particles per cell, the filtered temperature does not noticeably change.
- By increasing the initial particle/cell number, MC particle number density becomes smoother and nearly the same as filtered fluid density.

Sandia's High Pressure/Speed Sprays

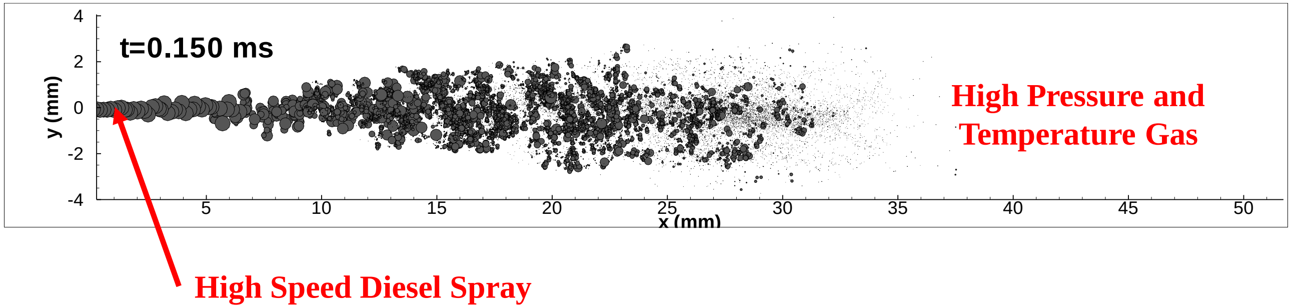

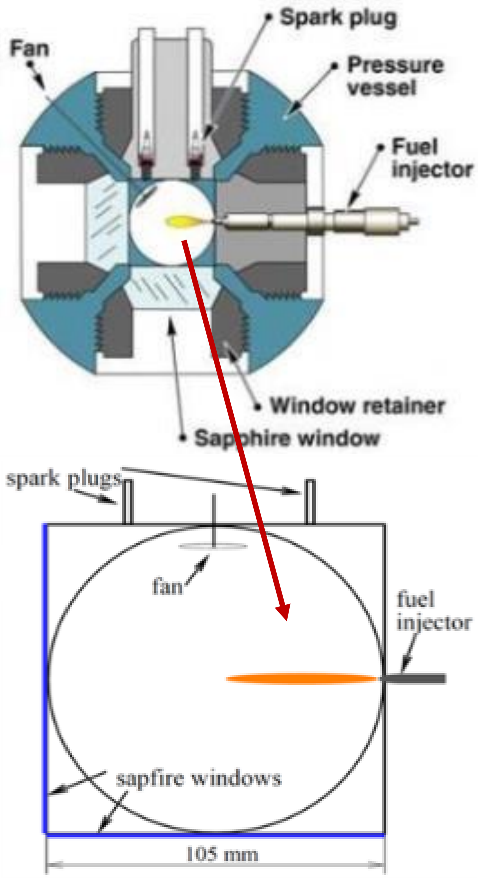

Evaporating and Reacting Spray Data from Sandia Laboratory:

- **Spray CET** with Evaporation and Mixing (Hexadecane Spray)
- **Spray A** with Evaporation and Mixing (Dodecane Spray)
- **Spray H** with Auto-Ignition and Combustion (Heptane Spray)

Highlights of Spray Simulations with LES/FMDF

- **Detailed Study of High Speed Evaporating Sprays and Spray Induced Flow/Turbulence**
  - Different Chamber Temperatures and Pressures
  - Different Injector Nozzle Sizes
  - Different Injection Pressures
- **Detailed Study of Turbulent Spray Flames**
  - Spray Auto-Ignition Process, Ignition Delays and Flame Lifted Length
  - Effects of different Chamber Temperatures and Oxygen Concentrations

LES/FMDF of Turbulent Spray Combustion (Spray H)

Surrounding Gas Properties: T=1000 K, ρ=14.8 kg/m^3, 21%O_2

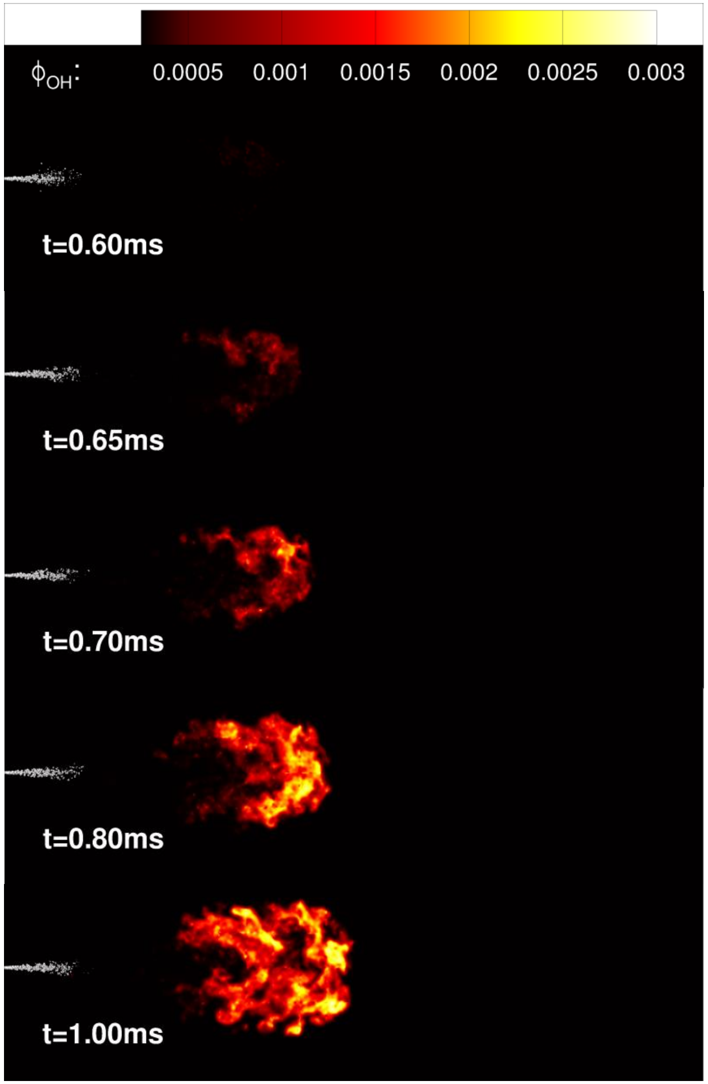

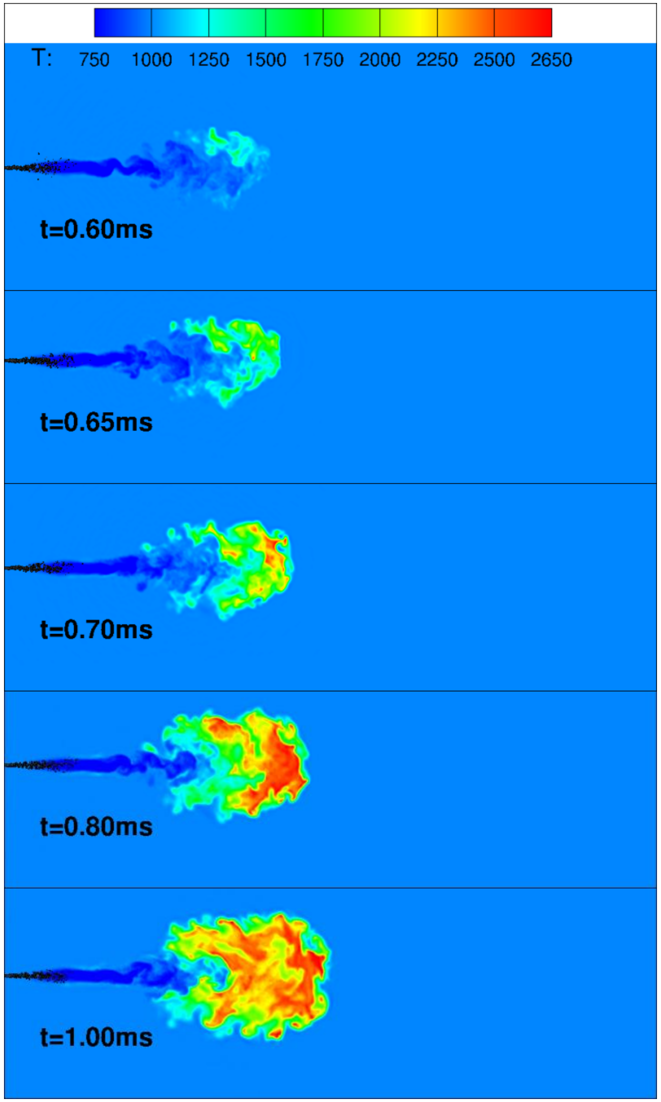

Auto-Ignition Process: OH mass fraction

Auto-Ignition Process: Temperature

Consistency and Numerical Accuracy of LES/FMDF

- LES-FD and FMDF-MC parts of the hybrid LES/FMDF solver are consistent even with a Evaporating and Reacting Spray

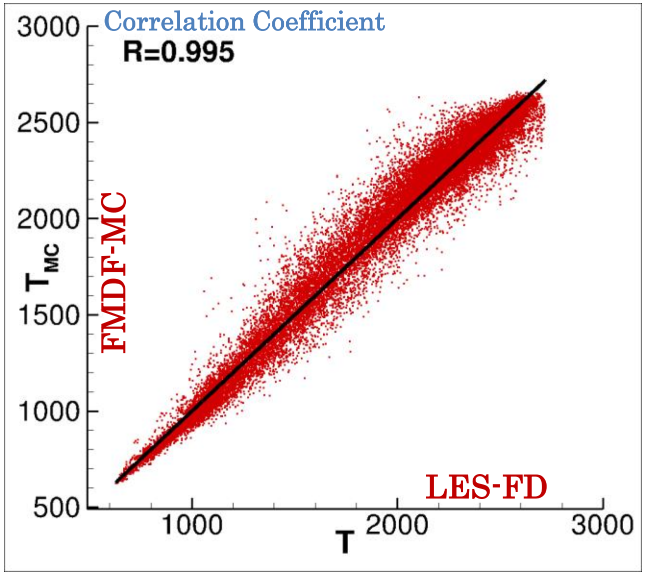

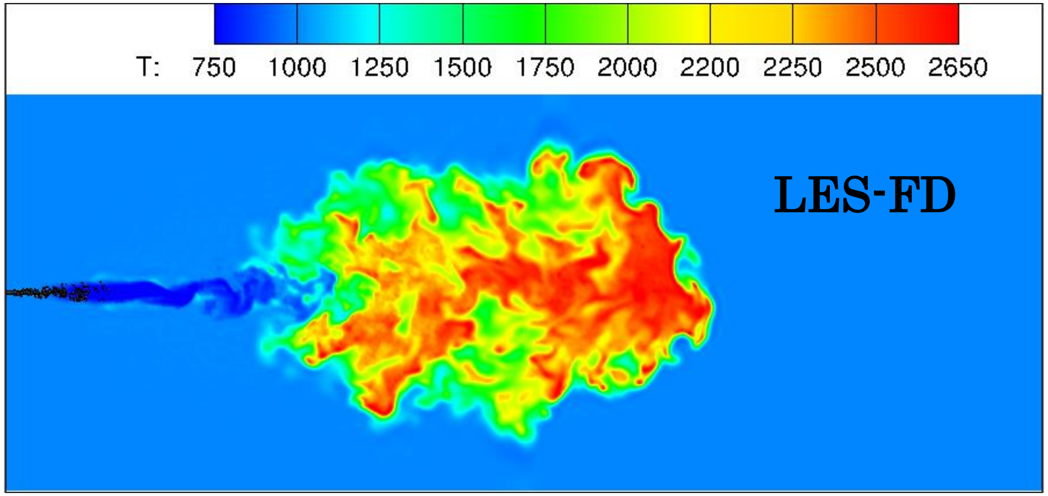

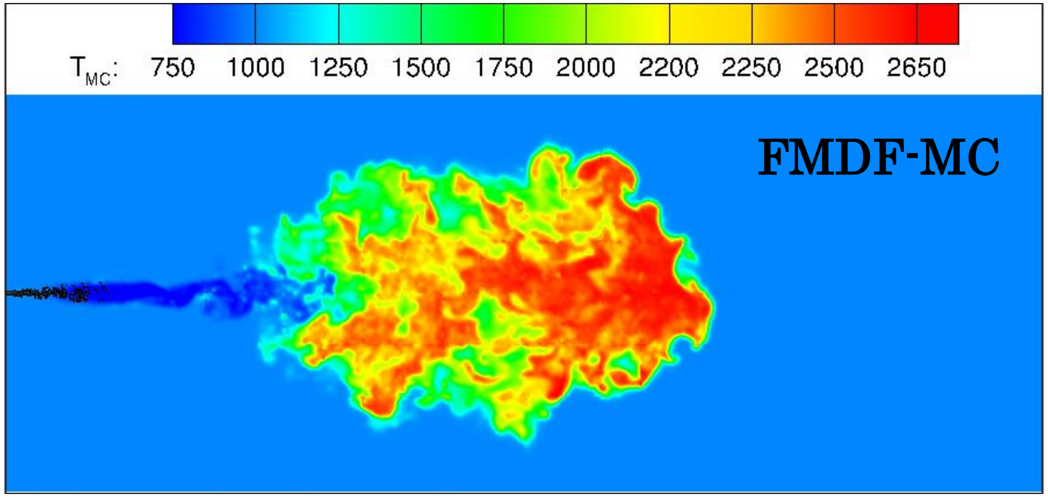

Temperature

Evaporating Sprays without Combustion - Comparison with Experiment

Liquid and vapor penetration –Comparison with Experiment

Spray A

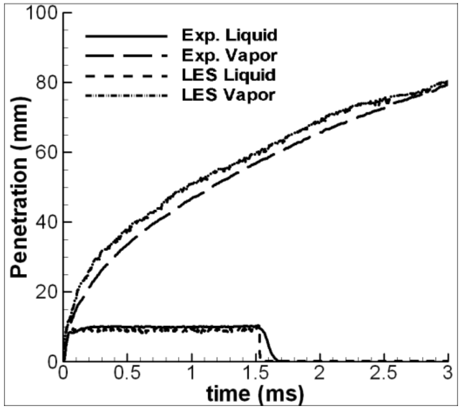

Spray H

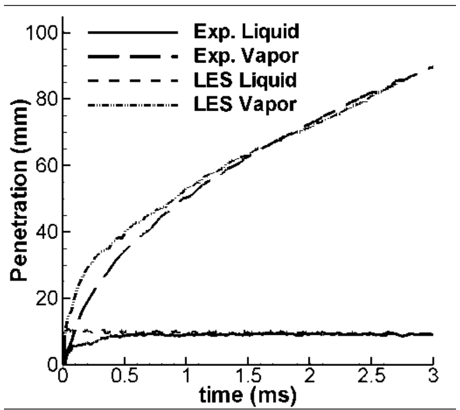

Spray CET

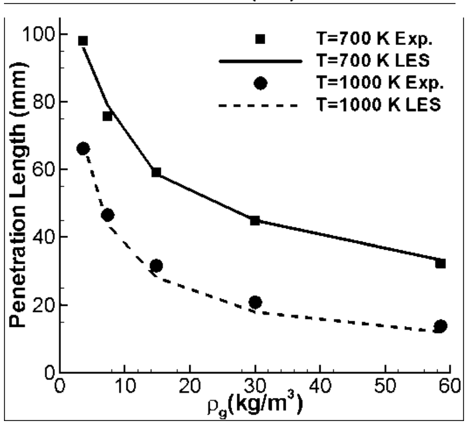

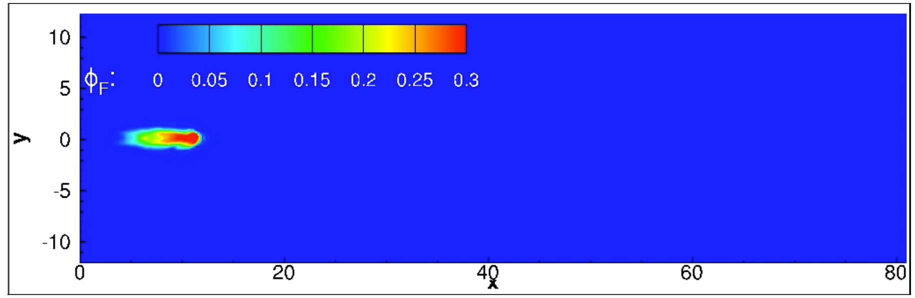

Fuel Vapor (Spray A)

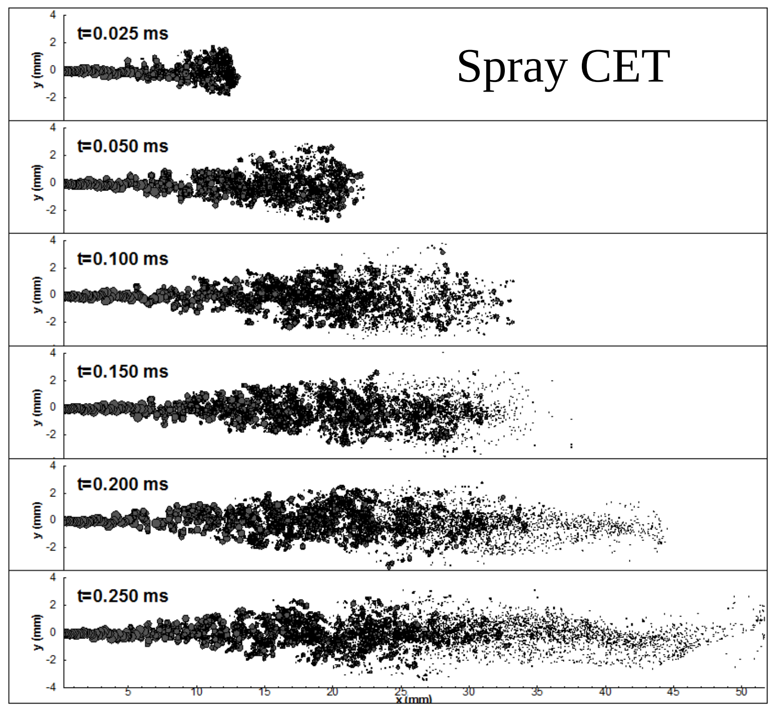

Cascade of Breakup events;
Droplets Driven by Induced Flow

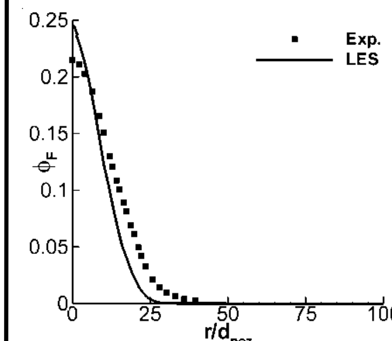

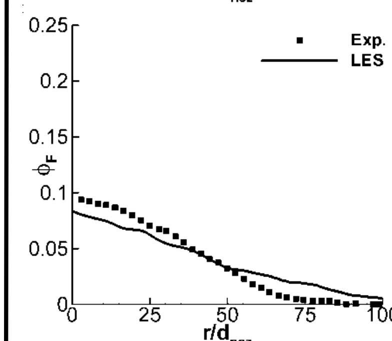

Fuel Vapor Profiles at Different Axial Locations (Spray H)

Diesel Spray with Combustion – Spray H

LES/FMDF Conducted with 44 Species Skeletal Mechanism for N-Heptane via ISAT

Lifted Flame of Auto-Igniting Spray

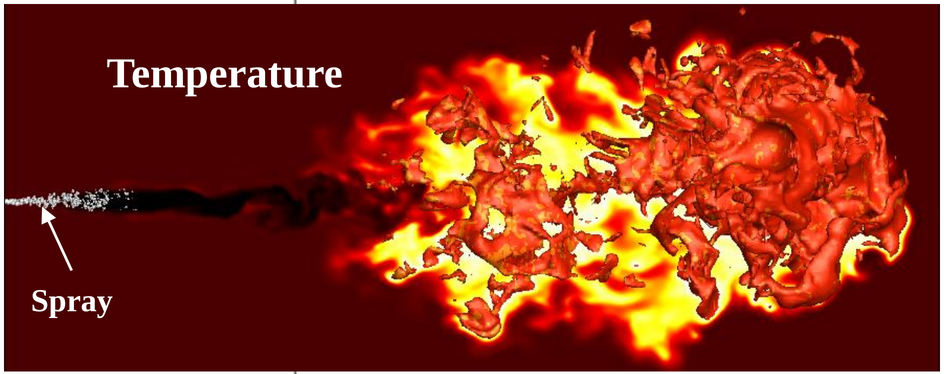

Flame Starts in Spray Generated Turbulent Zones at Tip of Fuel Vapor Jet

Comparison with Experiment - Flame Lift-off Length , Liquid &Vapor Penetration Lengths

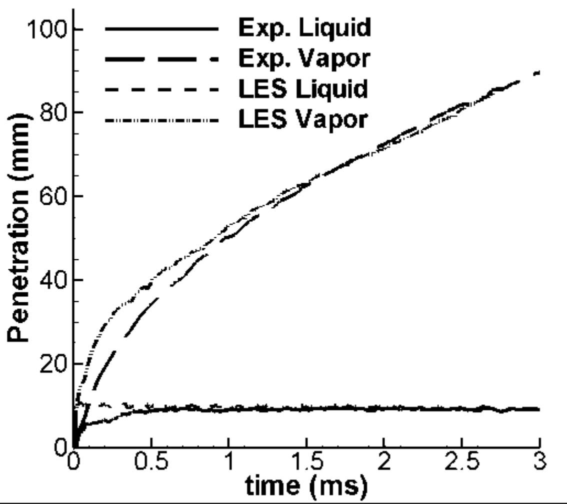

Liquid and Evaporated Fuel Vapor Penetration Depths

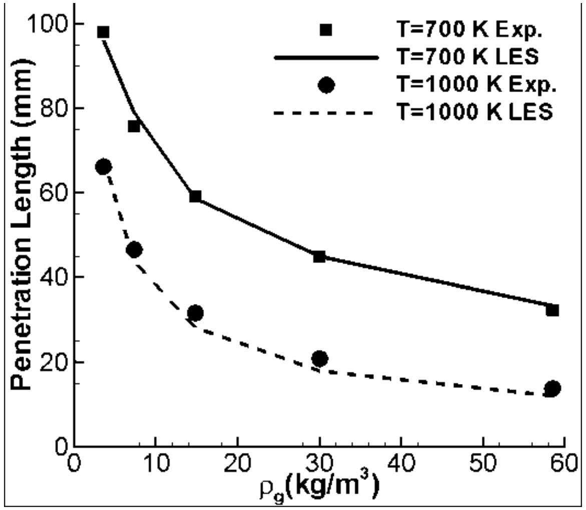

Liquid Penetration for various Gas Temperatures and Densities

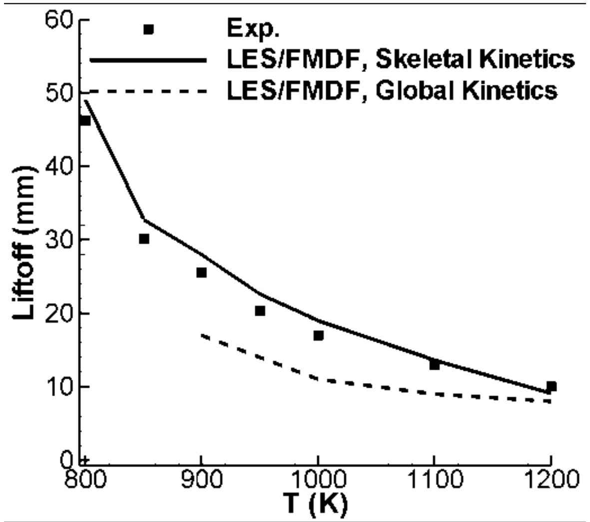

Flame Lift-off Length at different Ambient Temperatures

Summary, Current Status, and Future Challenges

- ❑ Extension and application of scalar FMDF method to Multiphase Flows in Complex Configurations with efficient LES-FD+FMDF-MC Solver
- ❑ LES/FMDF simulations of complex combustion problems (e.g. reacting diesel spray via ISAT, supersonic hydrogen cavity combustion via detailed kinetics, Colorless distributed combustion, and turbulent-jet-assisted combustion in rapid compression machine via reduced mechanisms, etc.) are successfully conducted

- ❑ Main barriers to utilizing LES/FMDF for practical combustor simulations are related to LES of non-reacting flows in complex geometries and computational implementation of FMDF in production codes
  - ➢ Computing/modeling turbulent boundary layer in high Reynolds number flows,………..
  - ➢ Reliability of Kinetics and Computational demand of complex reaction mechanisms
  - ➢ An important issue in comparing LES/FMDF results with experiment is the "matching" of boundary/initial conditions

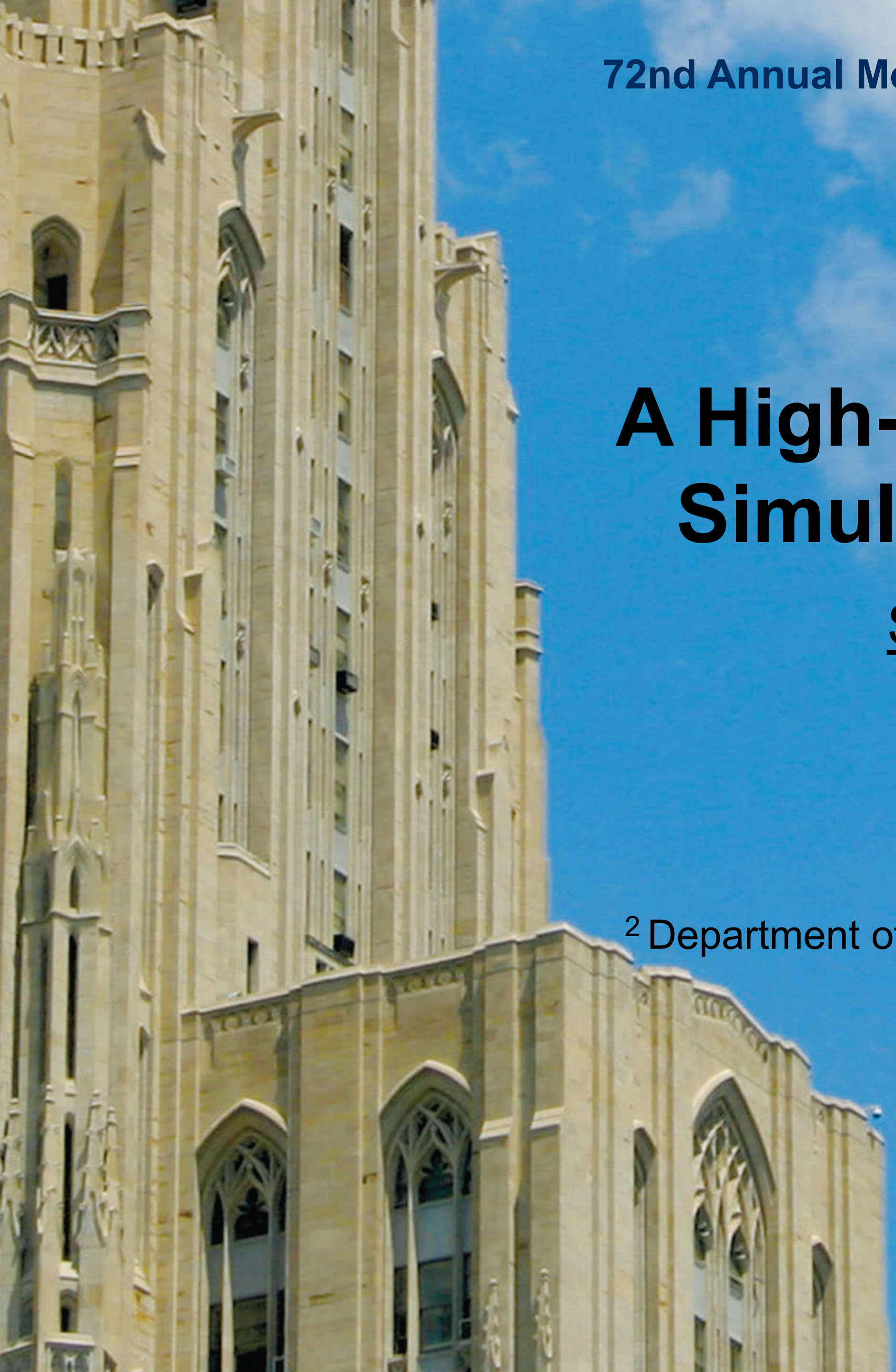

72nd Annual Meeting of the APS Division of Fluid Dynamics,

November 23-26, 2019, Seattle, WA

A High-Order FDF Large Eddy Simulator of Complex Flows

Shervin Sammak[1,2], Aidyn Aitzhan[2],
Arash G. Nouri[2] and Peyman Givi[2]

[1] Center for Research Computing,
University of Pittsburgh, Pittsburgh, PA

[2] Department of Mechanical Engineering and Materials Science,
University of Pittsburgh, Pittsburgh, PA

O’Brien’s contributions

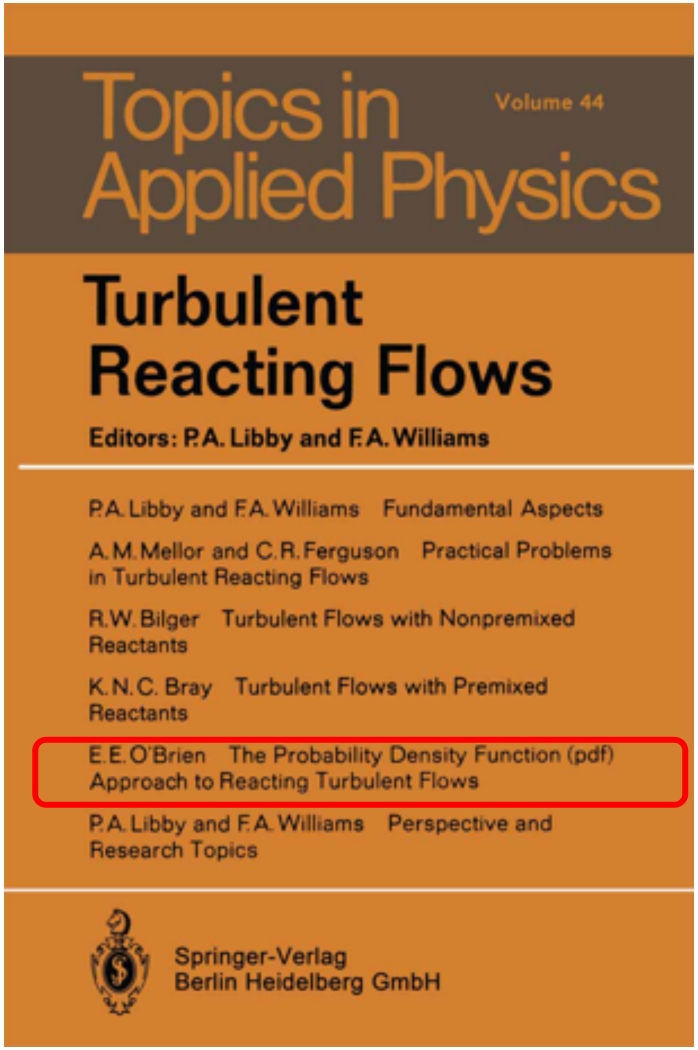

Topics in Applied Physics Volume 44

Turbulent Reacting Flows

Editors: P.A. Libby and F.A. Williams

P.A. Libby and F.A. Williams Fundamental Aspects

A.M. Mellor and C.R. Ferguson Practical Problems in Turbulent Reacting Flows

R.W. Bilger Turbulent Flows with Nonpremixed Reactants

K.N.C. Bray Turbulent Flows with Premixed Reactants

E.E. O'Brien The Probability Density Function (pdf) Approach to Reacting Turbulent Flows

P.A. Libby and F.A. Williams Perspective and Research Topics

Springer-Verlag Berlin Heidelberg GmbH

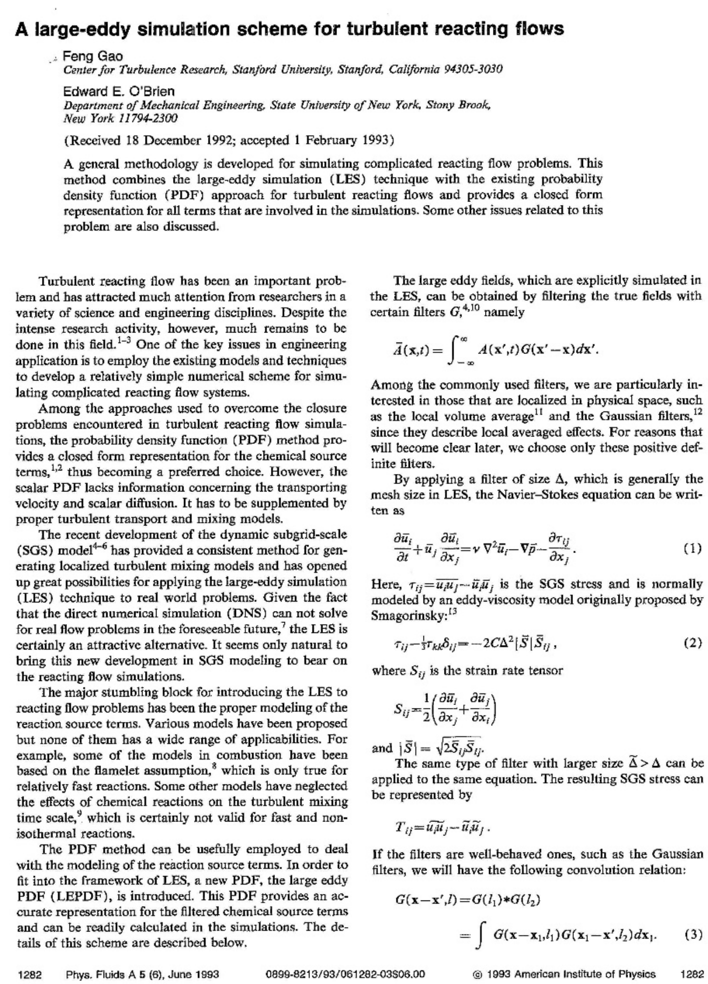

A large-eddy simulation scheme for turbulent reacting flows

Feng Gao
Center for Turbulence Research, Stanford University, Stanford, California 94305-3030

Edward E. O'Brien
Department of Mechanical Engineering, State University of New York, Stony Brook, New York 11794-2300

(Received 18 December 1992; accepted 1 February 1993)

A general methodology is developed for simulating complicated reacting flow problems. This method combines the large-eddy simulation (LES) technique with the existing probability density function (PDF) approach for turbulent reacting flows and provides a closed form representation for all terms that are involved in the simulations. Some other issues related to this problem are also discussed.

Turbulent reacting flow has been an important problem and has attracted much attention from researchers in a variety of science and engineering disciplines. Despite the intense research activity, however, much remains to be done in this field.[1–3] One of the key issues in engineering application is to employ the existing models and techniques to develop a relatively simple numerical scheme for simulating complicated reacting flow systems.

Among the approaches used to overcome the closure problems encountered in turbulent reacting flow simulations, the probability density function (PDF) method provides a closed form representation for the chemical source terms,[1,2] thus becoming a preferred choice. However, the scalar PDF lacks information concerning the transporting velocity and scalar diffusion. It has to be supplemented by proper turbulent transport and mixing models.

The recent development of the dynamic subgrid-scale (SGS) model[4–6] has provided a consistent method for generating localized turbulent mixing models and has opened up great possibilities for applying the large-eddy simulation (LES) technique to real world problems. Given the fact that the direct numerical simulation (DNS) can not solve for real flow problems in the foreseeable future,[7] the LES is certainly an attractive alternative. It seems only natural to bring this new development in SGS modeling to bear on the reacting flow simulations.

The major stumbling block for introducing the LES to reacting flow problems has been the proper modeling of the reaction source terms. Various models have been proposed but none of them has a wide range of applicabilities. For example, some of the models in combustion have been based on the flamelet assumption,[8] which is only true for relatively fast reactions. Some other models have neglected the effects of chemical reactions on the turbulent mixing time scale,[9] which is certainly not valid for fast and non-isothermal reactions.

The PDF method can be usefully employed to deal with the modeling of the reaction source terms. In order to fit into the framework of LES, a new PDF, the large eddy PDF (LEPDF), is introduced. This PDF provides an accurate representation for the filtered chemical source terms and can be readily calculated in the simulations. The details of this scheme are described below.

The large eddy fields, which are explicitly simulated in the LES, can be obtained by filtering the true fields with certain filters G,[4,10] namely

$$\bar{A}(\mathbf{x},t)=\int_{-\infty}^{\infty} A(\mathbf{x}',t)G(\mathbf{x}'-\mathbf{x})d\mathbf{x}'.$$

Among the commonly used filters, we are particularly interested in those that are localized in physical space, such as the local volume average[11] and the Gaussian filters,[12] since they describe local averaged effects. For reasons that will become clear later, we choose only these positive definite filters.

By applying a filter of size Δ, which is generally the mesh size in LES, the Navier–Stokes equation can be written as

$$\frac{\partial \bar{u}_i}{\partial t}+\bar{u}_j\frac{\partial \bar{u}_i}{\partial x_j}=\nu\nabla^2\bar{u}_i-\nabla\bar{p}-\frac{\partial \tau_{ij}}{\partial x_j}. \qquad (1)$$

Here, $\tau_{ij}=\overline{u_iu_j}-\bar{u}_i\bar{u}_j$ is the SGS stress and is normally modeled by an eddy-viscosity model originally proposed by Smagorinsky:[13]

$$\tau_{ij}-\tfrac{1}{3}\tau_{kk}\delta_{ij}=-2C\Delta^2|\bar{S}|\bar{S}_{ij}, \qquad (2)$$

where S_{ij} is the strain rate tensor

$$S_{ij}=\frac{1}{2}\left(\frac{\partial \bar{u}_i}{\partial x_j}+\frac{\partial \bar{u}_j}{\partial x_i}\right)$$

and $|\bar{S}|=\sqrt{2\bar{S}_{ij}\bar{S}_{ij}}$.

The same type of filter with larger size $\tilde{\Delta}>\Delta$ can be applied to the same equation. The resulting SGS stress can be represented by

$$T_{ij}=\widetilde{\bar{u}_i\bar{u}_j}-\tilde{\bar{u}}_i\tilde{\bar{u}}_j.$$

If the filters are well-behaved ones, such as the Gaussian filters, we will have the following convolution relation:

$$G(\mathbf{x}-\mathbf{x}',l)=G(l_1)*G(l_2)$$
$$=\int G(\mathbf{x}-\mathbf{x}_1,l_1)G(\mathbf{x}_1-\mathbf{x}',l_2)d\mathbf{x}_1. \qquad (3)$$

 0899-8213/93/061282-03S06.00

Outline

- Sensitivity analysis of LES and DNS of a 3D temporally developing mixing layer (basic research)
- Simulation of Volvo test case (applied research)

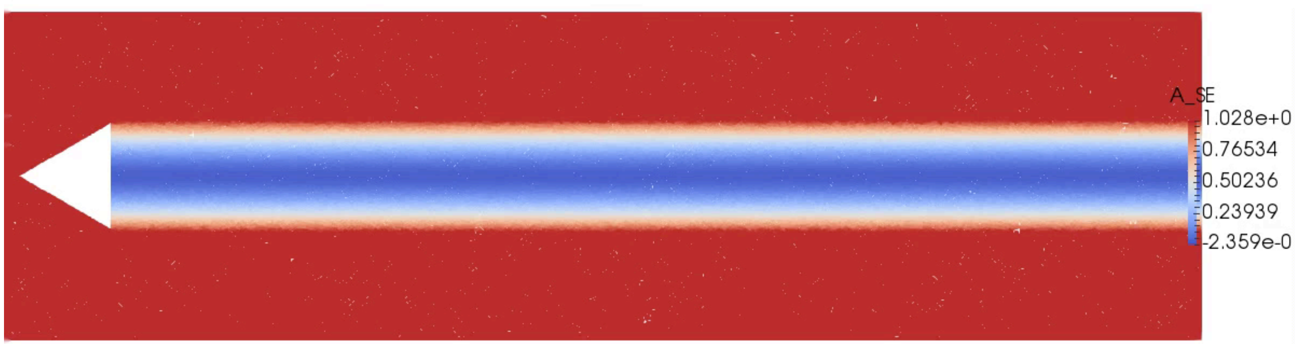

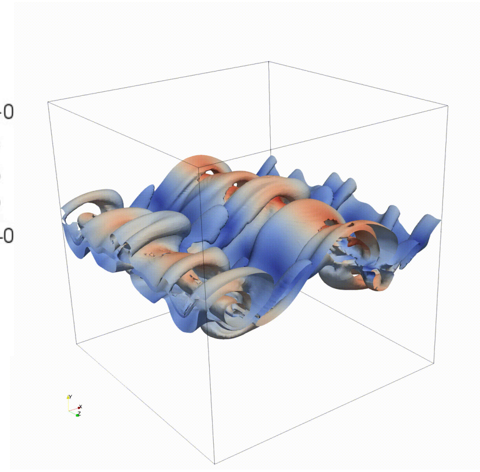

Filtered transport equations

- Filtering

$$\langle Q(\mathbf{x},t)\rangle_\ell = \int_{-\infty}^{+\infty} Q(\mathbf{x}',t)G(\mathbf{x}',\mathbf{x})d\mathbf{x}' \qquad \langle Q(\mathbf{x},t)\rangle_L = \langle \rho Q\rangle_\ell / \langle \rho\rangle_\ell$$

$$\frac{\partial \langle\rho\rangle_\ell}{\partial t} + \frac{\partial \langle\rho\rangle_\ell \langle u_j\rangle_L}{\partial x_j} = 0$$

$$\frac{\partial \langle\rho\rangle_\ell \langle u_i\rangle_L}{\partial t} + \frac{\partial \langle\rho\rangle_\ell \langle u_j\rangle_L \langle u_i\rangle_L}{\partial x_j} = -\frac{\partial \langle p\rangle_\ell}{\partial x_i} + \frac{\partial \langle\tau_{ij}\rangle_\ell}{\partial x_j} - \frac{\partial \Sigma_{ij}}{\partial x_j}$$

$$\frac{\partial \langle\rho\rangle_\ell \langle \phi_\alpha\rangle_L}{\partial t} + \frac{\partial \langle\rho\rangle_\ell \langle u_j\rangle_L \langle \phi_\alpha\rangle_L}{\partial x_j} = \frac{\partial}{\partial x_j}\left(\left\langle \gamma \frac{\partial \phi_\alpha}{\partial x_j}\right\rangle_\ell\right) - \frac{\partial M_j^\alpha}{\partial x_j}$$

<u>SGS stress</u> $\Sigma_{ij} = \langle\rho\rangle_\ell \left(\langle u_i u_j\rangle_L - \langle u_i\rangle_L \langle u_j\rangle_L\right)$

<u>SGS scalar flux</u> $M_j^\alpha = \langle\rho\rangle_\ell \left(\langle u_j \phi_\alpha\rangle_L - \langle u_j\rangle_L \langle \phi_\alpha\rangle_L\right)$

Scalar-FDF SGS closure

- Modeled (Fokker-Plank)

$$\frac{\partial F}{\partial t} + \frac{\partial \left(\langle u_j \rangle_L F \right)}{\partial x_j} = \frac{\partial}{\partial x_j} \left[(\gamma + \gamma_t) \frac{\partial \left(F / \langle \rho \rangle_l \right)}{\partial x_j} \right] + \frac{\partial}{\partial \psi_k} \left[\Omega_m F \left(\psi_k - \langle \phi_k \rangle_L \right) \right]$$

- SGS energy

$$\frac{\partial (\langle \rho \rangle_\ell \tau_{\alpha\alpha})}{\partial t} + \frac{\partial [\langle \rho \rangle_\ell \langle u_j \rangle_L \tau_{\alpha\alpha}]}{\partial x_j} = \frac{\partial}{\partial x_j} \left[(\gamma + \gamma_t) \frac{\partial \tau_{\alpha\alpha}}{\partial x_j} \right] + 2(\gamma + \gamma_t) \left[\frac{\partial (\langle \phi_\alpha \rangle_L)}{\partial x_j} \frac{\partial (\langle \phi_\alpha \rangle_L)}{\partial x_j} \right] - 2\Omega_m \langle \rho \rangle_\ell \tau_{\alpha\alpha}$$

Modeled FDF transport equation

- Stochastic differential equation

$$
\begin{aligned}
dX_i &= \left[\langle u_i\rangle_L + \frac{1}{\langle\rho\rangle_l}\frac{\partial}{\partial x_i}(\gamma+\gamma_t)\right]dt + \sqrt{\frac{2(\gamma+\gamma_t)}{\langle\rho\rangle_l}}dW_i \\
d\psi_k &= -\Omega_m\left(\psi_k - \langle\phi_k\rangle_L\right)dt + S_k(\boldsymbol{\psi})\,dt
\end{aligned}
$$

- Fokker-Plank equation (Modelled FDF)

$$
\begin{aligned}
\frac{\partial F}{\partial t} + \frac{\partial\left(\langle u_j\rangle_L F\right)}{\partial x_j} &= \frac{\partial}{\partial x_j}\left[(\gamma+\gamma_t)\frac{\partial\left(F/\langle\rho\rangle_l\right)}{\partial x_j}\right] + \frac{\partial}{\partial\psi_k}\left[\Omega_m F\left(\psi_k - \langle\phi_k\rangle_L\right)\right] \\
&\quad - \frac{\partial S_k(\boldsymbol{\psi})F}{\partial\psi_k}
\end{aligned}
$$

Spectral methodology

- Discontinuous elements in space.
- Using basis Functions to approximate solution.
- Finite element method using Riemann solver for fluxes.

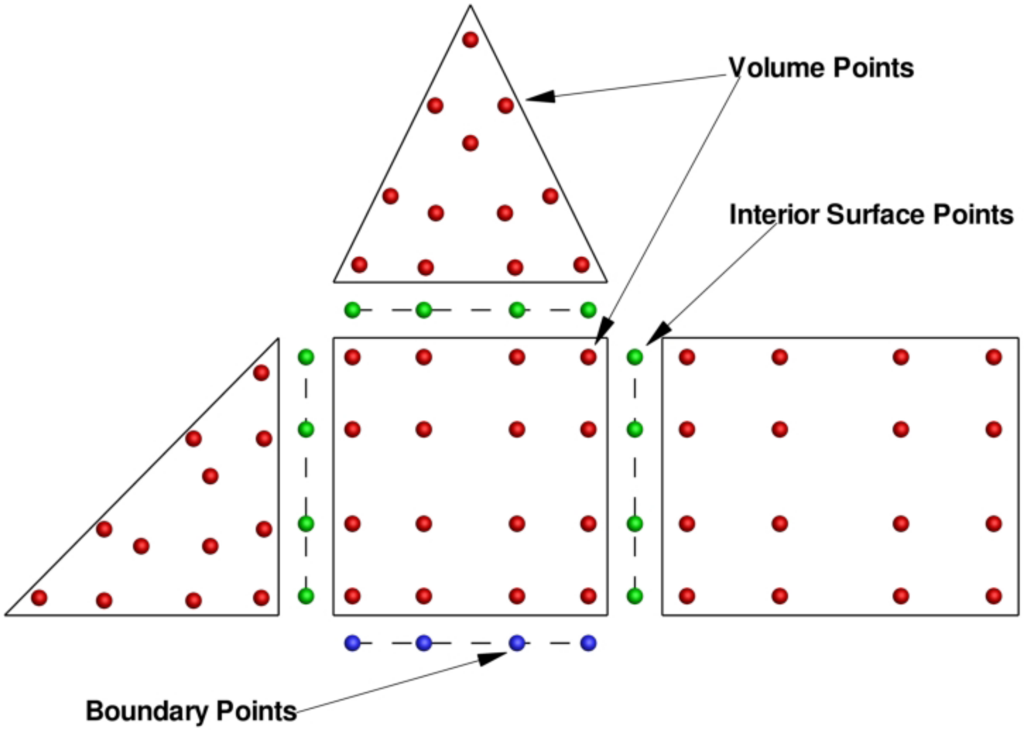

$$U_{app} = \sum_{j=1}^{s} a_j \mathcal{L}_{j,app}$$

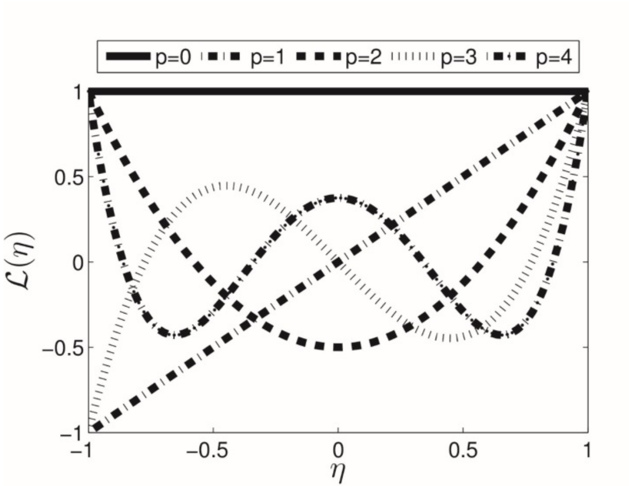

Spectral solver capabilities

- Hybrid mixed element unstructured meshes (tetrahedra, prisms, pyramids, and hexahedra)
- p-enrichment and h-refinement
- Curved mesh

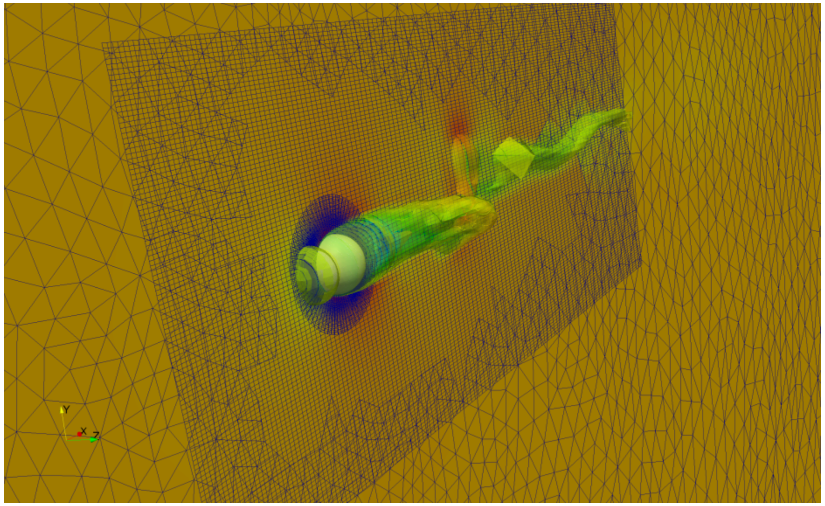

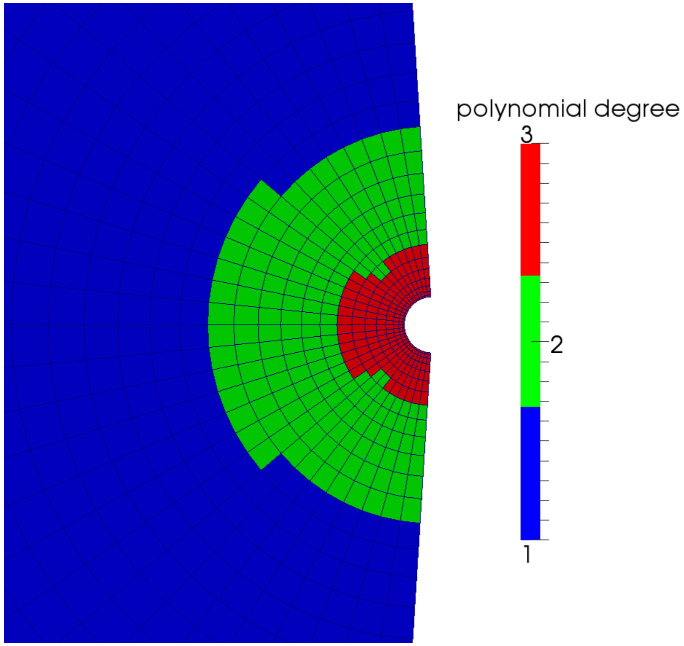

Spectral-FDF simulator

- Lagrangian Monte Carlo elements on Eulerian grids.

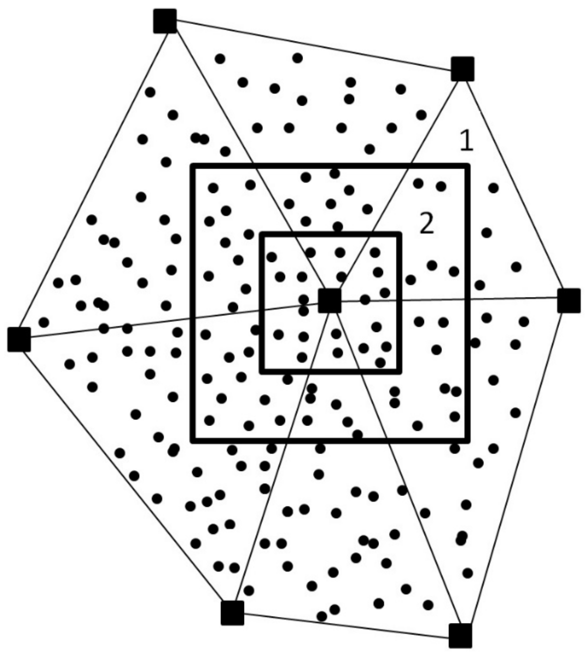

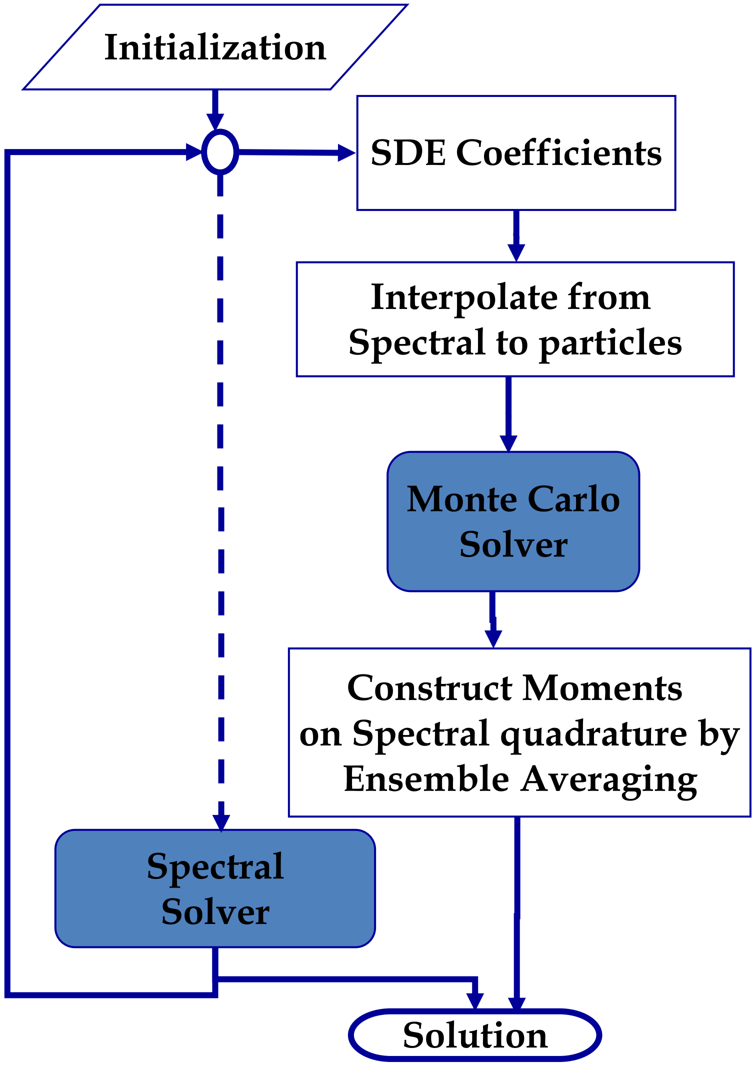

Mixing layer - Numerical procedure

- 1 DNS case
  - h=1/256
  - p=5
- 12 LES cases
  - h=1/128, 1/64, 1/32 and 1/16
  - Δ=1/32
  - p=3, 4 and 5
- Construct the L_2 norm error of subgrid scale energy (τ), resolved energy (R) and total energy (r).

Mixing layer - Reynolds stresses

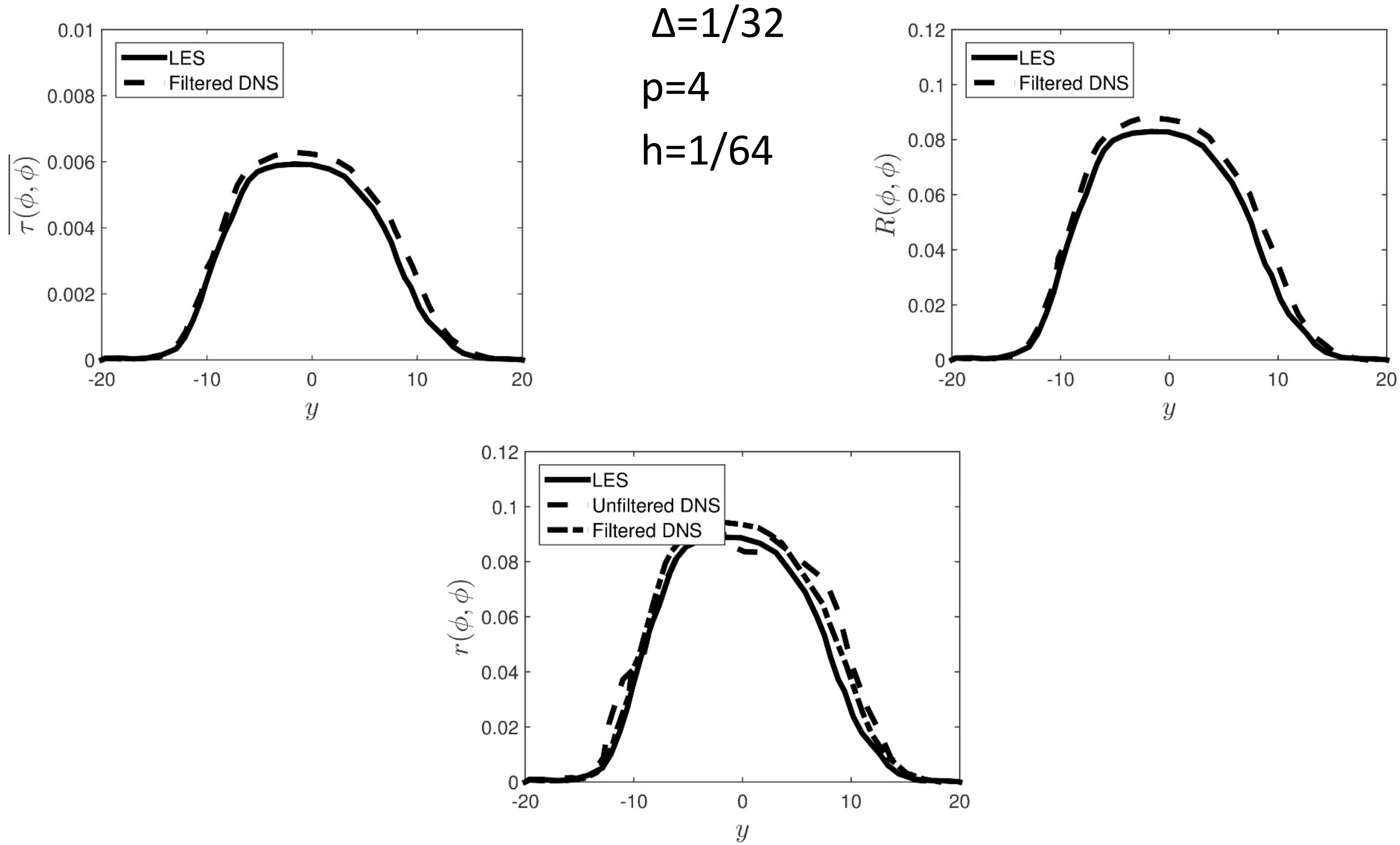

Mixing layer – h- & p- refinements

Δ=1/32

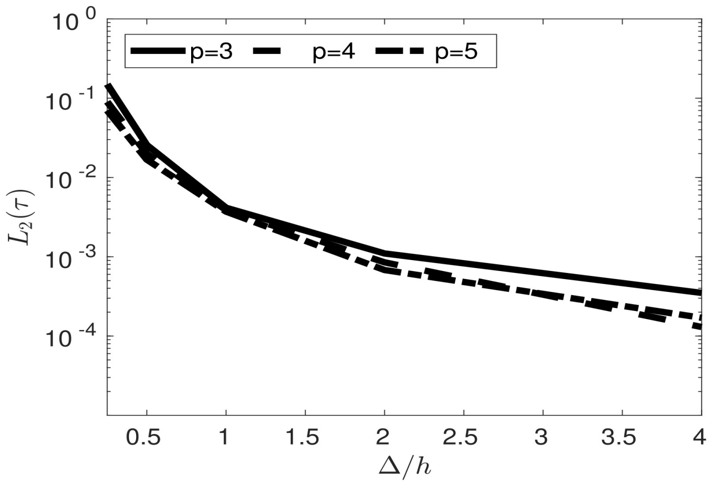

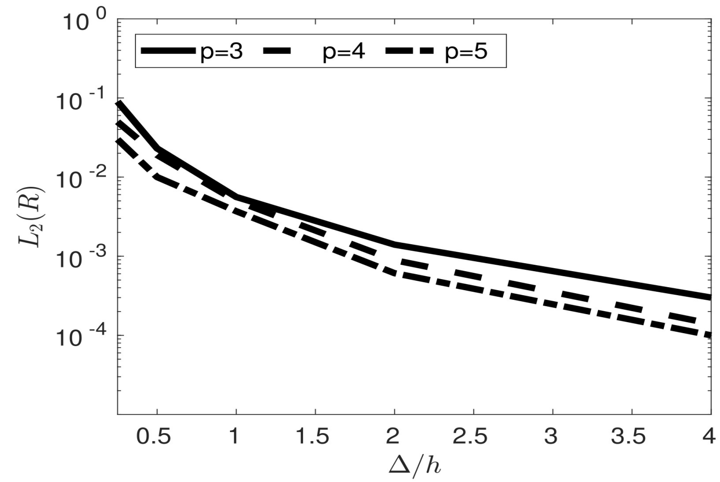

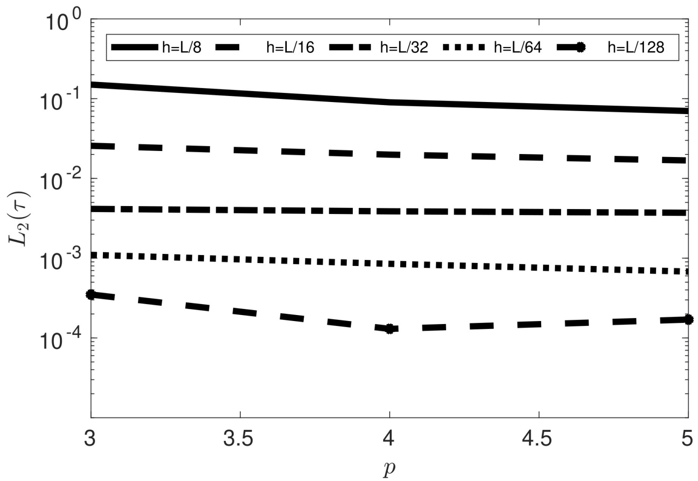

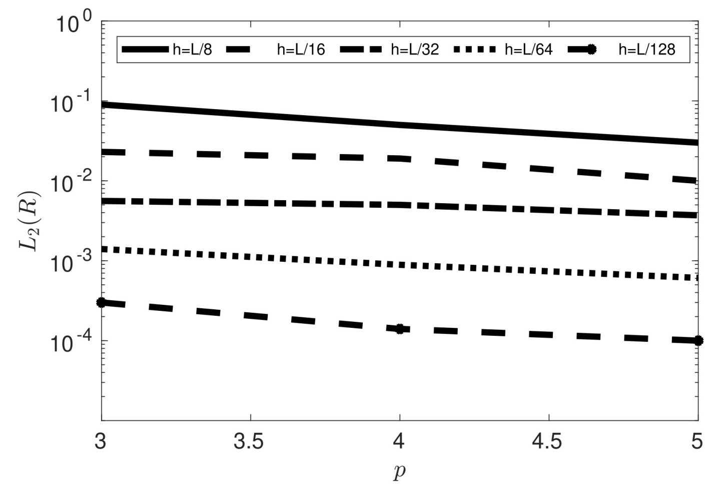

Volvo test case - Configuration

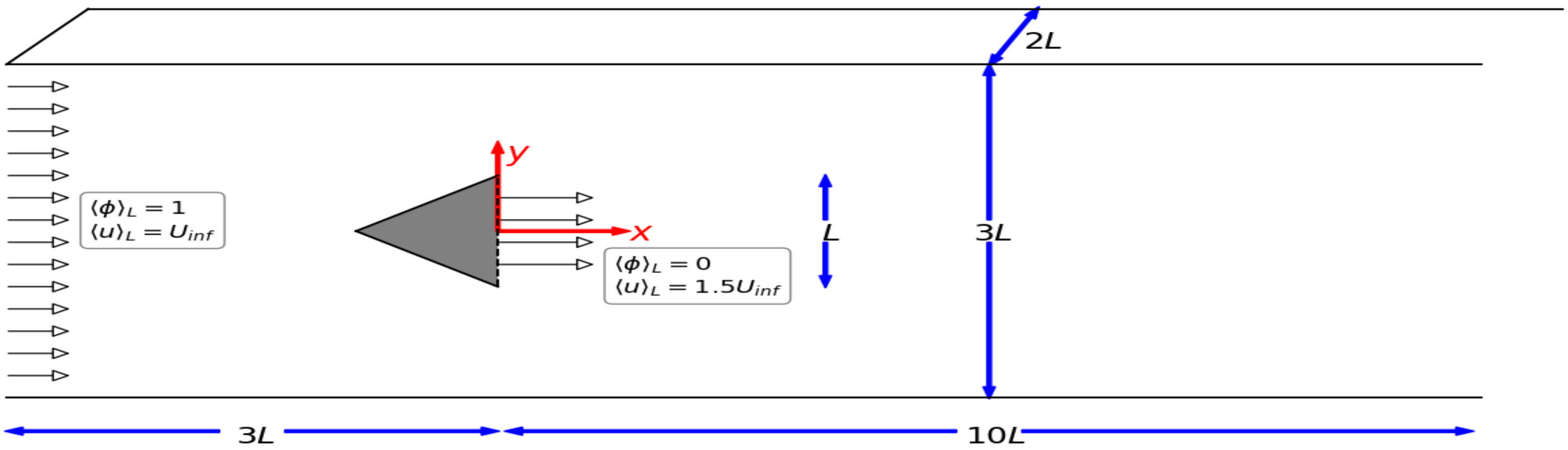

Volvo test case – Mesh & contour plot

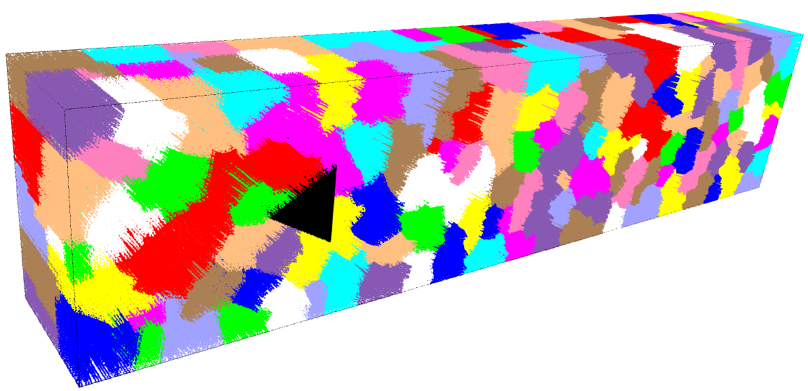

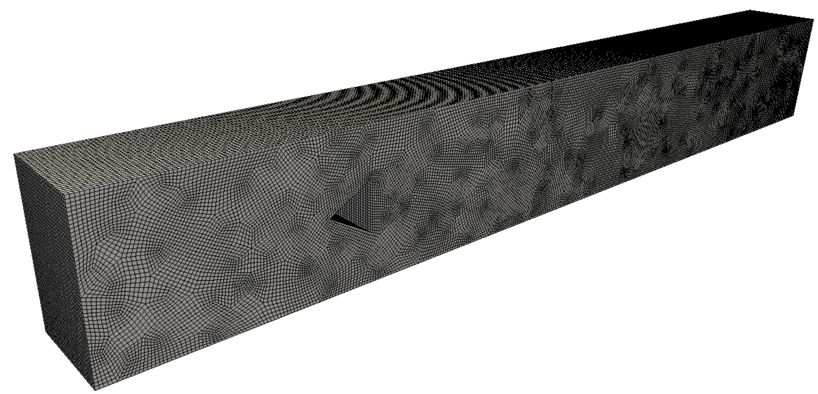

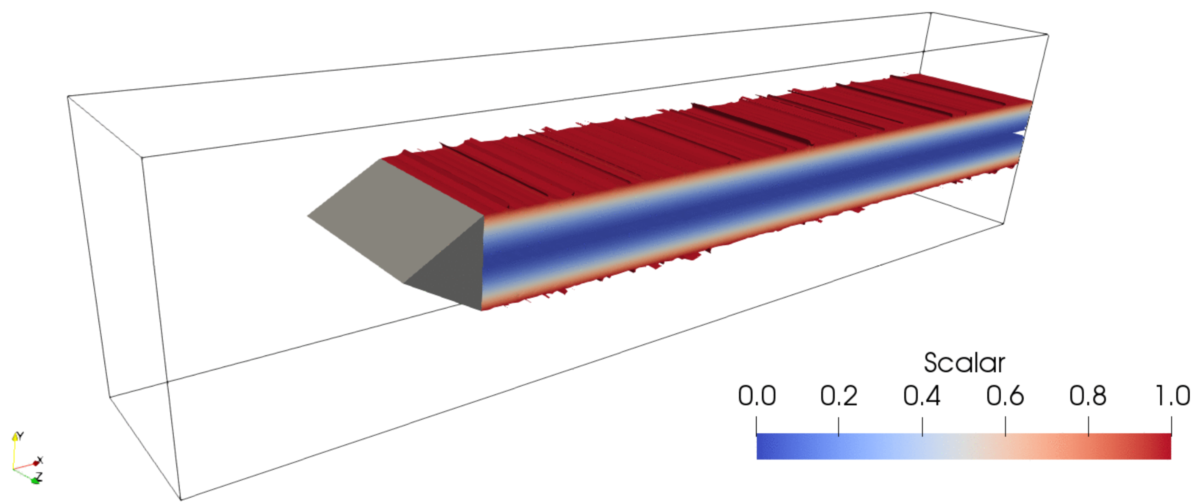

Volvo test case – Reynolds stresses

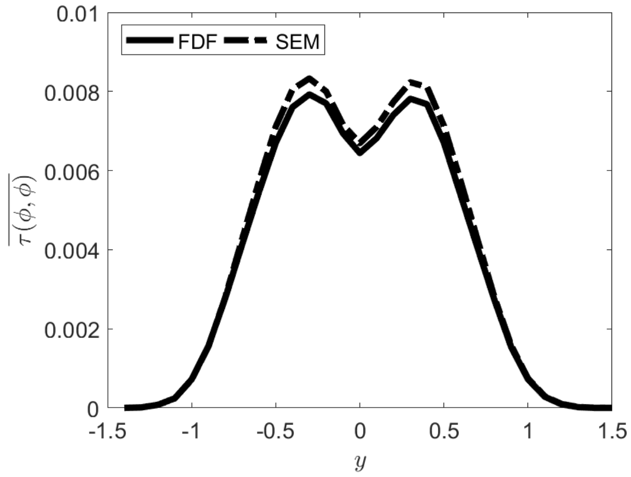

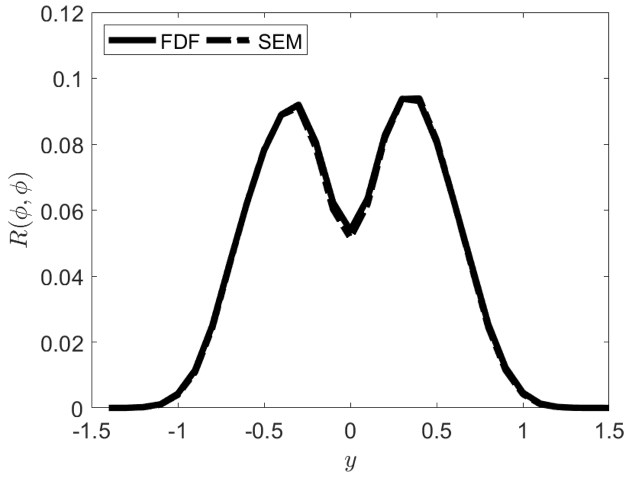

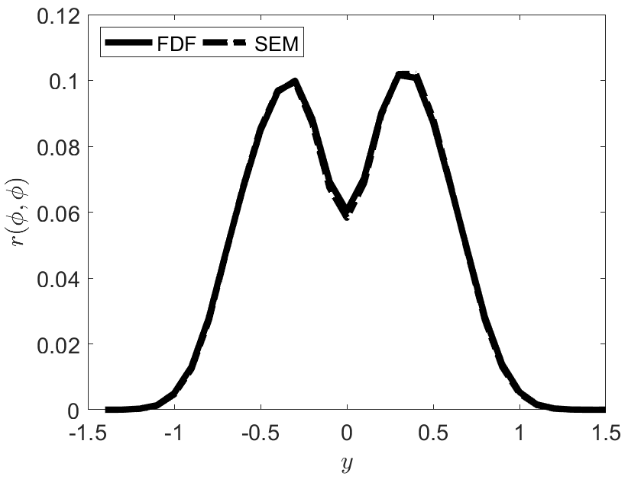

Summary

- High order FDF-LES simulator
  - Basic research
    - h-refinement
      - Similar to the p-enrichment, the LES Reynolds stresses converges to the DNS results for finer resolution.
    - p-enrichment
      - As p goes higher, the error converges to zero for all Reynolds stresses.
  - Applied research
    - FDF coupled with spectral/hp method
    - MC procedure extended for LES on arbitrary mesh

Thank you!

On Large Eddy Simulation/Filtered Density Function based Modeling of Circular Bluff Body Configurations

Ricardo Franco
Dr. Cesar Celis
Mechanical Engineering Section
Faculty of Sciences and Engineering
Pontificia Universidad Católica del Perú

DFD2019 **SEATTLE**
72nd Annual Meeting of the
American Physical Society
Division of Fluid Dynamics
November 23-26, 2019

Introduction

Smoke from forest fires covering the sky in Viña del Mar, Chile. November 16th 2019.

- Combustion is used to generate much of the heat and power we consume.
- Outdoor fine particulate matter due to air pollution, such as soot, is the fifth leading risk factor for death in the world. (Schraufnagel et al., 2019)
- Soot formation is highly problematic from an engineering and modeling perspective because of its complexity.
- It is of interest to further our understanding of soot to mitigate its negative effects but also harness its positive effects in other applications such as heat transfer.

Reacting flows and filtered density functions

- Ongoing research work on reacting flows in bluff body burner configurations including soot formation.
- Two approaches for soot formation modeling: sectional approach and method of moments (MoM).
- MoM will be initially considered because of its relatively low cost.
- As of now, LES/FDF *(Colucci et al., 1998)* is being considered as the best choice for comprehensive modeling of the combustion processes.

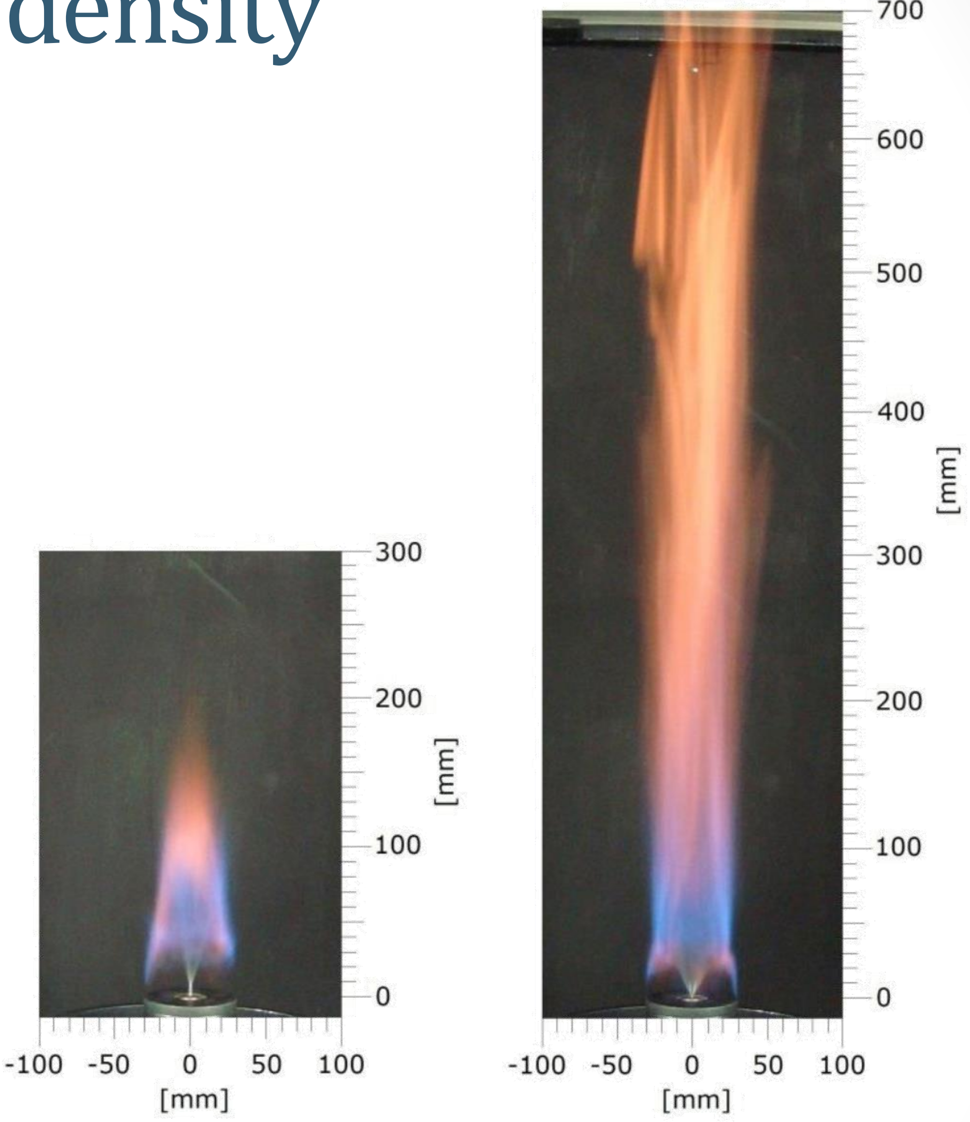

Experimental results of the reactive flow at different fuel jet speeds. *(Villanueva, J., 2013. PUC-Rio)*

Previous RANS analysis

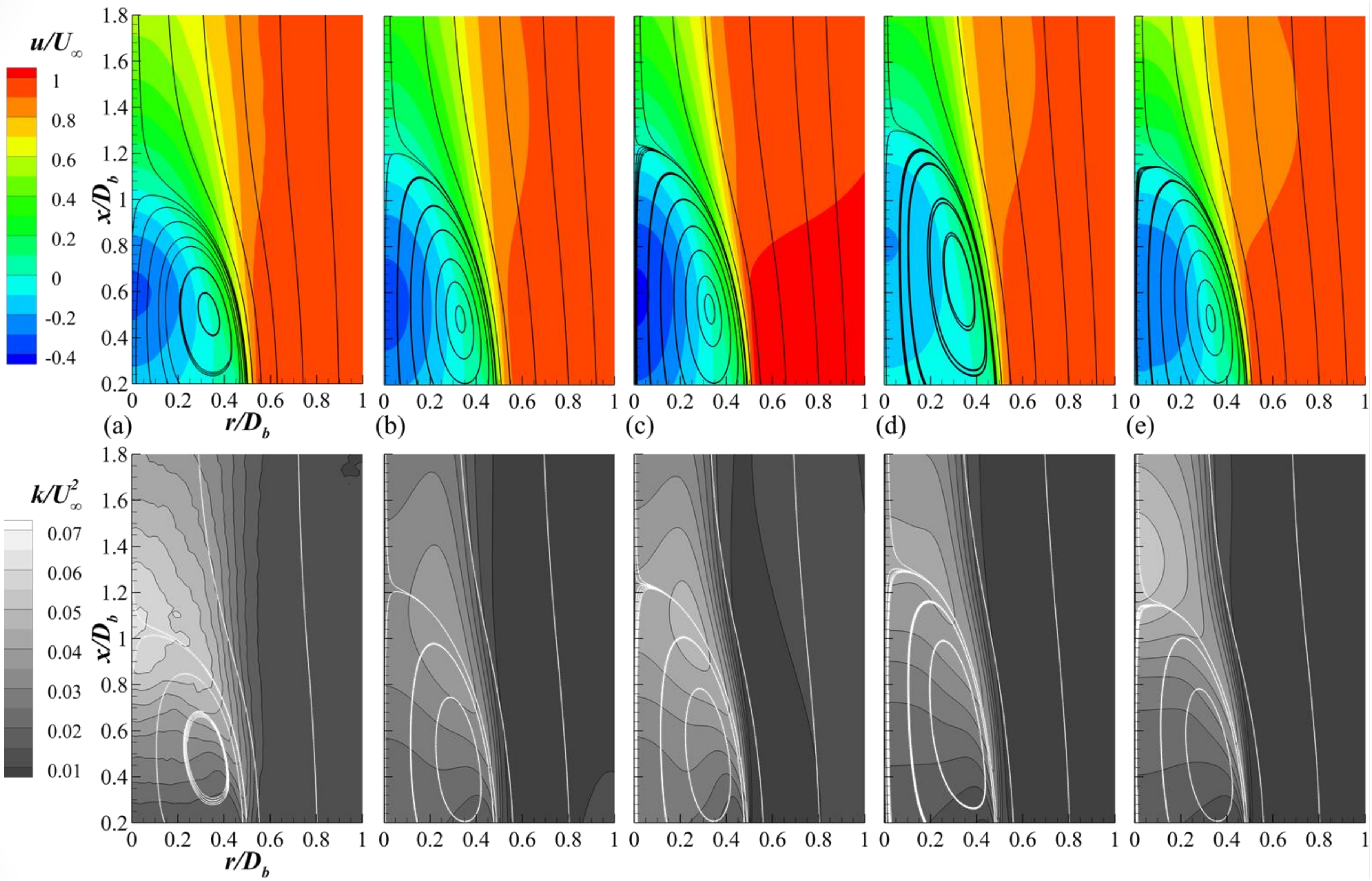

Axial velocity (Top) and TKE (bottom) contours. (a) Experimental results (b) Standard *k-ε* (c) *k-ω*SST (d) Quadratic *k-ε* (e) Cubic *k-ε*. *(Franco et al., 2019)*

Numerical modeling

- Fully scripted using *blockMesh* in OpenFOAM v1906.
- The same version of OpenFOAM was used to perform the simulations.
- Mesh displayed corresponds to preliminary low resolution cases.

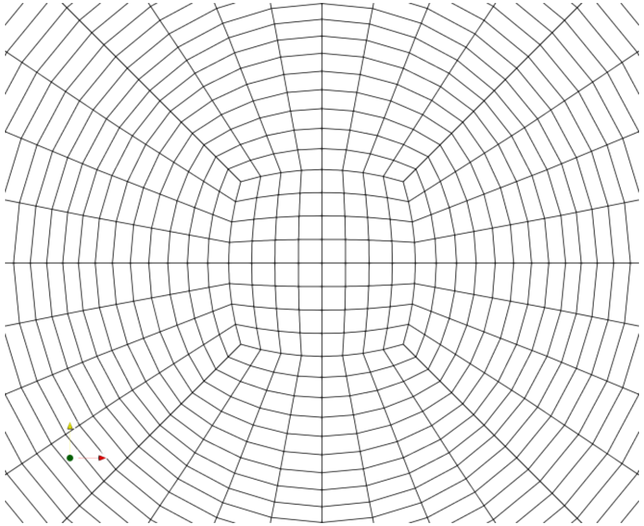

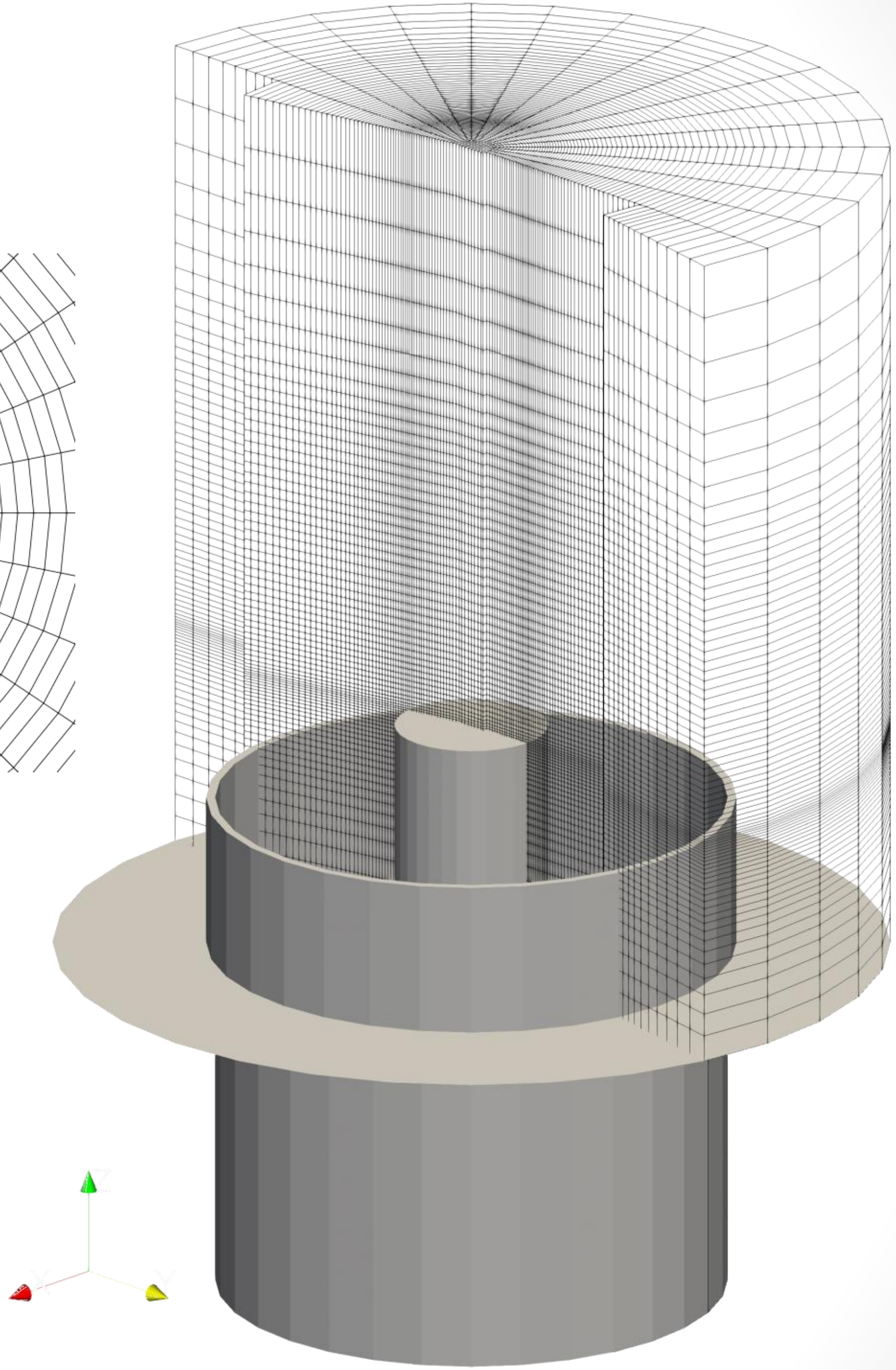

- For the inlet velocity field, a divergence free synthetic eddy method *(Poletto et al., 2013)* is used.
- SGS model: Wall adapting local Eddy-viscosity (WALE)

Preliminary VLES results

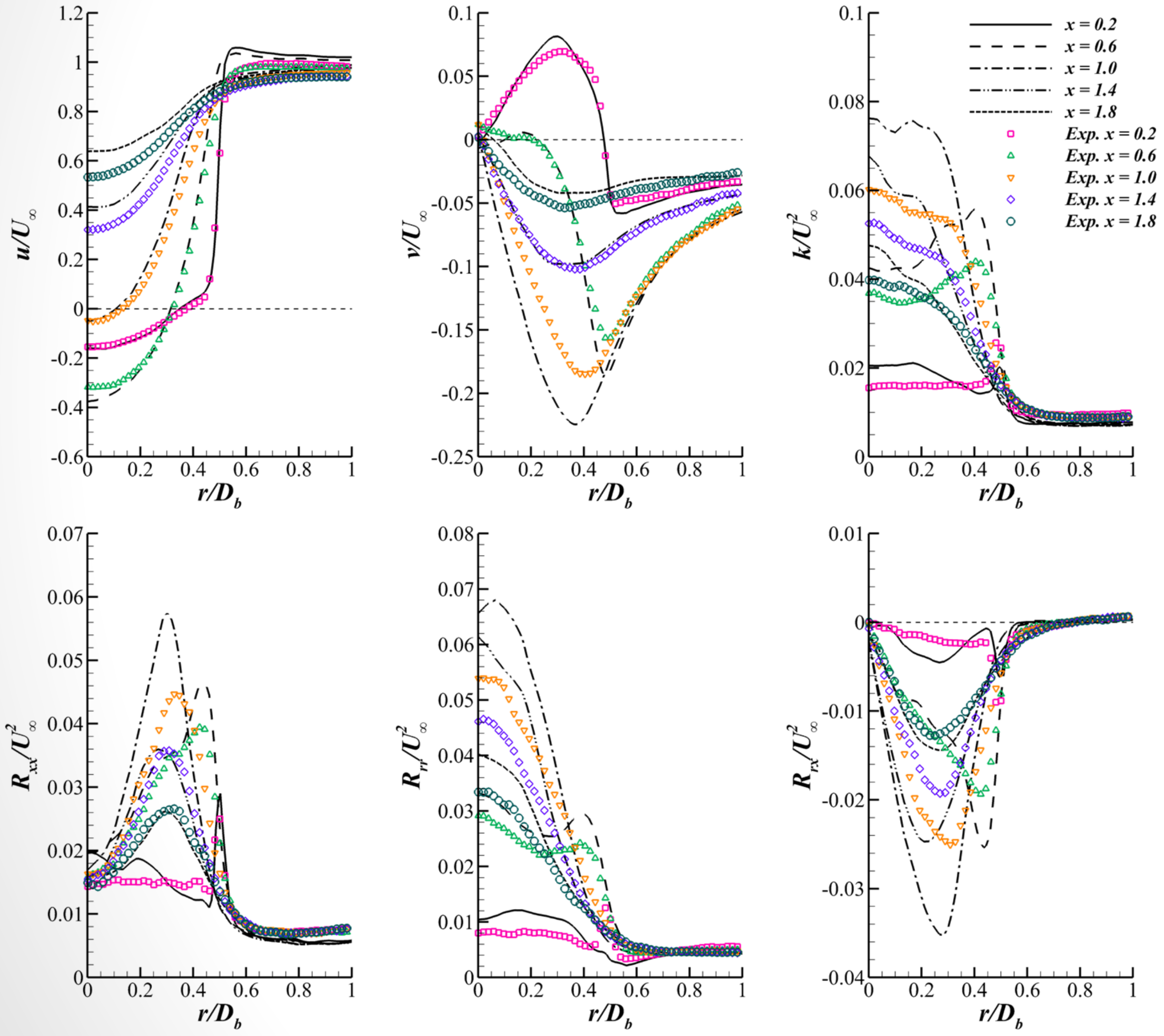

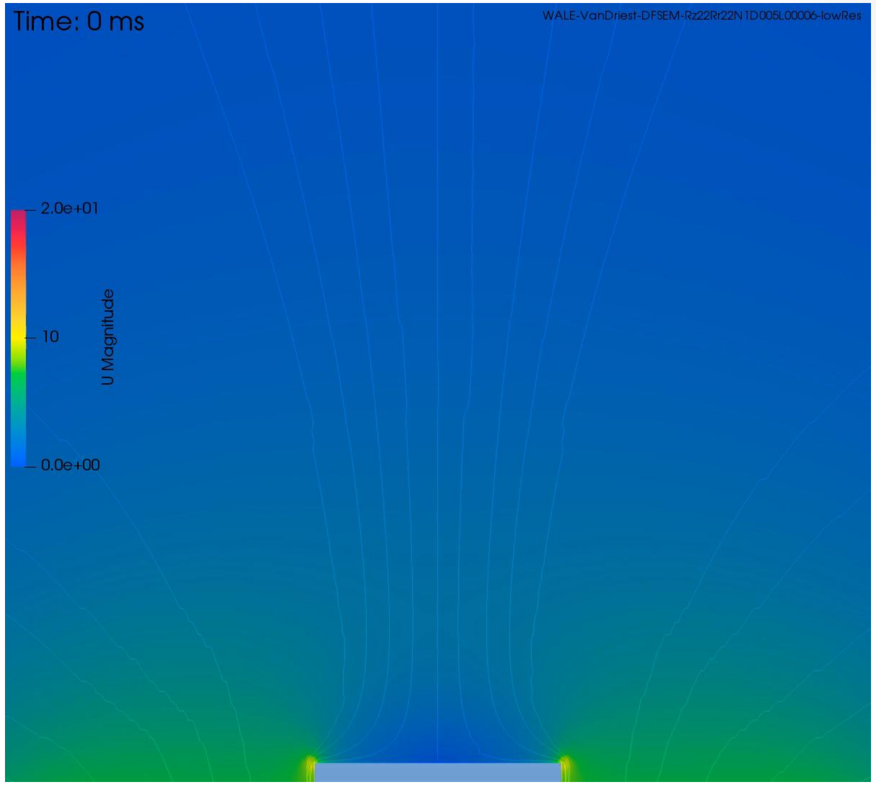

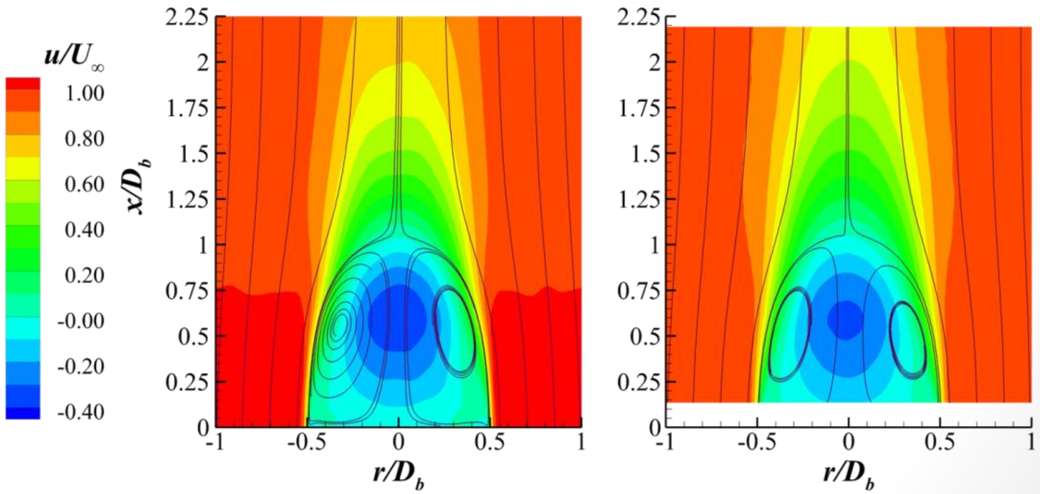

Preliminary LES results

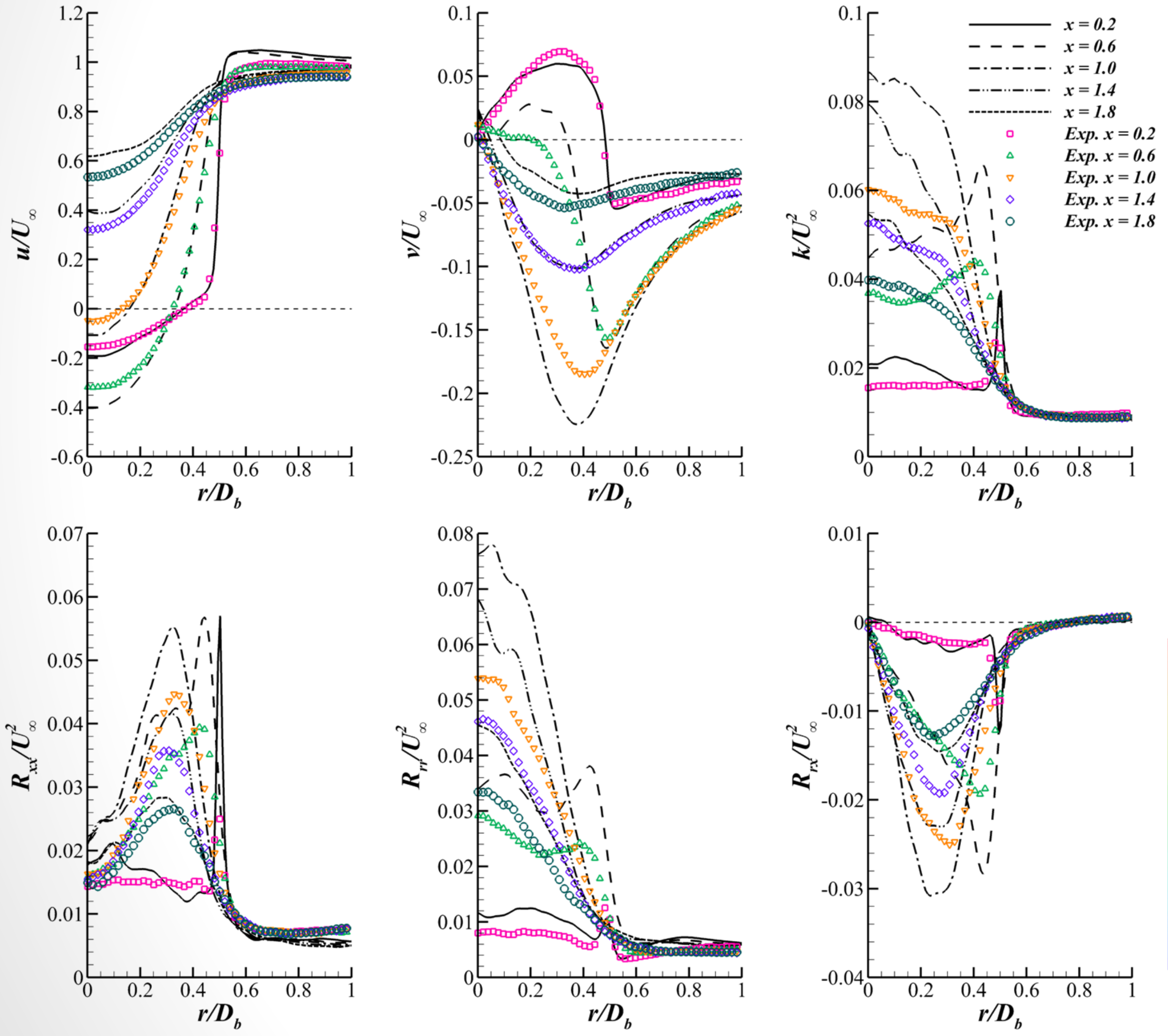

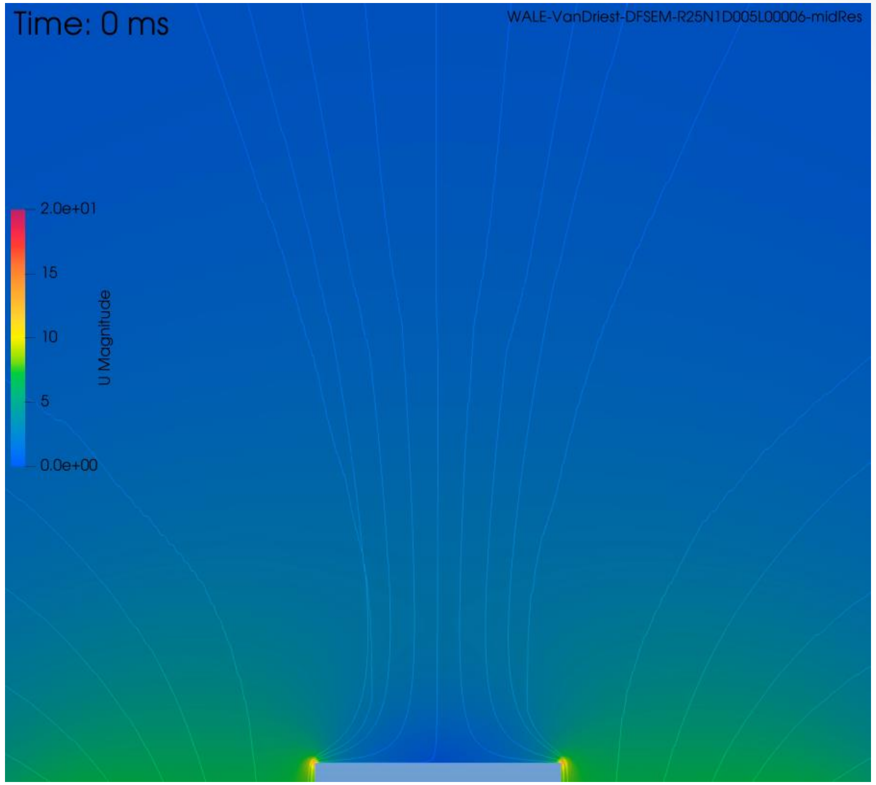

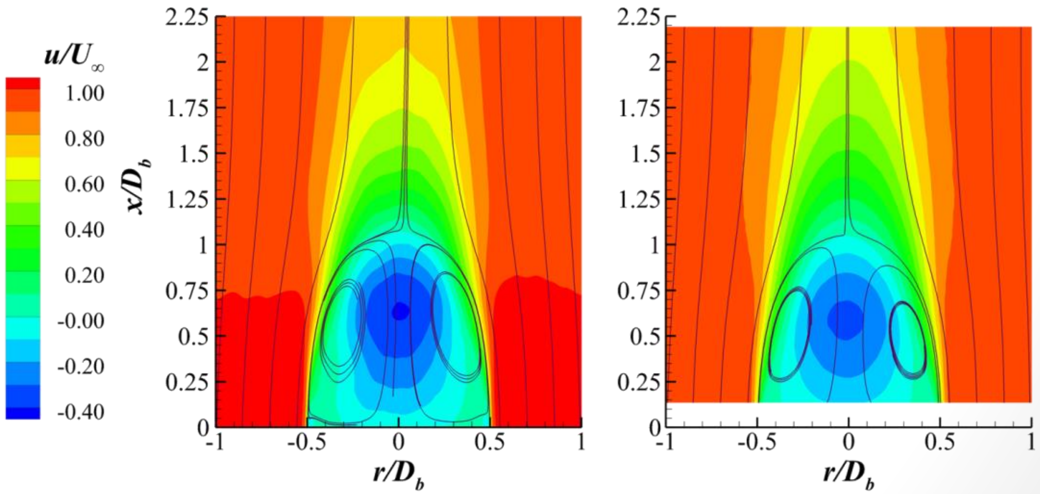

Reynolds stress components

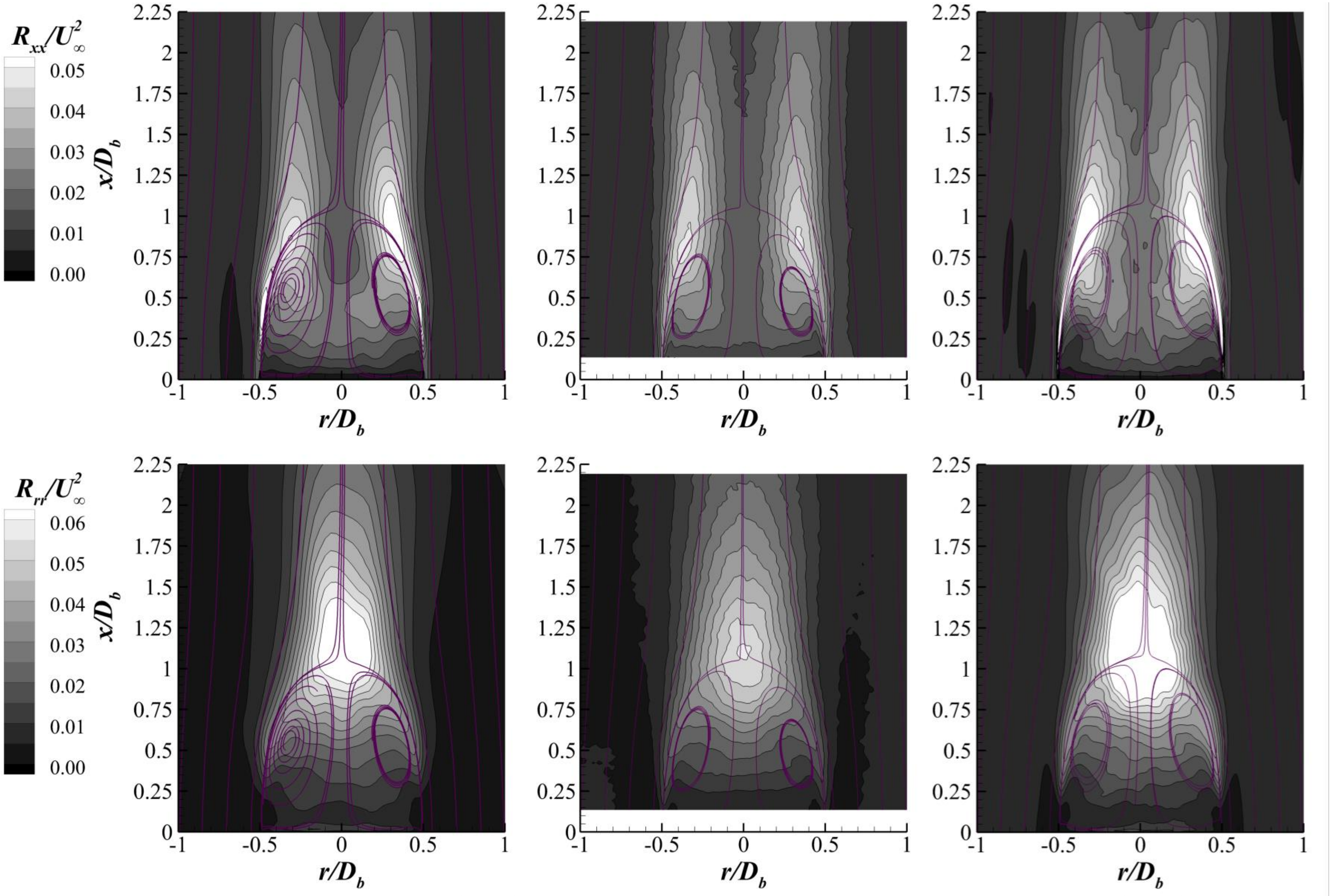

Reynolds axial stress *(Top)* and radial stress *(Bottom)* for the VLES case *(Left)*, experimental results *(Middle)* and LES case *(Right)*.

Final Remarks

- RANS models were found to be generally insufficient to correctly predict anisotropic turbulent structures, but nonlinear models did improve somewhat on linear ones.
- Preliminary LES results are promising. With little calibration of the boundary conditions, not only the turbulent structure but the overall flow structure as well resemble the experimental measurements.
- However, the turbulence itself at the wake is being greatly exaggerated by the model.
- Achieving proper turbulence levels is imperative in order to properly model the transport of chemical species and thus the reaction rates.

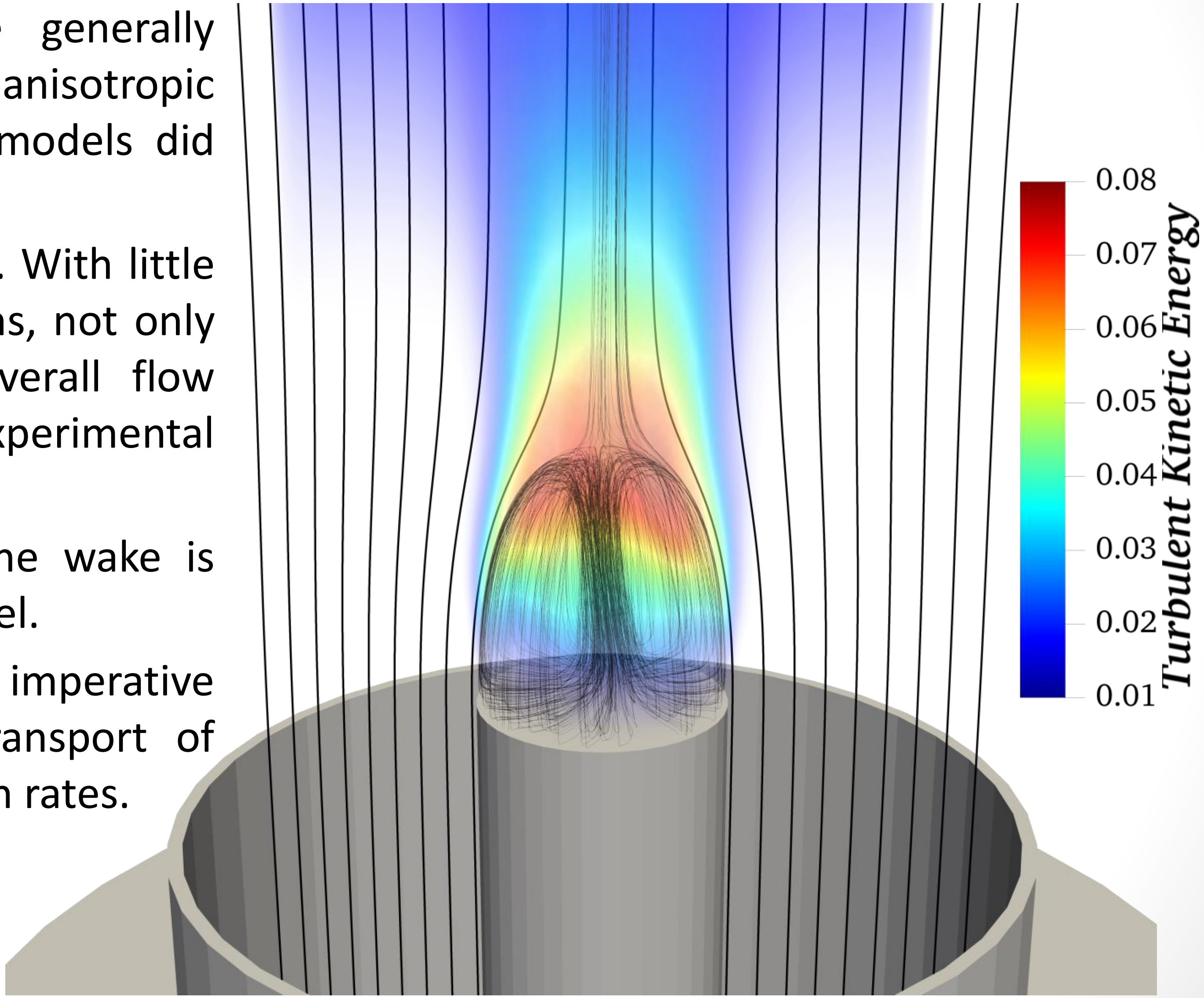

References

- Schraufnagel, D. E., Balmes, J. R., Cowl, C. T., De Matteis, S., Jung, S.-H., Mortimer, K., … Wuebbles, D. J. (2019). Air Pollution and Noncommunicable Diseases: A Review by the Forum of International Respiratory Societies 2019; Environmental Committee, Part 1: The Damaging Effects of Air Pollution. *CHEST*, *155*(2), 409–416. https://doi.org/10.1016/j.chest.2018.10.042
- Colucci, P. J., Jaberi, F. A., Givi, P., & Pope, S. B. (1998). Filtered density function for large eddy simulation of turbulent reacting flows. *Physics of Fluids*, *10*(2), 499–515. https://doi.org/10.1063/1.869537
- Cruz Villanueva, J. J., & Figueira da Silva, L. F. (2013). *Estudo experimental da combustão turbulenta de sprays de etanol usando PLIF-OH , PIV e Shadowgraphy Juan José Cruz Villanueva Estudo experimental da combustão turbulenta de sprays de etanol usando PLIF-OH , PIV e Shadowgraphy*.
- Cruz Villanueva, J. J., & Figueira da Silva, L. F. (2016). Study of the Turbulent Velocity Field in the Near Wake of a Bluff Body. *Flow, Turbulence and Combustion*, *97*(3), 715–728. https://doi.org/10.1007/s10494-016-9709-6
- Franco. R., Celis, C., & Figueira da Silva, L.F. (2019). On the suitability of RANS turbulence models for modeling circular bluff-body configurations. 25th ABCM International Congress of Mechanical Engineering.
- Lien, F. S., Chen, W. L., & Leschziner, M. A. (1996). Low-Reynolds-Number Eddy-Viscosity Modelling Based on Non-Linear Stress-Strain/Vorticity Relations. *Engineering Turbulence Modelling and Experiments*, *3*, 91–100. https://doi.org/10.1016/B978-0-444-82463-9.50015-0
- Shih, T.-H., Liou, W. W., Shabbir, A., Yang, Z., & Zhu, J. (1995). A new k-ϵ eddy viscosity model for high reynolds number turbulent flows. *Computers & Fluids*, *24*(3), 227–238. https://doi.org/https://doi.org/10.1016/0045-7930(94)00032-T
- Poletto, R., Craft, T., & Revell, A. (2013). A new divergence free synthetic eddy method for the reproduction of inlet flow conditions for les. *Flow, Turbulence and Combustion*, *91*(3), 519–539. https://doi.org/10.1007/s10494-013-9488-2

Thank you!

Molecular mixing in highly turbulent premixed flames

Xinyu Zhao, Patrick Meagher

University of Connecticut

11/24/2019

Motivation

- Mixing models are a critical component of the transported PDF method.
- Mixing forms
  - Linear mean square estimation (or IEM)
  - Modified Curl's model
  - Euclidean minimum spanning tree (EMST) model
  - Multiple mapping conditioning (MMC)
  - Shadow-position mixing model (SPMM)
- Mixing rates
  - Taylor macroscales
  - Dynamic rates
  - Hybrid models
  - Differential diffusion
- Mixing models for premixed combustion

An approach to the autoignition of a turbulent mixture

CÉSAR DOPAZO AND EDWARD E. O'BRIEN

Dept. of Mechanics, SUNY, Stony Brook, New York 11790, U.S.A.

The Joint Pdf of a Scalar and Its Gradient at a Point in a Turbulent Fluid

Direct Numerical Simulations of Reacting Flows in Homogeneous Turbulence

PDF models have been applied to complex premixed flames

Swirl # = 0.79

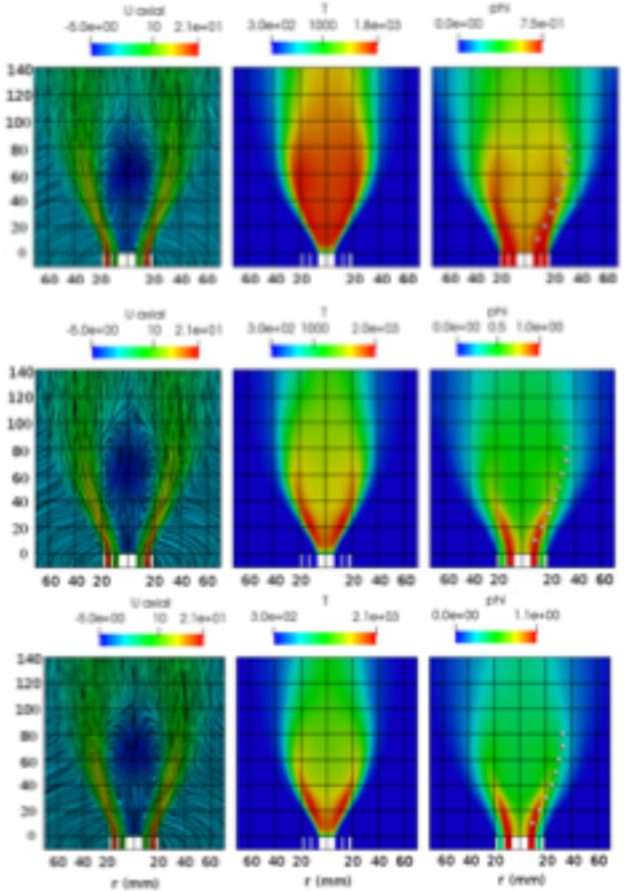

0.75/0.75

1.0/0.5

1.125/0.375

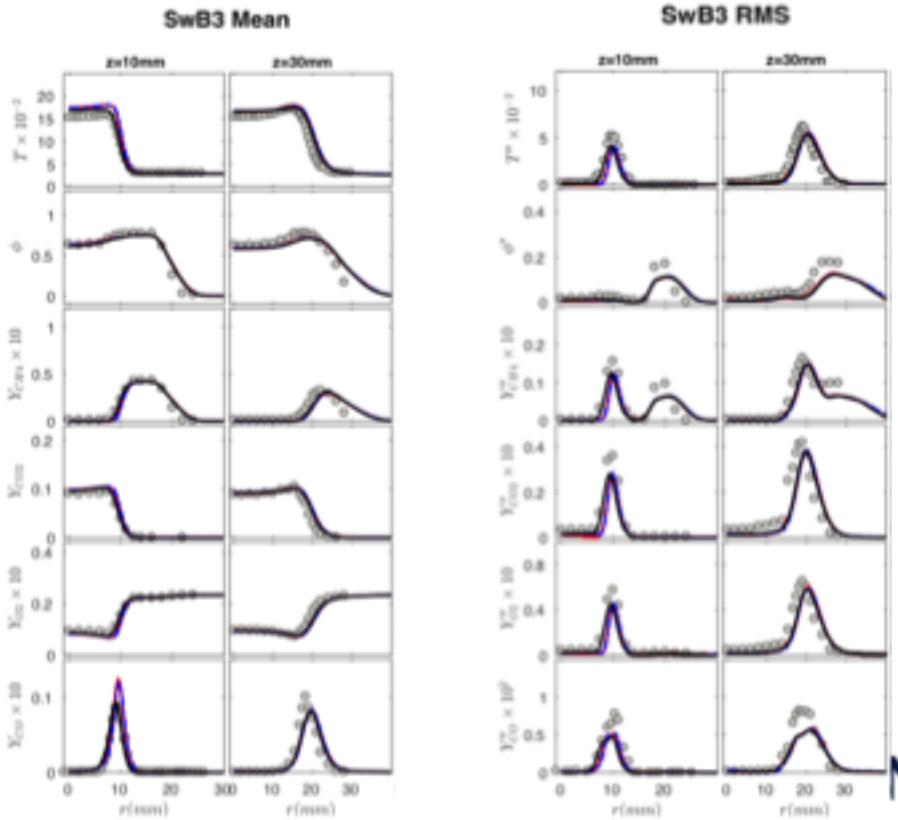

H. Turkeri, X. Zhao. In preparation. 2019

PDF models have been applied to complex premixed flames

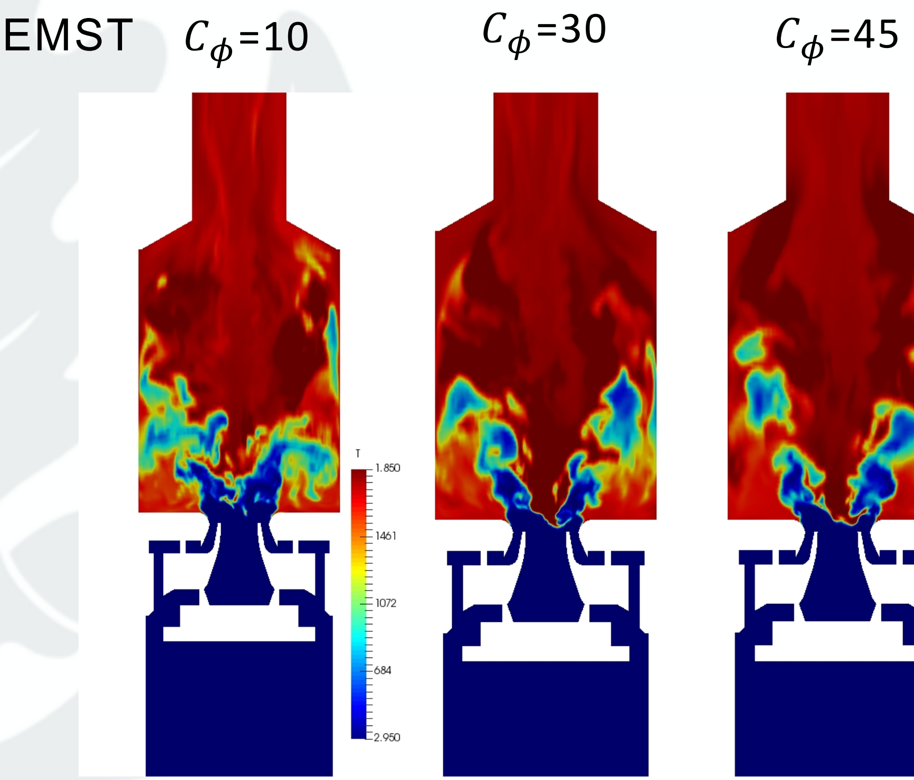

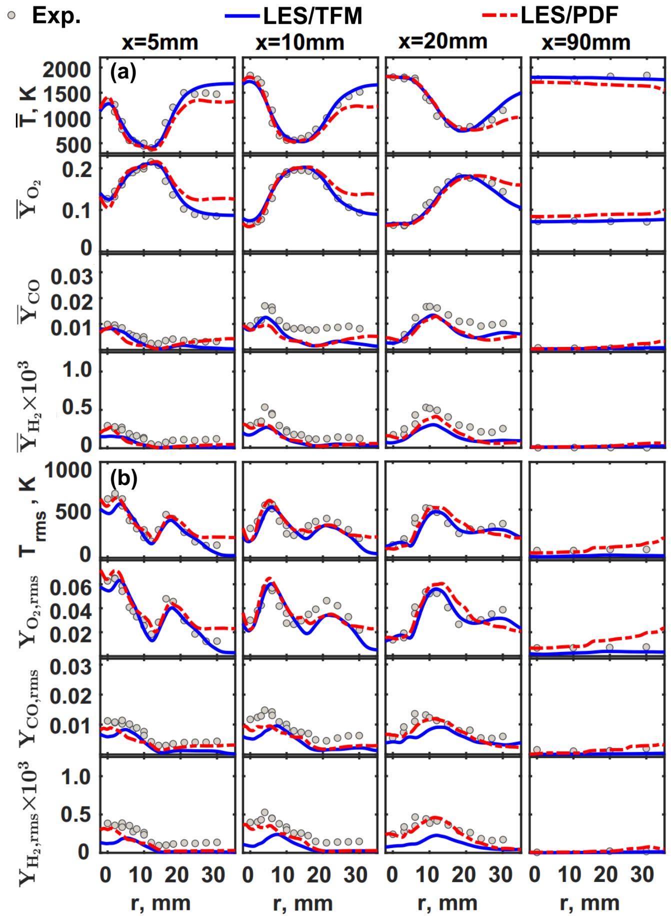

P. Zhang and X. Zhao. Under review with Proceedings of the Combustion Institute. 2019

Highly-turbulent premixed flame: transition to broken reaction zone regime

DNS databases using a 24-species reduced model for n-dodecane/air flames

$P = 30\ bar,\ \phi = 0.7,\ T_0 = 700\ K,\ Ka = 10^2, 10^3, 10^4$

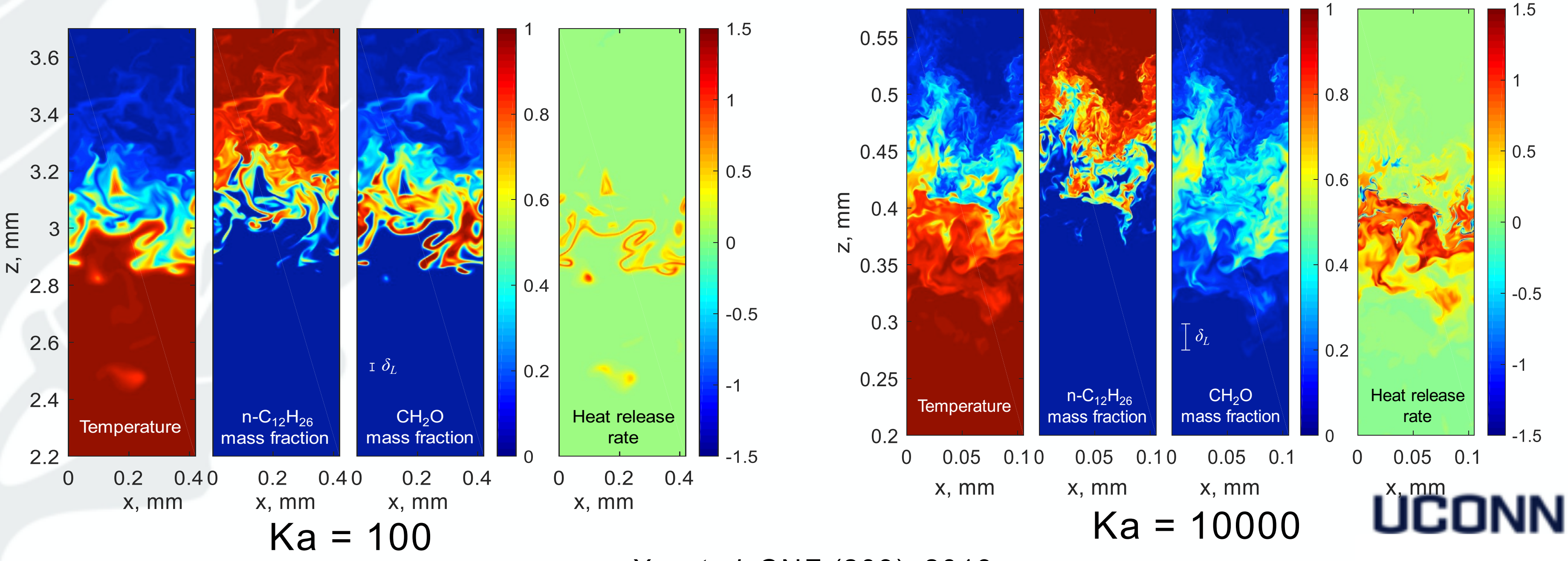

Xu *et al*, CNF (209), 2019

Mixing form: Euclidean Minimum Spanning Tree (EMST)

- Applies Prim's Algorithm to a set of points in compositional space
- Y^{i} is the mass fraction represented as a vector in $\mathbb{R}^{\mathrm{n}}$ where n is the number of species
  - ➢ $\mathrm{Y}_{\mathrm{j}}^{\mathrm{i}}$ is the mass fraction for the jth species at the i^{th} test point
  - ➢ $L^{(i,j)} = \left\|Y^{i} - Y^{j}\right\|$ is the Euclidian distance between test points i and j in the $\mathbb{R}^{\mathrm{n}}$ compositional space (edge length)
- Algorithm selects node pairs to generate tree with shortest total **edge length**
- Currently uses a fixed root node to reduce computational costs

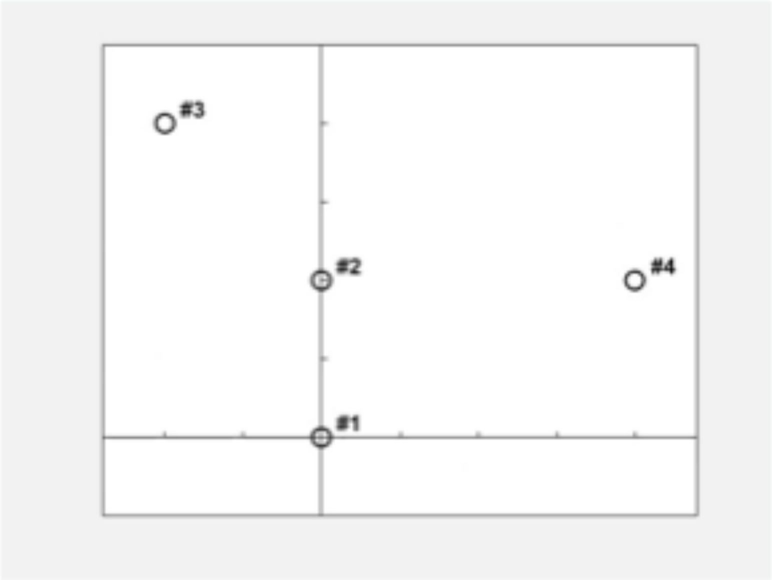

Z. Ren, S. Subramaniam & S.B. Pope (2002)

UCONN

Mixing form: EMST for laminar premixed flames

Without normalization

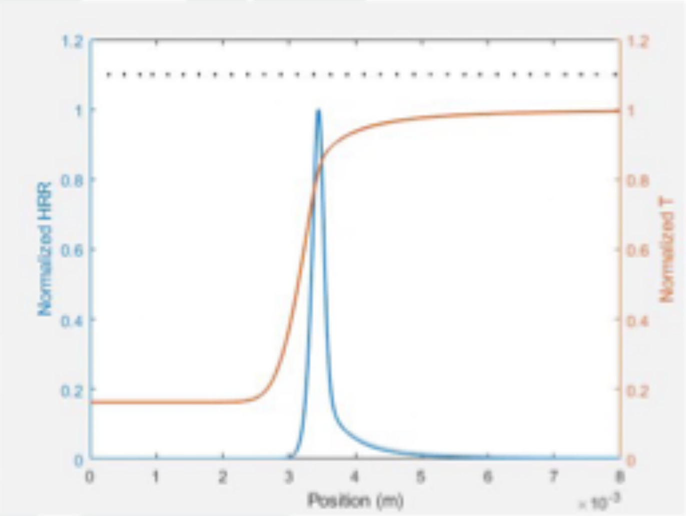

With normalization

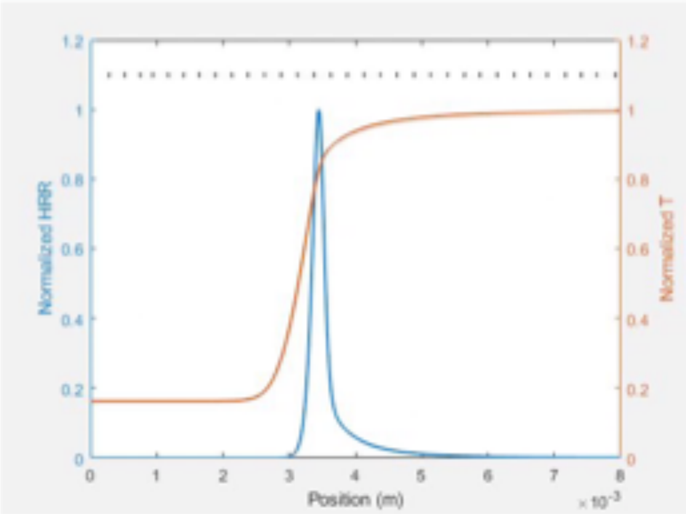

Echoes the findings in Kuron *et al.* CNF (177), 2017

Mixing form: EMST for Ka = 100 flame

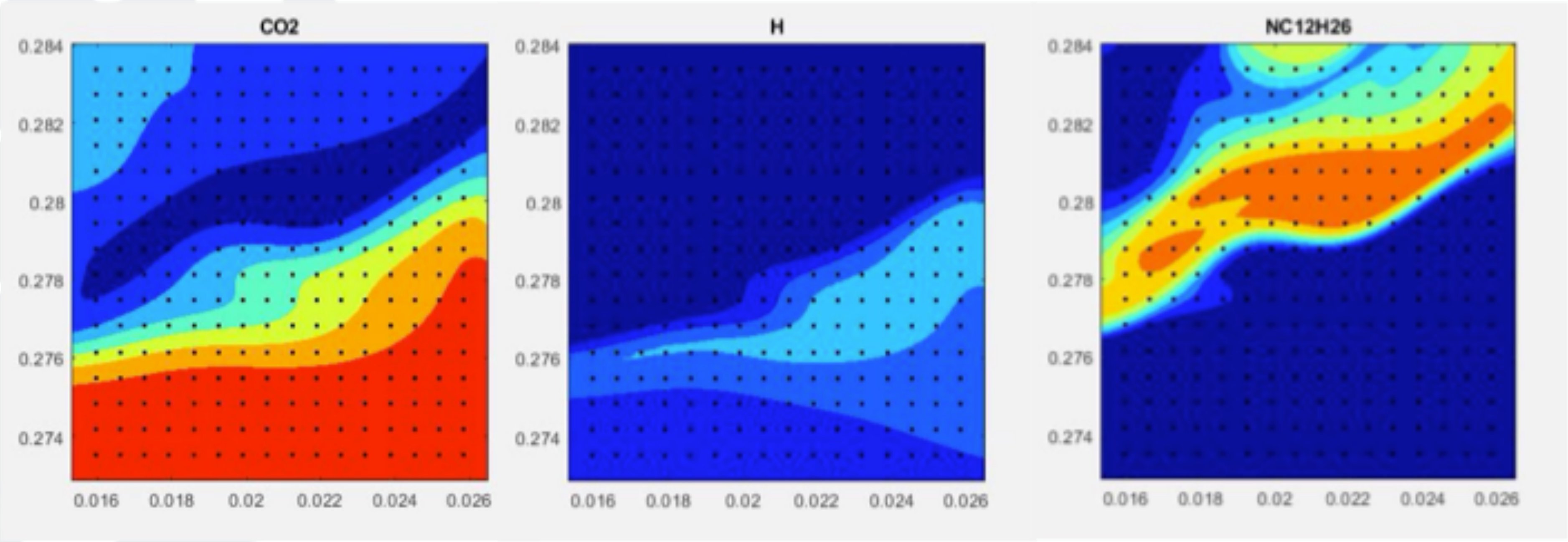

CO_2 H Fuel

Mixing form: EMST for Ka = 100 flame

With normalization

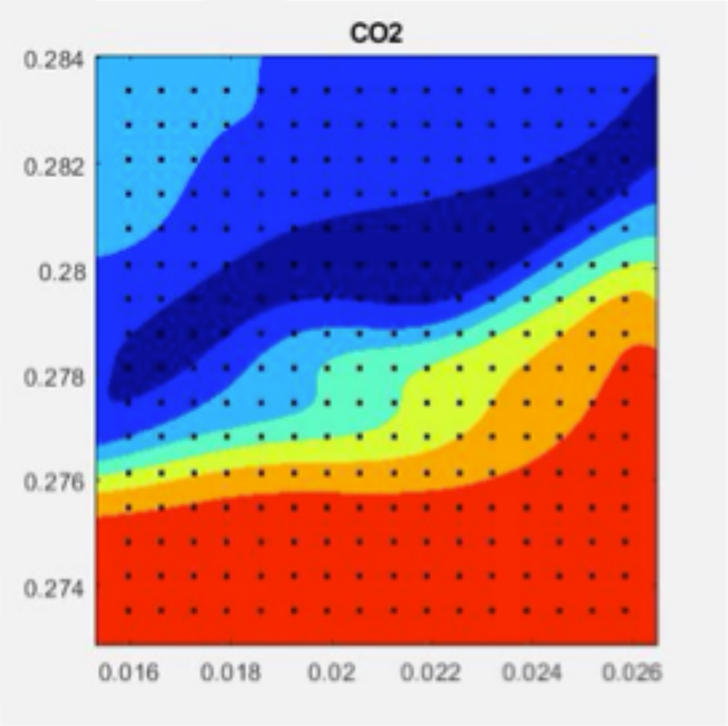

Without normalization

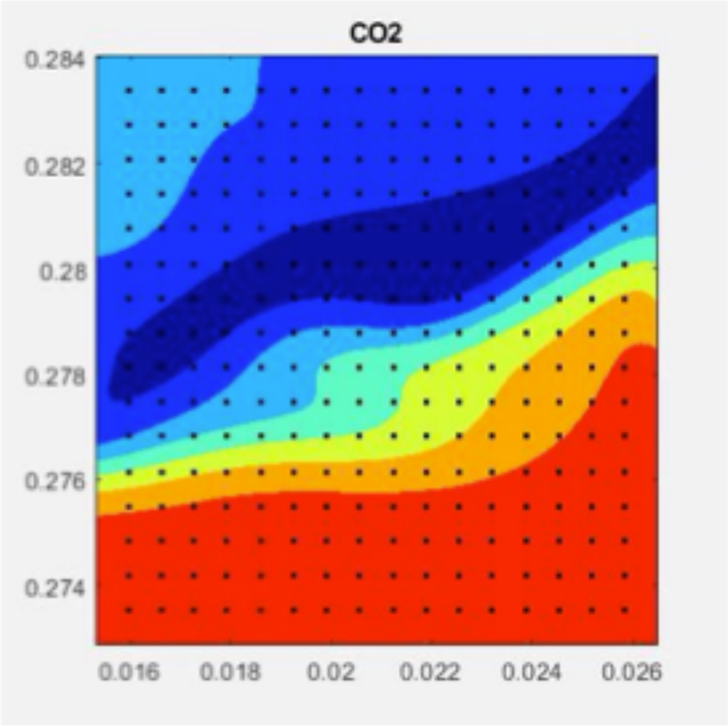

UCONN

Mixing form: EMST for Ka = 1000 flame

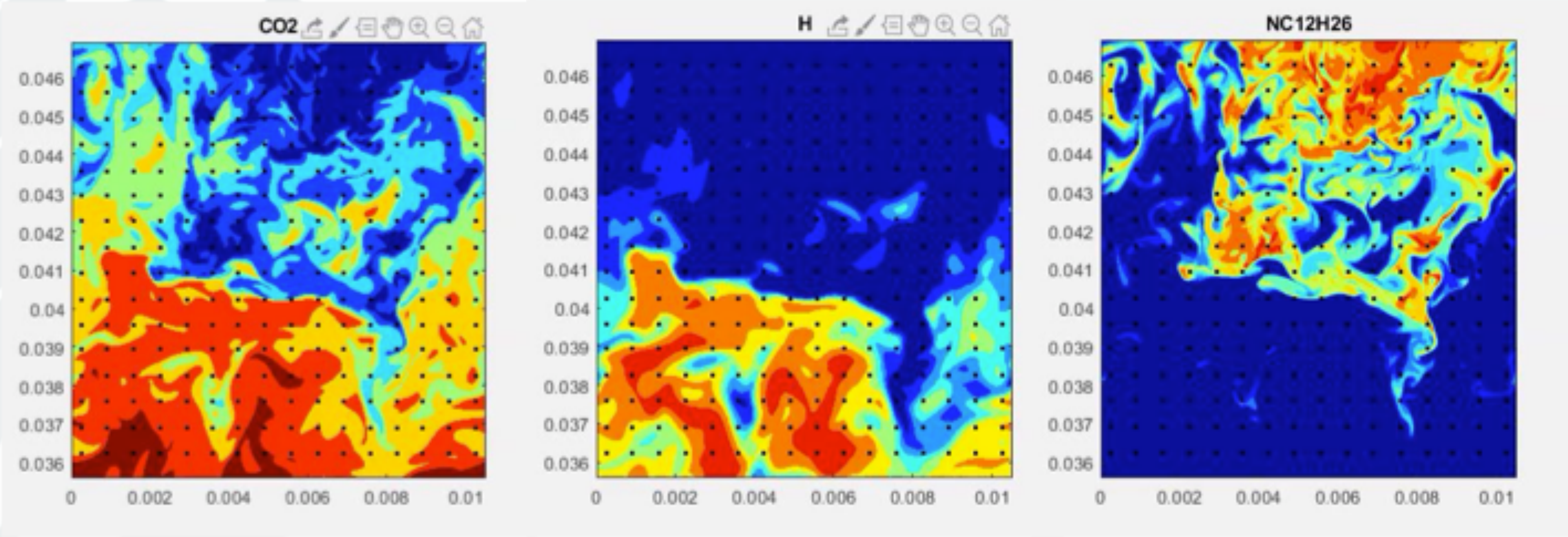

CO_2 H Fuel

Mixing form: EMST

64x64 Test Points, 100 micron Box, each species mass fraction vector normalized by max value Reported: Index distance between node pairs						
	Ka=100		Ka=1000		Ka=10000	
	Mean	STD	Mean	STD	Mean	STD
T=1200K	2.34	3.92	4.37	8.63	13.67	15.64
T=1500K	2.11	1.98	4.42	8.84	10.86	13.35
T=2100K	2.12	2.58	4.73	9.30	10.21	13.68

UCONN

Highly-turbulent premixed flame: diffusion-reaction balance

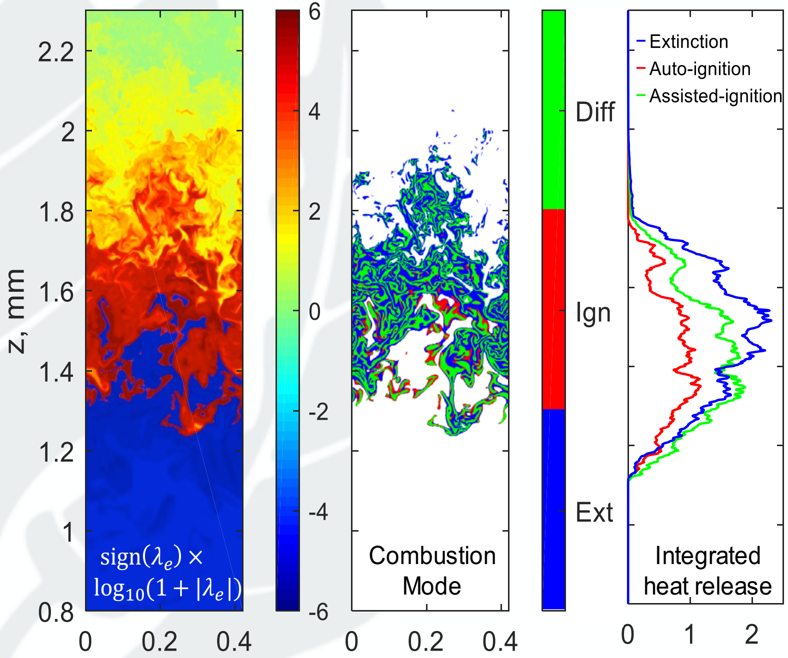

- For a diffusive system, chemical and diffusion source terms are computed as

$$\frac{DY_i}{Dt} = \frac{\omega_i \cdot W_i}{\rho} + \frac{\nabla \cdot (\rho D_i \nabla Y_i)}{\rho}$$

$$\frac{DC_i}{Dt} \approx \omega_i + \frac{\nabla \cdot (\rho D_i \nabla Y_i)}{W_i}$$

$$\frac{DT}{Dt} \approx \frac{-\sum_{n=1}^{K} \omega_i \cdot W_i \cdot e_i}{\rho \bar{c}_v} + \frac{\nabla \cdot (\lambda \nabla T)}{\rho \bar{c}_v}$$

S_{chem} S_{diff}

- Let **b** denote the left eigenvector returned from CEMA, the projected source terms are computed as

$$\phi_\omega = b \cdot S_{chem}$$
$$\phi_s = b \cdot S_{diff}$$

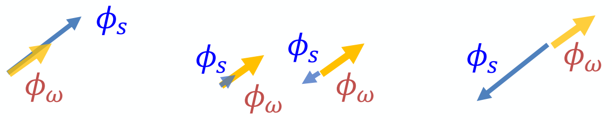

Xu et al. PCI (2018); Xu et al. CNF (2019).

Regime	Inlet distance	burning velocity (cm/s) with manipulation factor (β)		
		0.5	1.0	1.5
diffusion-controlled	1 cm	53.2 cm/s	75.2 cm/s	92.1 cm/s
auto-igniting	400 cm	519.0 cm/s	519.0 cm/s	519.0 cm/s

Observations

- EMST can capture the laminar flame structure.
- Different normalizations can alter the mixing rule and can be leveraged to improve the model for different regimes.
- For highly disturbed flames, the mixing behavior is more homogeneously randomized.
- The modeling of mixing rates can leverage local diffusion-reaction balance.

In Memory of O’Brien

Uniform mean scalar gradient in grid turbulence:

Asymptotic probability distribution of a passive scalar

Presenter: Xiaodan Cai, Ph.D.
United Technologies Research Center

November 24, 2019

A LEGACY OF PROFESSOR O’BRIEN

The founder of the PDF method for reacting turbulent flows

• • •

#+1. Closure for Stochastically Distributed Second-Order Reactants (1968, citation: 22)

#+2. Turbulent shear flow mixing and rapid chemical reactions: an analogy (1973, citation: 40)

#+3. An approach to the autoignition of a turbulent mixture (1974, citation: 393)

#+4. The **probability** density function (pdf) approach to reacting turbulent flows (1980, Citation: 252)

#+5. Joint **probability** density function of a scalar and its gradient in isotropic turbulence (1991, citation: 31)

• • •

“There are a few asymptotic situations in which fluid flows containing chemically reactive species can be successfully studied analytically.” Adapted From O’Brien

FOLLOWING PROFESSOR O’BRIEN

$$\frac{\partial Y}{\partial t} + \underset{\sim}{u}\cdot\nabla Y = D\nabla^2 Y + \dot{w}/\rho$$

A Concept Jump

$$\frac{\partial P}{\partial t} + \overline{\underset{\sim}{u}\cdot\nabla\mathcal{P}} + \frac{\partial}{\partial \hat{Y}}\left(\frac{\dot{w}}{\rho}P\right) = -D\frac{\partial}{\partial \hat{Y}}\left(\overline{\nabla^2 Y\mathcal{P}}\right.$$

$$-D\frac{\partial^2}{\partial \hat{Y}^2}\left(\overline{\frac{\partial Y}{\partial x_i}\frac{\partial Y}{\partial x_i}\mathcal{P}}\right)$$

Many concepts have been tried to model this term

Challenge

$$\frac{1}{2}\frac{\partial^2}{\partial \hat{Y}^2}[\langle\varepsilon(x,t|\hat{Y})\rangle P(\hat{Y};x,t)],$$

If PDF of temperature evolution is known, the mean and fluctuation of reactants are known

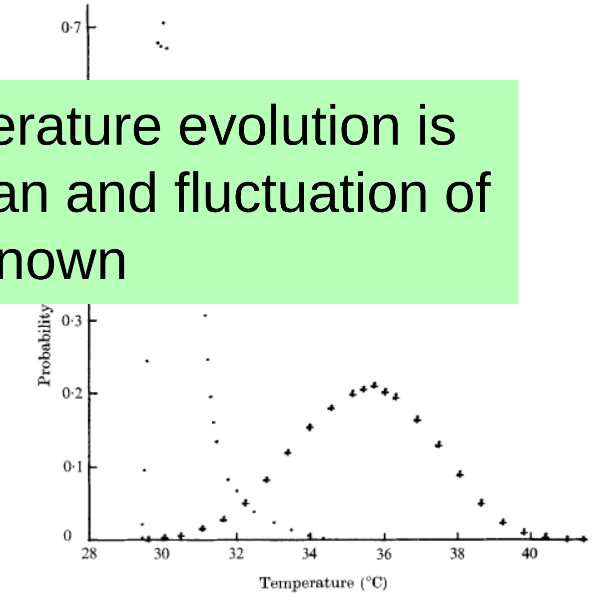

Established Connection

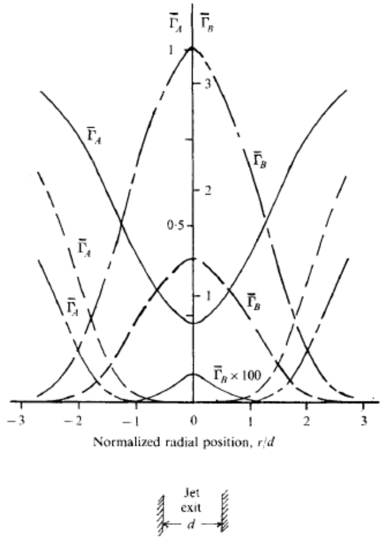

FIGURE 2. Mean concentration of reacting species 15 diameters downstream of jet exit as a function of radial position. $\Gamma_A(S_2) = 1$. ——, $\Gamma_B(S_1) = 1$; — — —, $\Gamma_B(S_1) = 5$; - - -, $\Gamma_B(S_1) = 10$.

WORKING WITH PROFESSOR O’BRIEN

β: Scalar Gradient

$$\frac{\partial \varphi}{\partial t} + U\frac{\partial \varphi}{\partial x} + \nabla\cdot(\mathbf{v}\varphi) = D\,\nabla^2\varphi - \beta v.$$

$$\mathsf{F}_v = \langle v' | \varphi' = \Phi\rangle \qquad \epsilon' = \langle D(\nabla\varphi/\varphi_{\mathrm{rms}})^2\rangle$$

$$\rho = \langle v'\varphi'\rangle \qquad \chi = \frac{\langle D(\nabla\varphi)^2 | \varphi' = \Phi\rangle}{\langle D(\nabla\varphi)^2\rangle}$$

$$\frac{\partial P}{\partial t} + U\frac{\partial P}{\partial x} + \nabla\cdot(\mathsf{F}P) - \frac{\partial}{\partial\Phi}\left[\left(\mathsf{F}\cdot\frac{\nabla\varphi_{\mathrm{rms}}}{\varphi_{\mathrm{rms}}} - \frac{\nabla\cdot\langle \mathbf{v}\varphi^2\rangle}{2\varphi_{\mathrm{rms}}^2}\right)\Phi P\right]$$
$$-D\,\nabla^2 P = -\frac{\partial^2}{\partial\Phi^2}\left[D\left\langle\left(\frac{\nabla\varphi}{\varphi_{\mathrm{rms}}}\right)^2 \middle| \varphi' = \Phi\right\rangle P\right]$$
$$+\frac{\partial}{\partial\Phi}[\beta'\mathsf{F}_v P - (\epsilon' + \beta'\rho)\Phi P], \qquad (4)$$

Assumptions

Approximations

$$\frac{\partial}{\partial\Phi}[\chi(\Phi)P(\Phi)] = \left\{\frac{\beta'}{\epsilon'}\cdot[\mathsf{F}_v(\Phi) - \Phi\rho] - \Phi\right\}P,$$

$$P(\Phi) = \frac{c}{\chi}\exp\left(-\int_{-\infty}^{\Phi}\frac{\Phi}{\chi}\,d\Phi\right)\cdot\exp\left(-\int_{-\infty}^{\Phi}\frac{\beta'(\rho\Phi - \mathsf{F}_v)}{\epsilon'\chi}\,d\Phi\right).$$

Analytical Solution

“There are a few asymptotic situations in which fluid flows containing chemically reactive species can be successfully studied analytically.”

A FRIEND OF PROFESSOR O'BRIEN

His modesty and warmness are deeply felt by the people around him
His rigor and creativeness have big impacts on the field he loves

Modeling Radiative Heat Transfer and Turbulence-Radiation Interactions Using PDF and FDF Methods

Dan Haworth
The Pennsylvania State University

Collaborator: Michael F. Modest

The benefits of PDF/FDF methods extend immediately to radiative emission . . .

Mean flow transport | Chemical reaction | Radiative emission

$$
\frac{\partial \rho f_\phi}{\partial t} + \underline{\frac{\partial \rho \tilde{u}_i f_\phi}{\partial x_i}} + \underline{\frac{\partial \rho S_\alpha f_\phi}{\partial \psi_\alpha}} \underline{- \delta_{\alpha(h)} \frac{\partial \dot{Q}_{\mathrm{rad,em}} f_\phi}{\partial \psi_\alpha}}
$$

$$
= \underline{-\frac{\partial}{\partial x_i}\left[\left\langle u_i'' \middle| \psi \right\rangle \rho f_\phi\right]} + \underline{\frac{\partial}{\partial \psi_\alpha}\left[\left\langle \frac{\partial J_i^\alpha}{\partial x_i} \middle| \psi \right\rangle f_\phi\right]} \underline{- \delta_{\alpha(h)} \frac{\partial}{\partial \psi_\alpha}\left[\left\langle \dot{Q}_{\mathrm{rad,ab}} \middle| \psi \right\rangle f_\phi\right]}
$$

Turbulent transport | Molecular transport | Radiative absorption

. . . and using particle-based representations, radiative absorption is readily accommodated

Consistent hybrid Lagrangian particle/finite-volume transported composition PDF/FDF method

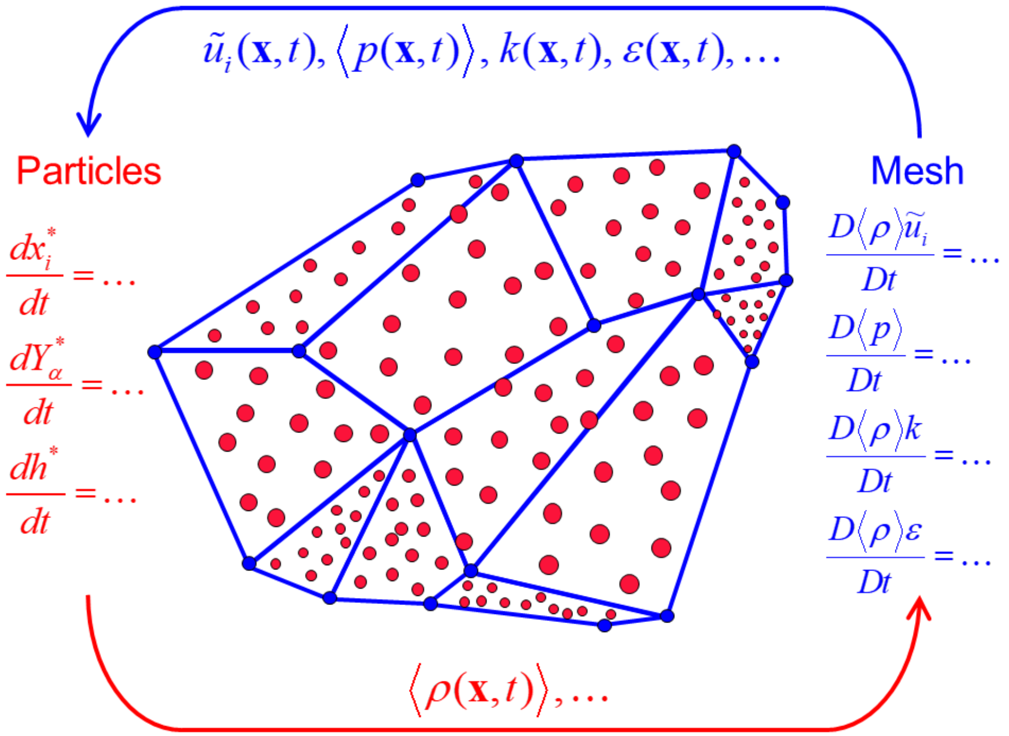

Photon Monte Carlo ray-tracing method with line-by-line spectral resolution

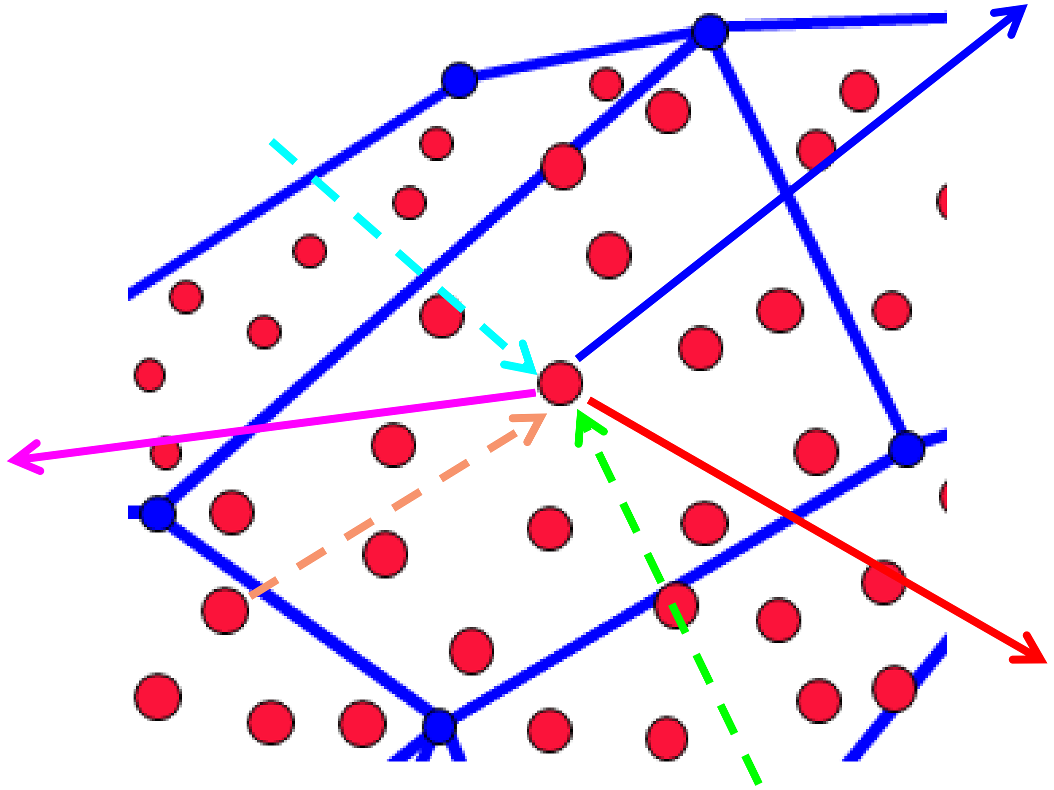

PennState

Radiation and TRI have been explored for a series of four piloted non-premixed turbulent jet flames . . .

- Sandia/TUD flame D
  - Modest (but discernable) radiation effects
- Sandia/TUD flame D + soot
  - Correlation based soot model: $f_v = f_v(\Phi)$
- Scaled-up (4x) Sandia/TUD flame D
  - Dominated by spectral molecular gas radiation
- Scaled-up (4x) Sandia/TUD flame D + soot
  - Spectral molecular gas radiation + broadband soot radiation

Gupta, Haworth & Modest ProCI 34 (2013)

PennState

. . . that range from optically thin to optically thick

Flame	D_{jet} (mm)	$U_{jet,b}$ (m/s)	Optical thickness
D	7.2	49.6	0.049
D+soot	7.2	49.6	0.050
4D	28.8	12.4	0.248
4D+soot	28.8	12.4	0.345

Gupta, Haworth & Modest ProCI 34 (2013)

Moderate-resolution LES has been performed to facilitate parametric studies

- ~1.1 million finite-volume cells
  - ~84% of TKE resolved
- ~15 particles per cell
- One-equation SFS turbulence model
- Synthesized turbulence at inlet
  - Klein et al. (2003)

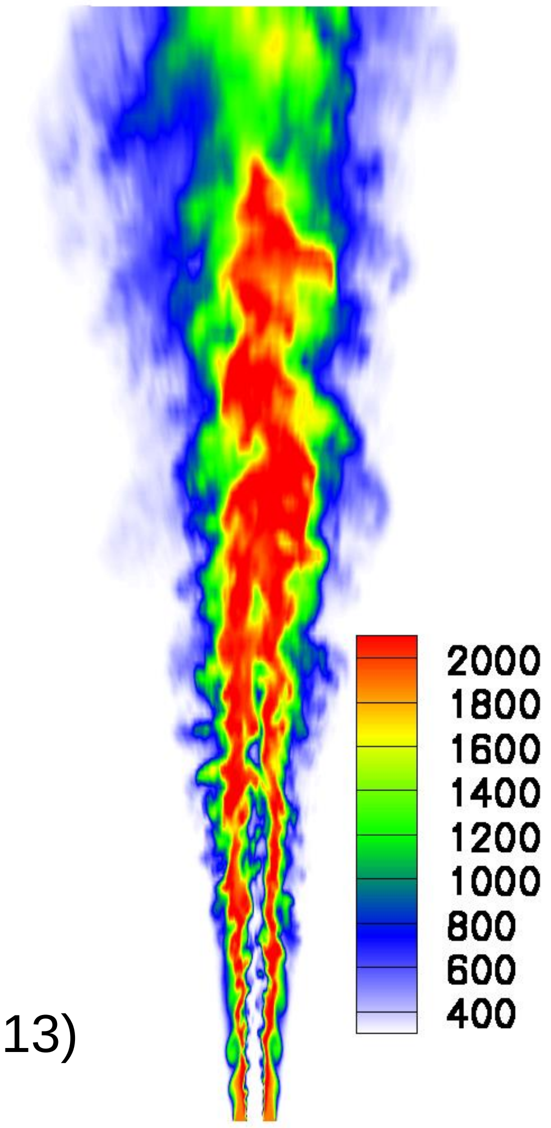

Gupta, Haworth & Modest ProCI 34 (2013)

Several simulations have been performed to isolate resolved-scale versus subfilter-scale contributions to emission and absorption turbulence-radiation interactions (TRI)

	Case name	Emi. calc.	Abs. calc.	Emission		Absorption	
				ReS TRI	SFS TRI	ReS TRI	SFS TRI
	TRI0	Mean	Mean	–	–	–	–
Frozen-field analysis	TRI1F	Cell	Mean	Y	–	–	–
	TRI2F	Cell	Cell	Y	–	Y	–
	TRI3F	Part.	Cell	Y	Y	Y	–
	TRI4F	Part.	Part.	Y	Y	Y	Y
Fully coupled runs	TRI2C	Cell	Cell	Y	–	Y	–
	TRI3C	Part.	Cell	Y	Y	Y	–
	TRI4C	Part.	Part.	Y	Y	Y	Y

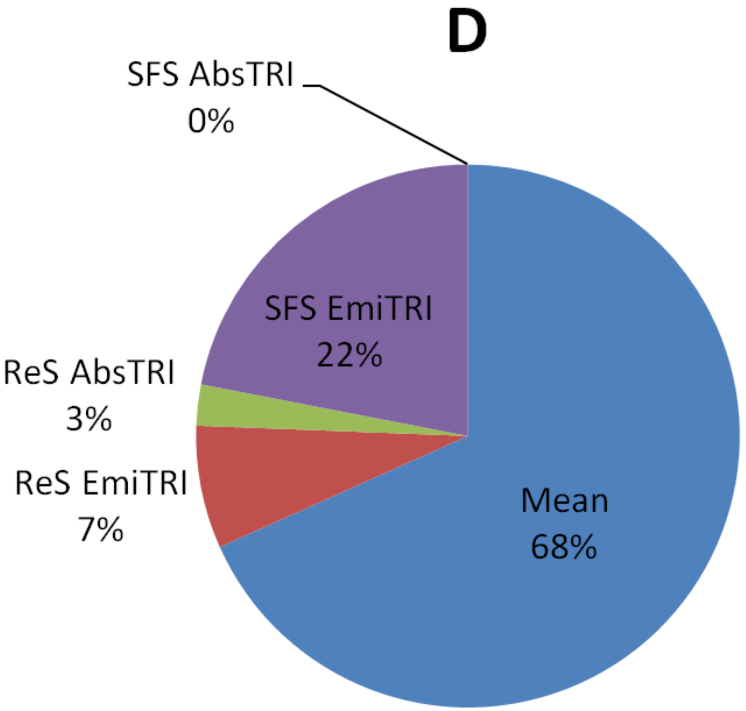

- Emission TRI are always important
- Subfilter-scale contributions to emission TRI exceed resolved-scale contributions
- Absorption TRI are important only for optically thick systems
- Subfilter-scale contributions to absorption TRI are negligible

Based on frozen-field radiant fractions

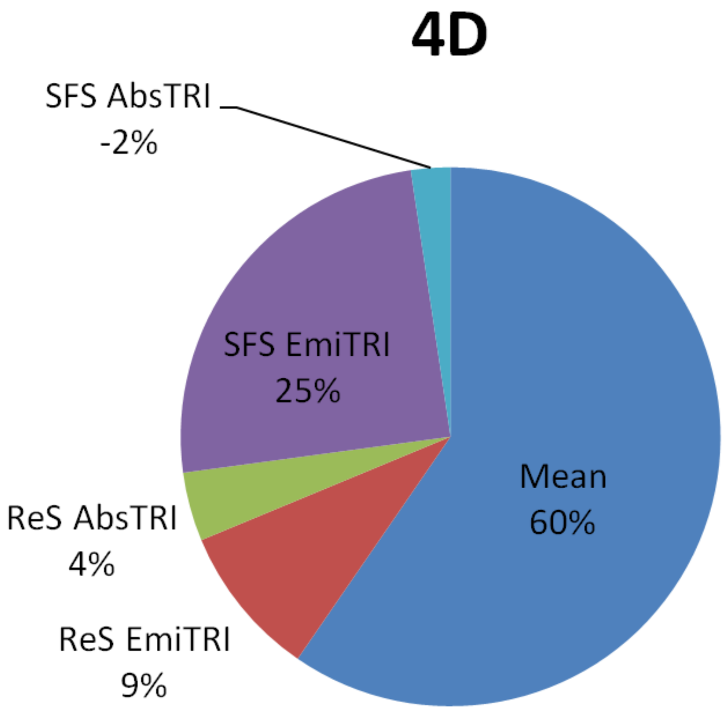

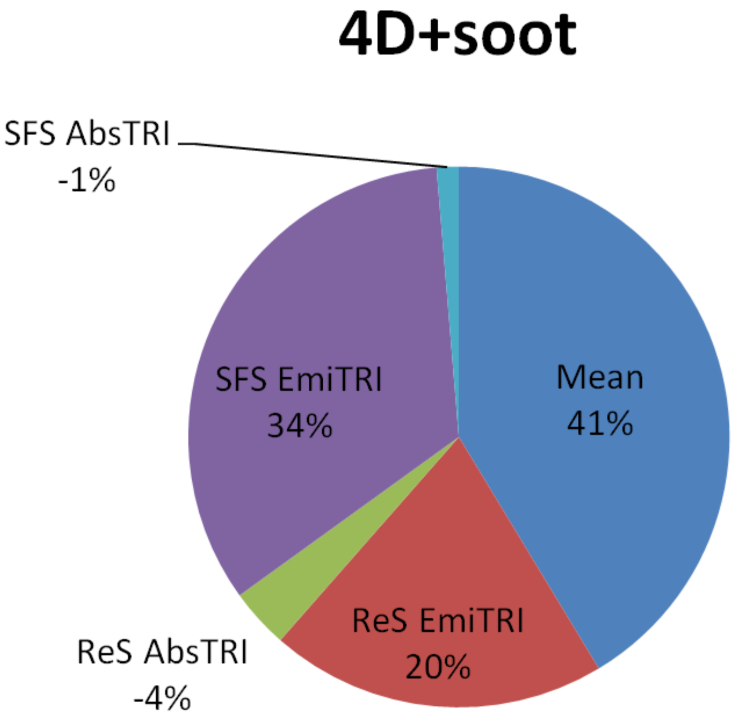

There are competing effects at high pressures

- Radiation effects expected to be *enhanced* by:
  - Higher pressures
    - Molecular gas emission is proportional to participating species concentration
    - Soot emission is proportional to soot volume fraction, which increases as ~p^2 for moderately high pressures (to ~40 bar)
  - Higher levels of exhaust-gas recirculation (containing CO_2 and H_2O) in practical combustion systems
- Radiation effects expected to be *diminished* by:
  - Lower temperatures that are of interest for some advanced combustion strategies
  - Relatively small length and time scales (in car and truck engines)

PennState

PMC/LBL has been used to explore spectral radiation characteristics in an engine-relevant environment*

- Ambient mixture (reacting)
  - 900 K, 22.8 kg/m^3 (60 bar)
  - 15% O_2, 6.2% CO_2, 3.6% H_2O
- n-Dodecane fuel
  - 150 MPa, 5.5 ms duration
- Unsteady RANS
  - 2D axisymmetric (wedge) mesh
  - Nonuniform, ~12K finite-volume cells
  - Standard two-equation turbulence model
- Stochastic Lagrangian parcel fuel injection and spray models
- 54-species chemical mechanism
- Semi-empirical two-equation soot model
- WSR or PDF models
  - 50-100 particles per cell for PDF

*ECN Spray A
www.sandia.gov/ecn/

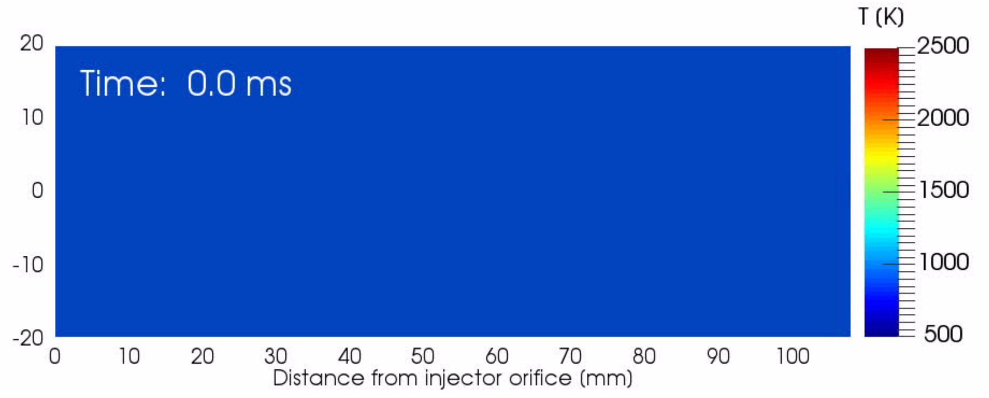

Ferreyro Fernandez et al. (2018)
Combust. Flame 190:402-415

PennState

PDF-based model gives correct global soot level

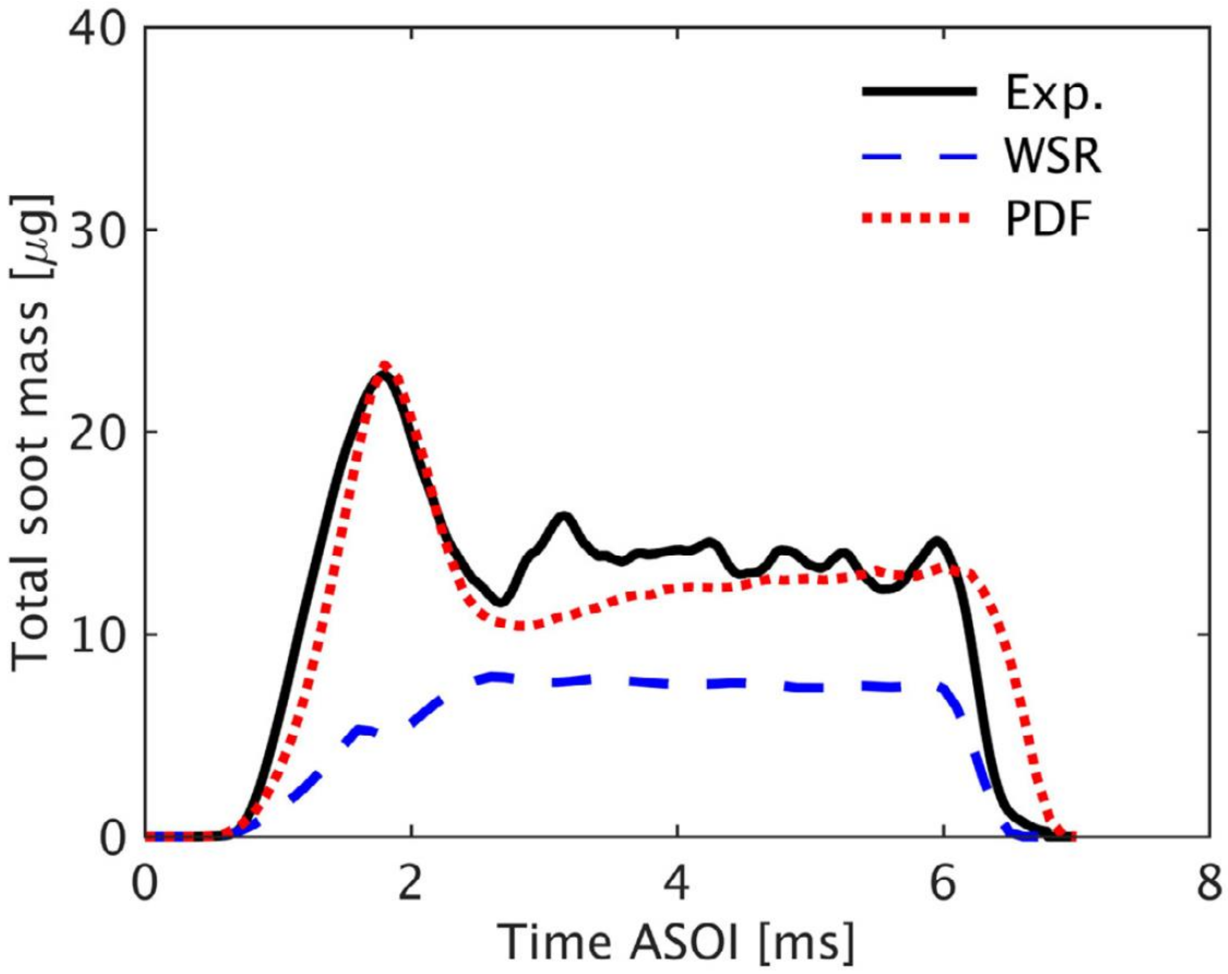

Ferreyro Fernandez et al. (2018) Combust. Flame 190:402-415

Spectral radiation is computed @ 3 ms aSOI using PMC/LBL

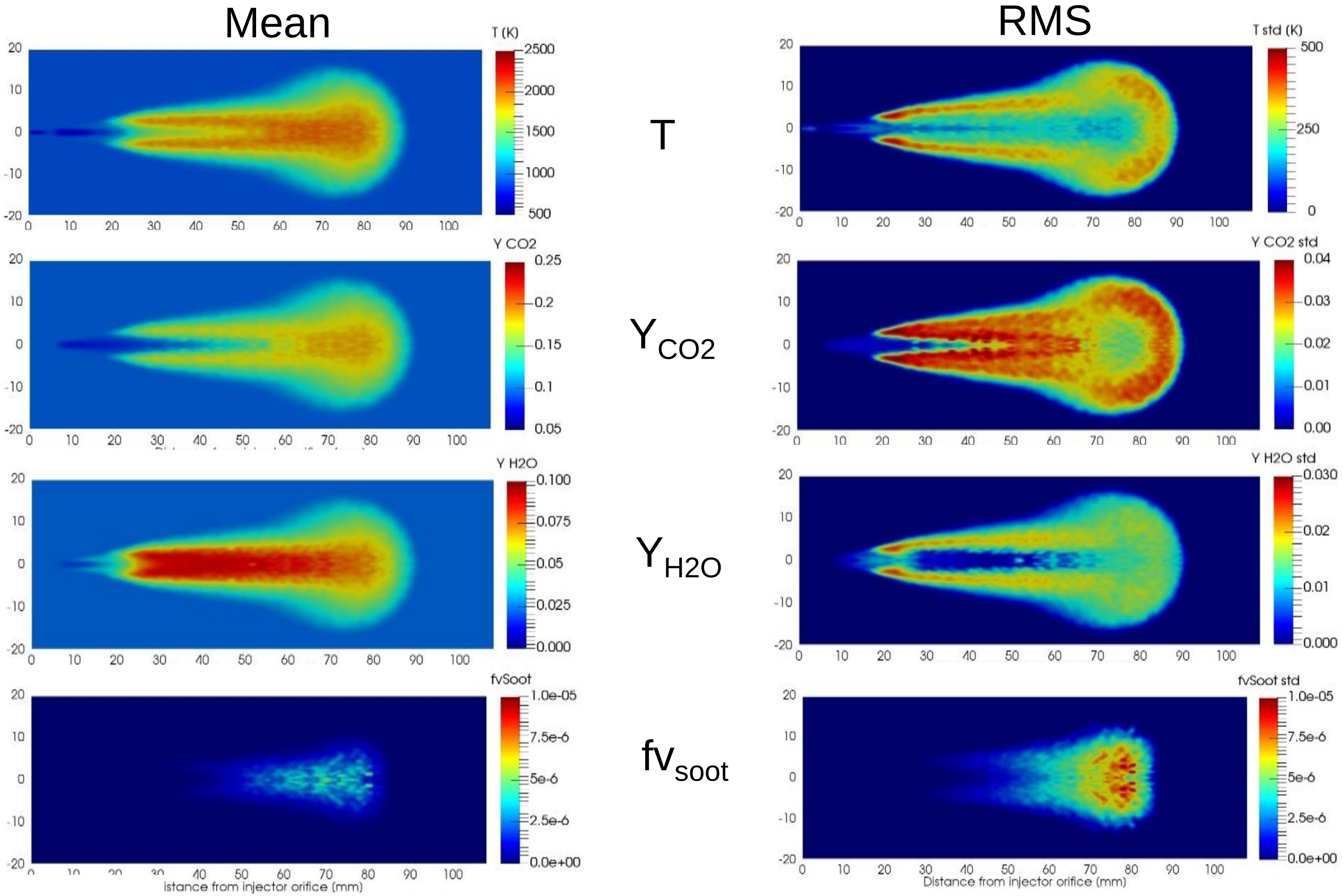

PennState

Ferreyro Fernandez et al. (2018) Combust. Flame 190:402-415

Molecular gas radiation dominates

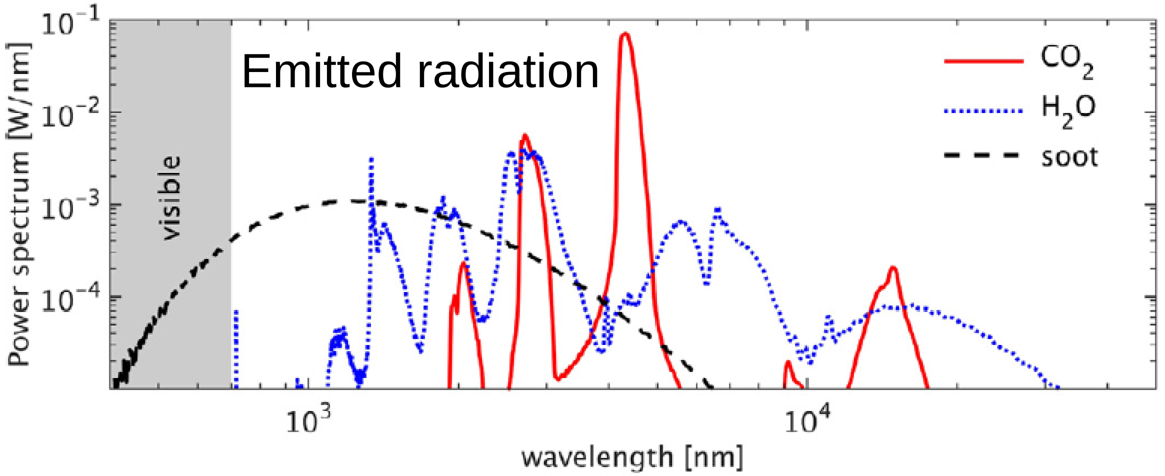

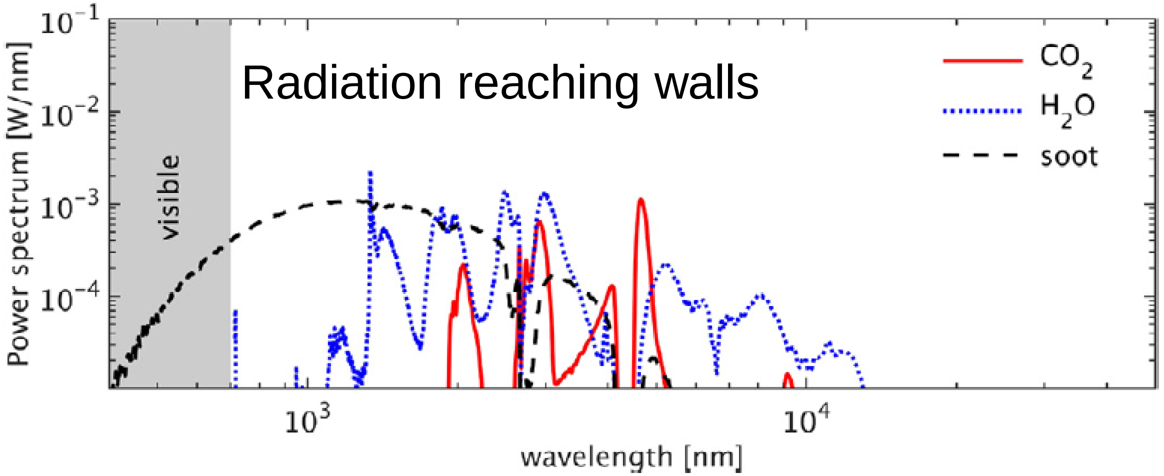

Source	Total emission (W)	Flame-zone emission (W)	Radiation reaching wall (W)
CO	0.20	0.20	0.05
CO2	221.5	21.7	5.3
H2O	32.4	4.6	8.9
Soot	1.30	1.3	1.1
Total	254.4	27.7	15.3

Fuel power = 1572 W
Radiant fraction ≈ 1%
Soot radiant fraction ≈ 0.07%*
CO_2 and H_2O dominate

*0.068%, per Skeen et al. SAE 2014-01-1252

Ferreyro Fernandez et al. (2018)
Combust. Flame 190:402-415

PennState

PDF/PMC/LBL provides new insight into radiative transfer in high-pressure turbulent combustion systems

- Consideration of spectral radiation properties and reabsorption is essential
- Molecular gas radiation usually dominates soot radiation
- Radiation redistributes energy, in addition to contributing to heat losses
- Global radiation effects are relatively small (~10%), and are the net result of high spectral emission and high spectral reabsorption
- A simplified model has been developed for high-pressure hydrocarbon-air combustion systems, with or without soot*

*C. Paul, D.C. Haworth, M.F. Modest (2019) ProCI 37:4617-4624

PennState

Deep Learning of Single-Point PDF Closure for Turbulent Scalar Mixing

M. Raissi, H. Babaee, and P. Givi

E.E. O' Brien, Ph.D. Thesis (1960)

E. E. O'Brien, *On the Statistical Behavior of a Dilute Reactant in Isotropic Turbulence*, Ph.D. Thesis, Johns Hopkins University, Baltimore, MD, 1960.

$$\frac{\partial P}{\partial t} + \frac{\partial^2(\epsilon_{\alpha\beta} P)}{\partial \psi_\alpha \partial \psi_\beta} = -\frac{\partial \left[P S_\alpha(\psi) \right]}{\partial \psi_\alpha}$$

$$\epsilon_{\alpha\beta} = E\left(\Gamma \nabla \phi_\alpha \cdot \nabla \phi_\beta \,\middle|\, \Phi(\mathbf{x}, t)\right)$$

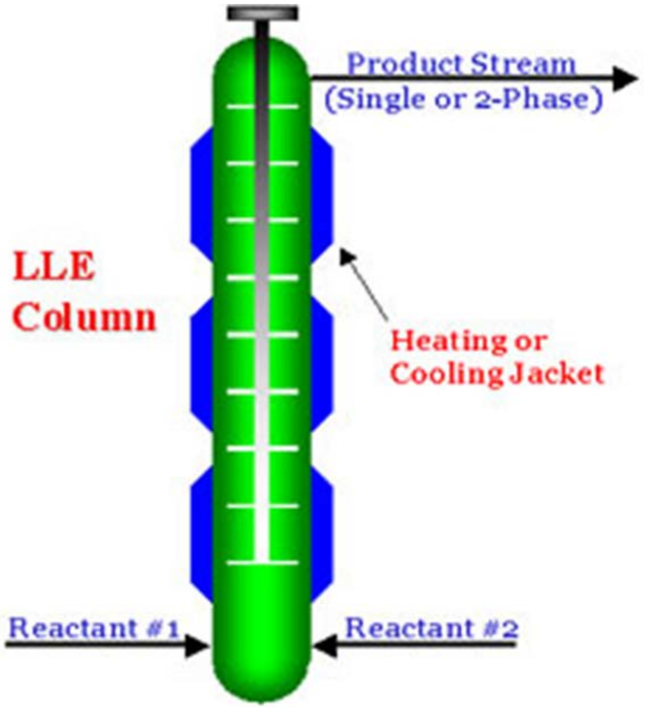

$$P(\psi) = \frac{1}{2}\left[\delta(\psi - \psi_F) + \delta(\psi - \psi_O)\right]$$

DNS of Scalar Mixing

171

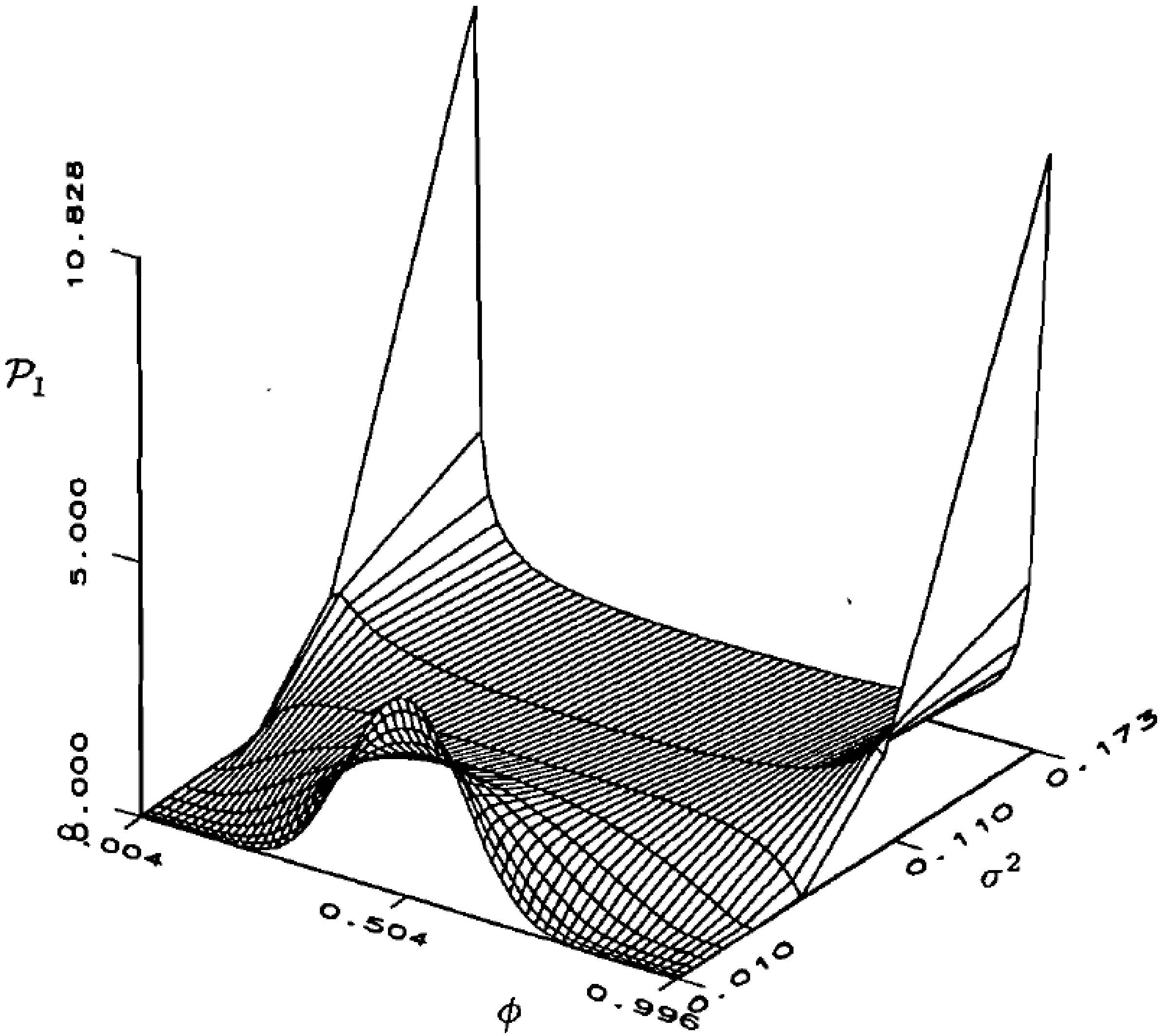

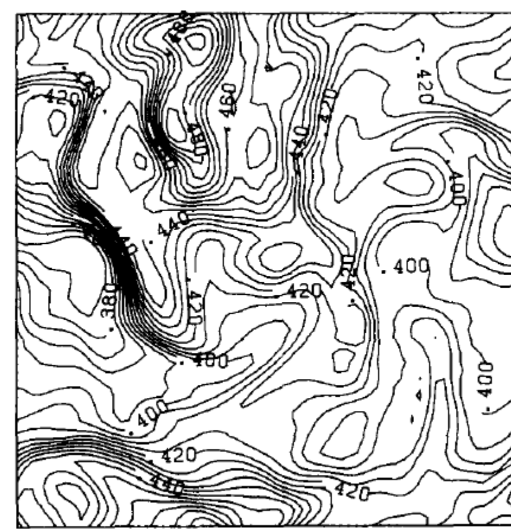

Kraichnan Amplitude Mapping Closure (AMC)

The conditional dissipation rate of an initially binary scalar in homogeneous turbulence

Edward E. O'Brien
Department of Mechanical Engineering, State University of New York at Stony Brook, Stony Brook, New York 11794-2300

Tai-Lun Jiang
Department of Mechanical and Aerospace Engineering, University at Buffalo, Amherst, New York 14260

(Received 30 April 1991; accepted 6 August 1991)

It is shown that a necessary and sufficient condition for the scalar dissipation rate, conditioned on scalar value ϕ, to be independent of ϕ is that the one-point scalar probability distribution function (pdf) is Gaussian. It is then shown that the amplitude mapping closure yields a closed-form, separable expression for the ϕ dependence of the conditional dissipation rate in the case of an initial double-delta scalar pdf. If the initial binary scalar field is located at $\phi = \pm 1$, the solution is $\exp\{-2[\mathrm{erf}^{-1}(\phi)]^2\}$, a result that is strongly supported by earlier direct numerical simulations.

When a scalar field is mixed by a turbulent field, the mean square gradient of the scalar is an important quantity in the description of scalar evolution. In particular, it is the quantity which determines the rate of decay of scalar variance, $\sigma(t)$, in homogeneous turbulence[1]

as its only unknown function the expectation of the normalized scalar mean square gradient, conditioned on the value of the normalized scalar.

Historically, it has been the practice to propose *ad hoc* closure approximations for $E\{\xi^2|\phi\}$, or quantities related

AMC for Scalar Mixing

PoF92.PDF - Adobe Acrobat Pro DC

Binary and trinary scalar mixing by Fickian diffusion—Some mapping closure results

Tai-Lun Jiang and Peyman Givi
Department of Mechanical and Aerospace Engineering, State University of New York, Buffalo, New York 14260

Feng Gao
Center for Turbulence Research, Stanford University, Stanford, California 94305

(Received 16 September 1991; accepted 4 December 1991)

The amplitude mapping closure of Kraichnan [Bull. Am. Phys. Soc. **34**, 2298 (1989); Phys. Rev. Lett. **63**, 2657 (1989)] is used for statistical description of the mixing process by Fickian diffusion of a stochastically distributed scalar variable. This closure is invoked in the context of an evolution equation for the single-point probability density function (pdf) of the scalar from initially symmetric binary and trinary states. In the binary case, a simple recipe is provided for the time scaling relation which is very useful in model implementation. In the trinary case, it is shown that after a fixed elapsed time, the pdf relaxes to a distribution similar to that of the binary mixing. The magnitude of this time is independent of the initial extent of departure from a binary state; however, the rate of evolution toward an asymptotic Gaussian state depends on the level of the departure. In both cases, the closure predictions for the scalar flatness factor and the correlation of the mean square scalar–scalar gradients agree well with those obtained by direct numerical simulations (DNS). However, some features of the results are different from those of earlier DNS of mixing in stationary turbulence. These differences are likely attributed to inadequacy of the amplitude mapping closure at the single-point level in accounting for the effects of turbulence stretching.

I. INTRODUCTION

Development of the amplitude mapping closure by Kraichnan and co-workers[1,2] has had a significant impact on statistical modeling of turbulent reacting flows. This closure has proven its capability in probability density function (pdf) modeling of scalar variables in turbulent flows, and has demonstrated its physical plausibility in a number of validation studies by means of comparative assessments against direct numerical simulation (DNS) data.[2-5] Because of its demonstrated relative strength and its sound mathematical-physical basis, it is anticipated that this closure will be extensively utilized in statistical treatment of turbulence, and will gradually replace the closures currently in use in probability modeling of turbulent combustion phenome-

nal" information for predicting the evolution of these scales. With availability of such information (by whatever means), the problem reduces to that of establishing a time scaling relation by which the mapping closure can be enacted. The mechanism of utilizing this relation is demonstrated here by two simple examples. The examples chosen are those for which the desired information can be furnished by simple analytical procedures. However, an outline is provided of the implementation of this mechanism for more complex conditions.

The second problem is the provision of some analytical results for higher-order statistics generated by the mapping closure. This problem is suitable for addressing the relaxation property of the predicted pdf, including the temporal evolution of the scalar variance, the scalar flatness, and the

AMC ≡ Johnson-Edgeworth Translation (JET)

Combust. Sci. and Tech., 1993, Vol. 91, pp. 21-52
Photocopying permitted by license only

Johnson-Edgeworth Translation for Probability Modeling of Binary Scalar Mixing in Turbulent Flows

R. S. MILLER, S. H. FRANKEL, C. K. MADNIA, and P. GIVI *Department of Mechanical and Aerospace Engineering, State University of New York, Buffalo, NY 14260*

(Received August 14, 1992; in final form November 2, 1992)

Abstract—A family of Probability Density Functions (PDF's) generated by *Johnson-Edgeworth* Translation (JET) is used for statistical modeling of the mixing of an initially binary scalar in isotropic turbulence. The frequencies obtained by this translation are shown to satisfy some of the characteristics of the PDF's generated by the *Amplitude Mapping* Closure (AMC) (Kraichnan, 1989; Chen *et al.*, 1989). In fact, the solution obtained by one of the members of this family is shown to be identical to that developed by the AMC (Pope, 1991). Due to this similarity and due to the demonstrated capabilities of the AMC, a justification is provided for the use of other members of JET frequencies for the modeling of the binary mixing problem. This similarity also furnishes the reasoning for the applicability of the *Pearson Family* (PF) of frequencies for modeling of the same phenomena. The mathematical requirements associated with the applications of JET in the modeling of the binary mixing problem are provided, and all the results are compared with data generated by Direct Numerical Simulations (DNS). These comparisons indicate that the *Logit-Normal* frequency portrays some subtle features of the mixing problem better than the other closures. However, none of the models considered (JET, AMC, and PF) are capable of predicting the evolution of the conditional expected dissipation and/or the conditional expected diffusion of the scalar field in accordance with DNS. It is demonstrated that this is due to the incapability of the models to account for the variations of the scalar bounds as the mixing proceeds. A remedy is suggested for overcoming this problem which can be useful in probability modeling of turbulent mixing, especially when accompanied by chemical reactions. While in the context of a single-point description the evolution of the scalar bounds cannot be predicted, the qualitative analytical-computational results portray a physically plausible behavior.

1 INTRODUCTION

The problem of binary mixing in turbulent flows has been the subject of widespread investigations over the past two decades (Dopazo, 1973; Pope, 1979; Pope, 1985; Pope,

Data Driven PDF Closure Development

1. Conditional Expected Dissipation

$$\frac{\partial P}{\partial t} + \frac{\partial^2(\boxed{\mathcal{E}}P)}{\partial \psi^2} = 0, \quad -1 \leq \psi \leq +1$$

$$\mathcal{E} = \mathcal{E}(t, \psi) =< \xi | \psi(t, \boldsymbol{x}) = \psi >$$

$$\xi \;= \Gamma \nabla \psi \cdot \nabla \psi$$

2. Conditional Expected Diffusion

$$\frac{\partial P}{\partial t} + \frac{\partial(\boxed{D}P)}{\partial \psi} = 0$$

$$D = D(t, \psi) =< \Gamma \nabla^2 \psi | \psi(t, \boldsymbol{x}) = \psi >$$

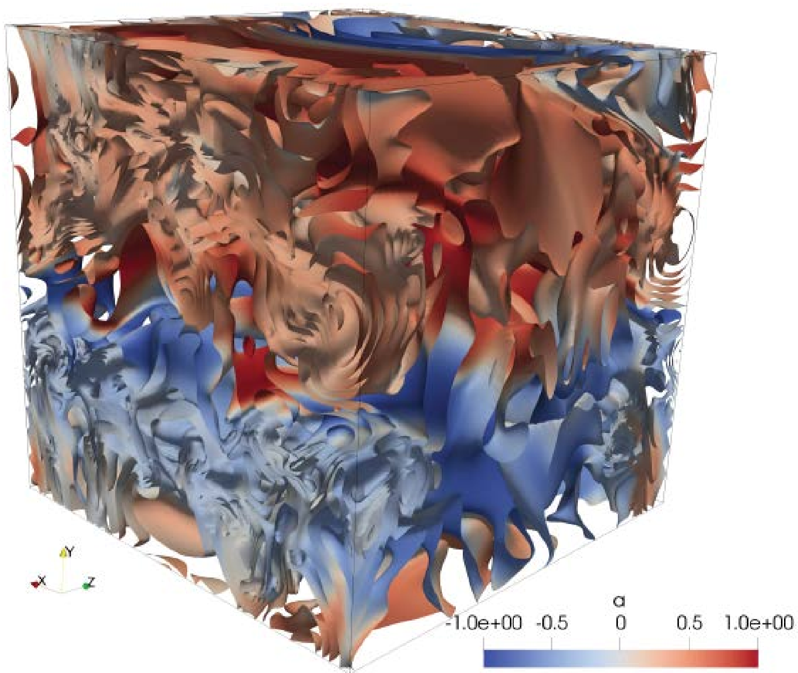

LMSE Model

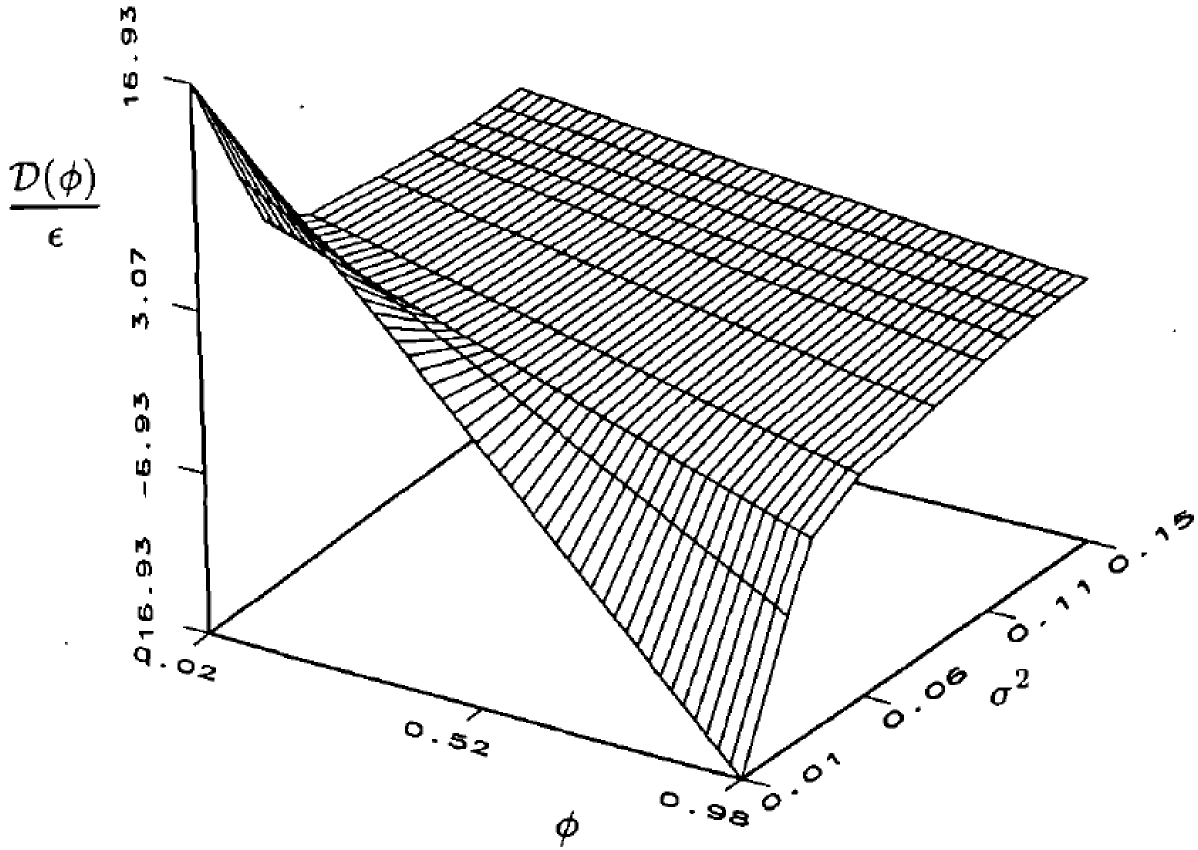

16.93
$\frac{\mathcal{D}(\phi)}{\epsilon}$
3.07
-6.93
-16.93
0.02
0.52
0.98
ϕ
0.01
0.06
0.11
0.15
σ^2

Challenges

1. Conditional Expected Dissipation

$$\frac{\partial P}{\partial t} + \frac{\partial^2(\boxed{\mathcal{E}}P)}{\partial \psi^2} = 0, \quad -1 \leq \psi \leq +1$$

$$\mathcal{E} = \mathcal{E}(t,\psi) =< \xi | \psi(t,\boldsymbol{x}) = \psi >$$

$$\xi \;= \Gamma \nabla \psi \cdot \nabla \psi$$

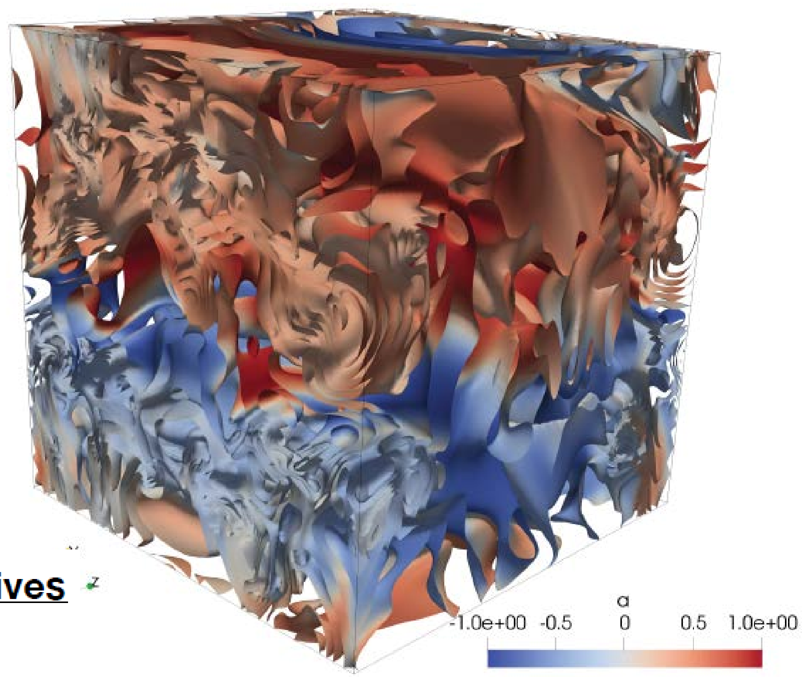

- No direct observations on $\mathcal{E}$
- Obtaining data on $\mathcal{E}$ involves space-time derivatives
- Sparse observations on P → DNS, Experiment

→ Model $\mathcal{E}$

Physics Based + Data Driven

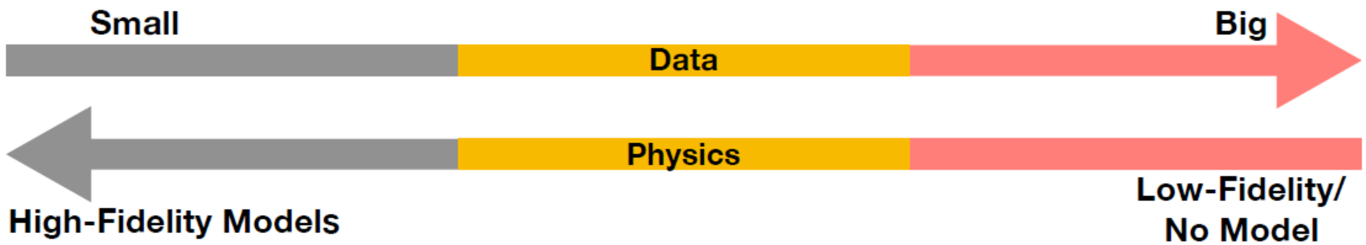

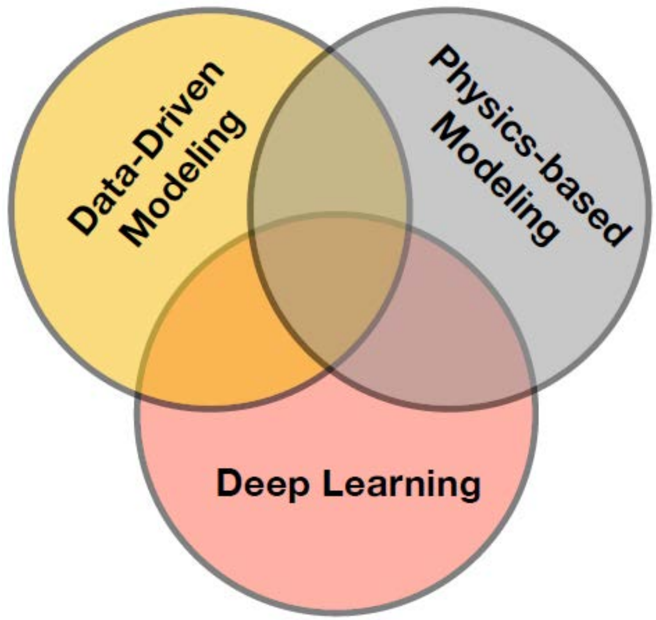

No Data Left Behind

No Model Left Behind

Disruptive Technology

Physics-Informed Deep Learning

Hidden Physics Models

$$u_t = \mathcal{N}\left(t, x, u, u_x, u_{xx}, \ldots\right)$$

Physics Informed Deep Learning (Part I): Data-driven Solutions of Nonlinear Partial Differential Equations, M. Raissi, P. Perdikaris, G. Karniadakis
https://arxiv.org/abs/1711.10561.

Observed PDF

Can we find conditional expected dissipation/diffusion given some observations on PDF ?

Data + Physics

$$\frac{\partial \boxed{P}}{\partial t} + \frac{\partial^2 (\boxed{\mathcal{E}} P)}{\partial \psi^2} = 0$$

Data on P

Learn $\mathcal{E}$

Data-Driven Inverse Problem

Physics Informed Neural Networks

Physics Uninformed | **Physics Informed**

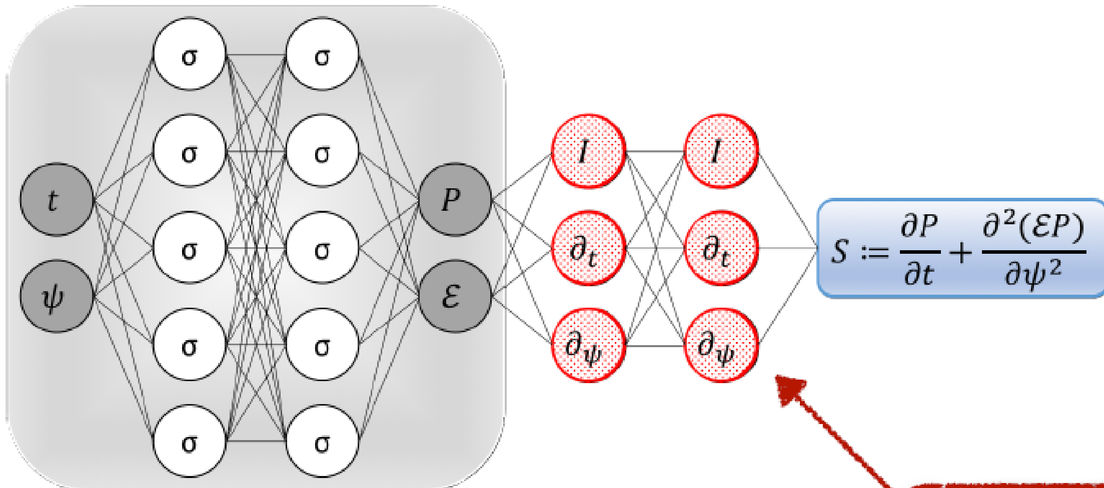

Exact Differentiation!

$$S := \frac{\partial P}{\partial t} + \frac{\partial^2(\mathcal{E}P)}{\partial \psi^2}$$

$$\sum_{n=1}^{N} |P(t^n, \psi^n) - P^n|^2 + \boxed{\sum_{n=1}^{N} |S(t^n, \psi^n)|^2}$$

Enforcing Physics (PDF Transport)

Deep Learning of Turbulent Scalar Mixing, M. Raissi, H. Babaee, P. Givi https://arxiv.org/abs/1811.07095.

Physics Informed Neural Networks

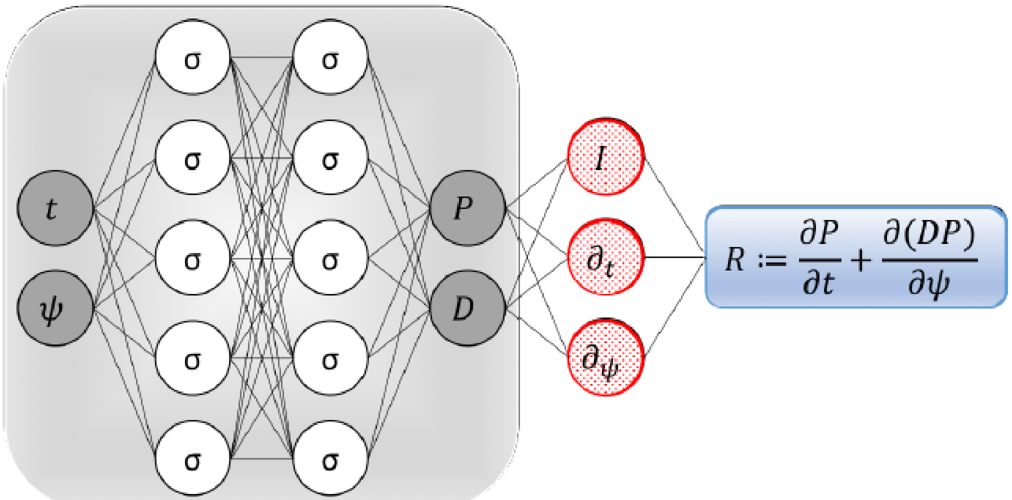

$$R := \frac{\partial P}{\partial t} + \frac{\partial (DP)}{\partial \psi}$$

$$\sum_{n=1}^{N} |P(t^n, \psi^n) - P^n|^2 + \boxed{\sum_{n=1}^{N} |R(t^n, \psi^n)|^2}$$

Enforcing Physics (PDF Transport)

Deep Learning of Turbulent Scalar Mixing, M. Raissi, H. Babaee, P. Givi https://arxiv.org/abs/1811.07095.

AMC/JET Solution

- **The PDF Evolution (driving to a Gaussian state):**

$$P(\tau,\psi)=\frac{G}{2}\exp\left\{-(G^2-1)\left[\mathrm{erf}^{-1}(\psi)\right]^2\right\}$$
$$G(\tau)=\sqrt{\exp(2\tau)-1}.$$

- **The Variance:**

$$\frac{<\sigma^2>(\tau)}{<\sigma^2>(0)}=\frac{2}{\pi}\arctan\left(\frac{1}{G\sqrt{G^2+2}}\right)$$

- **The Conditional Expected Dissipation:**

$$\frac{\mathcal{E}(t,\psi)}{\epsilon(t)}=\left(\sqrt{\frac{1+\sin\left[\frac{\pi\sigma^2(t)}{2\sigma^2(0)}\right]}{1-\sin\left[\frac{\pi\sigma^2(t)}{2\sigma^2(0)}\right]}}\right)\exp\left\{-2\left[\mathrm{erf}^{-1}(\psi)\right]^2\right\}$$

- **The Conditional Expected Diffusion:**

$$\frac{D(t,\psi)}{\epsilon(t)}=\left(\frac{-\sqrt{\pi}}{\sin\left[\frac{\pi\sigma^2(t)}{2\sigma^2(0)}\right]}\sqrt{\frac{1+\sin\left[\frac{\pi\sigma^2(t)}{2\sigma^2(0)}\right]}{1-\sin\left[\frac{\pi\sigma^2(t)}{2\sigma^2(0)}\right]}}\right)\exp\left\{-\left[\mathrm{erf}^{-1}(\psi)\right]^2\right\}\mathrm{erf}^{-1}(\psi)$$

Data Driven Modeling

Observation on PDF

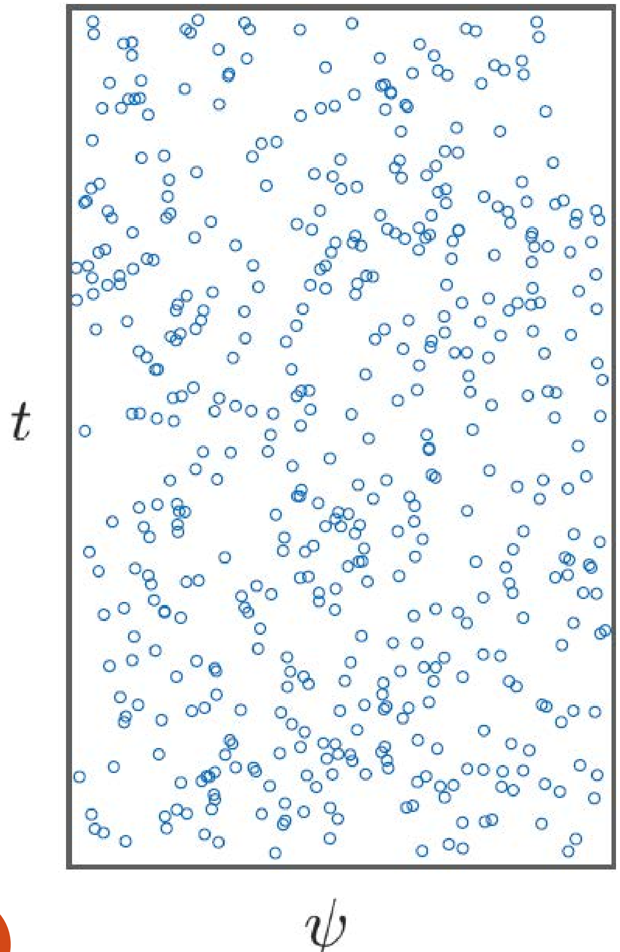

+

$$\boxed{\frac{\partial P}{\partial t} + \frac{\partial^2(\mathcal{E}P)}{\partial \psi^2} = 0}$$

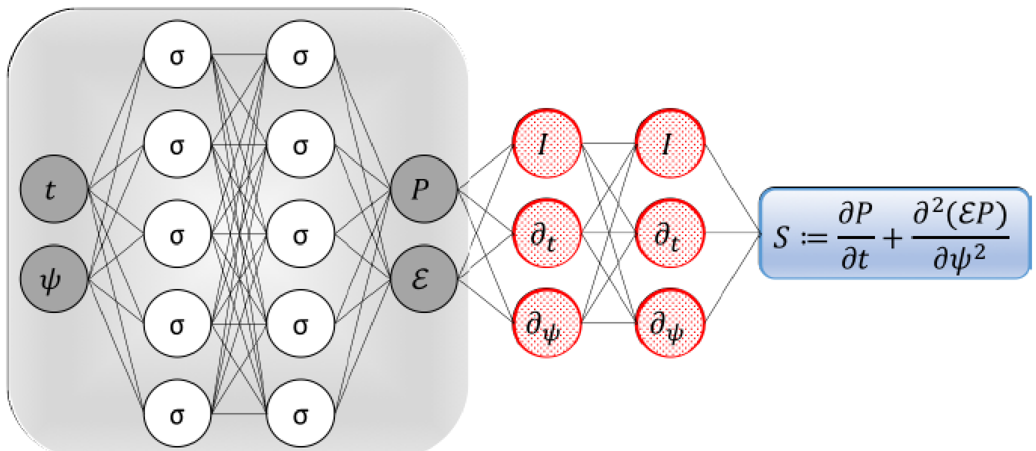

$$\sigma(x) = x \ \mathrm{sigmoid}(x)$$

Hidden layers: 10

Neurons per layers: 50

Conditional Expected Diffusion

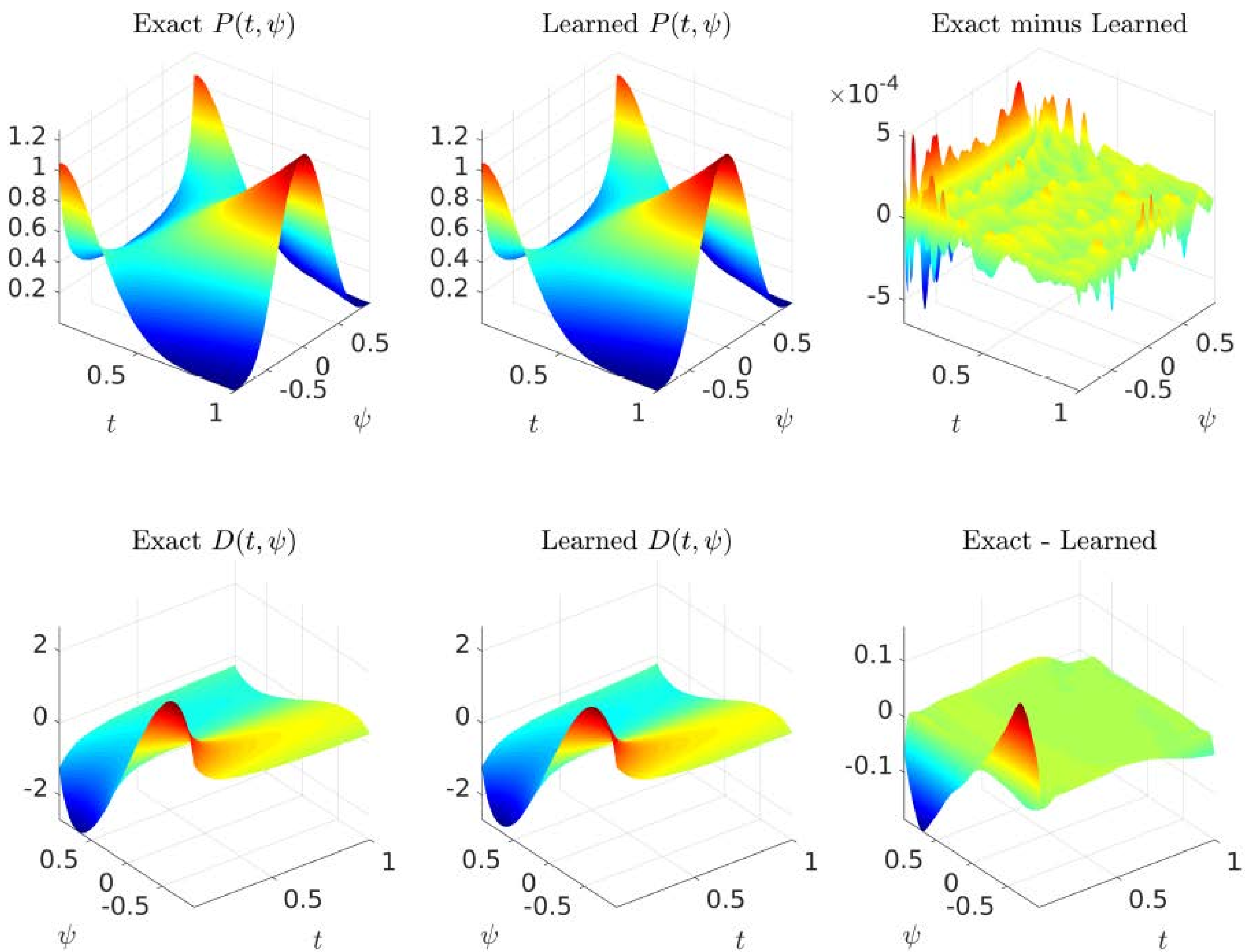

Deep Learning of Turbulent Scalar Mixing, M. Raissi, H. Babaee, P. Givi https://arxiv.org/abs/1811.07095.

Conditional Expected Diffusion

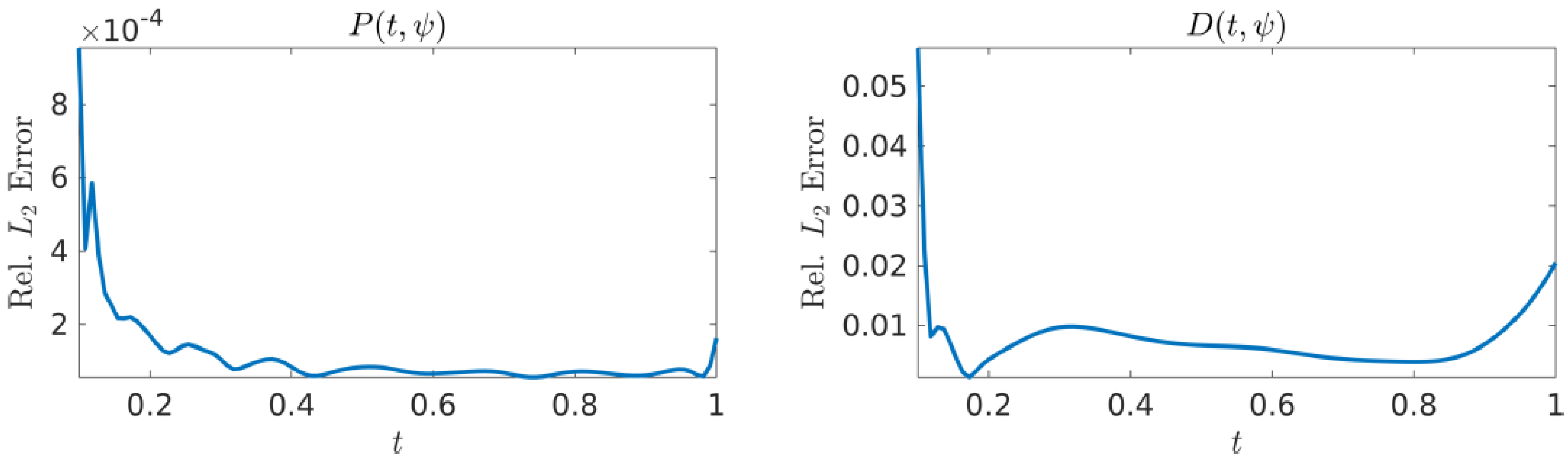

Conditional Expected Dissipation

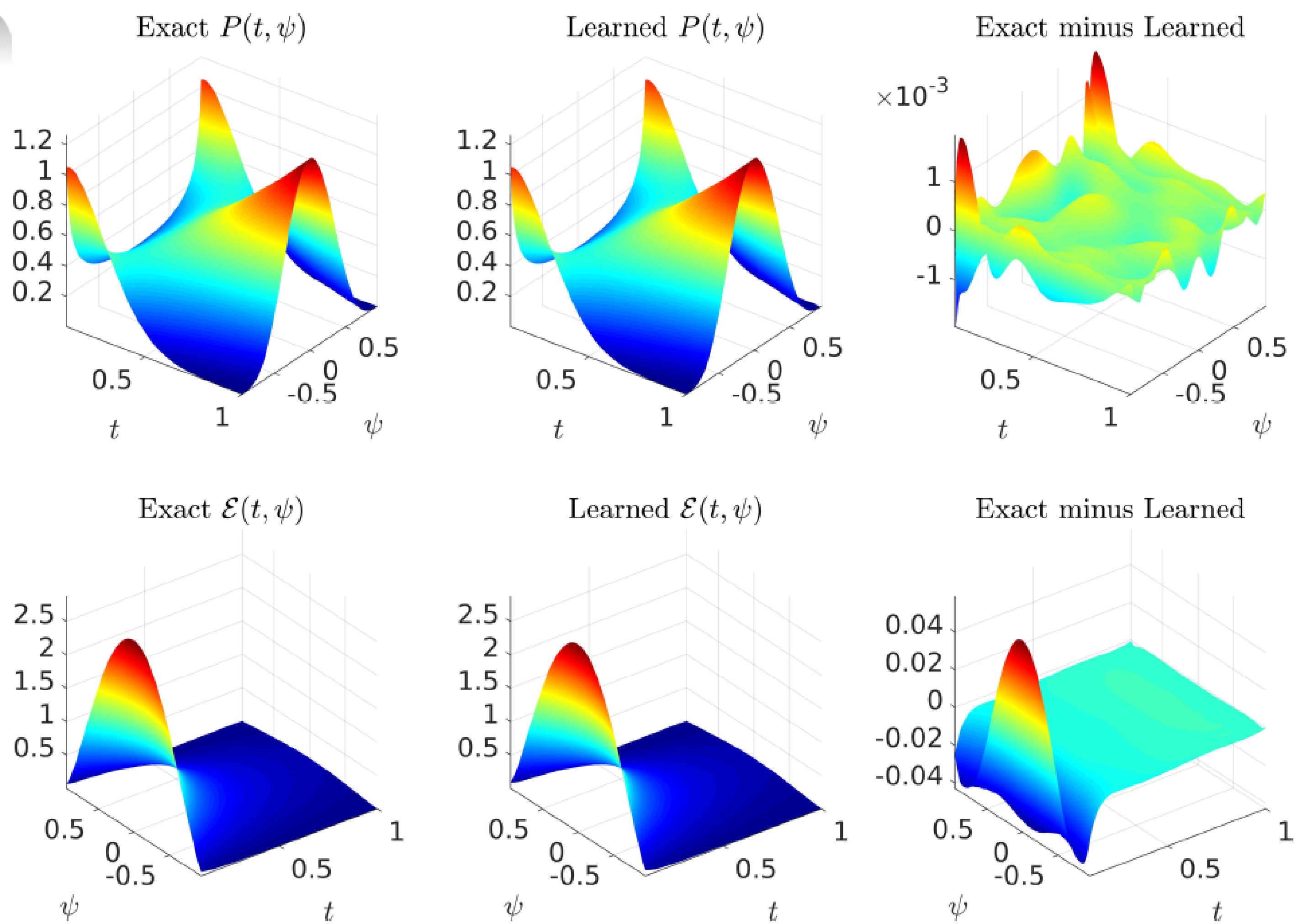

Deep Learning of Turbulent Scalar Mixing, M. Raissi, H. Babaee, P. Givi https://arxiv.org/abs/1811.07095.

Conditional Expected Dissipation

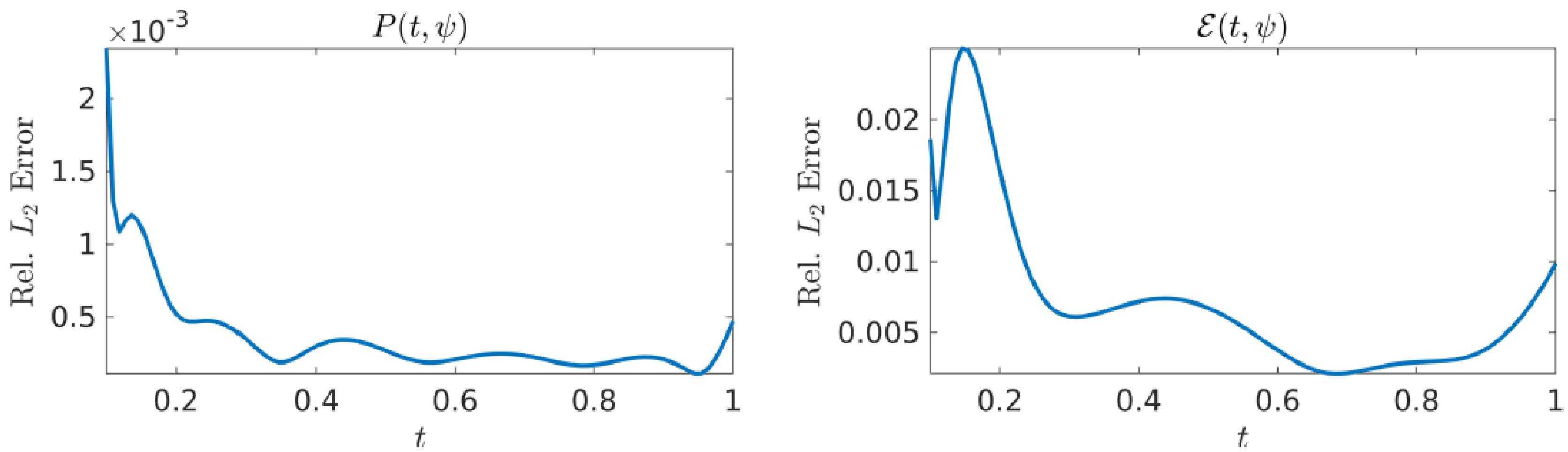

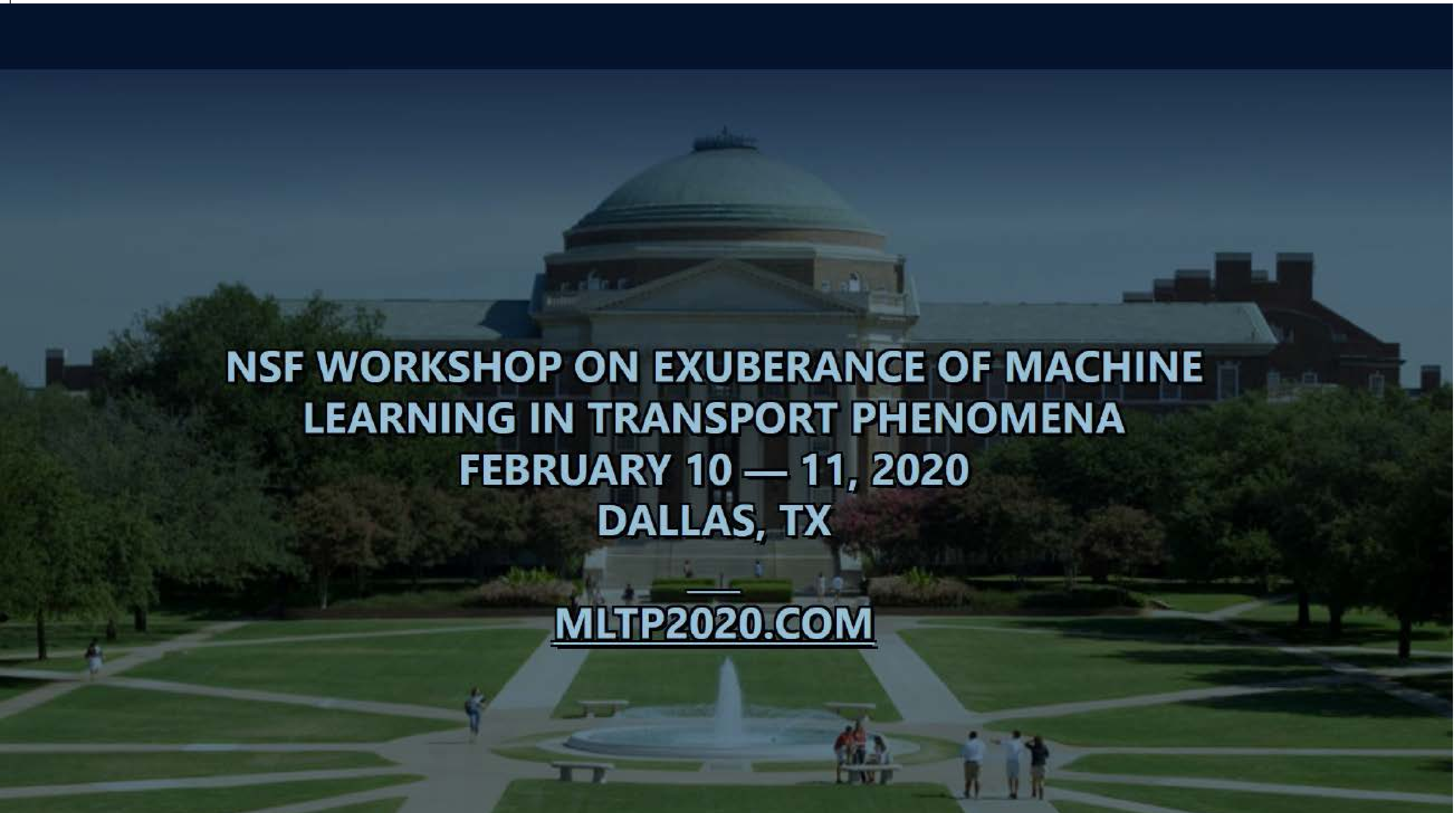
NSF WORKSHOP ON EXUBERANCE OF MACHINE
LEARNING IN TRANSPORT PHENOMENA
FEBRUARY 10 — 11, 2020
DALLAS, TX
MLTP2020.COM

Thank you!

Neural Network Regression

$$\left.\begin{aligned} y_i = f(x_i) + \epsilon_i, \quad \epsilon_i \sim \mathcal{N}\left(0, \sigma^2\right), \quad i = 1, \ldots, N \\ \mathbf{y} = f(\mathbf{x}) + \epsilon, \quad \epsilon \sim \mathcal{N}\left(\mathbf{0}, \sigma^2\mathbf{I}\right) \end{aligned}\right\}\ \text{Data}$$

$$\left.\begin{aligned} f(x) &= W^L h^L + b^L \\ h^L &= \tanh(W^{L-1} h^{L-1} + b^{L-1}) \\ &\vdots \\ h^1 &= \tanh(W^0 x + b^0) \end{aligned}\right\}\ \text{Prior}$$

$$\left.\begin{aligned} \mathbf{y} \sim \mathcal{N}\left(f(\mathbf{x}), \sigma^2\mathbf{I}\right) \\ \min_{W,b}\ (\mathbf{y} - f(\mathbf{x}))'(\mathbf{y} - f(\mathbf{x})) \\ \min_{W,b} \sum_{i=1}^{N} |y_i - f(x_i)|^2 \end{aligned}\right\}\ \text{Training}$$

$$\left. f(x^*) \right\}\ \text{Prediction}$$

Goodfellow, Ian, et al. *Deep learning*. Vol. 1. Cambridge: MIT press, 2016.

INVESTIGATION OF SCALAR-SCALAR-GRADIENT FILTERED DENSITY FUNCTION

Chenning Tong
Clemson University

Supported by NSF

Introduction

- In scalar FDF methods, reaction rate term closed
- Scalar FDF contains no small-scale scalar information. Mixing needs modeling
- Effects of reaction on mixing (diffusion/dissipation) must also be modeled
- Difficult to apply to different combustion regimes without assumptions about flame structure

Scalar-scalar-gradient FJDF

$$f_{\varphi\psi}\left(\hat{\varphi},\hat{\psi};\underline{x},t\right)=\int\delta\left[\varphi\left(\underline{x}',t\right)-\hat{\varphi}\right]\prod_{i=1}^{3}\delta\left[\psi_i\left(\underline{x}',t\right)-\hat{\psi}_i\right]G\left(\underline{x}'-\underline{x}\right)d\underline{x}'$$

$$\frac{\partial f_{\varphi\psi}}{\partial t}+\frac{\partial}{\partial x_k}\left\{\left\langle u_k\middle|\hat{\varphi},\hat{\psi}\right\rangle_L f_{\varphi\psi}\right\}=-\frac{\partial}{\partial\hat{\varphi}}\left\{\left\langle D\frac{\partial^2\varphi}{\partial x_k\partial x_k}\middle|\hat{\varphi},\hat{\psi}\right\rangle_L f_{\varphi\psi}\right\}$$
$$-\frac{\partial}{\partial\hat{\psi}_i}\left\{\left\langle D\frac{\partial^2\psi_i}{\partial x_k\partial x_k}\middle|\hat{\varphi},\hat{\psi}\right\rangle_L f_{\varphi\psi}\right\}+\frac{\partial}{\partial\hat{\psi}_i}\left\{\left\langle \psi_k\frac{\partial u_i}{\partial x_k}\middle|\hat{\varphi},\hat{\psi}\right\rangle_L f_{\varphi\psi}\right\}$$
$$-\frac{\partial}{\partial\hat{\varphi}}\left\{\omega(\hat{\varphi})f_{\varphi\psi}\right\}-\frac{\partial}{\partial\hat{\psi}_i}\left\{\hat{\psi}_i\omega(\hat{\varphi})f_{\varphi\psi}\right\}$$

Alternative mixing terms

$$\left\langle D\frac{\partial\psi_i}{\partial x_k}\frac{\partial\psi_j}{\partial x_k}\middle|\hat{\varphi},\hat{\psi}\right\rangle_L,\ D\hat{\psi}_j\left\langle\frac{\partial\psi_i}{\partial x_j}\middle|\hat{\varphi},\hat{\psi}\right\rangle_L$$

Introduction

- Scalar-scalar-gradient FJDF contains information on the scalar dissipation (Pope 1990)
- Effects of reaction on scalar dissipation (mixing) closed
- Capable of handling different regimes
- Diffusion of the scalar-gradient needs modeling
- We investigate the FJDF and the mixing terms in its transport equation

Turbulent jet facility

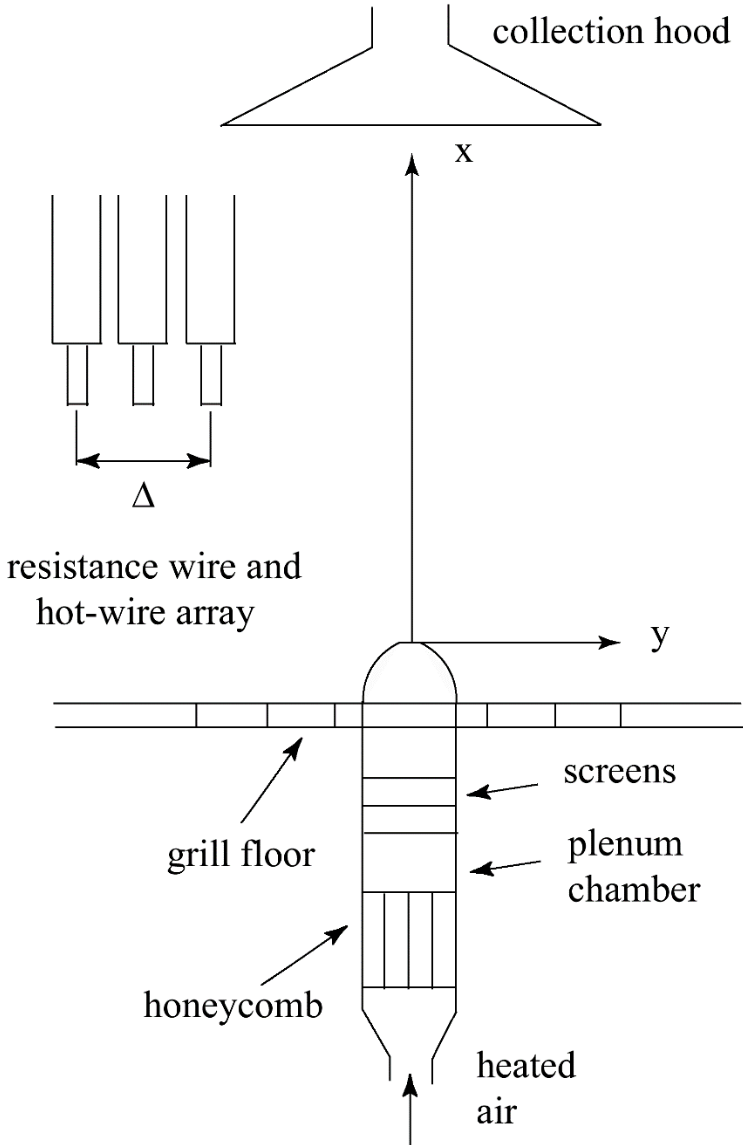

$$R_{ej} = 40{,}000$$

$$R_{\lambda} = 233$$

Passive temperature fluctuations used as a conserved scalar

Δ=20 mm, η_{φ} =0.22 mm

Scalar-scalar-gradient FJDF

$$f_{\varphi\psi}\left(\hat{\varphi},\hat{\psi};\underline{x},t\right)=\int\delta\left[\varphi\left(\underline{x}',t\right)-\hat{\varphi}\right]\prod_{i=1}^{3}\delta\left[\psi_i\left(\underline{x}',t\right)-\hat{\psi}_i\right]G\left(\underline{x}'-\underline{x}\right)d\underline{x}'$$

$G(x)$ is a top hat filter

FJDF a random variable

Analyze conditionally averaged FJDF

$$\left\langle f_{u\psi}\middle|\left\langle\varphi\right\rangle_L,\left\langle\varphi''^2\right\rangle_L\right\rangle$$

Scalar-scalar-gradient FJDF

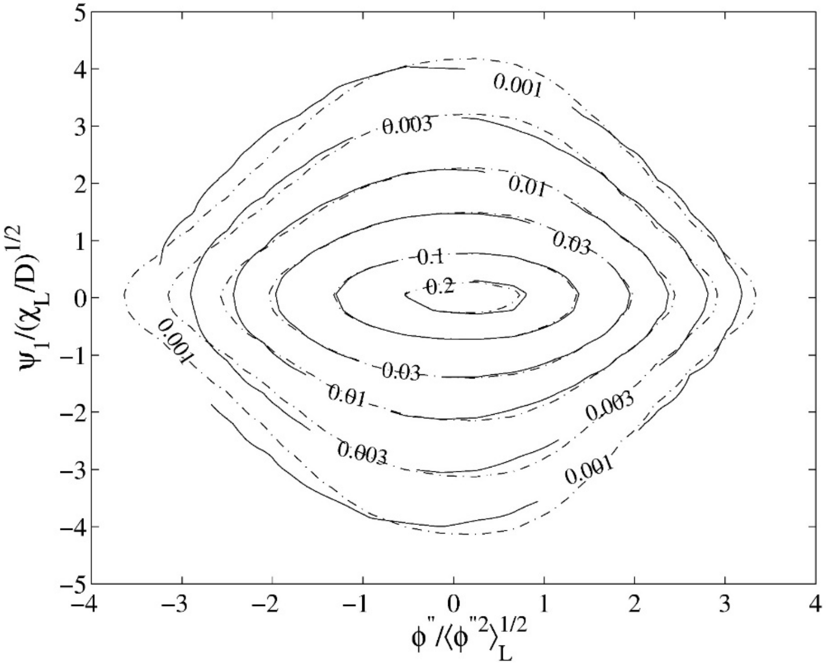

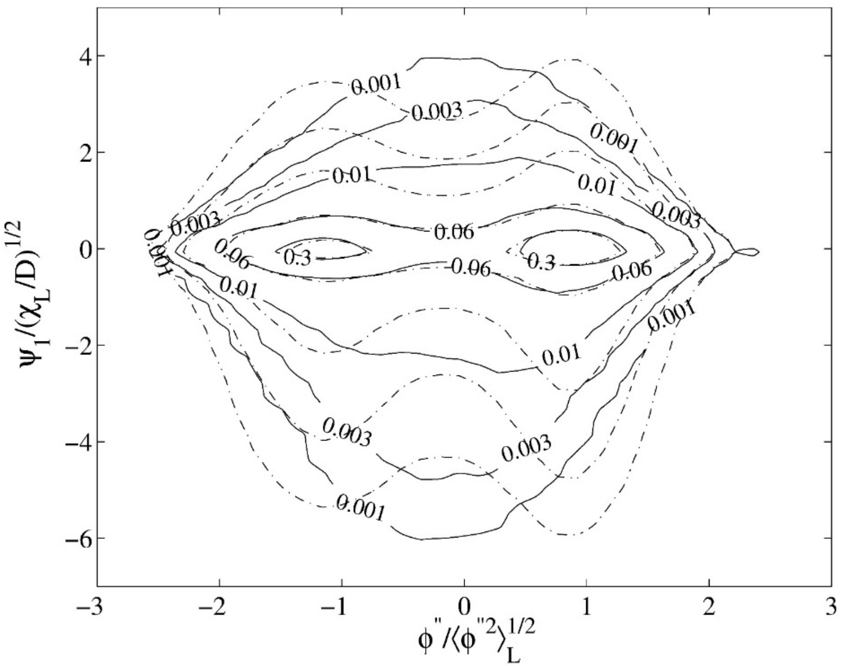

$\langle\varphi\rangle_L = \langle\varphi\rangle$ $\quad \langle\varphi''^2\rangle_L/\langle\varphi''^2\rangle = 0.3$

$\langle\varphi''^2\rangle_L/\langle\varphi''^2\rangle = 11$

Scalar-scalar-gradient FJDF

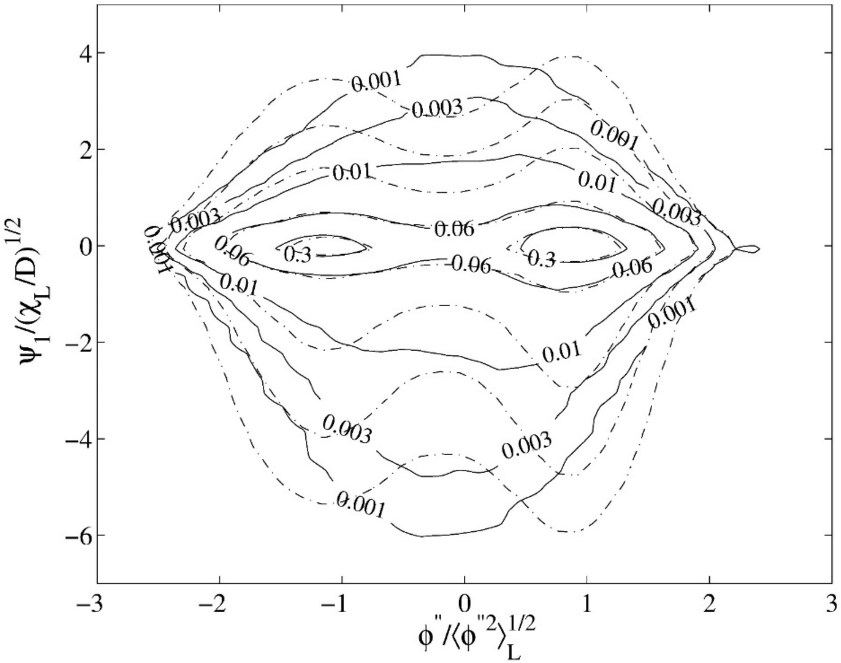

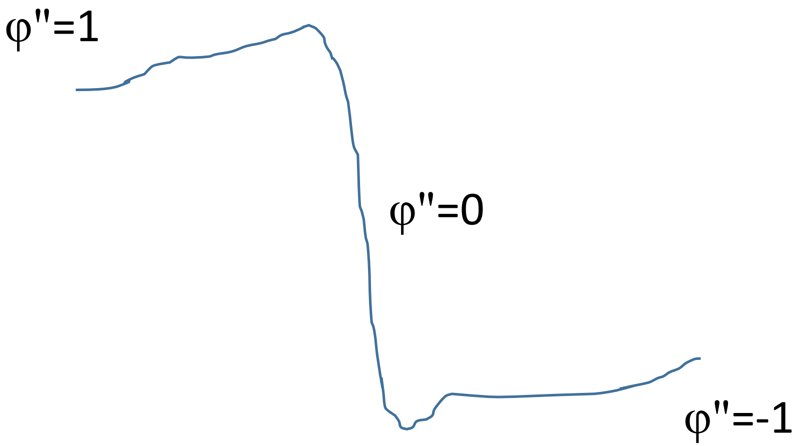

$\langle\varphi''^2\rangle_L/\langle\varphi''^2\rangle=11$

Conditional scalar gradient FDF

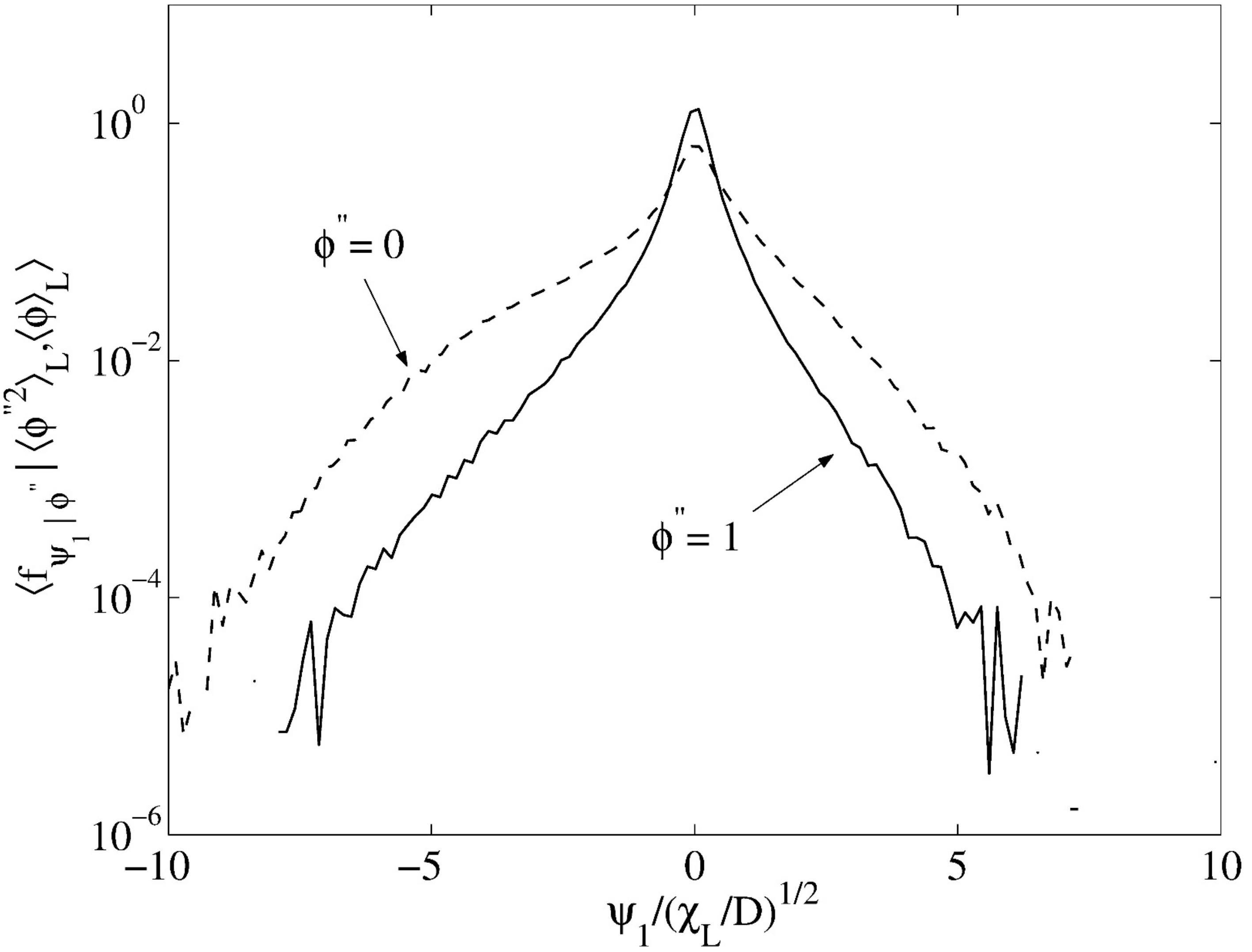

Conditionally filtered scalar-gradient diffusion

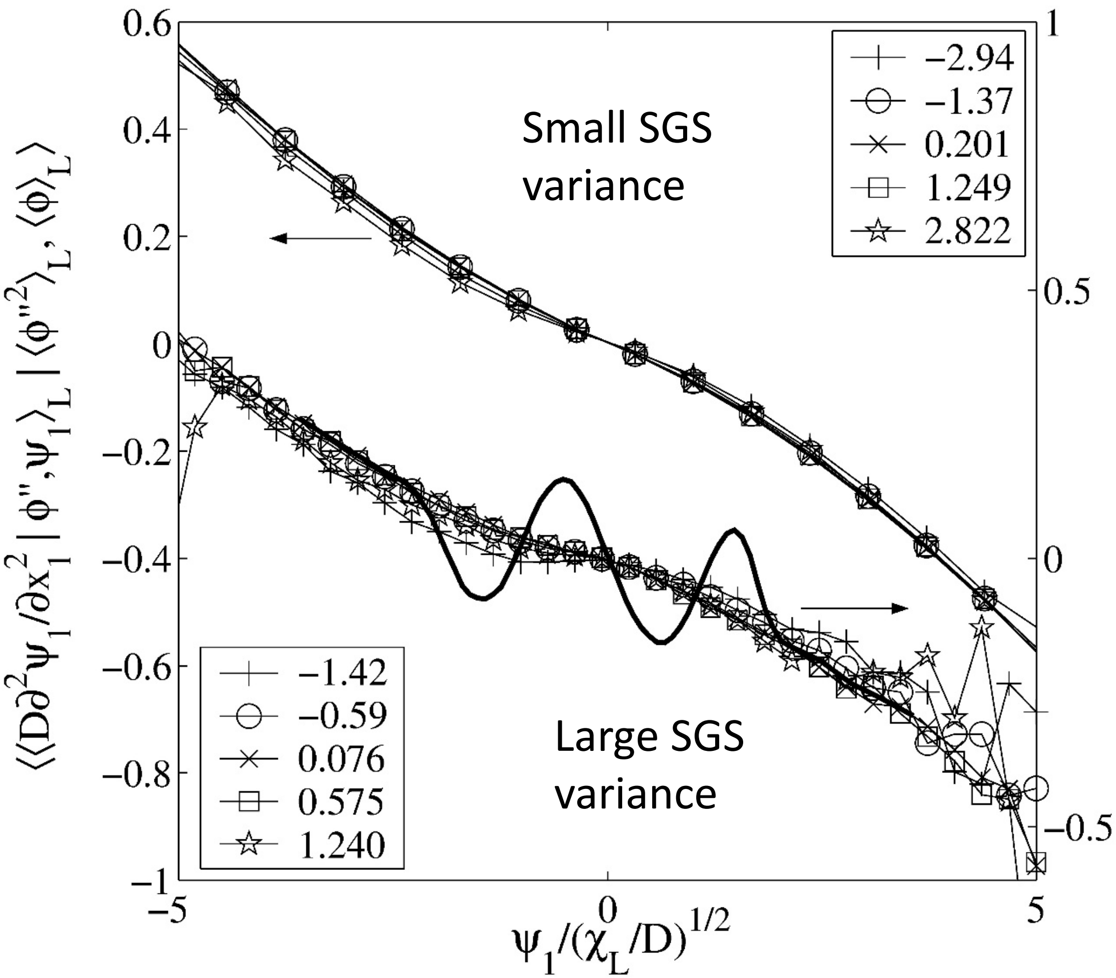

Conditionally filtered scalar-gradient dissipation

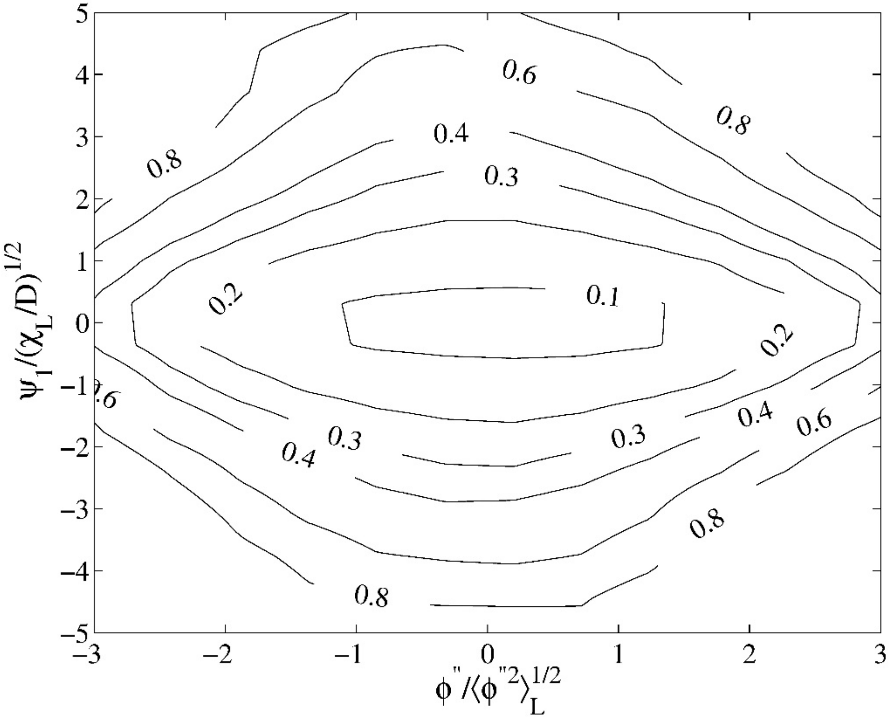

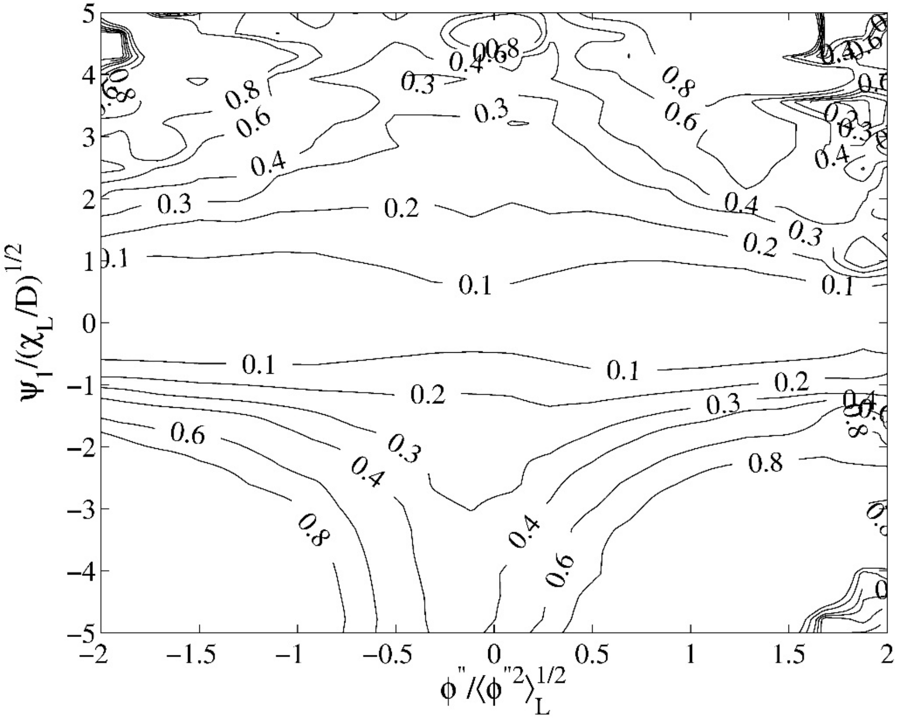

$\langle\varphi\rangle_L = \langle\varphi\rangle$ $\quad \langle\varphi''^2\rangle_L/\langle\varphi''^2\rangle = 0.3$

$\langle\varphi''^2\rangle_L/\langle\varphi''^2\rangle = 11$

Conditionally filtered scalar-gradient production

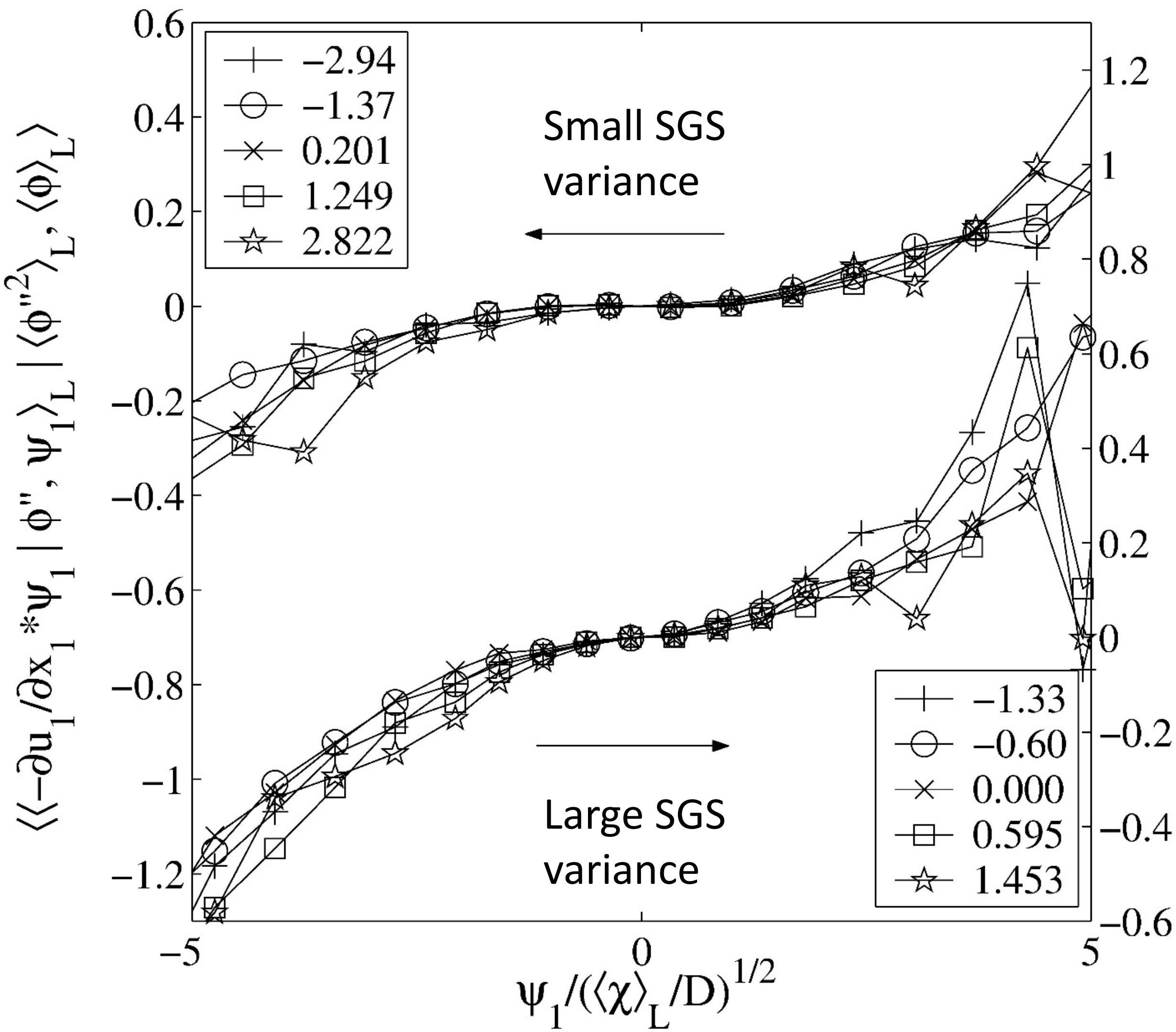

Conclusions

1. Two SGS mixing regimes. Scalar and scalar gradient nearly independent for small SGS variance

2. Scalar-scalar-gradient FJDF is bimodal, consistent with ramp-cliff structure for large SGS variance

3. High values of scalar-gradient dissipation for large SGS variance concentrated in the cliff

4. Greater scalar-gradient production for large SGS variance

5. Implications for modeling the FJDF

High order methods for the solution of transport equations

Gustaaf Jacobs, Hareshram Natarajan
Aerospace Engineering, San Diego State University

AFOSR
AIR FORCE OFFICE OF SCIENTIFIC RESEARCH

FA 9550-16-1-0008

DSEM LES

Discontinuous spectral element method [Kopriva 98]

- Approximate solution with higher-order (Jacobi) polynomial
- Collocation spectral method
- Map physical domain to master element
- Elements are connected through Riemann solvers

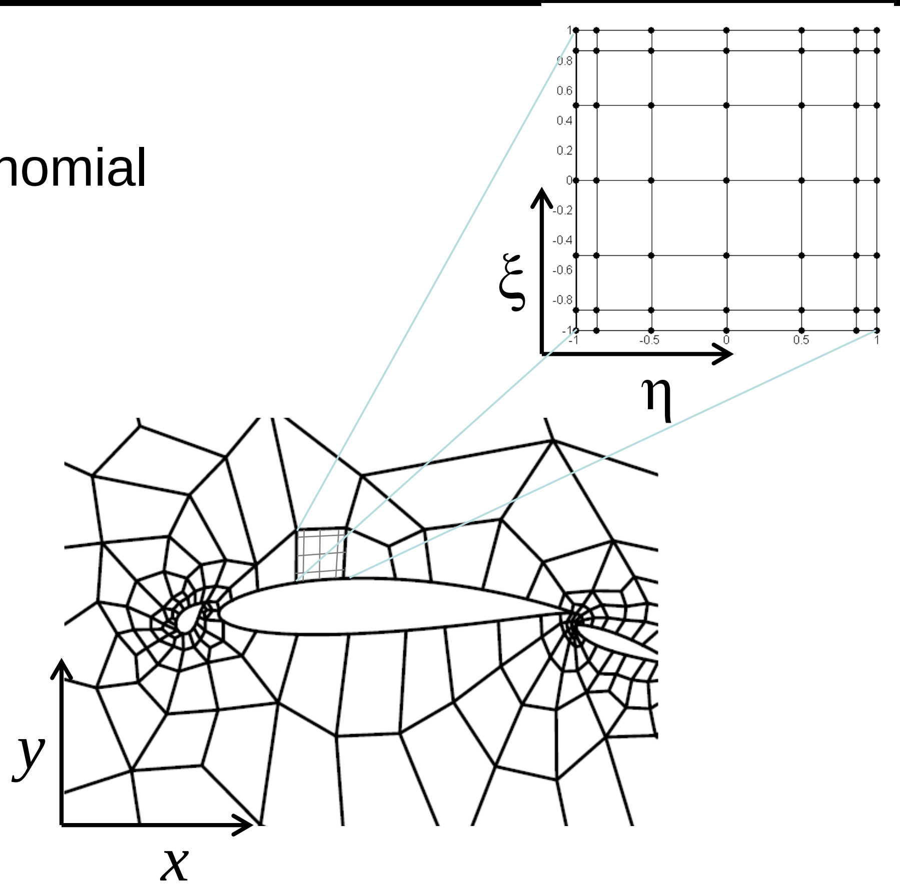

- Unstructured grids and non-overlapping elements
- High-order resolution
- Local and parallel
- Low dissipation and dispersion errors
- Explicit scheme

Can we formulate a numerical method to solve transport equations which is consistent with the DSEM-LES: preserve the favorable properties of DSEM?

Sengupta, K., Jacobs, G.B. and Mashayek, F. (2009), *Int. J. Num. Meth. Fluids,* 61(3)

Lagrangian vs semi-Lagrangian Methods

Lagrangian

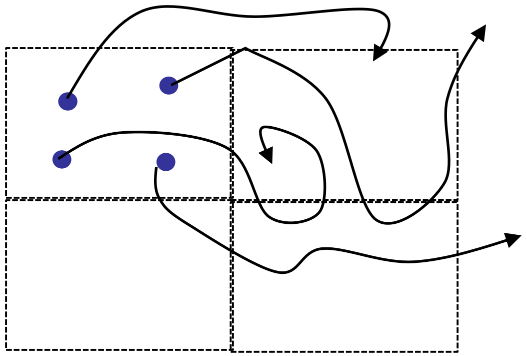

- Particles tracked over the entire flow field
- FDF obtained by local sampling
  - ➢ Conservative
  - ❖ Coupling with Eulerian solvers, tracking particles, locality

Semi-Lagrangian

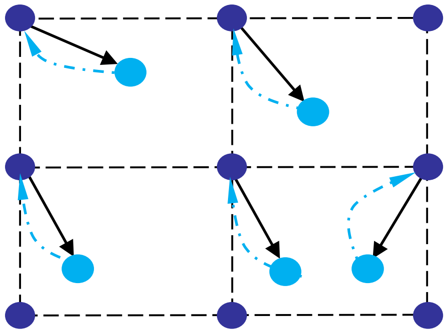

- ▪ Local, parallel, semi-fixed grid
- ❖ Conservation

Objective: Formulate a semi-Lagrangian method consistent with DSEM

DSEM-SL Numerical method

1)The physical domain is divided into E non-overlapping elements. $\Omega = \bigcup_{e=1}^{E} \Omega_e$.

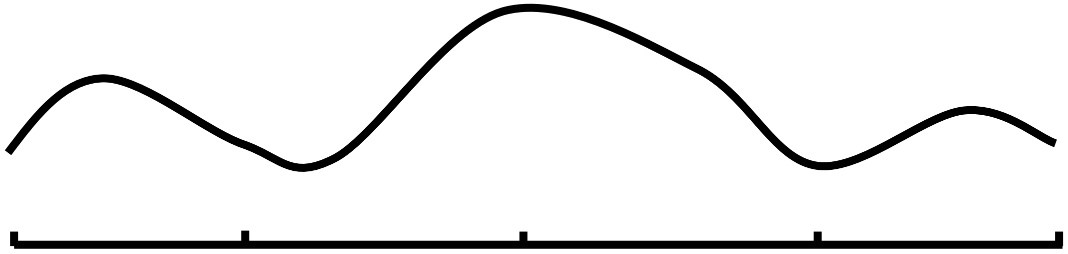

2)Initialize particles.

Within each element, the particles are initialized on the Chebyshev-Gauss quadrature nodes.

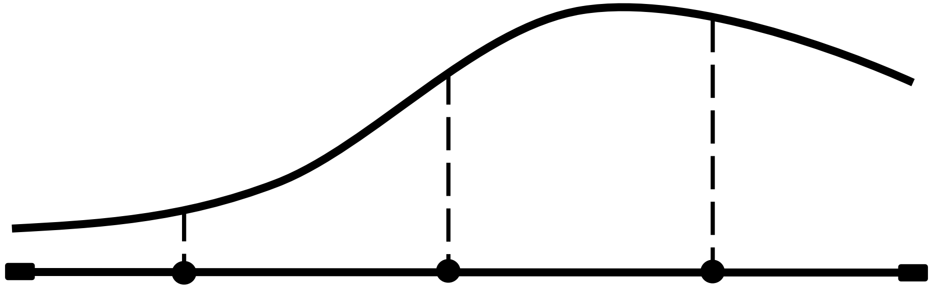

Chebyshev- Gauss quadrature nodes

$$\xi_i^p = cos\left(\frac{(2i+1)\pi}{2P}\right)$$

Boundary points

$$\phi^n(\xi) = \sum_{i=0}^{P-1} \hat{\phi}^n(\xi_i^p) l_i(\xi)$$

$l_i(\xi)$: Lagrange polynomials

$$l_i(\xi) = \Pi_{\mathrm{j}=0, i\neq \mathrm{j}}^{\mathrm{N}-1} \frac{\xi - \xi_i^p}{\xi_j^p - \xi_i^p}$$

[Natarajan and Jacobs, C&F, 2020]

DSEM-SL Numerical method

3) Explicit forward time integration.

N_s number of samples.

For each sample, trace the particles in 1 time step.

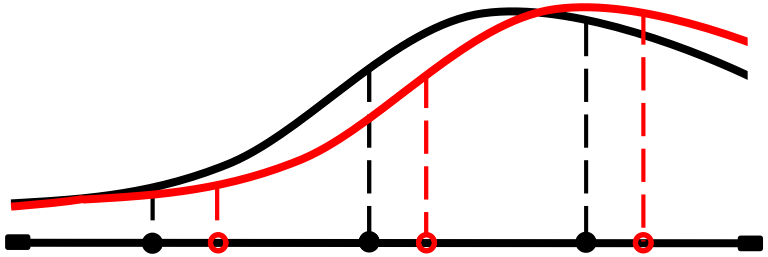

Advected position,

$$\xi^{\star} = \xi^{p} + \boxed{\Delta t\, u(\xi^{p}, t^{n})} + \boxed{\sigma\, N(0, \Delta t)}$$

Drift Term   Diffusion Term

Initial position, ξ^{p}

Advected solution, $\phi^{\star}(\xi)$

$$\phi^{\star}(\xi) = \sum_{i=0}^{N-1} \hat{\phi}^{\star}(\xi_i^{\star})\, l_i^{\star}(\xi)$$

$l_i^{\star}(\xi)$: Lagrange polynomials

$$l_i^{\star}(\xi) = \Pi_{\mathrm{j}=0, i\neq \mathrm{j}}^{\mathrm{N}-1} \frac{\xi - \xi_i^{\star}}{\xi_j^{\star} - \xi_i^{\star}}$$

4) Boundary treatment

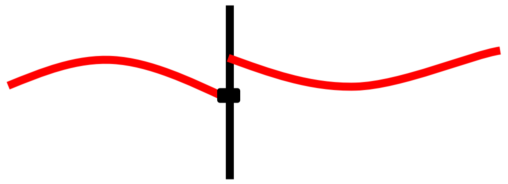

- Current approach
  - Element boundaries fixed
  - Upwinding to update the boundary values at next time,

    $\hat{\phi}^{n+1}\left(\xi_{left}\right)$ and $\hat{\phi}^{n+1}\left(\xi_{right}\right)$
  - Easy to parallelize

5) Remapping for each sample

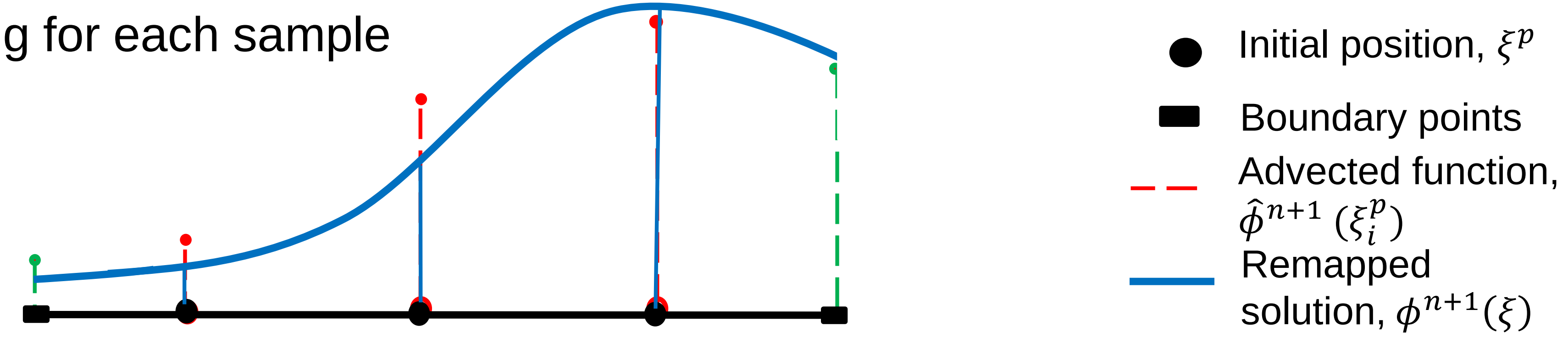

Boundary constraints

$$\sum_{i=0}^{N-1} \phi^{n+1}(\xi^p)\, l_i(\xi_{right}) = \hat{\phi}^{n+1}(\xi_{right})$$

$$\sum_{i=0}^{N-1} \phi^{n+1}(\xi^p)\, l_i(\xi_{left}) = \hat{\phi}^{n+1}(\xi_{left})$$

Least squares is used to solve the overdetermined system for each sample

DSEM-SL Numerical method

6) Solution

$$
\begin{array}{r}
\\
\\
\\
\\
\text{Boundary} \\
\text{constraint} \\
\text{Mass constraint} \\
\text{Energy constraint}
\end{array}
\begin{bmatrix}
1 & 0 & \dots & 0 \\
0 & 1 & \dots & 0 \\
\vdots & & & \\
0 & 0 & \dots & 1 \\
l_0(\xi_{right}) & l_0(\xi_{right}) & \dots & l_{N-1}(\xi_{right}) \\
l_0(\xi_{left}) & l_0(\xi_{left}) & \dots & l_{N-1}(\xi_{left}) \\
w_0 & w_1 & \dots & w_{N-1} \\
A_0 & A_1 & \dots & A_{N-1}
\end{bmatrix}
\begin{bmatrix}
\widehat{\phi^{n+1}}(\xi_0^p) \\
\vdots \\
\widehat{\phi^{n+1}}(\xi_{N-1}^p)
\end{bmatrix}
=
\begin{bmatrix}
\hat{\phi}^{n+1}(\xi_0^p) \\
\hat{\phi}^{n+1}(\xi_1^p) \\
\vdots \\
\hat{\phi}^{n+1}(\xi_{N-1}^p) \\
\hat{\phi}^{n+1}(\xi_{right}^p) \\
\hat{\phi}^{n+1}(\xi_{left}^p) \\
M^n + \Delta t\, \mathcal{F}_m^n \\
E^n + \Delta t\, \mathcal{F}_e^n
\end{bmatrix}
$$

(N+4) x N   N x 1   (N+4) x 1

Results: 1D Advection equation

$$\frac{\partial \phi}{\partial t} + u \frac{\partial \phi}{\partial x} = -\phi \frac{\partial u}{\partial x}$$

Conditions

- $\phi(x,0) \quad = \sin\left(2\tan^{-1}\left[\exp(-1)\tan\left(\frac{x}{2}\right)\right]\right); x \in [0,1]$
- $u \quad = -\sin(x)$
- Periodic boundary conditions

Numerical Parameters

- H, No. of elements $\quad = \; 3,4,5,6$
- P, Polynomial order $\quad = \; 3,4,5,6,7$
- $\lambda \quad = \; 1; \quad (\Delta t = \lambda \, \Delta x_{min})$

Time evolution: 1D Advection equation

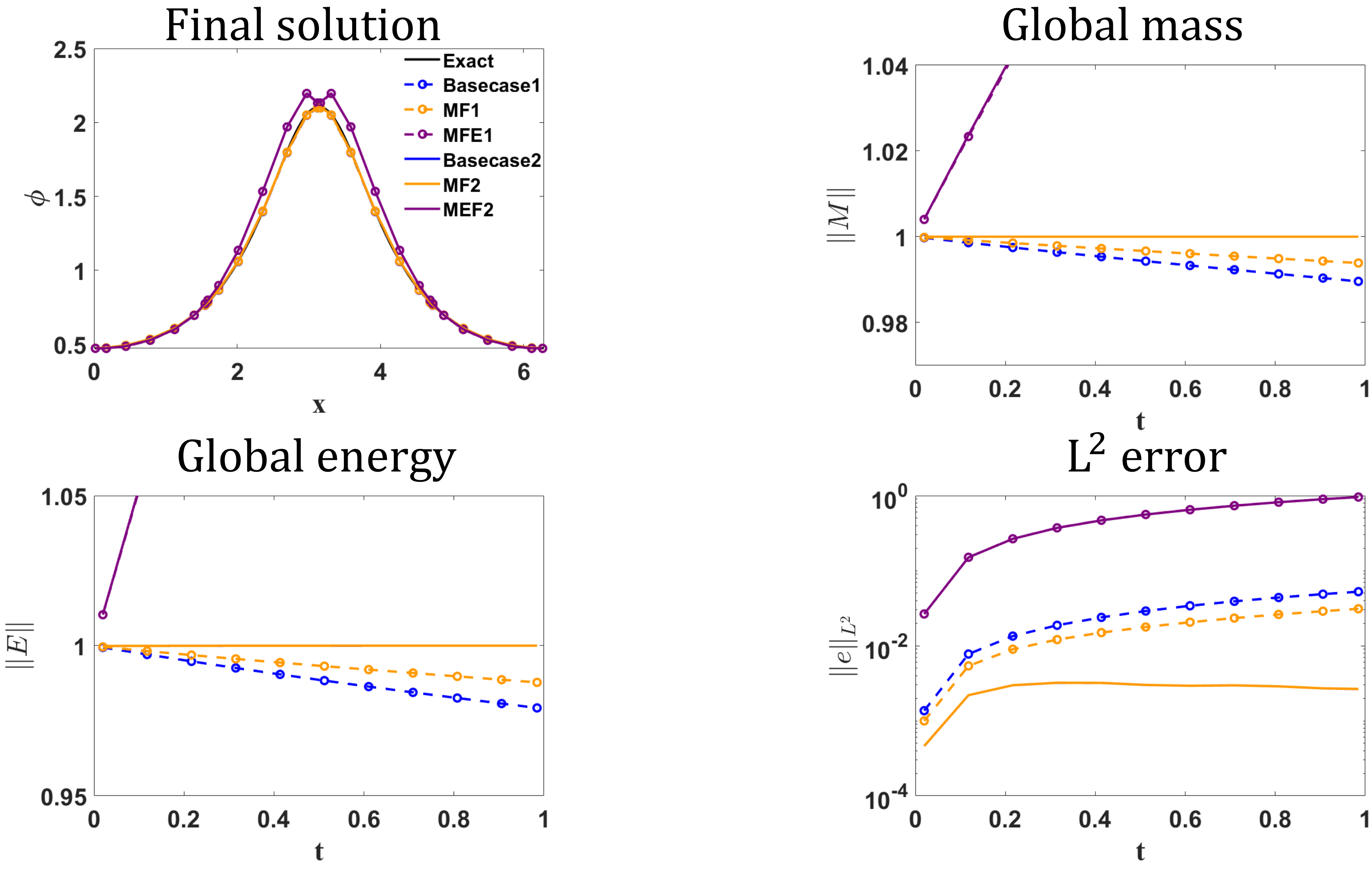

P convergence: 1D Advection equation

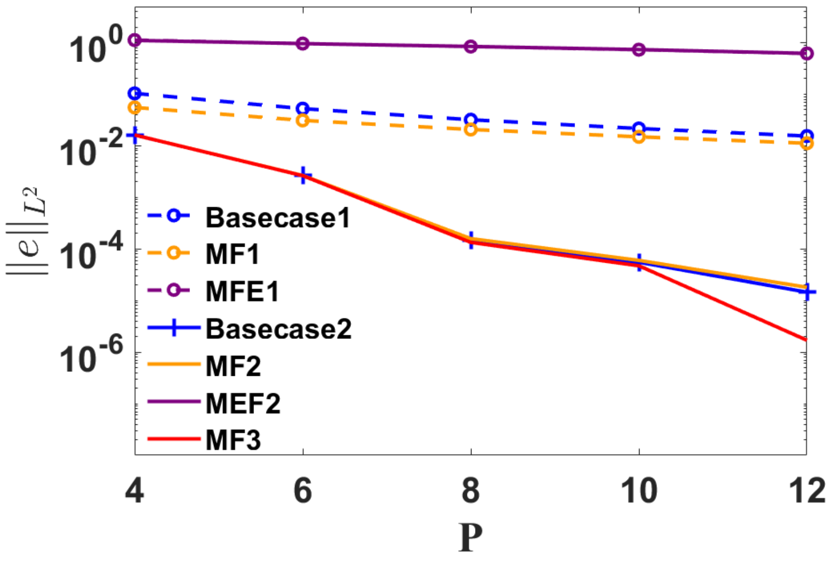

$\lambda = 1$

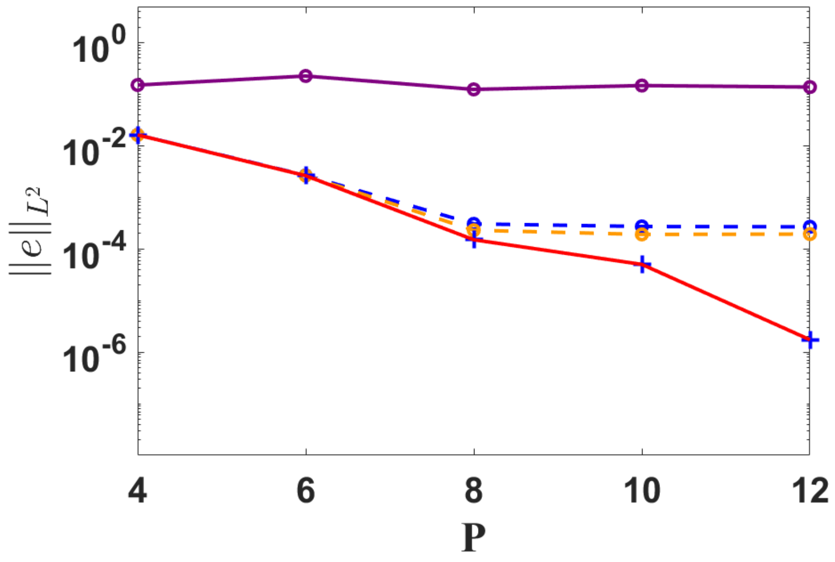

$\Delta t = 1e - 4$

Results: 2D Advection equation

$$\frac{\partial \phi}{\partial t} + u\frac{\partial\ \phi}{\partial x} + v\frac{\partial \phi}{\partial y} = 0$$

Conditions

- $\phi(x, y, 0) \ = \ \sin(2\pi x)\sin(2\pi y) \ ; x, y \in [0, 1]$
- $u \qquad = 2$
- $v \qquad = 1$
- Periodic boundary conditions

Numerical Parameters

- H, No. of elements = 4x4
- P, Polynomial order = 3,4,5,6,7
- λ = 1;

Time evolution: 2D Advection equation

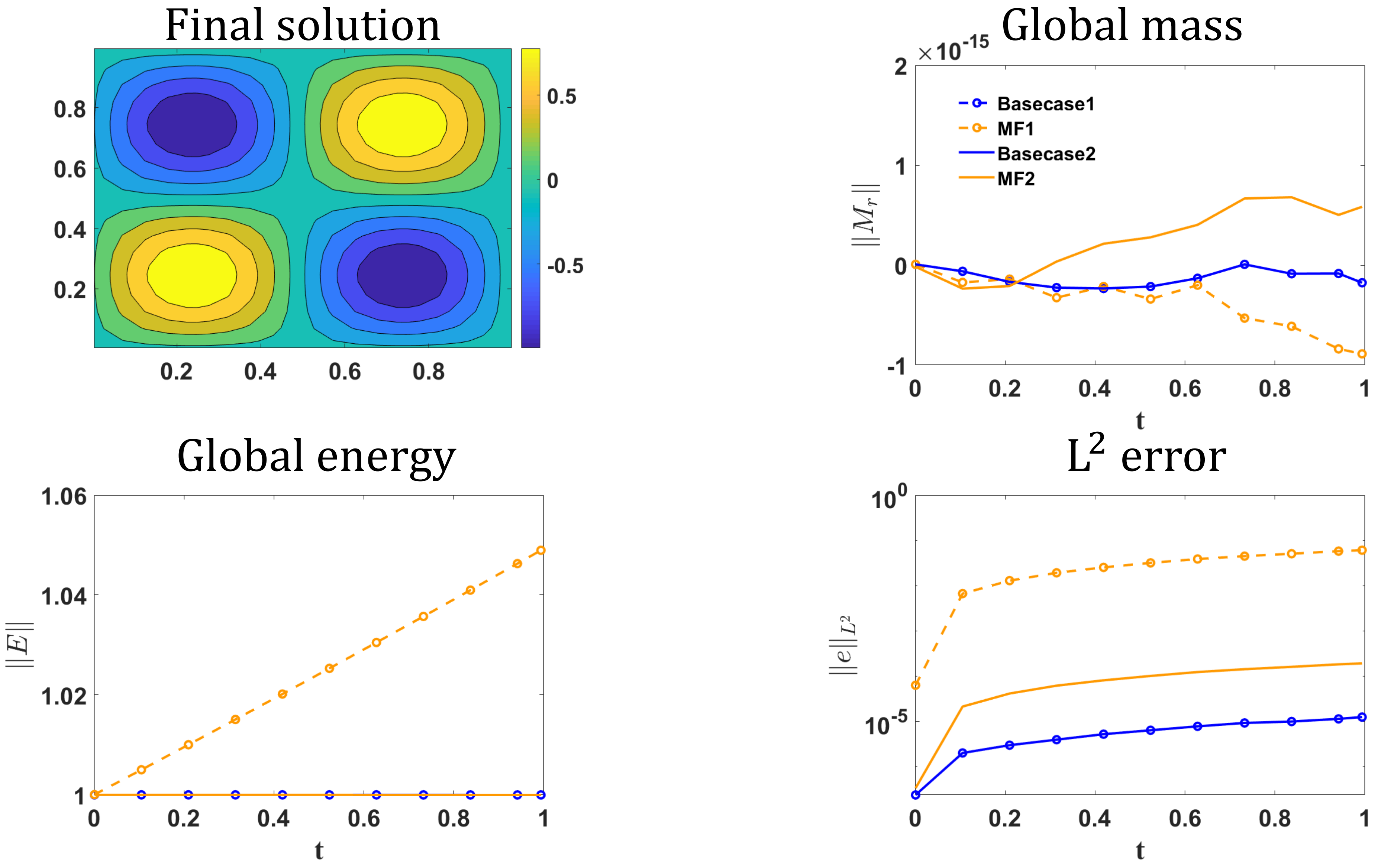

Conclusions

- A semi-Lagrangian method is developed for the solution of transport equations that is consistent with Eulerian DSEM solvers:
  - Local and parallel
  - High-order convergent
  - Boundary fitted
  - Extends easy to multi-dimensions

LES Approaches to combustion

Imperial College London

Combustion LES and the stochastic fields method

D Fredrich and W P Jones

Department of Mechanical Engineering

Imperial College London

London SW7 2AZ

In Memoria of Professor Ted O'Brien

APS Division of Fluid Dynamics
November 23–26, 2019 Seattle, Washington

The Preccinsta Combustor

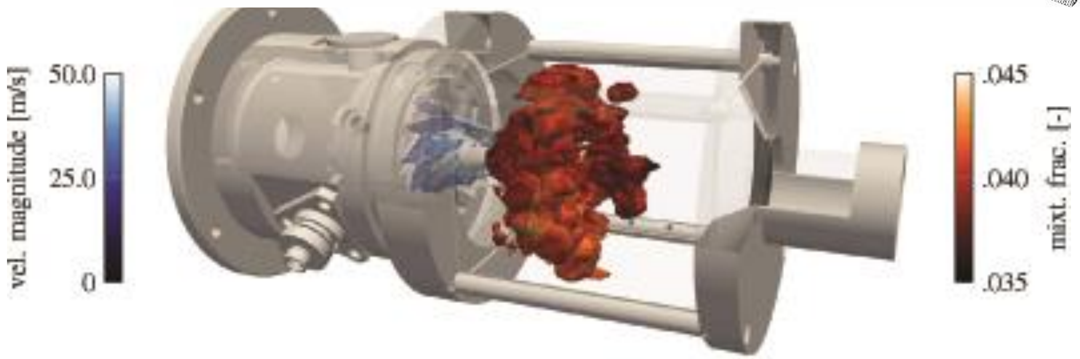

Iso-surfaces of the instantaneous CH4 mass fraction (left) and heat release rate (right) coloured by, respectively, the velocity magnitude and mixture fraction - $\phi = 0.7$.

Filtered Equations of Motion

$$\frac{\partial \overline{\rho}}{\partial t} + \frac{\partial \overline{\rho}\widetilde{u}_i}{\partial x_i} = 0$$

$$\frac{\partial \overline{\rho}\widetilde{u}_i}{\partial t} + \frac{\partial \overline{\rho}\widetilde{u}_i\widetilde{u}_j}{\partial x_i} = -\frac{\partial \overline{p}}{\partial x_j} + \frac{\partial}{\partial x_i}\mu\left[\left(\frac{\partial \overline{u}_i}{\partial x_j} + \frac{\partial \overline{u}_j}{\partial x_i}\right) - \frac{2}{3}\frac{\partial \overline{u}_k}{\partial x_k}\delta_{ij}\right] - \frac{\partial \tau_{ij}^{sgs}}{\partial x_i}$$

$$\frac{\partial \overline{\rho}\widetilde{n}_\alpha}{\partial t} + \frac{\partial \overline{\rho}\widetilde{u}_i\widetilde{n}_\alpha}{\partial x_i} = \overline{\rho\dot{\omega}_\alpha} - \frac{\partial}{\partial x_i}\left[\overline{J}_{\alpha,i} + \overline{\rho}\left(\widetilde{u_i n_\alpha} - \widetilde{u}_i\widetilde{n}_\alpha\right)\right]$$

$$\frac{\partial \overline{\rho}\widetilde{h}_t}{\partial t} + \frac{\partial \overline{\rho}\widetilde{u}_i\widetilde{h}_t}{\partial x_i} = \frac{\partial \overline{p}}{\partial t} - \frac{\partial}{\partial x_i}\left[\overline{J}_{h,i} + \overline{\rho}\left(\widetilde{u_i h_t} - \widetilde{u}_i\widetilde{h}_t\right)\right]$$

Sub-grid stresses: Dynamic Smagorinsky model

Combustion: Sub-Grid Pdf Equation Method

Fine grained pdf
$$F\left(\underline{\psi};\mathbf{x},t\right)=\prod_{\alpha=1}^{N_s}\delta\left(\psi_\alpha-\phi_\alpha\left(\mathbf{x},t\right)\right)$$

Sub-grid Pdf
$$\bar{\rho}\tilde{P}_{sgs}\left(\underline{\psi};\mathbf{x},t\right)=\int_\Omega\rho\left(\mathbf{x}',t\right)\mathrm{F}\left(\underline{\psi};\mathbf{x}',t\right)G(\mathbf{x}-\mathbf{x}';\Delta)\,dx'$$

The modelled sub-grid Pdf Equation [1], [2]

$$\bar{\rho}\frac{\partial\tilde{P}_{sgs}\left(\underline{\psi}\right)}{\partial t}+\bar{\rho}\tilde{u}_j\frac{\partial\tilde{P}_{sgs}\left(\underline{\psi}\right)}{\partial x_j}-\frac{\partial}{\partial x_j}\left(\frac{\mu}{\sigma}\frac{\partial\bar{P}_{sgs}\left(\underline{\psi}\right)}{\partial x_j}\right)+\sum_{\alpha=1}^{N}\frac{\partial\bar{\rho}\dot{\omega}_\alpha\left(\underline{\psi}\right)\tilde{P}_{sgs}\left(\underline{\psi}\right)}{\partial\psi_\alpha}$$

$$-\frac{\mu}{\sigma}\sum_{\alpha=1}^{N}\sum_{\beta=1}^{N}\frac{\partial\tilde{\varphi}_\alpha}{\partial x_i}\frac{\partial\tilde{\varphi}_\beta}{\partial x_i}\frac{\partial^2 P\left(\underline{\psi}\right)}{\partial\psi_\alpha\partial\psi_\beta}=\frac{\partial}{\partial x_i}\left(\frac{\mu_{sgs}}{\sigma_{sgs}}\frac{\partial\tilde{P}_{sgs}\left(\underline{\psi}\right)}{\partial x_i}\right)$$

$$-\frac{C_d}{\tau_{sgs}}\sum_{\alpha=1}^{N}\frac{\partial}{\partial\psi_\alpha}\left[\left(\psi_\alpha-\tilde{\phi}_\alpha\left(\mathbf{x},t\right)\right)\bar{\rho}\tilde{P}\left(\underline{\psi}\right)\right]$$

Stochastic Field Solution Method

Represent *PDF* by *N* stochastic fields [3]

$\xi_\alpha^n(\mathbf{x},t)$ is advanced from t to $t+dt$ according to:

$$\bar{\rho} d\xi_\alpha^n = -\bar{\rho}\tilde{u}_i \frac{\partial \xi_\alpha^n}{\partial x_i} dt + \frac{\partial}{\partial x_i}\left[\left(\frac{\mu}{\sigma} + \frac{\mu_{sgs}}{\sigma_{sgs}}\right)\frac{\partial \xi_\alpha^n}{\partial x_i}\right] dt$$

$$+\left(2\bar{\rho}\frac{\mu_{sgs}}{\sigma_{sgs}}\right)^{1/2} \frac{\partial \xi_\alpha^n}{\partial x_i} dW_i^n(t) - 0.5 C_d \bar{\rho} \tau_{sgs}^{-1}\left(\xi_\alpha^n - \tilde{\phi}_\alpha^n\right) dt + \bar{\rho}\dot{\omega}_\alpha^n\left(\underline{\xi}^n\right) dt$$

where $1 \le n \le N$, $\quad dW_i^n \approx \eta_i^n \sqrt{dt}$

and η_i^n is a [-1,+1] dichotomic vector

Chemistry: *15 step / 19 species CH_4 mechanisms (Lu et al. 2008)*

PRECCINSTA: Spatial pressure oscillation

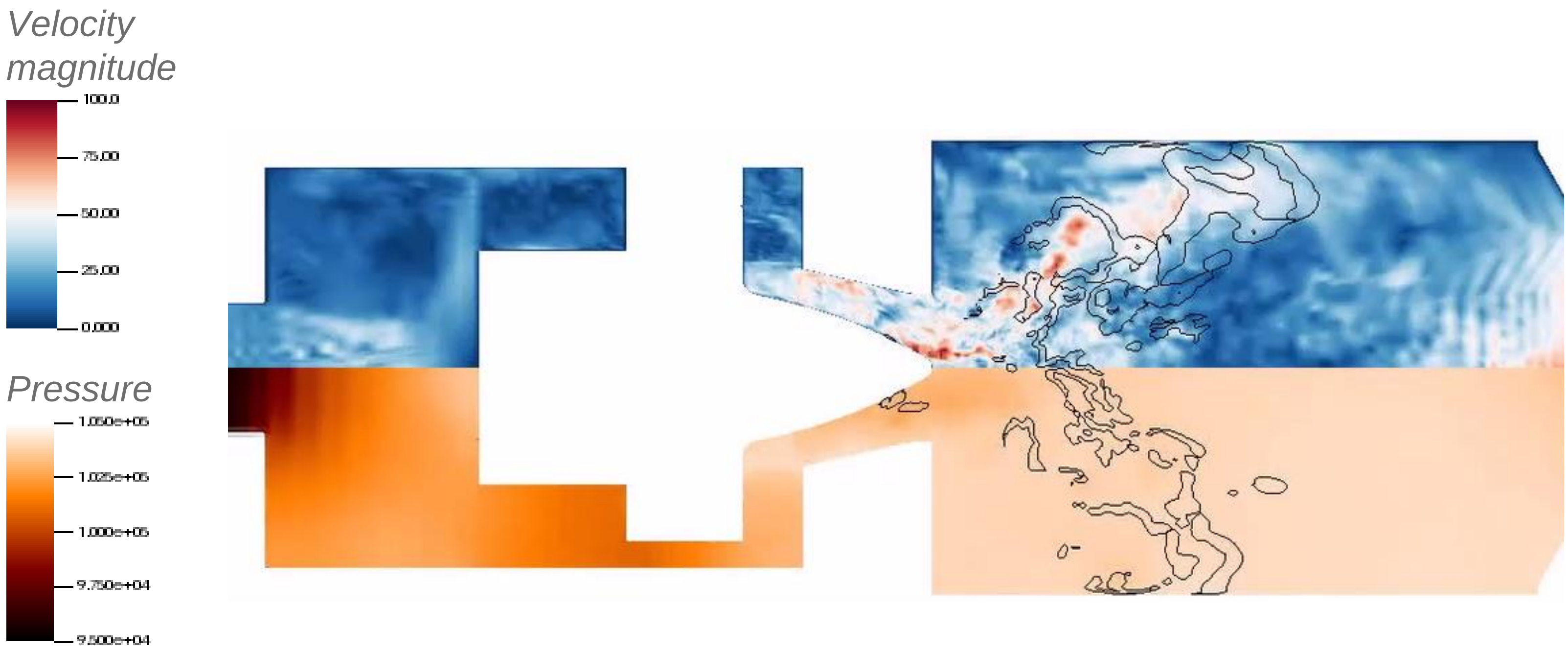

PRECCINSTA: Self-excited oscillation

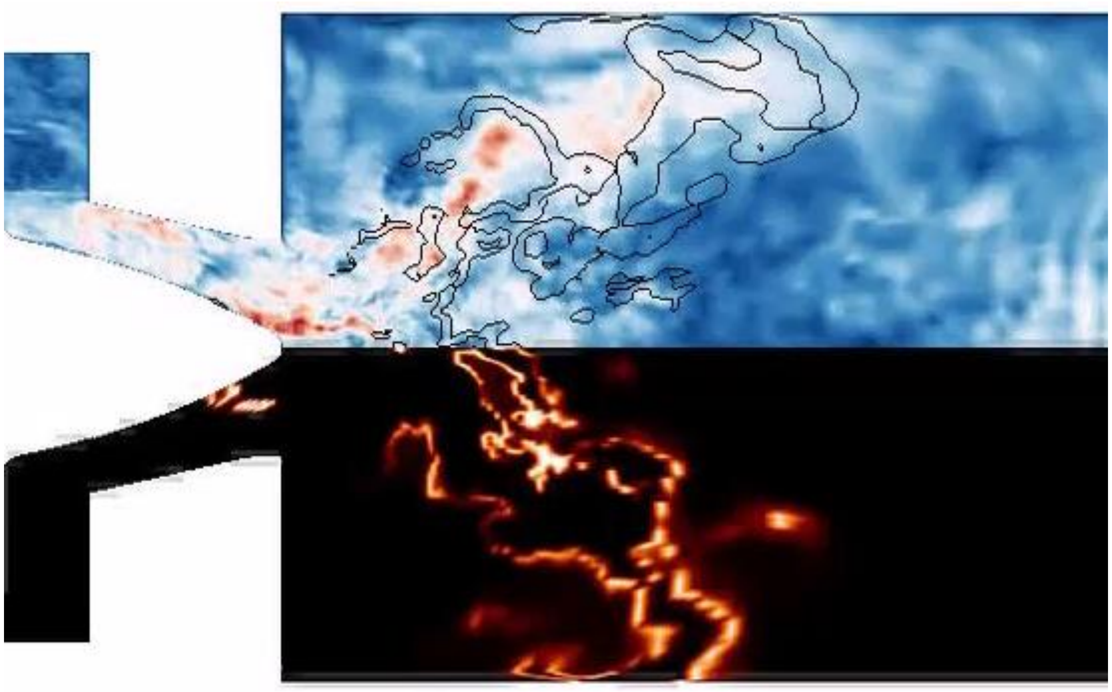

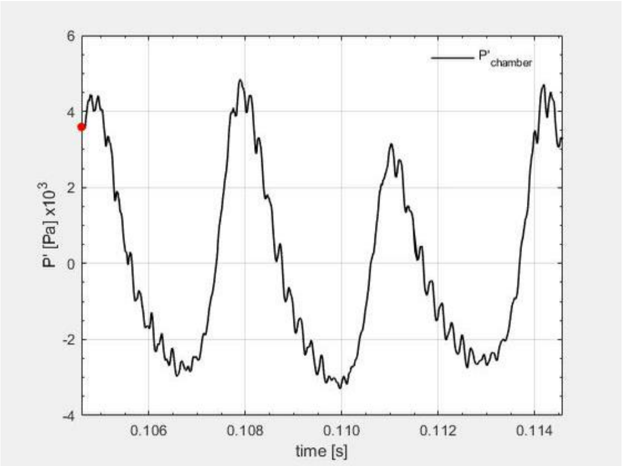

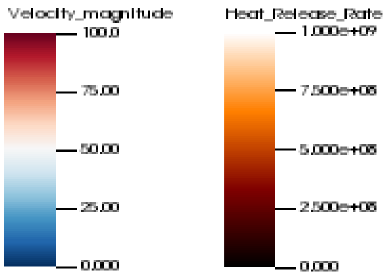

PRECCINSTA: Limit-cycle oscillation

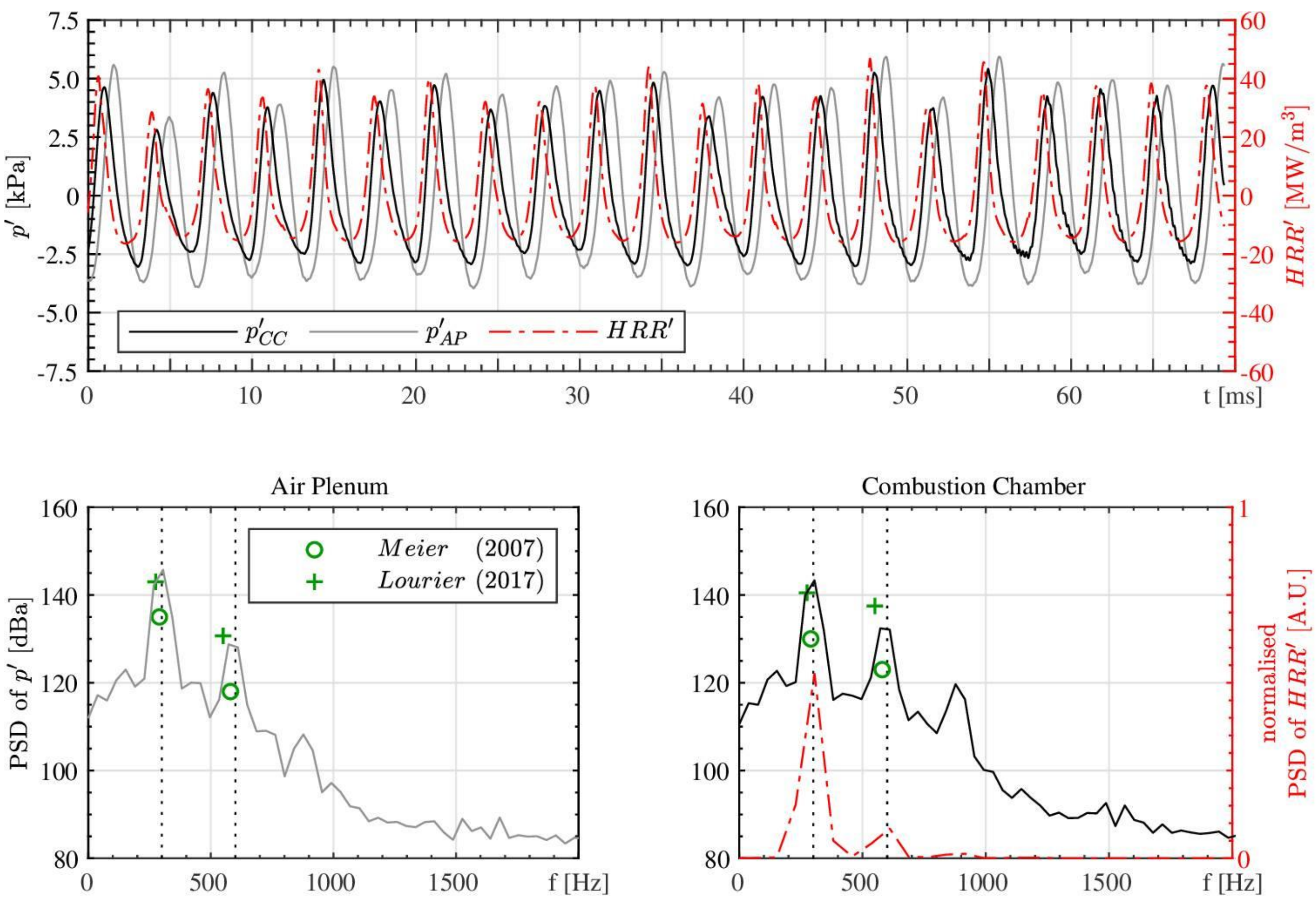

Conclusions

- The LES Stochastic field pdf method together with detailed but reduced chemistry has been previously applied to a wide range of flames – non-premixed, partially premixed, premixed and spray flames - to good effect.

For Compressible flow

- Self-excited combustion instabilities captured using BOFFIN-LESc
- Successful identification and description of various oscillation drivers

Imperial College London

References

1. O'Brien E.E. (1980), The probability density function (pdf) approach to reacting turbulent flows. In: Libby P.A., Williams F.A. (eds) Turbulent Reacting Flows. Topics in Applied Physics, **44**. Springer, Berlin, Heidelberg.

2. Dopazo, C. and O’Brien E.E. (1976), Statistical Treatment of Non-Isothermal Chemical Reactions in Turbulence, Combustion Science and Technology, **13**:1-6,99-122.

3. Jones W.P. and Navarro-Martinez S. (2007) , Large eddy simulation of autoignition with a sub-grid probability density function , Comb. Flame **150** 170–187.

Imperial College London

Acknowledgements

SIEMENS

EPSRC
Engineering and Physical Sciences Research Council

archer

UK CTRF
UK CONSORTIUM ON TURBULENT REACTING FLOWS

Physics-Based vs. Data-Driven Modeling for Turbulence and Combustion

Sharath S. Girimaji
Texas A&M University

American Physical Society – Division of Fluid Dynamics
72nd Annual Meeting, Seattle, 2019

Dedicated to a gentleman and scholar

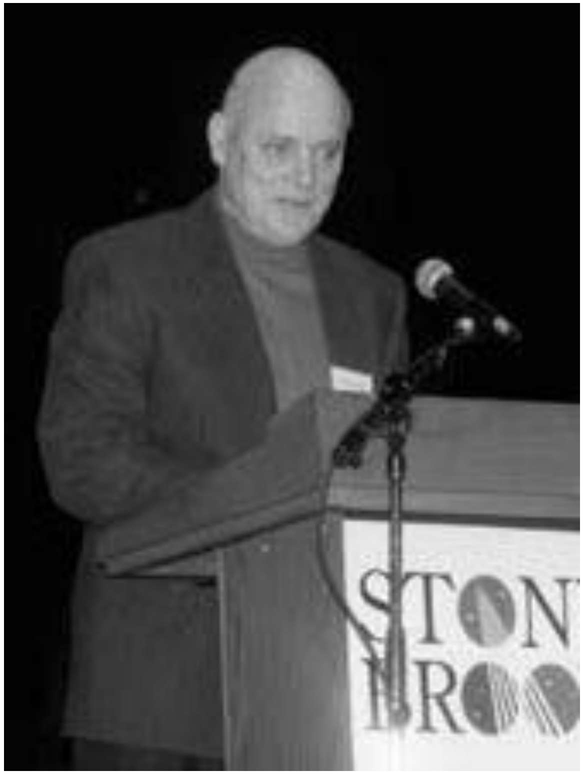

Prof. Ted O'Brien

Context of Talk

- Data-Driven Modeling (DDM) / Machine Learning (ML) has been very successful in many areas of science and engineering
- Will DDM/ML help to `solve' the age-old problem of turbulence

The purpose of this talk:

1. Ask questions of ML – as a skeptic
2. Seek answers – as an optimistic pragmatist

`Rise and Fall of turbulence theories'

Many `promising' approaches have flattered to deceive

1. Renormalization Group (Ken Wilson, 1980s – Nobel Prize)
   - Extremely successful for Quantum Electro Dynamics
2. Lattice Gas Automata (Steve Wolfram, 2000s)
   - Successful in many areas of biological process modeling
3. Many mathematical tools: POD, wavelets, fractals etc.

These approaches only marginally `solved' the turbulence problem
- Only added to the `mystique' or turbulence

Therefore it is fair ask the question
- `Is DDM/ML another *hype* or a game-changer?'

Typical Application

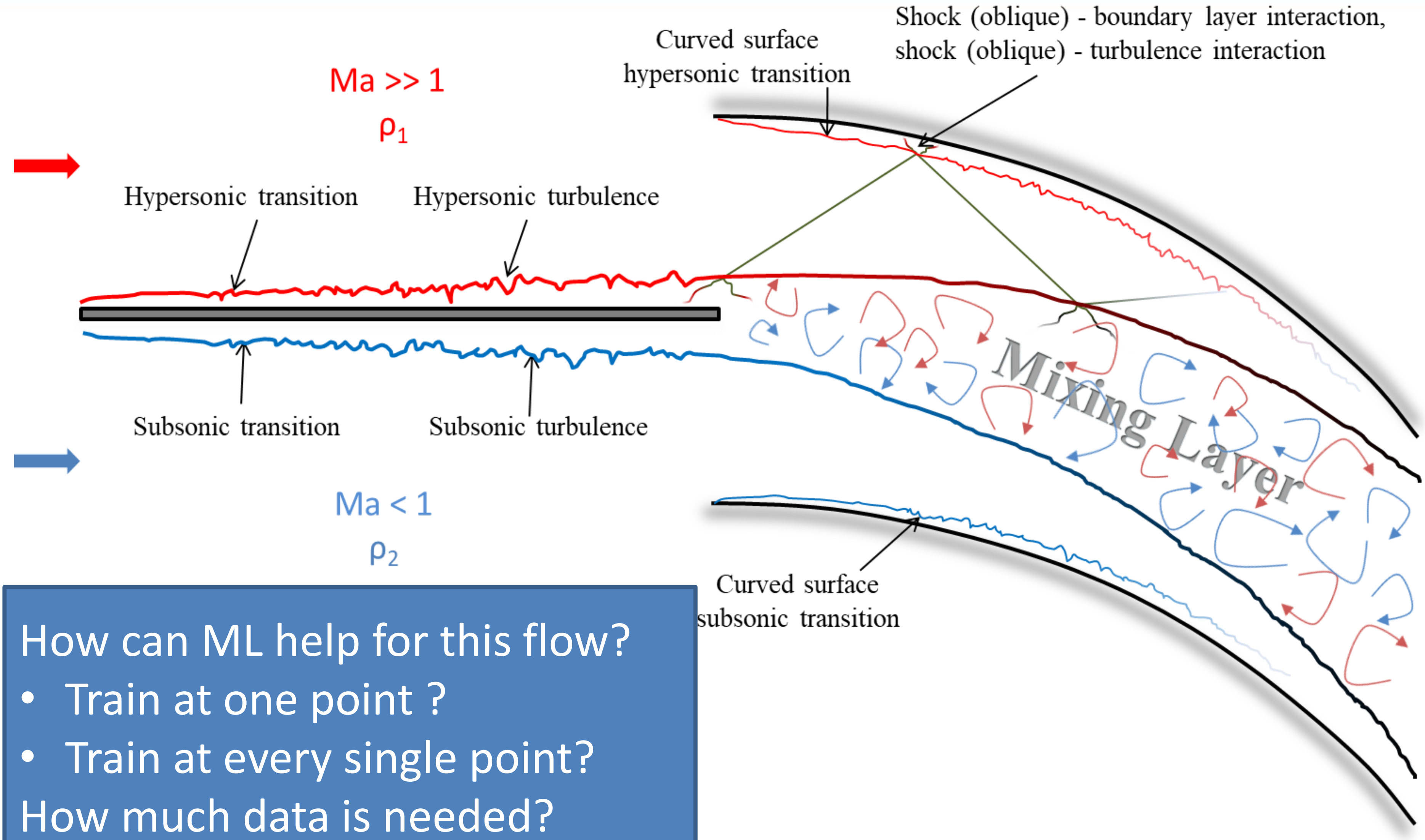

How can ML help for this flow?

- Train at one point ?
- Train at every single point?

How much data is needed?

Statistical modeling and unclosed processes

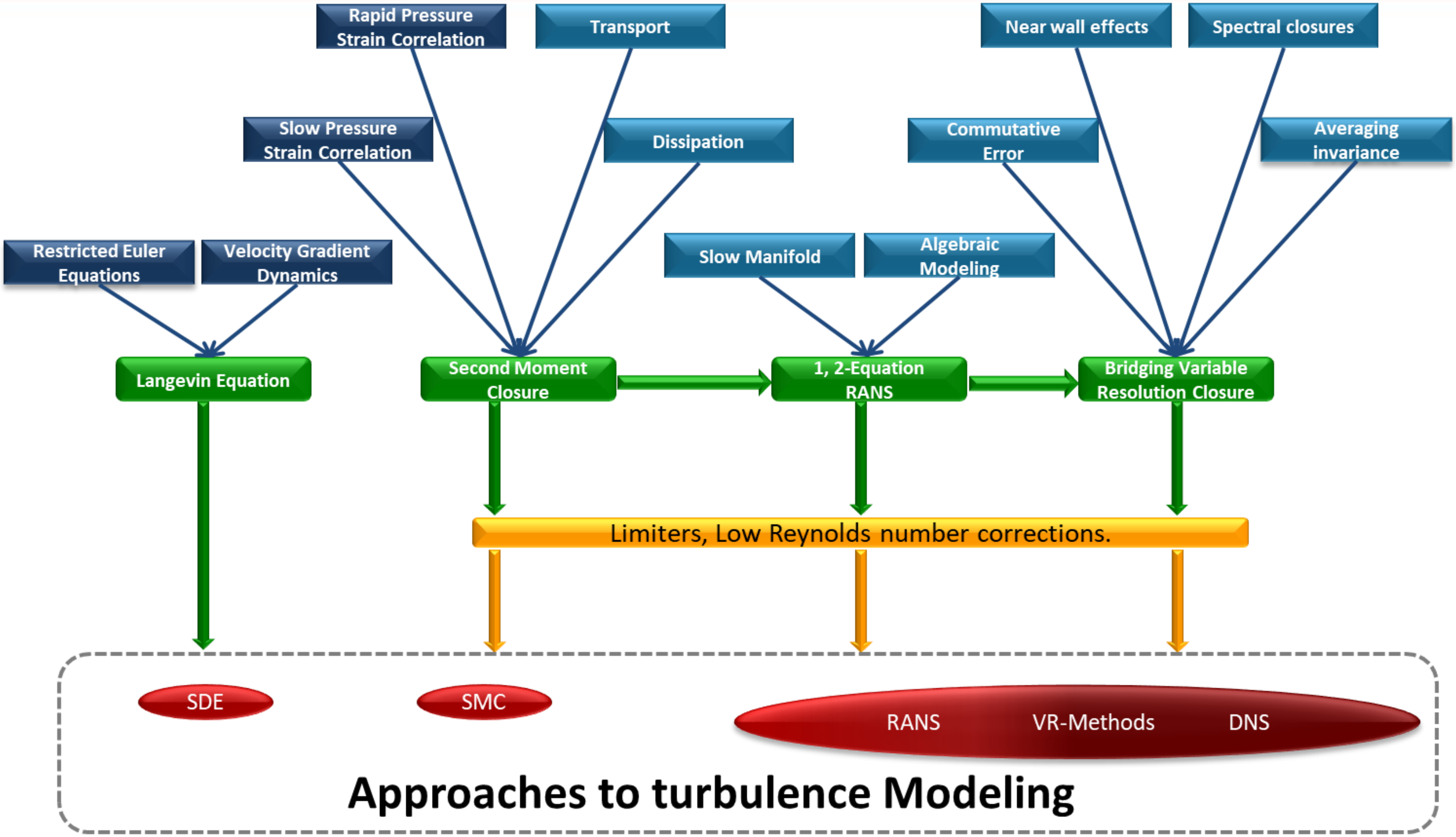

- **Where can ML help?**
- **How can ML help?**

Important Questions for DDM/ML

1. **Can DDM/ML help at all levels of modeling: RANS - SRS?**
   - Currently predominatly used for constitutive relation
2. **Is DDM/ML predictive or just data regurgitation?**
   - In many cases data not available
3. **Can we standardize the training procedure?**
   - Too many Neural Network Architectures – can get any answer we want
   - Which features? How many features?
   - What is the right objective function?
4. **Are we Training the ML right?**
   - Open-loop vs. Closed loop training
5. **Can ML recover from flaws on RANS leading to substantial improvements in results?**
   - RANS can be incorrect in many flows.

Current Status of ML?

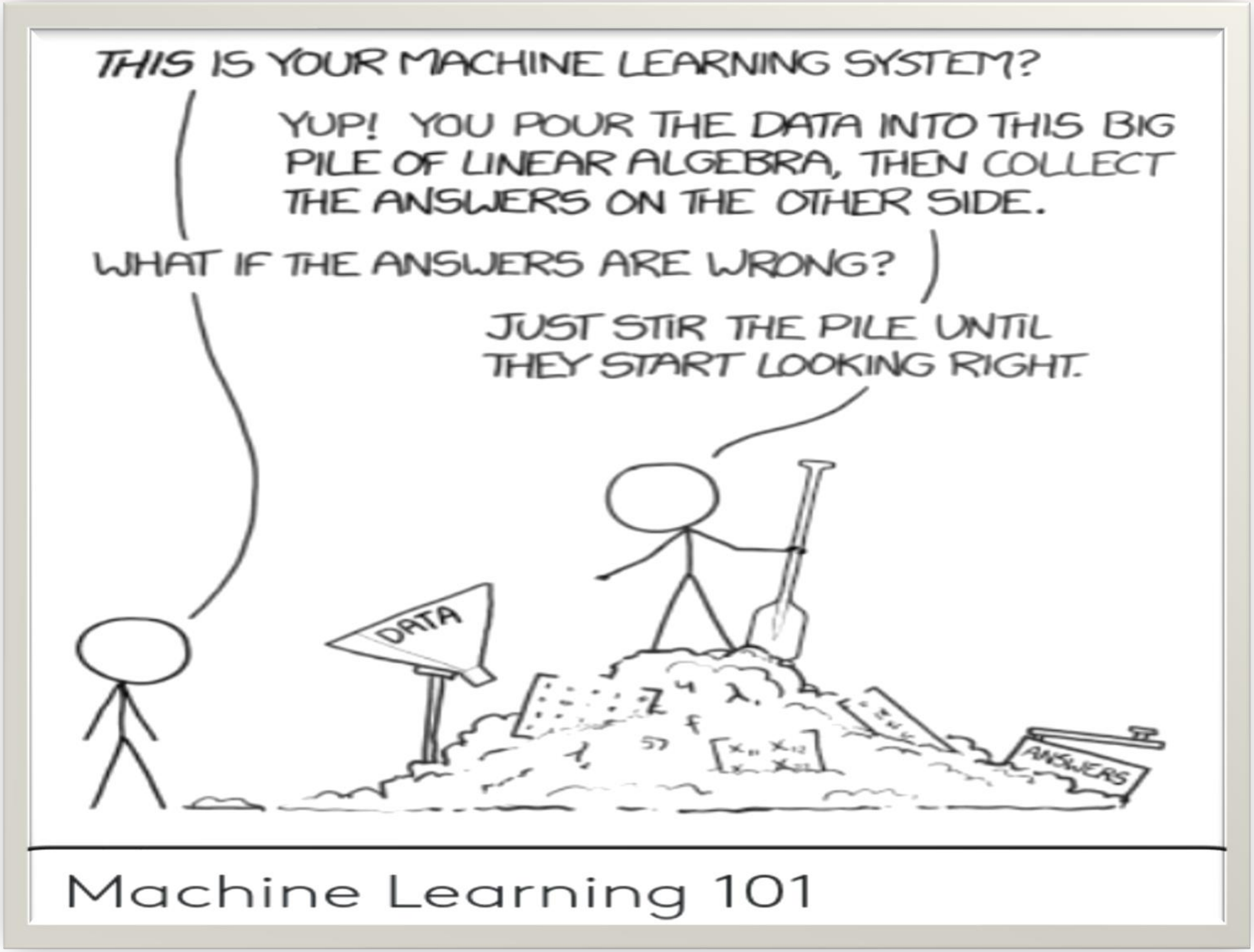

Two-equation RANS Model

How many **closure coefficients** do exist in RANS model?

- Algebraic Constitutive Closure Coefficients (CCC):

$$\langle u_i u_j \rangle = -\tau_{ij} = 2k b_{ij}(s_{ij}, w_{ij}) + \frac{2}{3} k \delta_{ij}, \qquad \boldsymbol{b}(\boldsymbol{s}, \boldsymbol{w}) = \sum_{\lambda=1}^{10} G_\lambda (I_{1:5}) \boldsymbol{T}^\lambda$$

- Transport Eqn. Closure Coefficients (TCC):

$$\rho \frac{\partial k}{\partial t} + \rho \langle U_j \rangle \frac{\partial k}{\partial x_j} = \tau_{ij} \frac{\partial \langle U_i \rangle}{\partial x_j} - \beta^* \rho k \omega + \frac{\partial}{\partial x_j}\left[(\mu + \sigma^* \mu_t) \frac{\partial k}{\partial x_j} \right]$$

$$\rho \frac{\partial \omega}{\partial t} + \rho \langle U_j \rangle \frac{\partial \omega}{\partial x_j} = \alpha \frac{\omega}{k} \tau_{ij} \frac{\partial \langle U_i \rangle}{\partial x_j} - \beta \rho \omega^2 + \frac{\partial}{\partial x_j}\left[(\mu + \sigma \mu_t) \frac{\partial \omega}{\partial x_j} \right]$$

These coefficients need calibration:

CCC: $G_1 \ldots G_{10}$

TCC: α, β, β^*, σ, σ^*

DDM/ML for RANS

Constitutive coefficients: Algebraic Equations

- Use of ML best developed for this piece of turbulence modeling
- Representation theory used for Feature Selection
- But in many instances, constitutive equation is not weakest link

Transport equations: Weakest links

- Can ML help modeling production and destruction of dissipation?
- How can ML help in turbulent transport modeling?
- Representation theory is not useful as these are scalar equations
- Objective functions may be integro-differential equations!

Transport equation modeling

Difficulty of ML techniques for transport equation modeling

- Channel flow test case (Re_τ=1000)
- RANS computations are reasonable for this flow
  - Physics-based modeling works adequately
  - Models well calibrated
- How does ML recover from wrong dissipation modeling?
  - We intentionally change correct RANS model coefficients and examine if ML recovers reasonable performance

Test Study

G_1	G_2	G_3	G_4	α	β	β*	σ	σ^*
-0.09	0	0	0	0.52	~~0.072~~ **0.054**	0.09	0.5	0.5

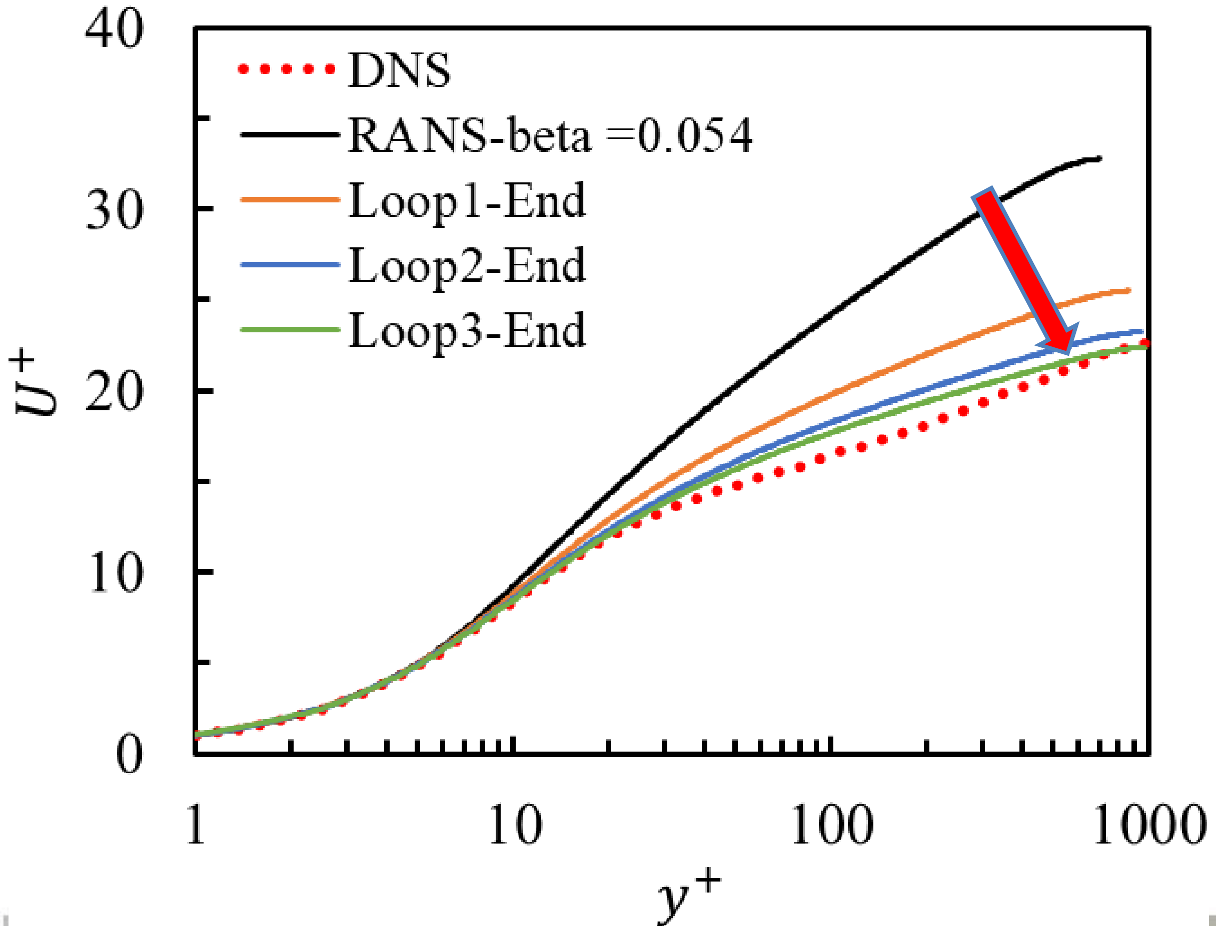

Test Study

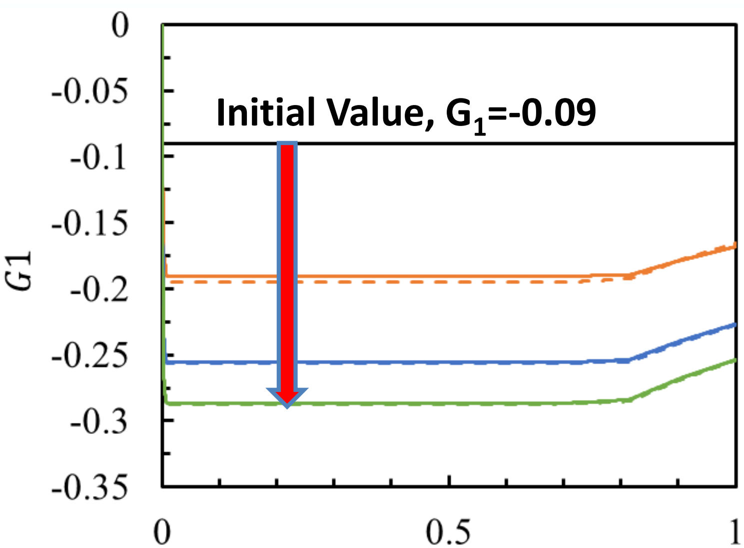

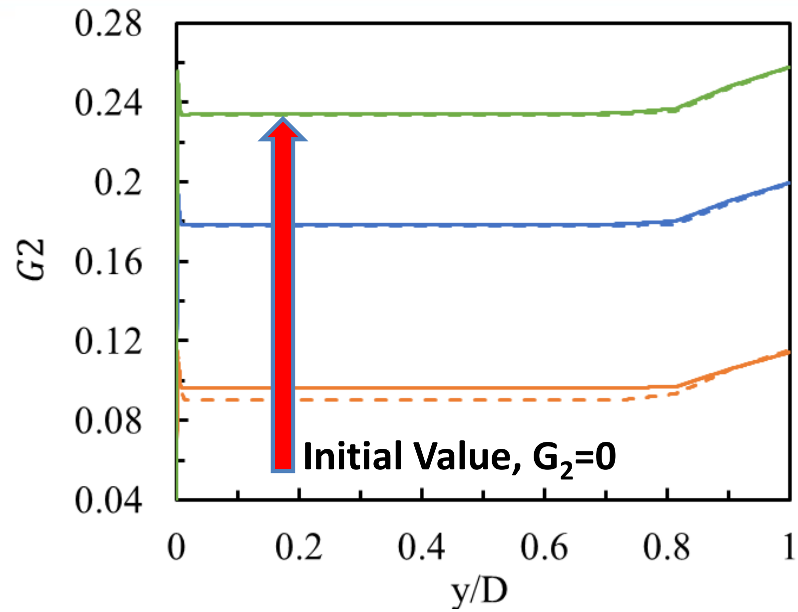

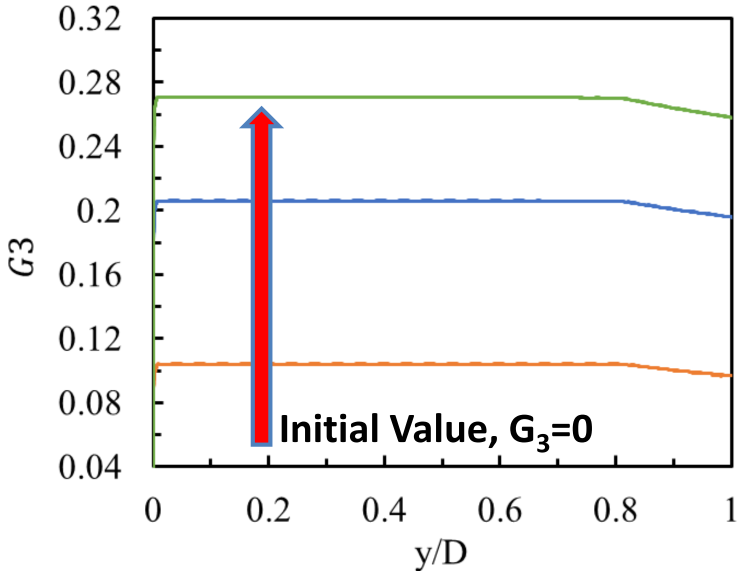

- The G_1 coefficient sharply decreases with training to compensate for small turbulent kinetic energy.
- G_2 and G_3 coefficients also go to unphysical values

Test Study

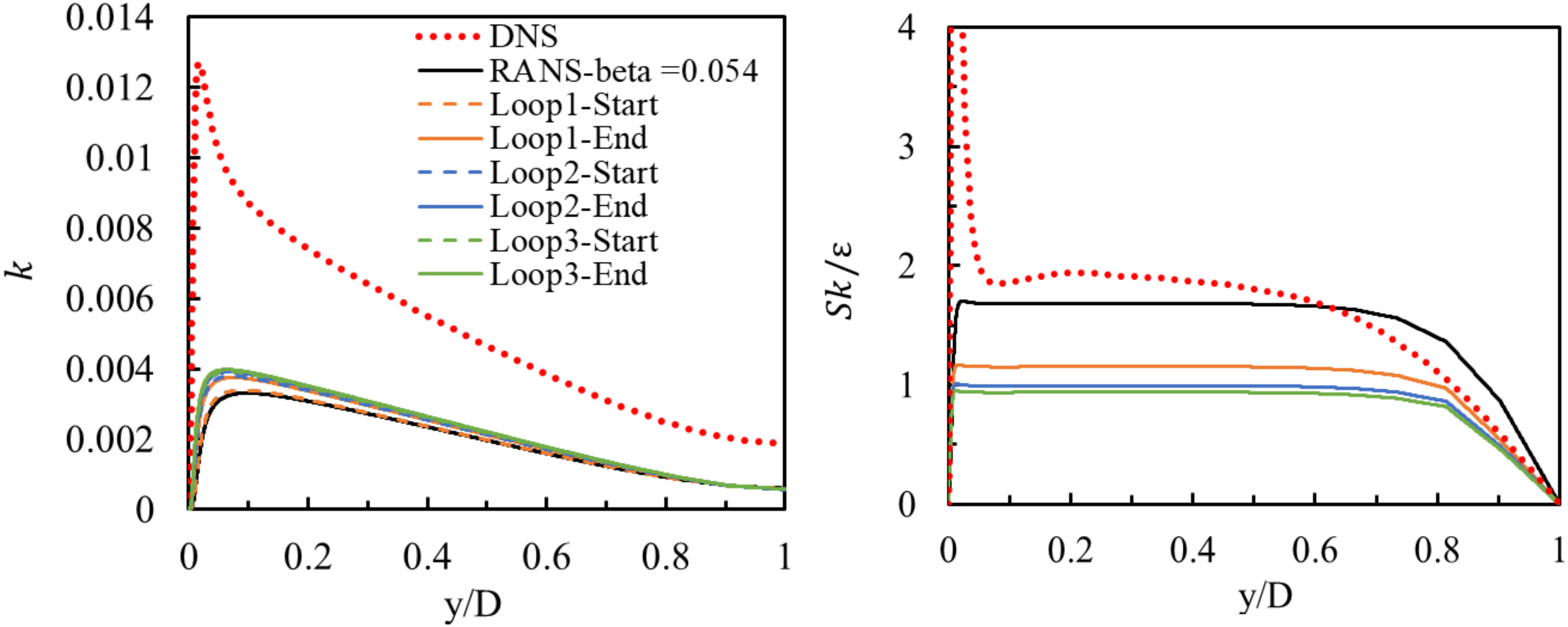

- All other quantities are completely off.

Outcome of test study

- DDM/ML is reasonable for statistics included in objective function (OF)
- Statistics not included in objective function (OF) – are worse than good `physics-based' model
- Challenge is to construct objective function (OF) and select Features that simultaneously optimizes:
  - *Mean flow, Reynolds stress, mean scalar, scalar variance, heat release, etc ?*
- Need physics-based analysis for construction objective functions and feature
  - **Need for physics merely takes a different form**

Parting Thoughts

- DDM/ML →a big hammer looking for a nail
- Turbulence modeling → Part Nail; Part Screw

- Both DDM/ML (Hammer) and Physics-Based Methods (Screw-Driver) needed

Thank you

Conclusions

- DDM/ML cannot make up all deficiencies in modeling
  - NN recovers from errors in G1, G2 and G3
  - NN cannot recover from errors in other coefficients
- Training practices and type of Neural Network have to standardized
- Physics-based modeling + DDM/ML can lead to improved predictive modeling
- Much more physics-based concepts are needed to correctly implement DDM/ML

Study-I

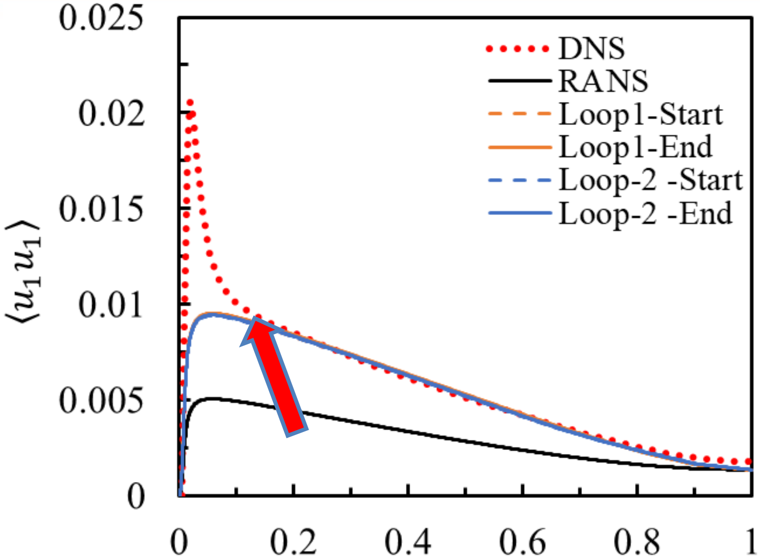

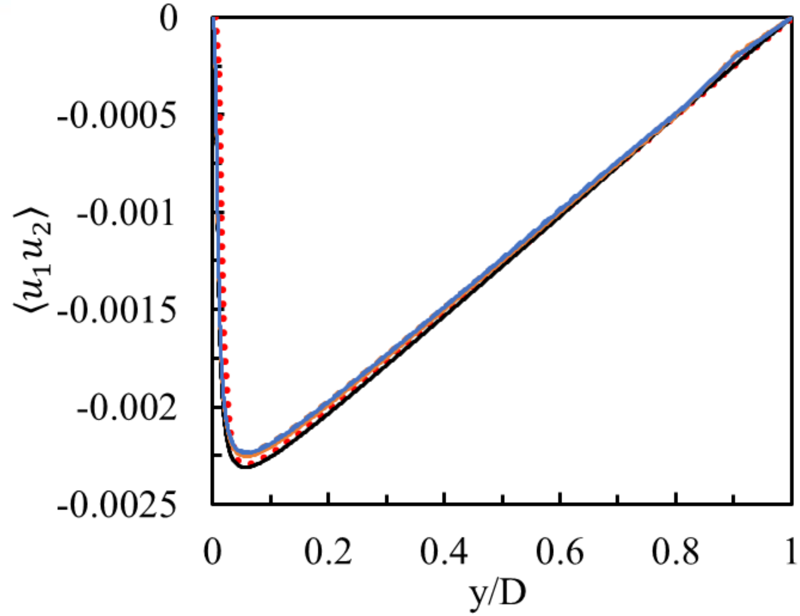

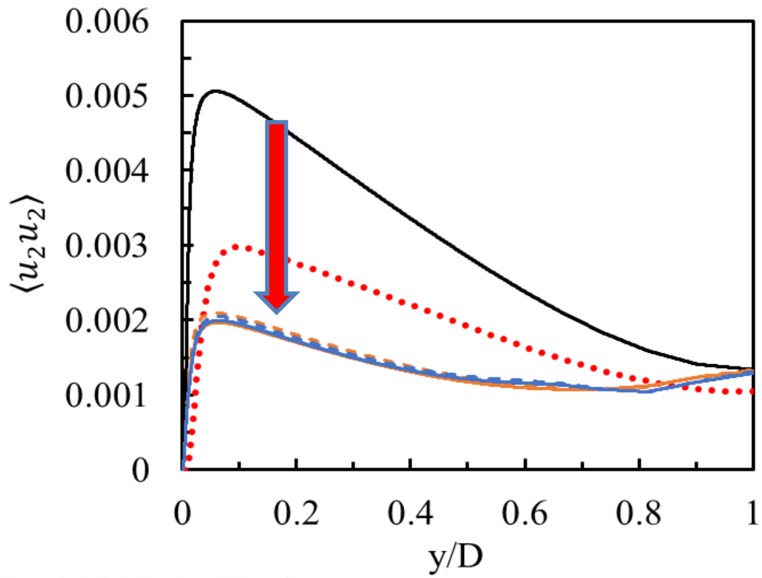

- $\langle u_1 u_2 \rangle$ does not change by training.
- $\langle u_1 u_1 \rangle$ and $\langle u_2 u_2 \rangle$ components improve by training.
- There is no significant difference between open-loop and closed-loop training in this study.

Study-II

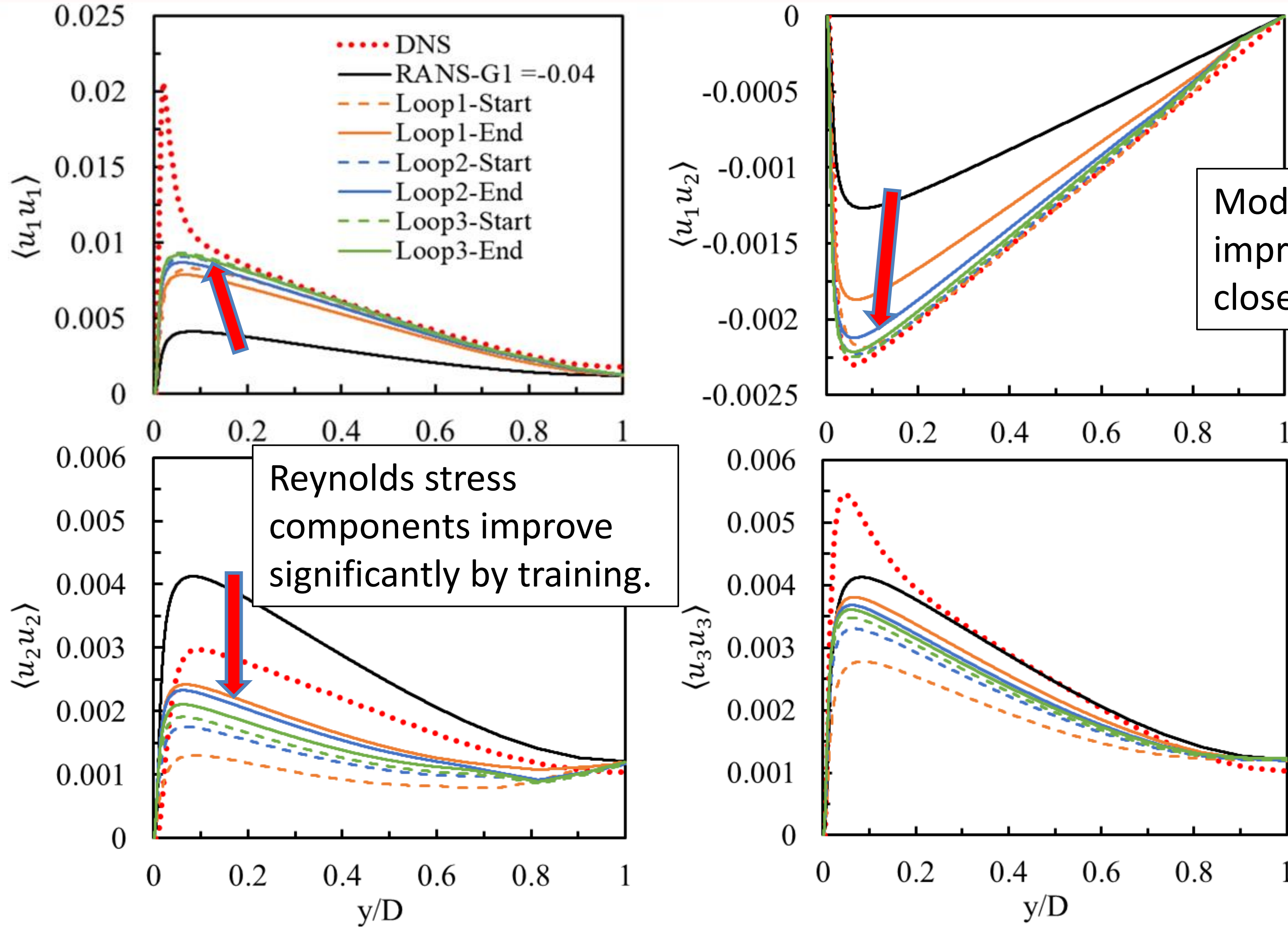

Model shows more improvements with closed-loop training.

Reynolds stress components improve significantly by training.

Study-III

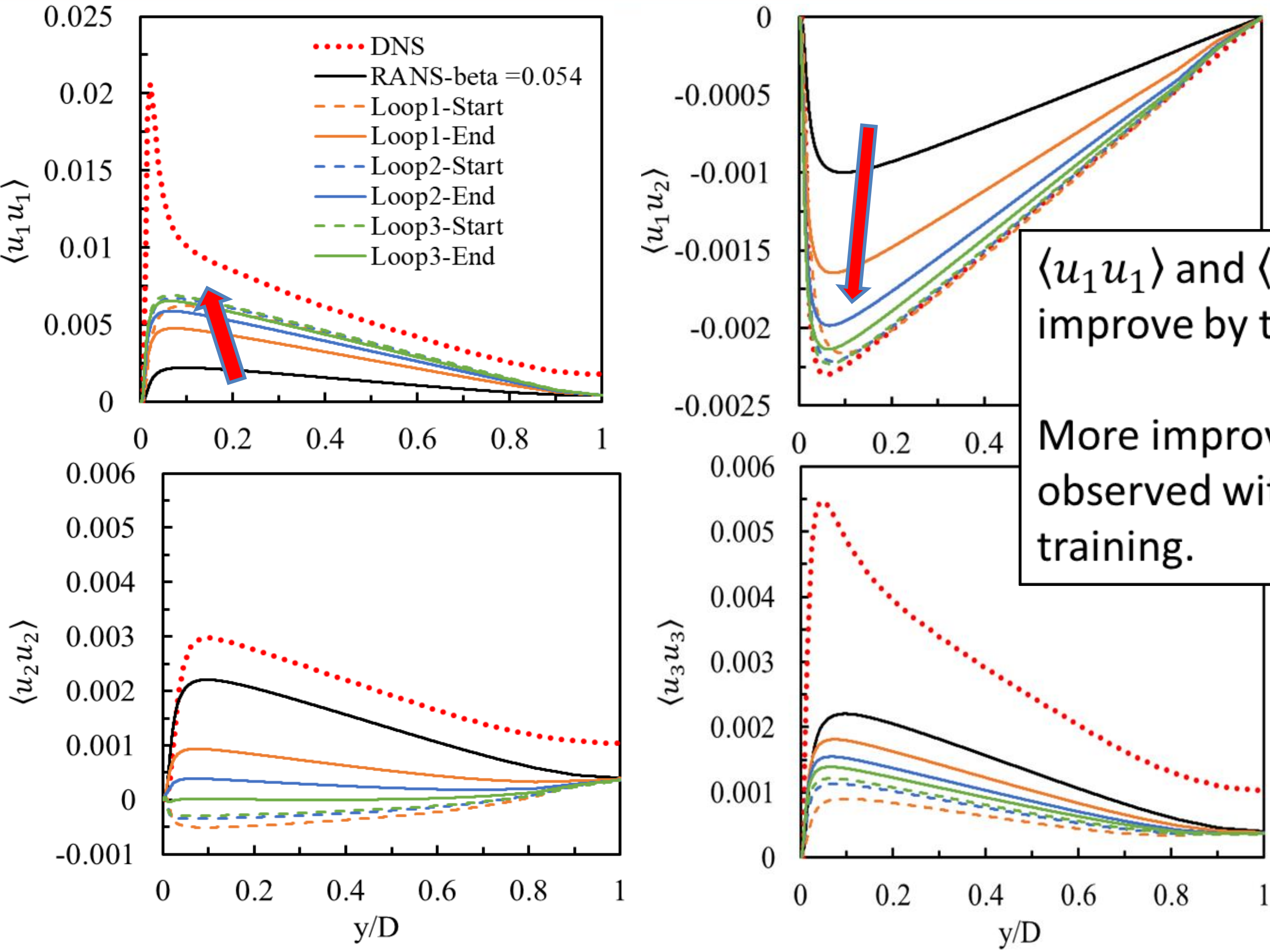

$\langle u_1 u_1 \rangle$ and $\langle u_1 u_2 \rangle$ components, improve by training.

More improvements are observed with closed-loop training.

Turbulence Phenomenon

H. Liepman: Rise and fall of theories (tools) of turbulence

So what is difficult about turbulence?

→ Non-linearity + Non-Locality

→ Spatio-temporal Chaos – acute dependence on I.C & B.C.

→ Butterfly effect: Does the flap of a butterfly's wings in Brazil set off a tornado in Texas? (Philip Merilees)

Concluding Remarks

- At A priori stage, NN should be constrained to give realizable values for all of the Reynolds stresses.

- <uiuj> values from the DNS should be used as a target in the learning process of NN rather than bij.

➢ Some people use TKE_DNS for normalizing the <uiuj> and use the obtained expression for bij in their optimization process. This seems not to be a good idea since although we are correcting bij values for our model, we will not get the improved <uiuj> due to the differences between TKE_DNS and TKS_RANS especially near the wall. (Julia Ling 2016, Kaandorp, Dwight. 2018)

➢ Some other use TKE_RANS for normalizing the <uiuj> and use the obtained expression for bij in their optimization process. This also seems not to be a good idea since by using TKE_RANS we will have large values of bij near the wall which might not be easily captured by NN optimization or might lead to unrealizable Reynolds stresses. (Geneva, Zabaras 2019)

Concluding Remarks

- A new recursive (closed-Loop) algorithm is proposed for RANS turbulence modeling.

- For the flow case that the standard k-ω RANS model performs well, It is observed that open-loop machine learning training improves the prediction of the RANS model for the normal Reynolds stress components. However, no more significant improvements is observed with closed-loop training.

- For the case that the C_μ= -G_1 value is changed from 0.09 to 0.04, it is observed that the k-ω RANS model performs poorly. It is revealed that the open-loop training can improve the performance of the model and more improvements can be achieved with close-loop training.

- The prediction of the k-ω RANS model when the coefficient β is tuned to a different value, showed to be far from the DNS data. It is illustrated that the for this case, ML training can be used to recover the Reynolds shear stress and velocity profile. However, It should be noted that other quantities like, turbulent kinetic energy (k) and SK/ε can not be fully recovered by training. For this case we also observed that closed-loop training excels the open-loop training.

Flows with spatially developing structures

Breakdown from one state of turbulence to another

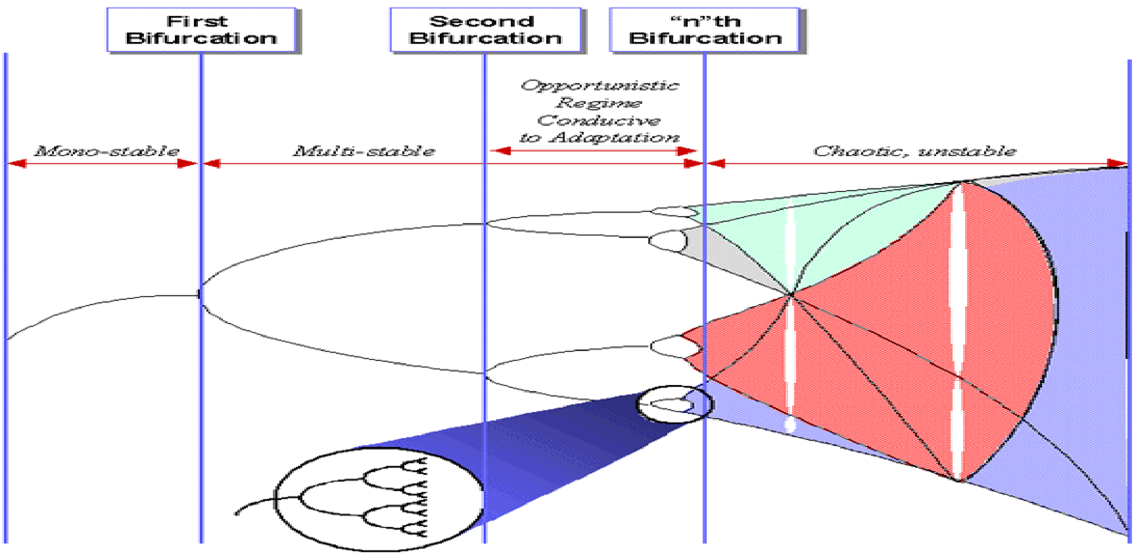

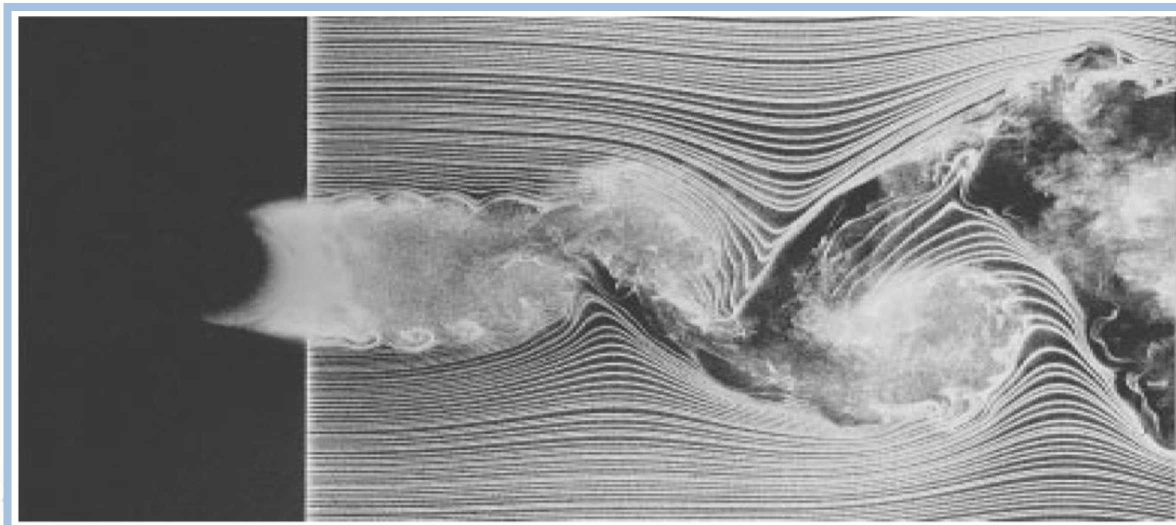

- Resolve what we cannot model
- Model what physics allows
- Have the wisdom to know the difference

Statistical modeling approaches and unclosed processes

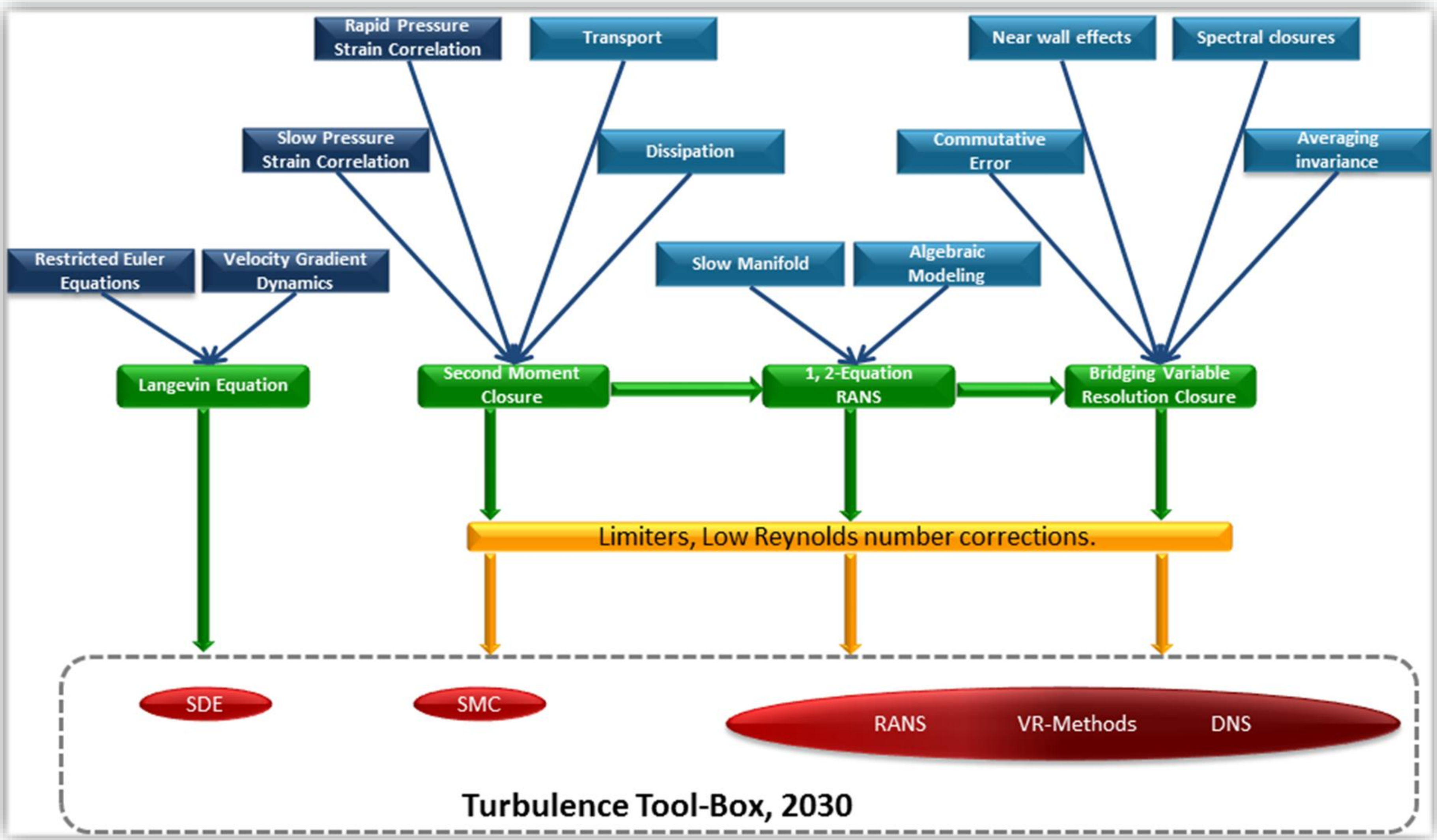

Traditional turbulence modeling

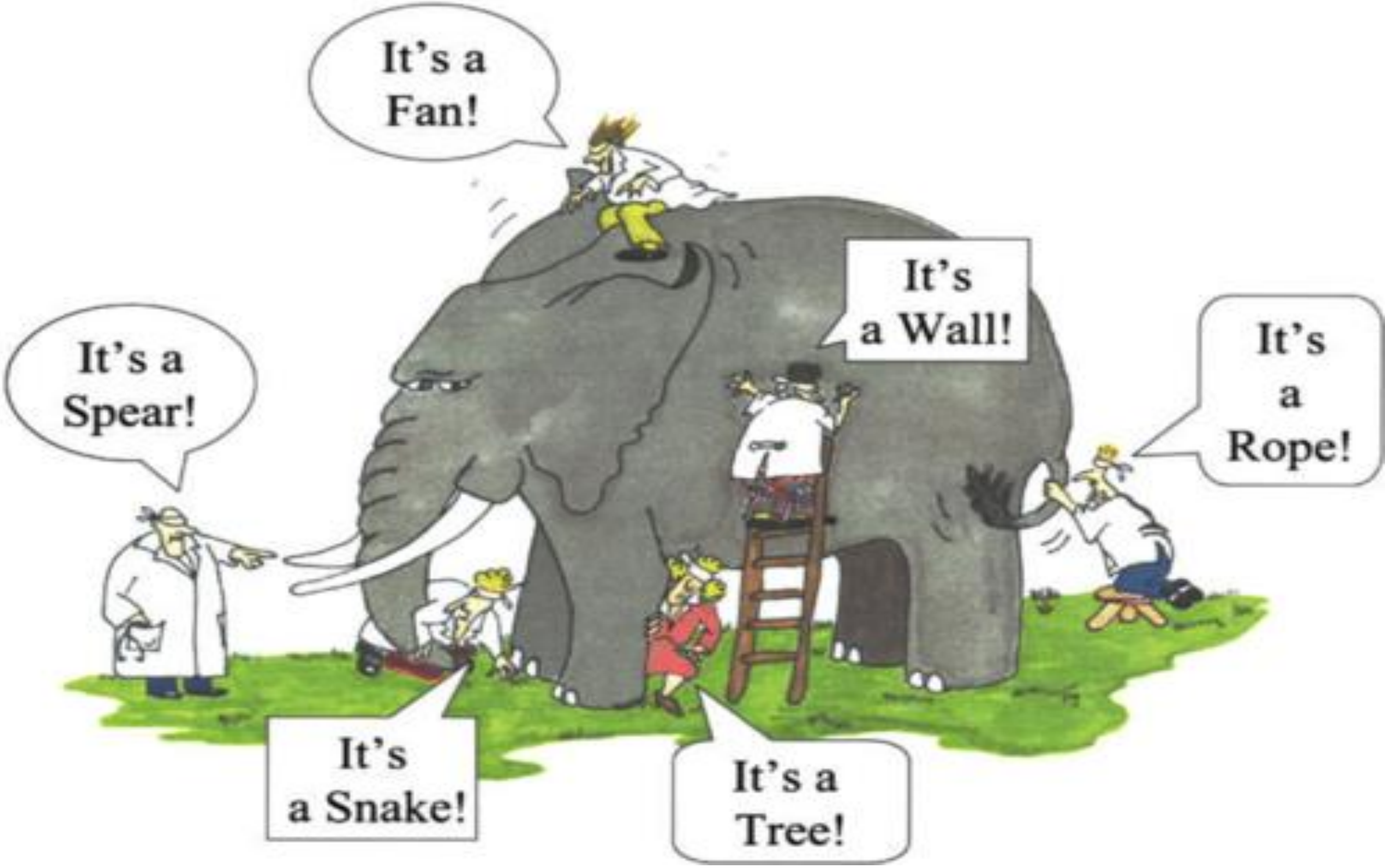

Age-old problem of turbulence

For many decades RANS & SRS: *Physics-based approaches*

In the last few years: *Data-driven approaches*

DDM/ML → model phenomena that cannot be described by equations.

- Turbulence equations are known but not easy to solve
- Modeling comes with many constraints –
  Conservation laws, Realizability, consistency etc
- `Constrained' ML is still in its infancy
- Turbulence is a complex phenomenon

Turbulence: A complex dynamical system

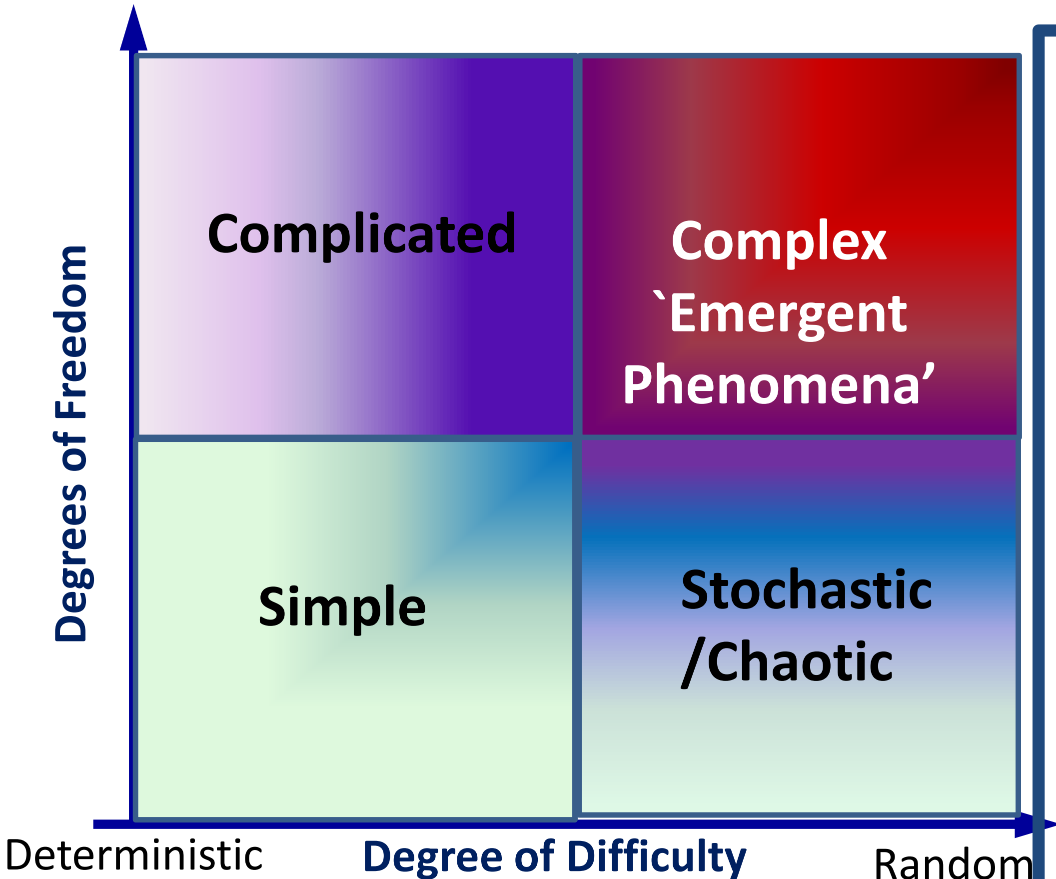

Mathematical Approaches

1. Simple → Most present methods
2. Chaotic → Probabilistic and dynamical systems
3. Complicated system → DDM/ML appears to be well suited
4. Complex or `emergent phenomena' → Is DDM/ML adequate

Amenability of Different Processes

- Constitutive coefficient: Algebraic Equations

→ use of ML straight forward

  - Features and Labels are reasonably easy to identify
  - Straight forward to define and optimize an objective function

- Transport Equation Coefficients: Differential Equations

→ use of ML is still unclear

-- Elliptic Equations are particularly challenging due to non-locality

-- Features, labels and objective functions are unclear

Chemical reaction term is algebraic and hence straight forward

- In Situ Adative Tabulation (Pope 2000) is akin to ML

APS-DFD 2019, G12.00004

Honoring Ted O'Brien

Differential Diffusion Modelling in Transported PDF Simulations of Turbulent Flames

Zhuyin Ren, Hua Zhou, Tianwei Yang

Tsinghua University

November 24 2019

Outline

- Background and Objectives
- Modelling strategy for filter and subgrid scale differential diffusion
- Results and Discussion
  - LES/FDF and RANS/PDF simulations of a jet-in-hot-coflow flame
  - Effects of resolved differential diffusion
  - Effects of subgrid-scale differential diffusion

Effects of differential diffusion on species mixing timescales

- Species mixing timescales

  $\tau_i = \langle Y_i'^2 \rangle / \langle \chi_i \rangle = \langle Y_i'^2 \rangle / 2(\rho D_i \nabla Y_i' \cdot \nabla Y_i')$

- DNS of turbulent premixed methane-air Bunsen flames

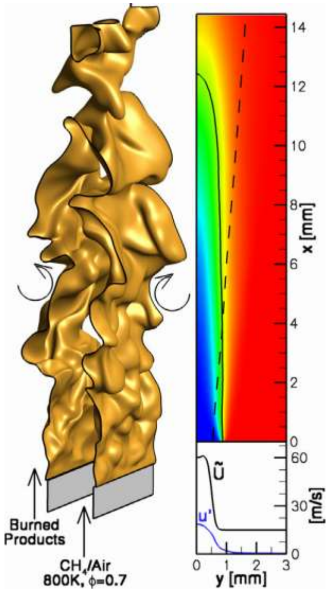

CaseA

$\tilde{U} = 60\ \mathrm{m/s}$,
$Re_{jet} = 840$,
$Ka = 100$,
$Da = 0.23$

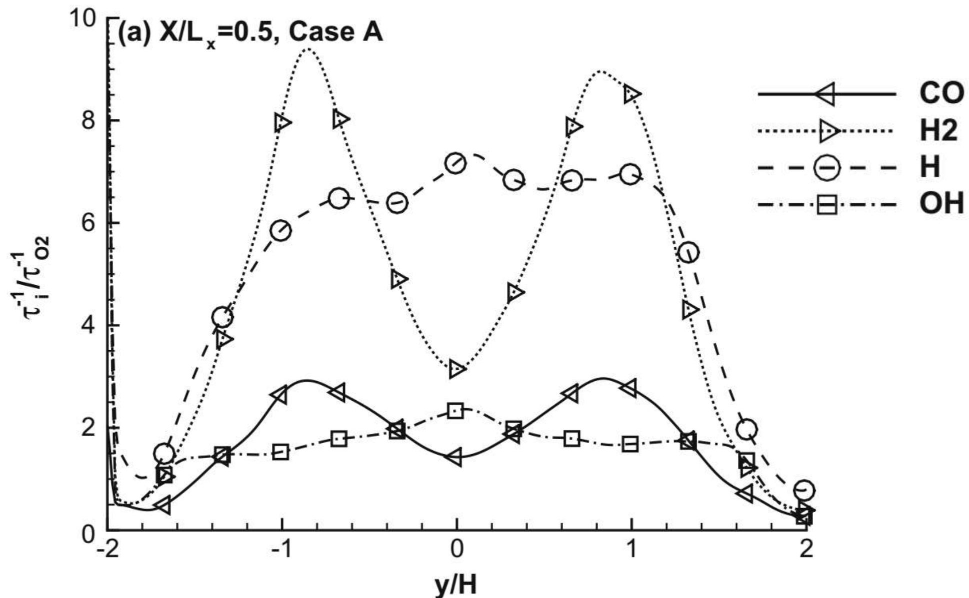

R. Sankaran, et al., PCI, 2007

E. Richardson. et al., CnF, 2010

- Difference in τ_i: up to a factor of 10
- Important to account for different mixing timescale among species

TPDF Method

- Transport equation of the joint composition PDF

$$\frac{\partial F}{\partial t}+\frac{\partial(\widetilde{U_i}F)}{\partial x_i}+\frac{\partial}{\partial \psi_k}(S_kF)=\frac{\partial}{\partial \psi_k}\left(\left\langle\frac{1}{\rho}\frac{\partial J_{i,k}}{\partial x_i}|\psi\right\rangle F\right)-\frac{\partial}{\partial x_i}(\langle u_i''|\psi\rangle F)$$

  - Eulerian TPDF equations are recast as stochastic differential equations of computational particles which evolve in physical and composition space

$$dx_k=[\widetilde{U_k}+\nabla(\tilde{\Gamma}_t\bar{\rho})/\bar{\rho}]dt+(2\tilde{\Gamma}_t)^{\frac{1}{2}}dW_k$$

$$\frac{d\phi_i}{dt}=S_i(\boldsymbol{\phi})+M(\phi_i)/\tau_\phi$$

- Nonlinear chemical reactions appear in closed form
- Modelling of molecular diffusion adds the largest amount of uncertainty

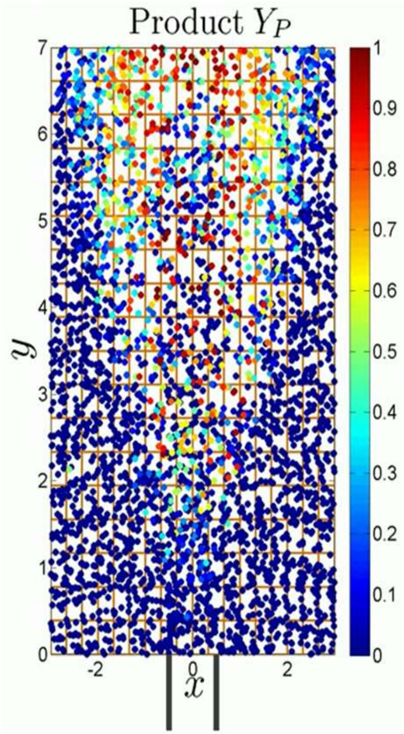

Modelling molecular diffusion in LES/FDF

- Mean-drift model

$$dX^* = \left[\widetilde{U} + \tilde{\nu}\nabla\left(\langle\rho\rangle\tilde{\Gamma}_t\right)\right]^* dt + \left(2\tilde{\Gamma}_t{}^*\right)^{1/2} dW$$

$$\frac{d\phi^*}{dt} = \left[\tilde{\nu}\nabla\cdot\left(\langle\rho\rangle\tilde{\Gamma}\nabla\widetilde{\phi}\right)\right]^* + S(\phi^*) + \Omega_M M(\phi^*)$$

Resolved molecular diffusion

- Filter-scale differential diffusion
- Uses species specific $\tilde{\Gamma}_i$
- Widely demonstrated

Subgrid mixing / micro-mixing

- Subgrid differential diffusion
- Requires a mixing model
- Remains open issues

Modelling subgrid differential diffusion

- Modelling challenge for subgrid differential diffusion with $Y_\beta^{(p)}$ as primitive variable

$$m^{(p)} \frac{dY_\beta^{(p)}}{\mathrm{d}t}|_q = -a^{(pq)}\left(Y_\beta^{(p)} - Y_\beta^{(q)}\right)$$

$$\frac{\mathrm{d}}{\mathrm{d}t}\left(\sum\nolimits_\beta Y_\beta^{(p)}\right) = -\frac{1}{m^{(p)}}\sum\nolimits_q \sum\nolimits_\beta a_\beta^{(pq)}\left(Y_\beta^{(p)} - Y_\beta^{(q)}\right) \neq 0 \quad \text{if } a_\beta^{(pq)} \text{ is different}$$

- Differential $a_\beta^{(pq)}$ results in violation of the realizability condition $\sum_\beta Y_\beta^{(p)} = 1$

- Mass-based implementation: mass-based quantities $m_\beta^{(p)}$ are taken as primitive variables

$$\frac{\mathrm{d}m_\beta^{(p)}}{\mathrm{d}t}|_q = \frac{dm^{(p)}Y_\beta^{(p)}}{\mathrm{d}t}|_q = -a_\beta^{(pq)}\left(Y_\beta^{(p)} - Y_\beta^{(q)}\right)$$

$$m^{(p)} = \sum\nolimits_{\beta=1}^{ns} m_\beta^{(p)} \qquad\qquad Y_\beta^{(p)} = \frac{m_\beta^{(p)}}{m^{(p)}}$$

- $m^{(p)}$ and $Y_\beta^{(p)}$ are reconstructed from $m_\beta^{(p)} \Longrightarrow \sum_\beta Y_\beta^{(p)}$ is guaranteed to be unity

IEM-DD and MC-DD models

- IEM-DD model

$$\frac{\mathrm{d}m_i^{(n)}}{\mathrm{d}t} = -\frac{\Omega_{M,i}\left(m_i^{(n)} - m^{(n)}\widetilde{Y_i}\right)}{2}, \quad i = 1,\dots,N_s,$$

$$\frac{\mathrm{d}H_s^{(n)}}{\mathrm{d}t} = -\frac{\Omega_{M,h_s}(H_s^{(n)} - m^{(n)}\widetilde{h_s})}{2}$$

- MC-DD model

$$m_i^{(p)} = (1-\alpha\theta_i)m_{i,0}^{(p)} + \alpha\theta_i m_0^{(p)}\widetilde{Y_i}^{(p,q)}, \quad i = 1,\dots,N_s,$$

$$H_s^{(p)} = \left(1-\alpha\theta_{N_s+1}\right)H_{s,0}^{(p)} + \alpha\theta_{N_s+1} m_0^{(p)}\widetilde{h_s}^{(p,q)}$$

$$\theta_i = \frac{3-\sqrt{9-8\omega_i}}{2}, i = 1,\dots,N_s+1$$

$$\omega_i = \Omega_{M,i}/\max\{\Omega_{M,1},\Omega_{M,2},\dots\Omega_{M,N_s+1}\}$$

- Verification in an inert mixing system

$$\Omega_{M,i} = \Omega_{M,h_s} \times (MW_{\mathrm{ave}}/MW_i)^{1/2}, \quad i = 1,\dots,N_s$$

$$\Omega_{M,h_s} = 333\ \mathrm{s}^{-1}$$

  - Decay of variance

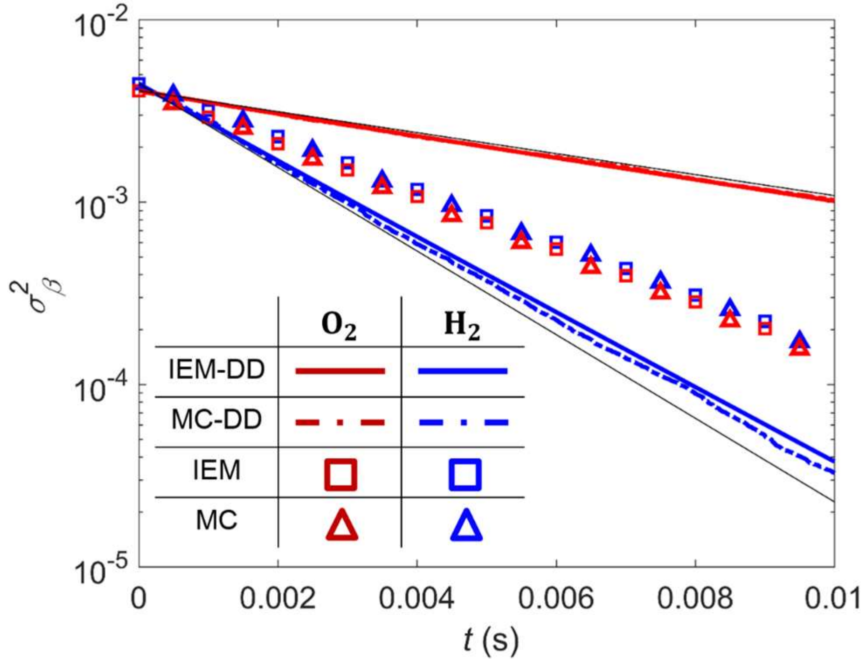

AJHC-HM1 flame

- Jet-in-Hot-Coflow (JHC) flames: Adelaide JHC (AJHC), Delft JHC (DJHC)
- AJHC flames
  - Turbulent nonpremixed CH_4/H_2 (volume ratio 1:1) flames stabilized on a jet issuing into a heated and diluted coflow

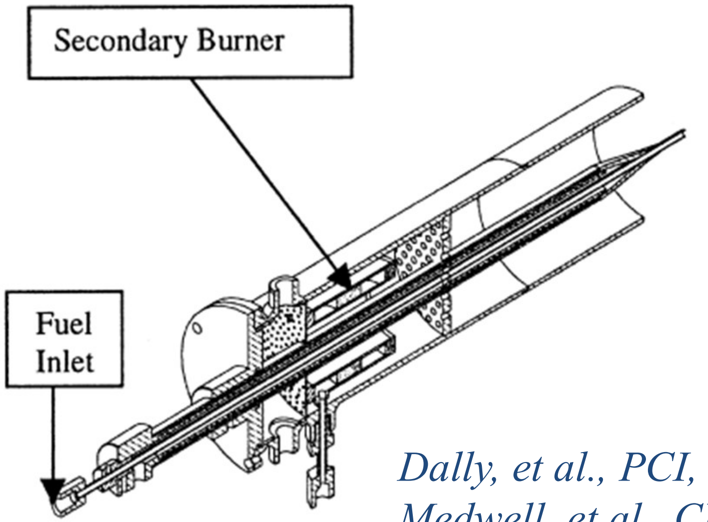

Dally, et al., PCI, 2002
Medwell, et al., CNF, 2007

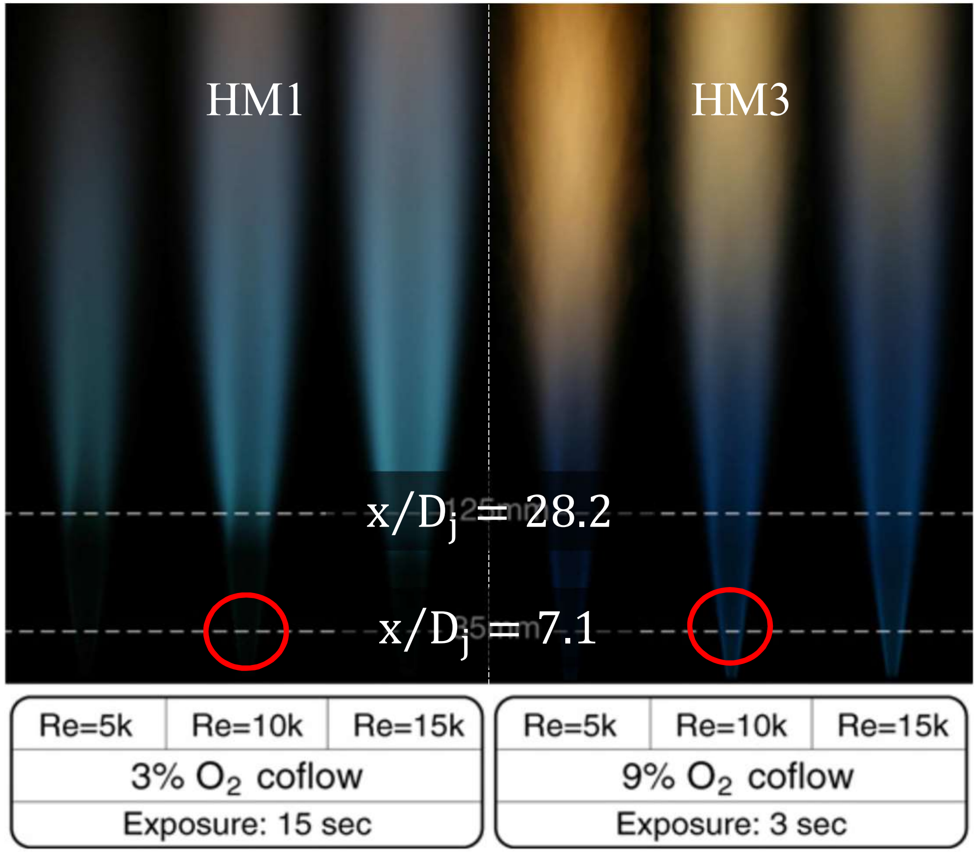

(MILD) (high temp. combust.)

LES/FDF - RANS/PDF Simulations

- Hybrid particle/mesh method

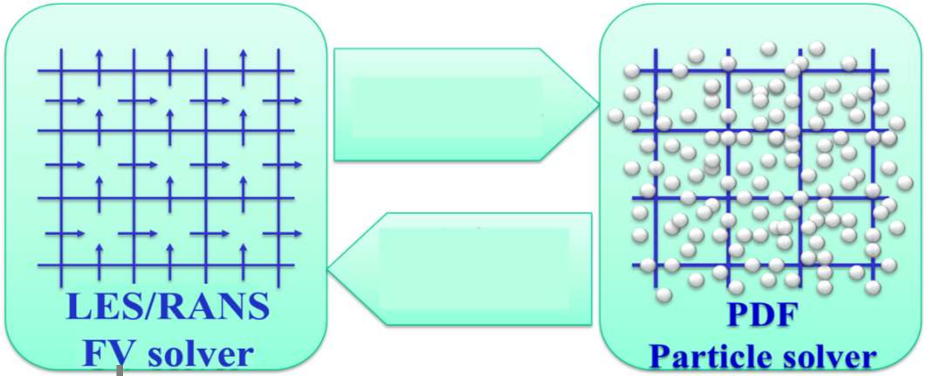

- Differential diffusion

➢ In LES/FDF, mean drift model is combined with MC-DD model to incorporate differential diffusion at both filter and subgrid scale

$$d\phi_i^*(t)/dt = \Omega_{M,i}^* M(\phi_i^*) + \left(\nabla \cdot \left(\bar{\rho}\tilde{\Gamma}_i \nabla \tilde{\phi}_i\right)/\bar{\rho}\right)^* + S_i(\boldsymbol{\phi}^*)$$

➢ Species-specific-diffusivity timescale model

$$\Omega_{M,i} = \frac{C_M\left(\tilde{\Gamma}_i + \tilde{\Gamma}_t\right)}{\Delta^2} \qquad C_M = 20.0$$

➢ In RANS/PDF, micro-mixing term $M(\phi_i^*)$ is modelled by IEM-DD / MC-DD

$$d\phi_i^*(t)/dt = \Omega_{M,i}^* M(\phi_i^*) + S_i(\boldsymbol{\phi}^*)$$

➢ Species-specific timescale model

$$\Omega_{M,i} = \Omega_{M,h_s} \times (MW_{\mathrm{ave}}/MW_i)^{1/2}$$

$$\Omega_{M,h_s} = C_\phi \Omega_t \qquad C_\phi = 2.5$$

Effects of resolved differential diffusion in LES/FDF

- Scalar radial profiles at x = 7.1 and 14.1D_j axial locations

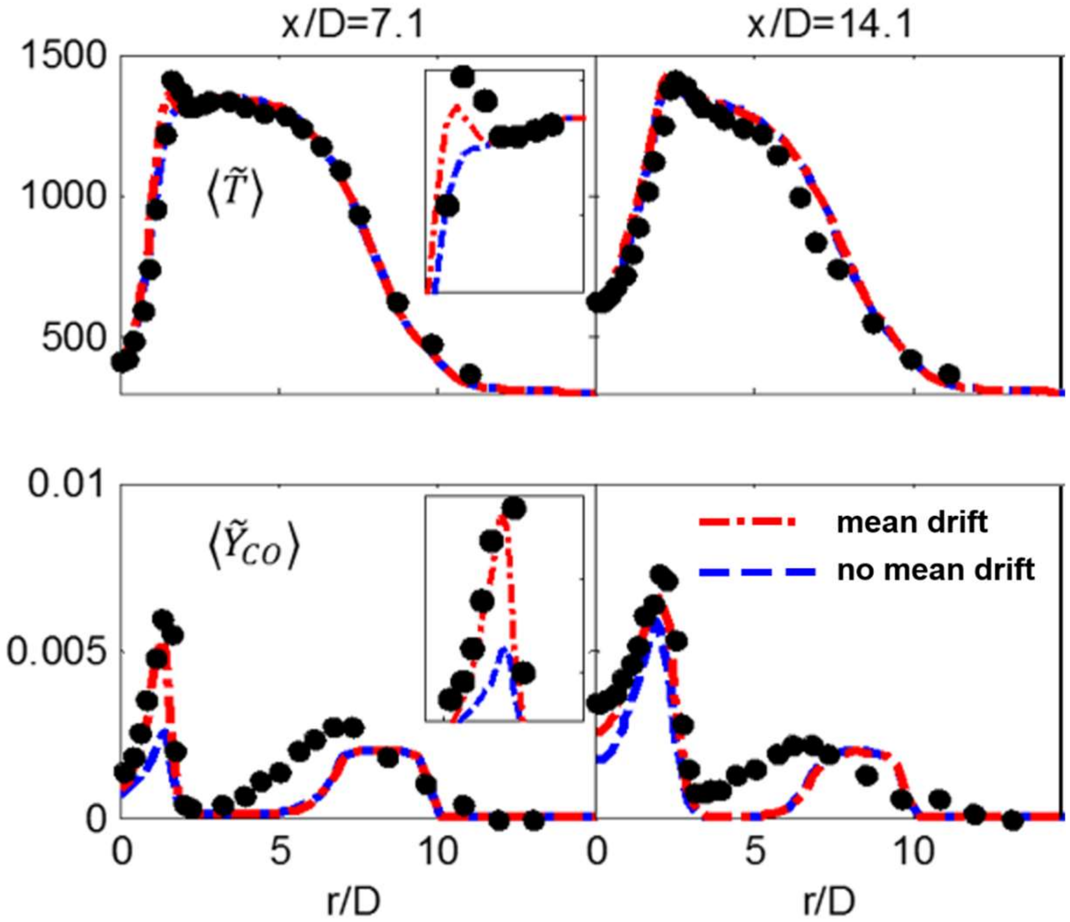

- x = 7.1D_j, temperature and CO are underpredicted without mean drift model, and is greatly improved with differential diffuision
- At the downstream, the effects of resolved differential diffusion gradually diminish --- the filter size is larger

Effects of subgrid differential diffusion

- Temperature radial profiles at x = 7.1 and 28.2D_j axial locations

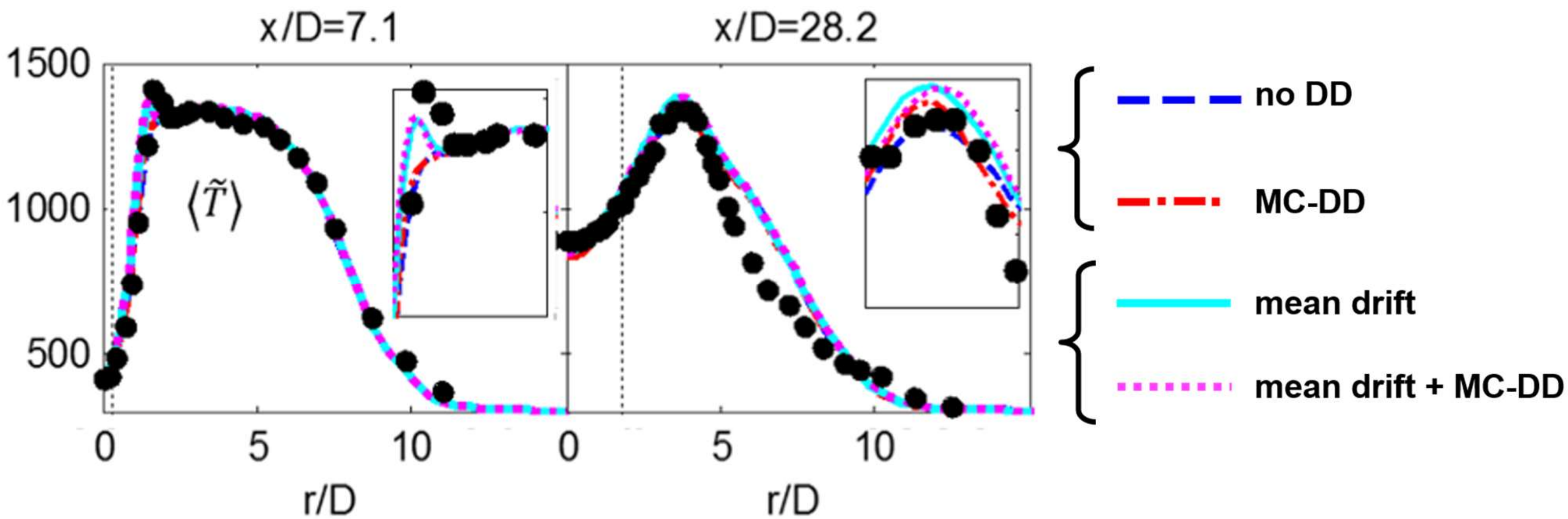

- x = 7.1D_j, minor difference between MC and MC-DD --- minor effects of subgrid differential diffusion
- x = 28.2D_j , subgrid differential diffusion makes slightly more notable difference --- the filter size is larger at the downstream

Effects of subgrid differential diffusion

- Scatter plots of mixture fraction versus temperature of computational particles at $x = 7.1D_j$

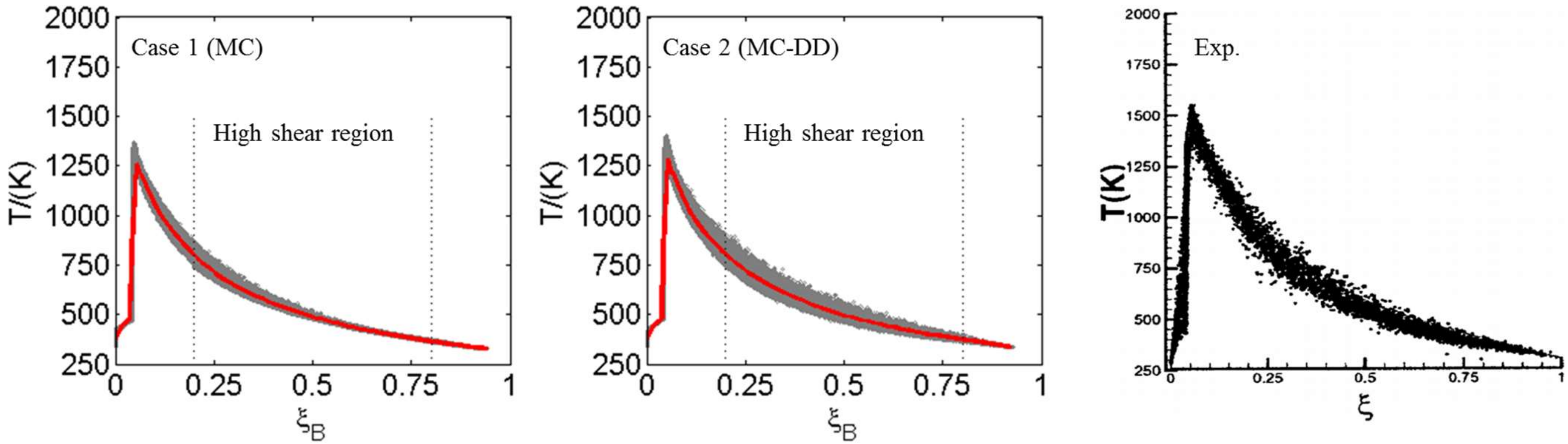

- High shear region corresponds to $0.2<\xi_B<0.8$
- The scatters of particle temperature versus mixture fraction shows notable differences between MC and MC-DD models in high shear region
- MC-DD model matches better with experimental measurement for the high shear region

Effects of micro-mixing with differential diffusion

- Scalar radial profiles at $x = 14.1D_j$ axial location

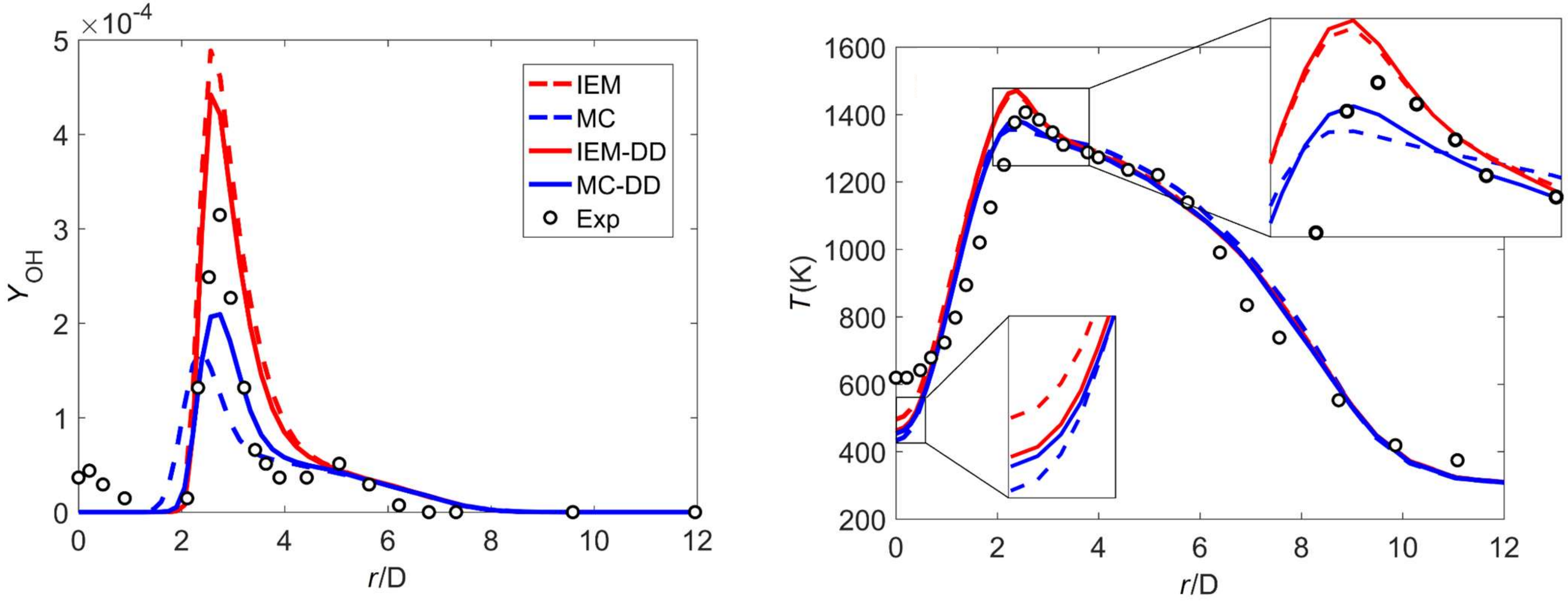

- The differences between IEM and IEM-DD are minor
- MC-DD yields slight improvement compared to MC in the peak value of OH and temperature at the critical flame location

Conclusions

- A modelling strategy to incorporate differential diffusion effects on both filter and subgrid scale is proposed

- LES/FDF and RANS/TPDF simulations for the flame HM1 have been carried out to investigate the effects of differential diffusion on flame characteristics

- For LES/FDF, the upstream predictions improve significantly by accounting for filter-scale differential diffusion. Accounting for subgrid differential diffusion show notable improvement for the conditional fluctuation of temperature in the high shear region

- For RANS/TPDF, the upstream predictions improve slightly by accounting for differential diffusion in micro-mixing

Acknowledgements

- This work is supported by National Natural Science Foundation of China 91841302.

Thanks for your attention!

Mathematical Models For Eulerian Conditional Statistics in a Complex Turbulent Flow

James C. Hill[1], Emmanuel Hitimana[2],
Michael G. Olsen[2]Rodney O. Fox[1]

[1]Iowa State University, CBE Dept.
[2] Iowa State University, ME Dept.

Paper G12.05: Session "Honoring Ted O'Brien"
72nd Annual Meeting of the APS Division of Fluid Dynamics
Seattle, WA, November 23-26, 2019

1. Method for solving turbulent reacting flow

- **Conditional Moment Closure Method:**
- $\frac{\partial\langle Y_\alpha|\xi\rangle}{\partial t} + \langle U|\xi\rangle . \nabla\langle Y_\alpha|\xi\rangle - \langle N|\xi\rangle \frac{\partial^2\langle Y_\alpha|\xi\rangle}{\partial \xi^2} = \langle W_\alpha|\xi\rangle$
- **$\langle U|\xi\rangle$ and $\langle N|\xi\rangle$ need to be modeled experimentally or analytically to achieve a closure**

2. Research objective

- **Measure conditional averages and compare predictions of the linear and the transported PDF gradient models**
- **Measurements made in a model scaled up multi-inlet vortex reactor (MIVR) using simultaneous stereo-PIV and PLIF**

  - Conditional velocity time averages ($\langle U_i|\xi\rangle$)
  - Conditional mixture fraction time averages ($\langle \Phi|\omega_i\rangle$)

Note: **U**= velocity, **ω**= sample space velocity
Φ= mixture fraction, ξ= sample space m.f.

3. The Multi-inlet Vortex Reactor (MIVR)

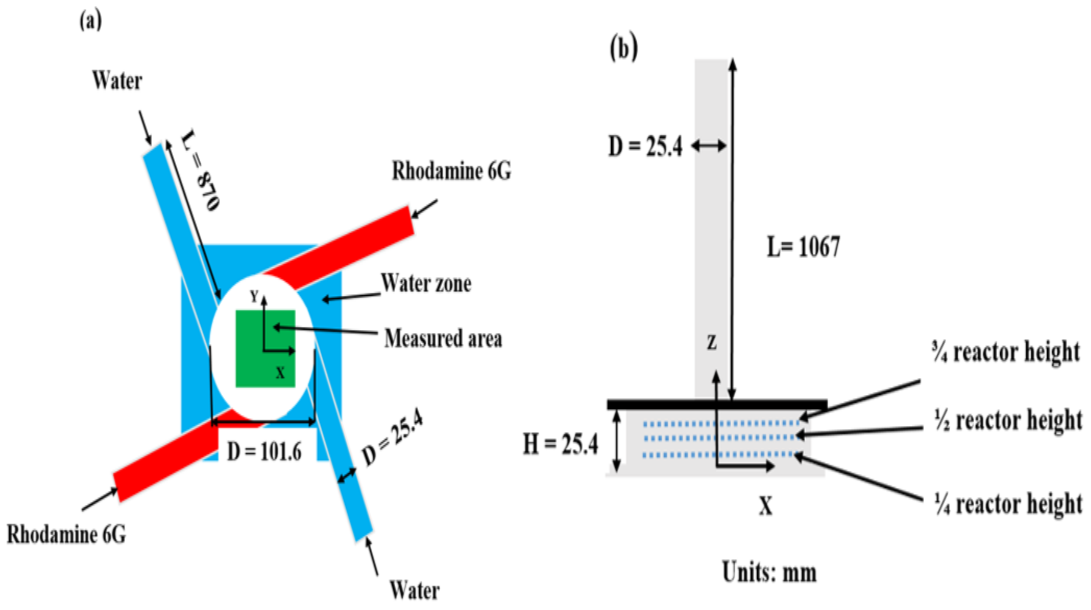

❖ The MIVR was developed for manufacturing nanoparticles using flash nanoprecipitation

Scaled up 16 times from the microscale MIVR

4. Measurement techniques: Particle Image Velocimetry (PIV) and Planar Laser Induced Fluorescence (PLIF)

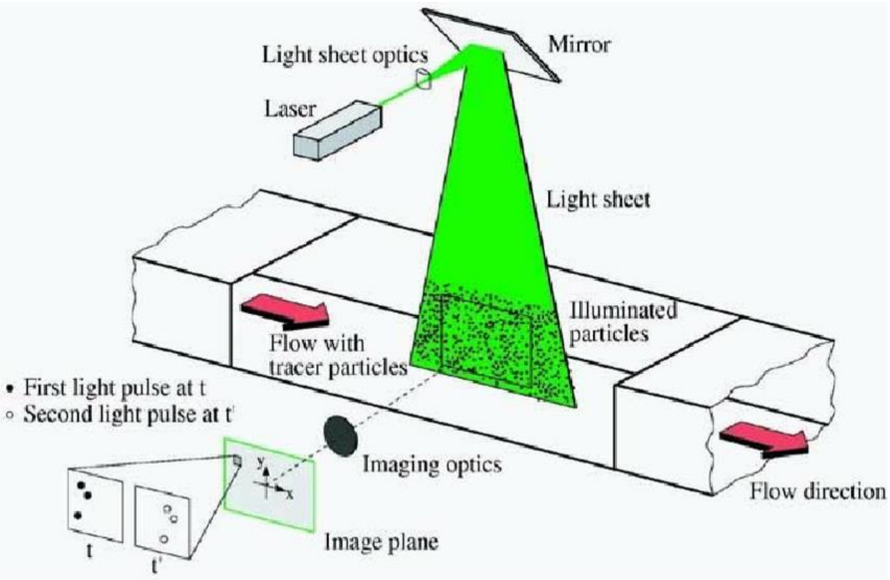

Fig. 3(a) Basic operation of PIV (Johnson et al., 2006)

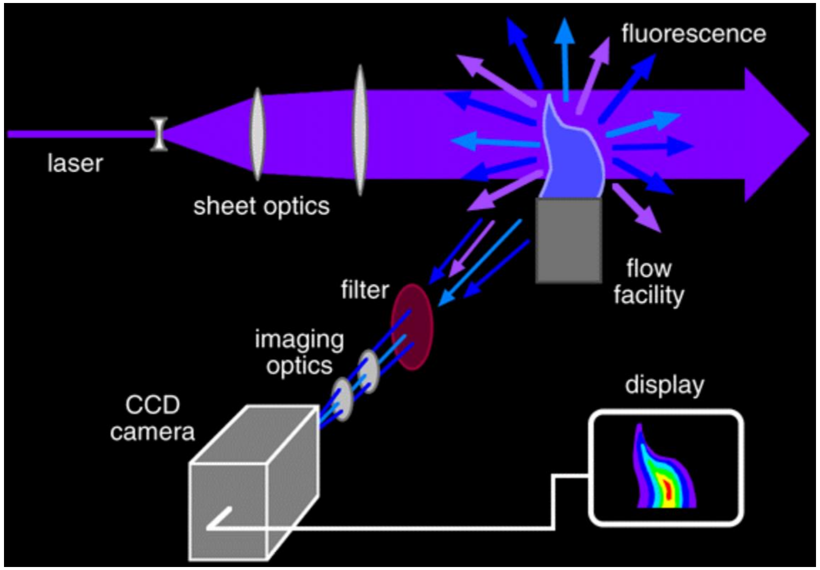

Fig. 3(b) Basic operation of PLIF (Seitzman et al., 1993)

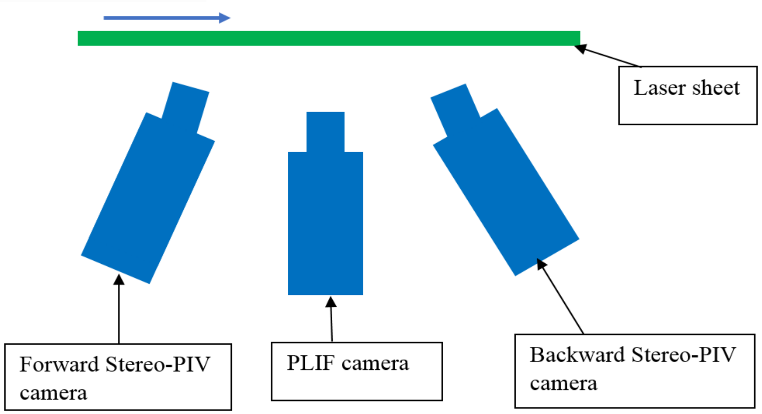

Fig. 3(c) Cameras arrangement

5. Typical instantaneous flow fields

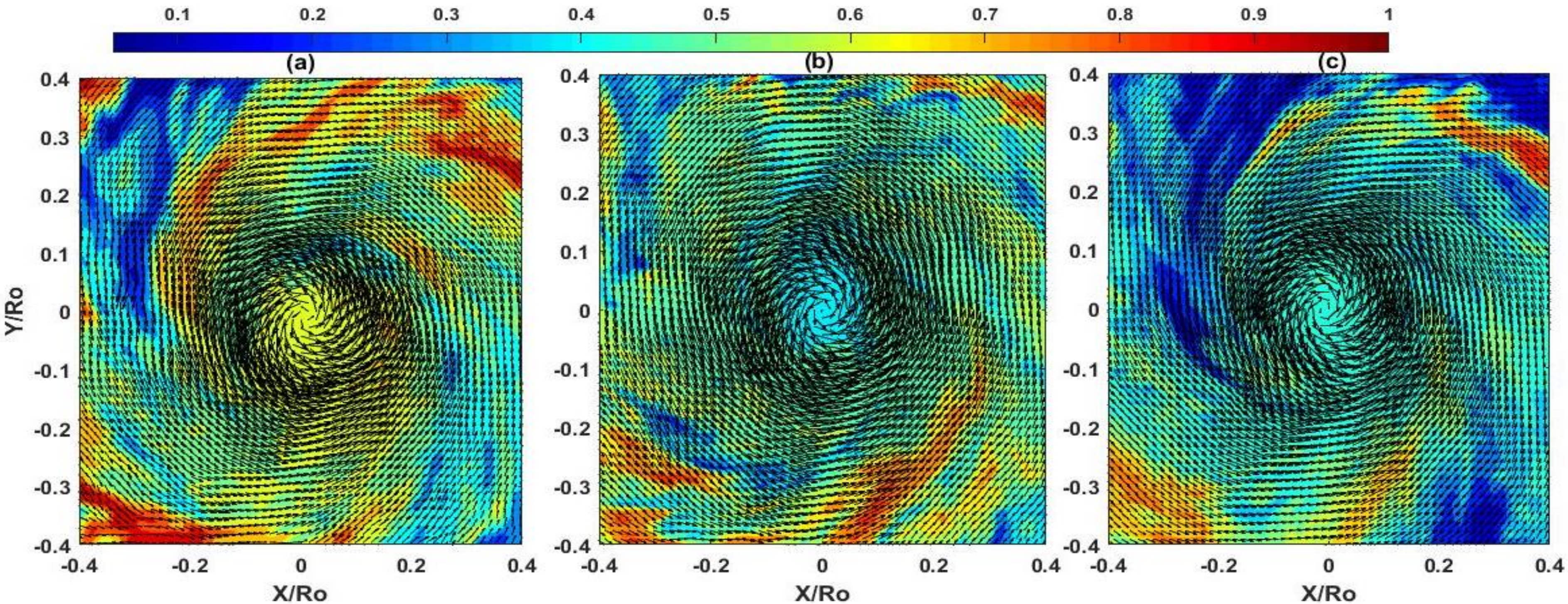

¼ plane **½ plane** **¾ plane**

Typical stereo-PIV/PLIF simultaneous results for Re=8125. The color and vectors represent the instantaneous mixture fraction and in-plane velocity field, respectively.

5. Mean velocity profiles

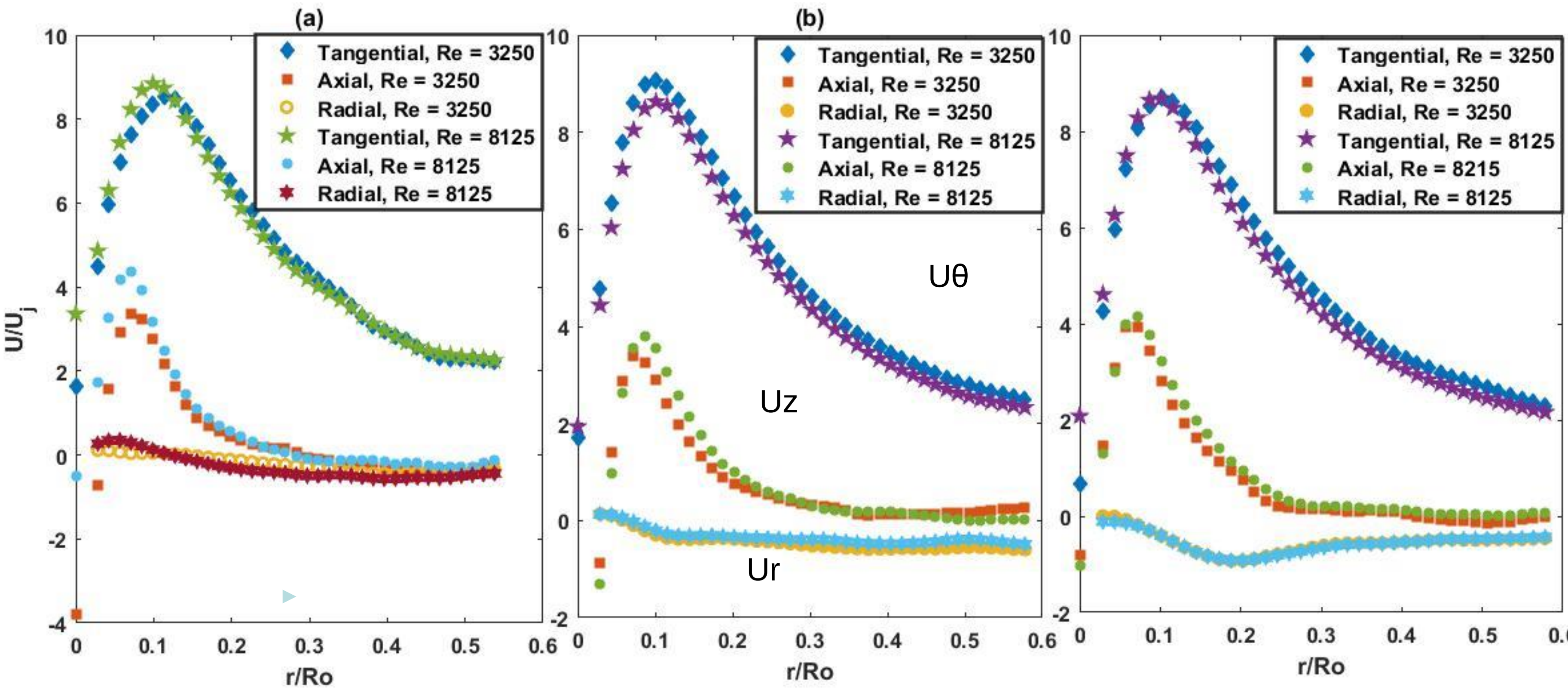

¼ plane **½ plane** **¾ plane**

6. Overview of the flow field: Mean concentration field

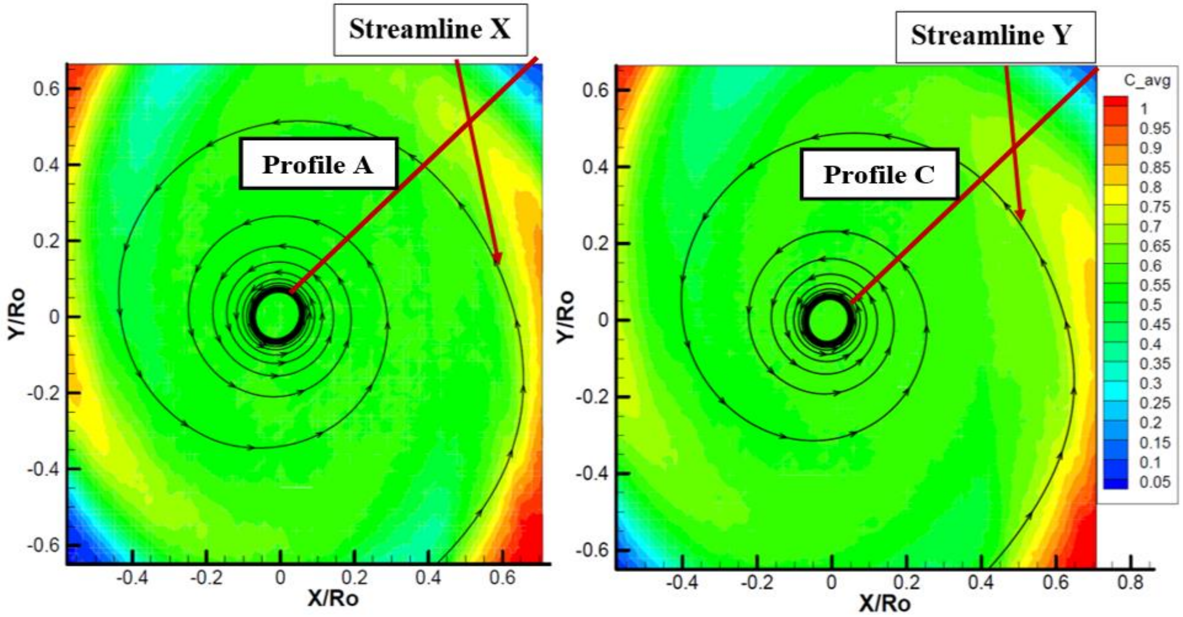

Re=8125 Re=3250

Example of "streamlines" along which statistics were computed at ½ plane. Mean concentration in color.

- Unmixed fluid spirals toward the center forming arm-like features
- The mean concentration is not axisymmetric

6. Overview of the flow field: Mixture fraction variance

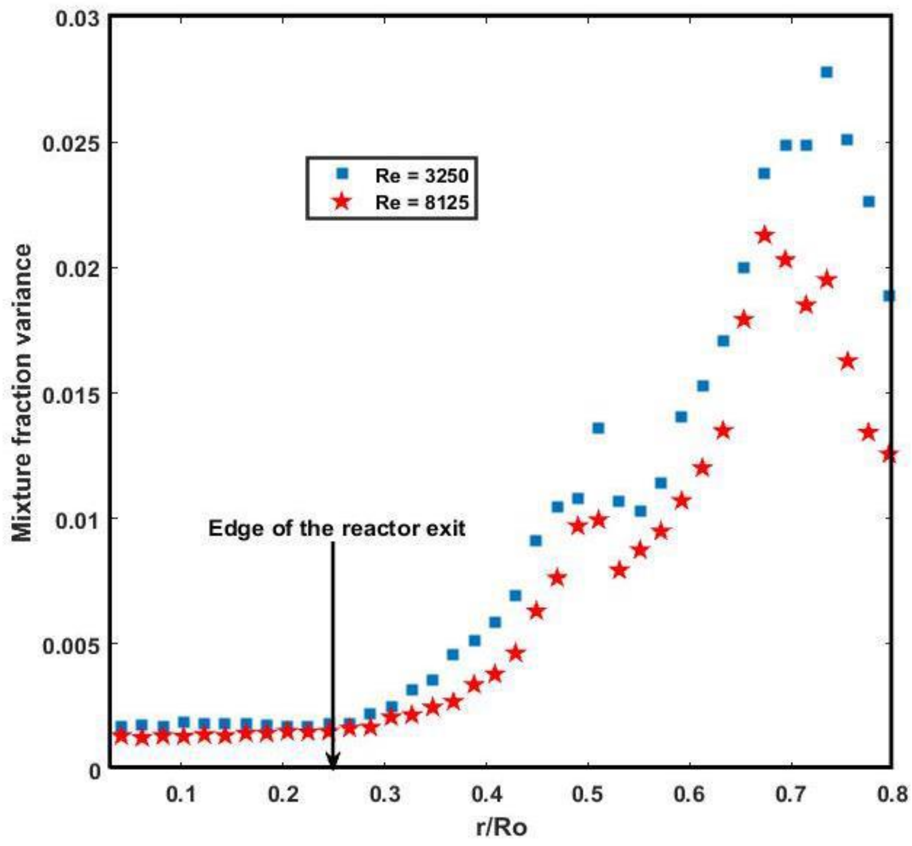

Mixture fraction variance at ½ plane through profiles A and C. Variance is maximum in spiral arms regions

7.1. Conditional velocity averages based on the linear model

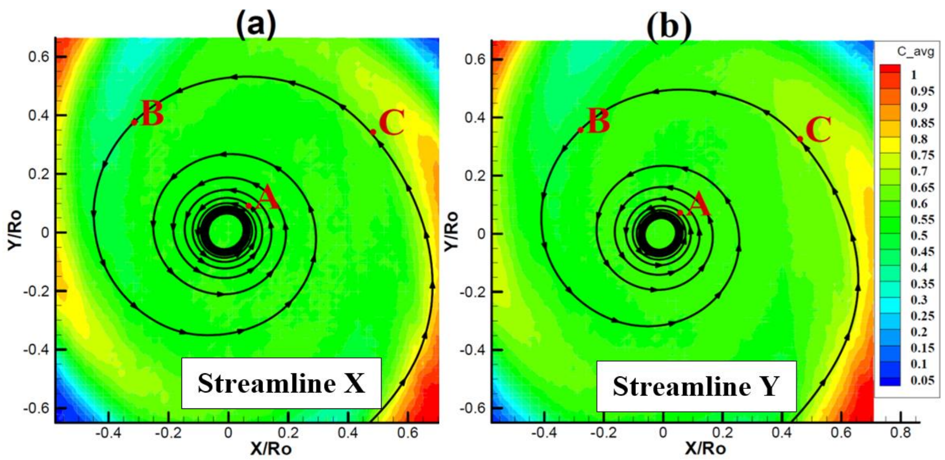

Re=8125 Re=3250

Mean concentration contour at ½ reactor height.
The streamline basepoints locations (A, B, C) shown in red

- $\langle U_i|\xi\rangle = \langle U_i\rangle + \langle u_i'\phi'\rangle \frac{(\xi-\langle\phi\rangle)}{\langle\phi'^2\rangle}$
- Assumes that joint PDF of velocity and mixture fraction is Gaussian

7.1. Conditional velocity averages based on the linear model (continued …)

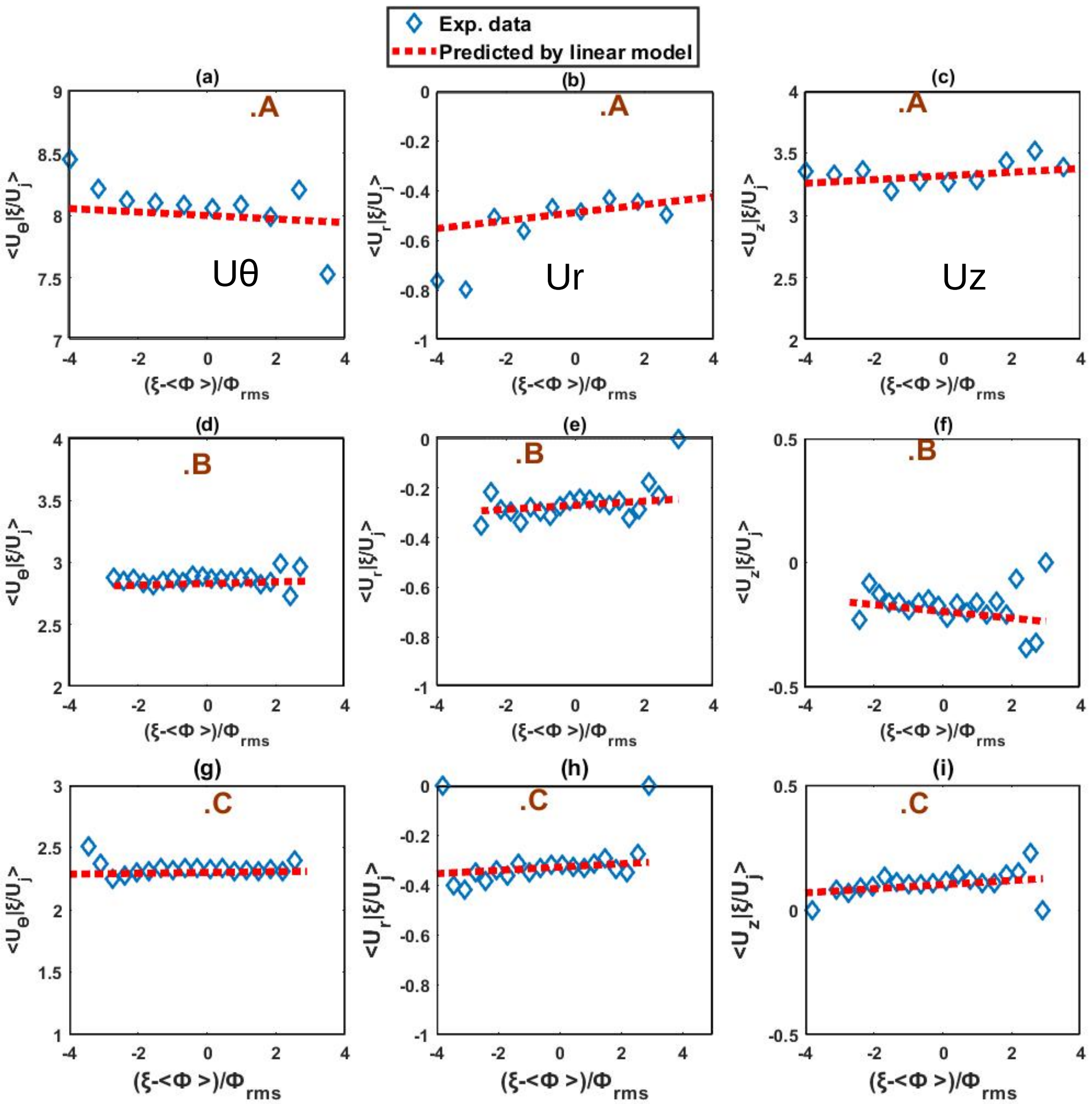

Compare experiment and linear model, ½ plane at Re=8125

7.2. Conditional velocity averages based on the Gradient PDF model

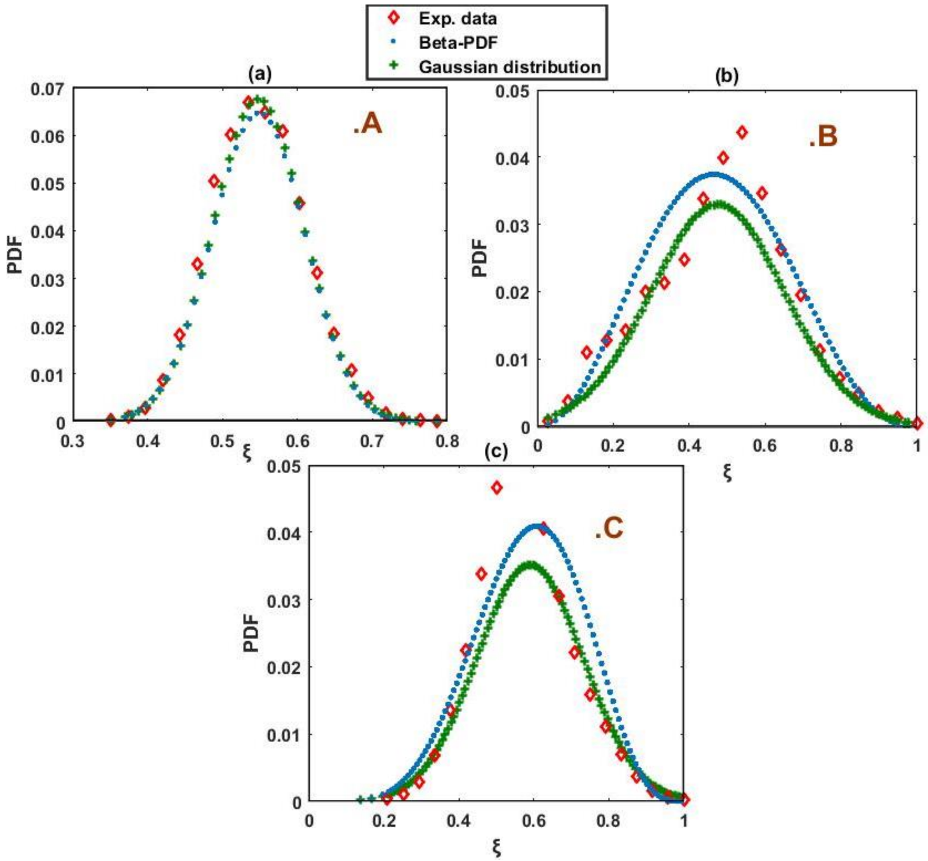

Fig. 10 *The probability density function of the mixture fraction fitted with Gaussian distribution and beta-PDF curves for Re = 8125 at ½ the reactor height. (a) For Basepoint A. (b) For basepoint B. (c) For basepoint C*

- ❖ $\langle U_i|\xi\rangle = \langle U_i\rangle - \frac{\mathrm{D}}{P_\Phi}\frac{\partial P_\Phi}{\partial r}$
- ❖ Based on the PDF of the scalar and its gradient
- ❖ Assumes isotropic turbulent diffusivity
- ❖ $\mathrm{D} = -\frac{\langle \phi' u_r' \rangle}{\frac{d\bar{\phi}}{dr}}$

7.2. Conditional velocity averages based on Gradient PDF model (continued …)

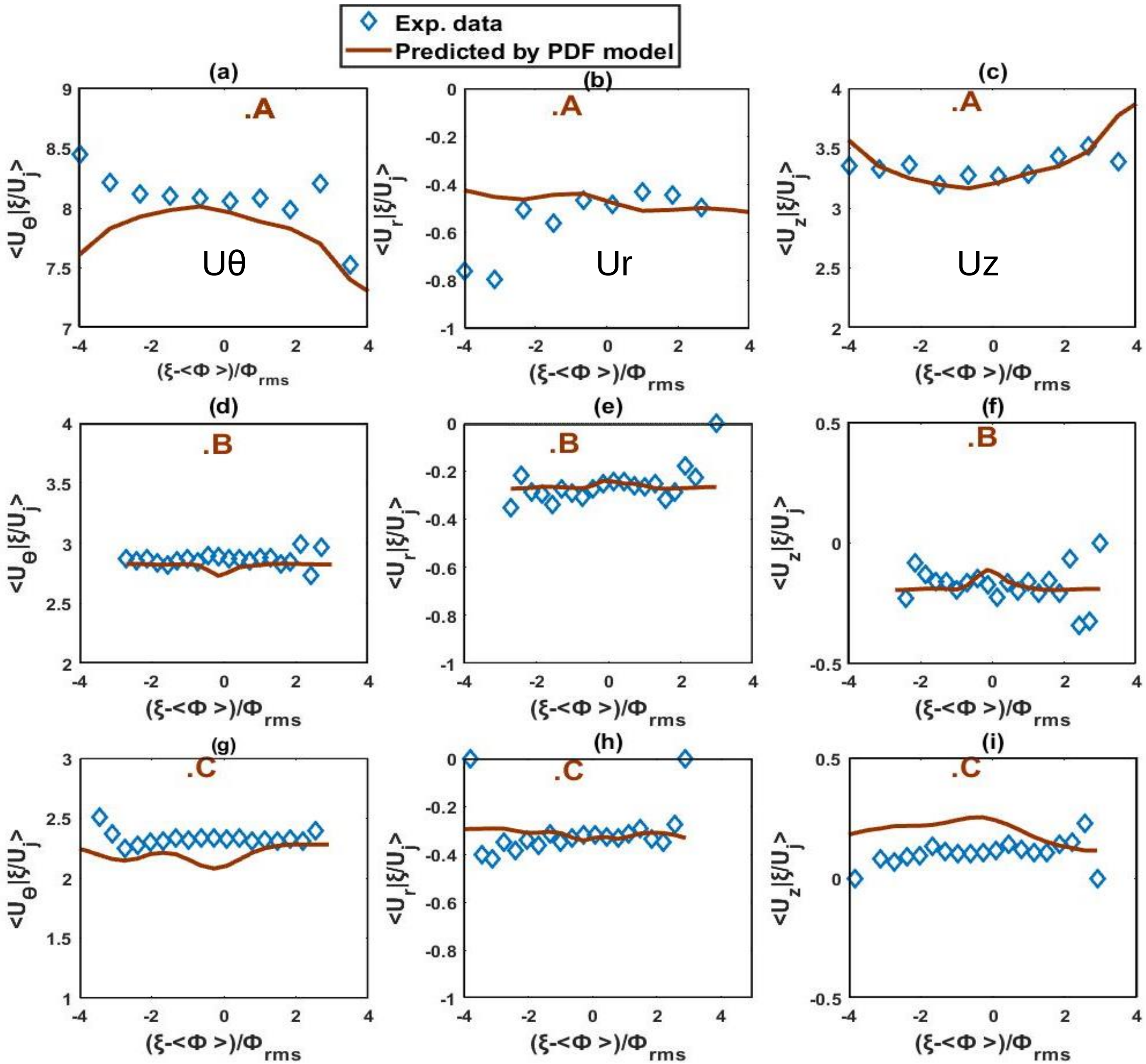

- A good prediction is obtained for the radial velocity
- Axial and tangential velocity are poorly predicted

Compare experiment and linear model, ½ plane at Re=8125

7.3. Conditional velocity averages based on modified Gradient PDF model

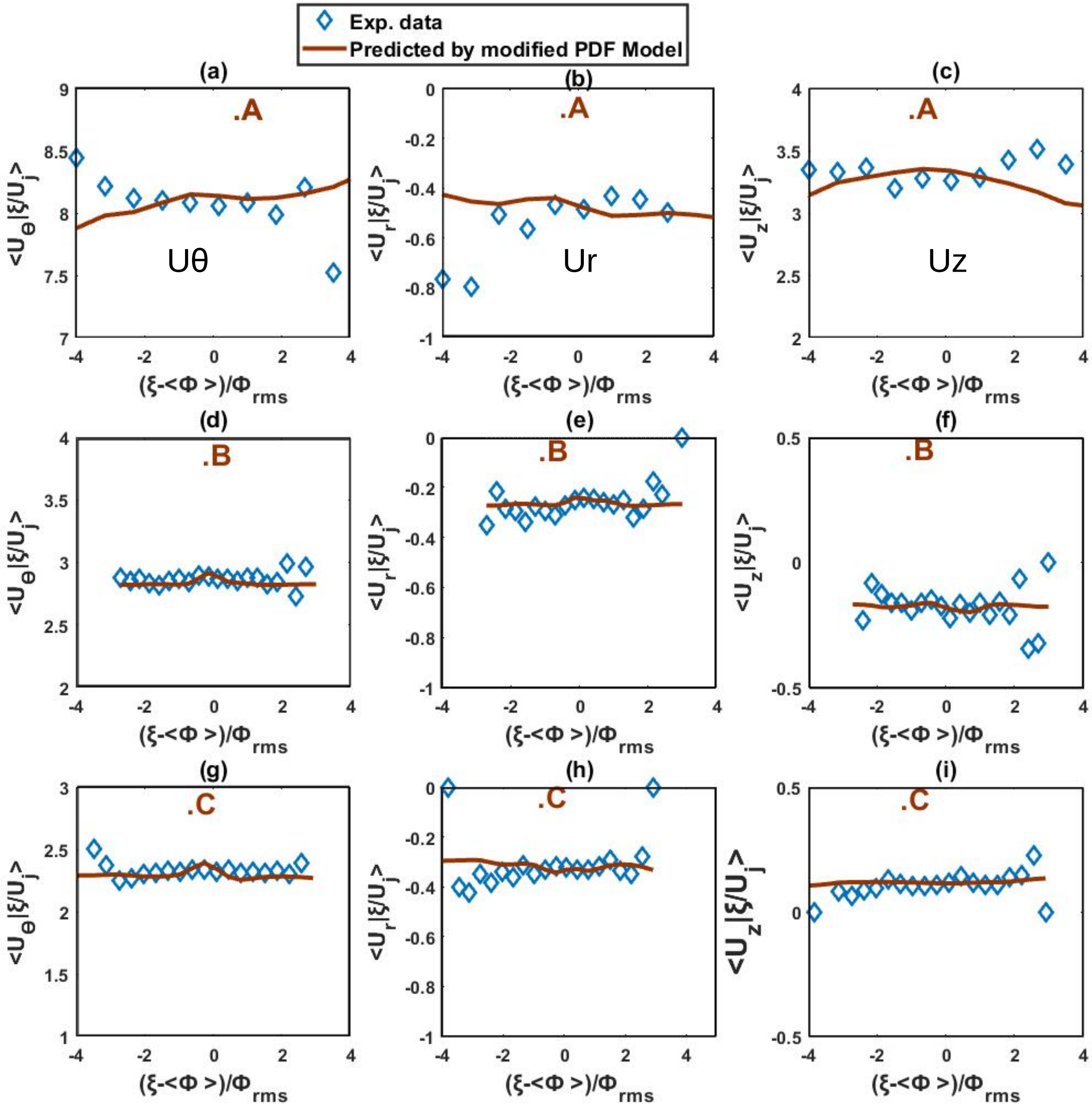

- The complex flow within the macro-MIVR results in noninotropic turbulent diffusivity
- $\mathrm{D}_{ir} = -\frac{\langle \phi' u_i' \rangle}{\frac{d\bar{\phi}}{dr}})$
- $\langle U_i | \xi \rangle = \langle U_i \rangle - \frac{\mathrm{D}_{ir}}{P_\phi} \frac{\partial P_\phi}{\partial r}$
- ½ plane, Re=8125

7.4. Conditional mixture fraction averages based on the linear model

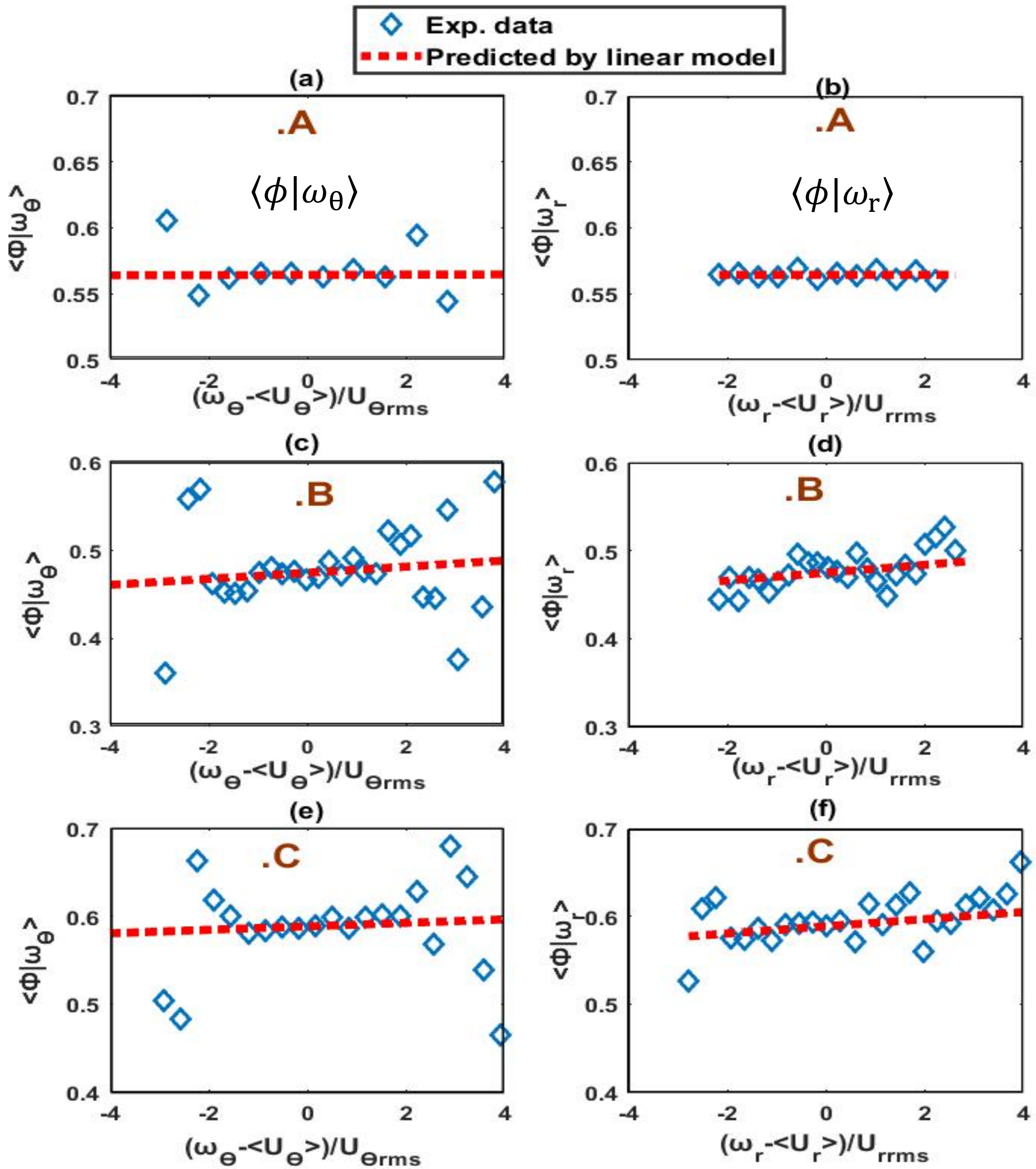

- Linear model for $\langle \phi | \omega_i \rangle$
- $\langle \phi | \omega_i \rangle = \langle \phi \rangle + \langle u_i' \phi' \rangle \frac{(\omega_i - \langle U_i \rangle)}{\langle u_i^2 \rangle}$
- ½ plane, Re=8125

8. Summary and conclusions

- The linear approximation and PDF gradient diffusion models are simple analytical tools used for predicting the conditional velocity and mixture fraction averages
- The linear model predicts $\langle U_i | \xi \rangle$ well in the low turbulence region away from the reactor center
- Near the reactor center, high velocity gradients coupled with low concentration gradients reduces the accuracy of the linear model predictions
- The Gradient PDF model with isotropic turbulent diffusivity performs poorly for tangential and axial conditional velocities
- The modified Gradient PDF model that considers three components of the turbulent diffusivity is better
- The mixture fraction conditioned on velocity components shows linear behavior near the reactor center, where the PDF of Φ is nearly Gaussian

9. Acknowledgments

- **Dr. Zhenping Liu**
- NSF/CBET-0934978

End.

Questions?

On the kinematics of scalar iso-surfaces in a turbulent, temporally developing jet

Brandon Blakeley, Weirong Wang, Duane Storti, James Riley
Department of Mechanical Engineering, University of Washington

APS Division of Fluid Dynamics
In honor of Ted O’Brien
24 November 2019

Turbulent mixing can be characterized by an interface that separates two regions of flow

- Flame surface (non-premixed)
  - Separates fuel from oxidant

Chris Shaddix, Yao Zhang, Sandia blog (2011)

Westerweel, J., et al. *JFM* (2009)

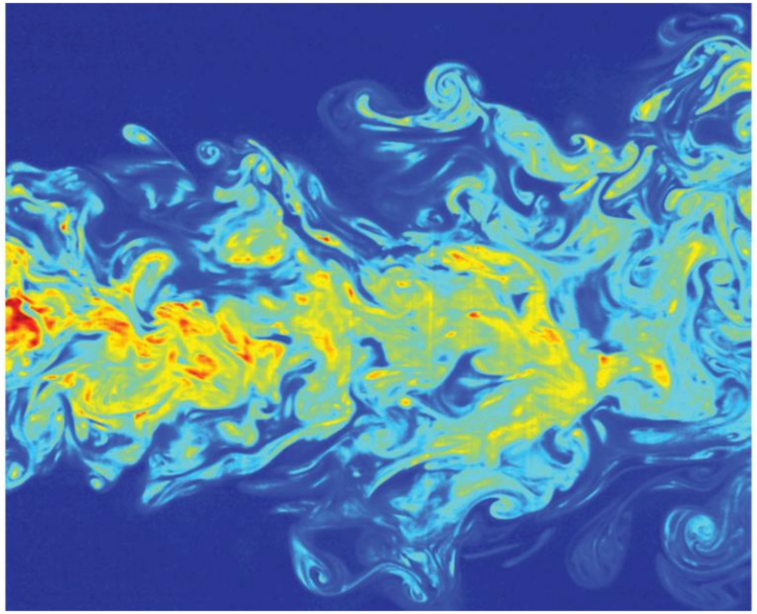

- Turbulent/non-turbulent interface
  - Separates rotational, turbulent flow from irrotational, ambient flow

Turbulent mixing can be characterized by an interface that separates two regions of flow

- Flame surface (non-premixed)
  - Separates fuel from oxidant
  - Mixture fraction, Z

Chris Shaddix, Yao Zhang, Sandia blog (2011)

- Turbulent/non-turbulent interface
  - Separates rotational, turbulent flow from irrotational, ambient flow
  - Vorticity magnitude, $|\omega|$

Westerweel, J., et al. *JFM* (2009)

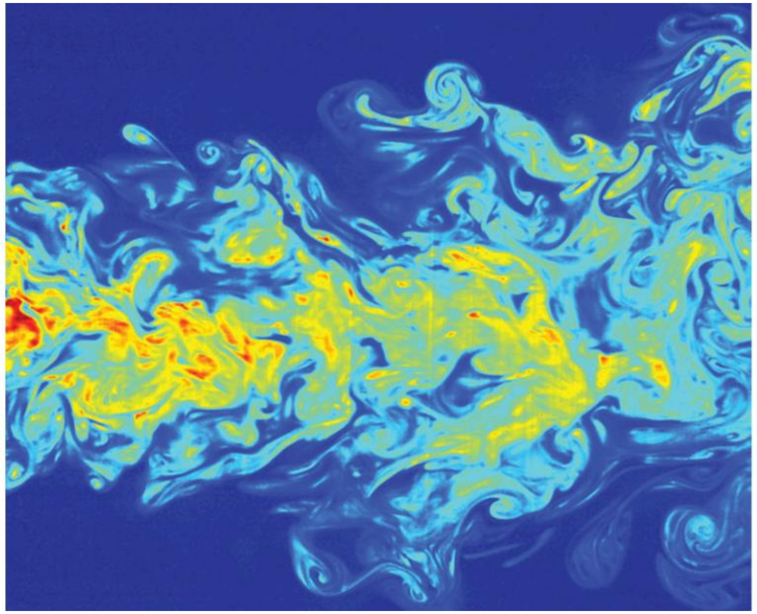

Turbulent mixing can be characterized by an interface that separates two regions of flow

- Flame surface (non-premixed)
  - Separates fuel from oxidant
  - Mixture fraction, Z
  - E.g. Coherent Flame Model (Marble and Broadwell, 1977)
- Turbulent/non-turbulent interface
  - Separates rotational, turbulent flow from irrotational, ambient flow
  - Vorticity magnitude, $|\omega|$

Chris Shaddix, Yao Zhang, Sandia blog (2011)

Westerweel, J., et al. *JFM* (2009)

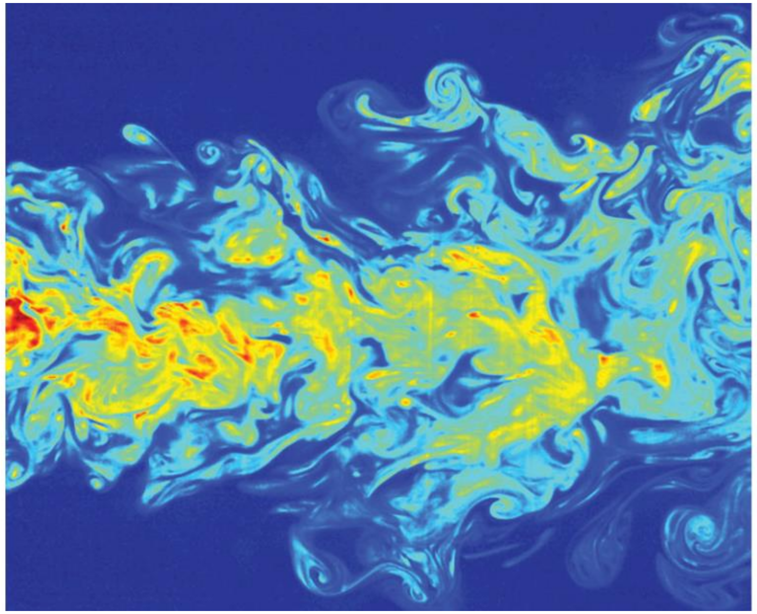

A transport equation can be derived for the mean iso-surface area per unit volume, Σ

Using notation from Van Kalmthout and Veynante, 1998:

$$\frac{\partial \Sigma}{\partial t} + \nabla \cdot (\langle \boldsymbol{u} \rangle_s \Sigma) = \langle \nabla \cdot \boldsymbol{u} \; - \boldsymbol{nn} : \nabla \boldsymbol{u} \rangle_s \Sigma$$

$$- \nabla \cdot (\langle w \boldsymbol{n} \rangle_s \Sigma) + \langle w (\nabla \cdot \boldsymbol{n}) \rangle_s \Sigma$$

E. Van Kalmthout and D. Veynante. PoF (1998)

A transport equation can be derived for the mean iso-surface area per unit volume, Σ

$$\overbrace{\frac{\partial \Sigma}{\partial t} + \nabla \cdot (\langle \boldsymbol{u} \rangle_s \Sigma)}^{\text{I and II: Convective derivative}} = \overbrace{\langle \nabla \cdot \boldsymbol{u} - \boldsymbol{nn}: \nabla \boldsymbol{u} \rangle_s \Sigma}^{\text{III: Production from strain-rate}}$$

$$- \underbrace{\nabla \cdot (\langle w \boldsymbol{n} \rangle_s \Sigma)}_{\text{IV: Normal displacement}} + \underbrace{\langle w (\nabla \cdot \boldsymbol{n}) \rangle_s \Sigma}_{\text{V: Effect of curvature}}$$

$$w = \frac{D \nabla^2 Z}{|\nabla Z|}, \qquad n = -\frac{\nabla Z}{|\nabla Z|}, \qquad \langle Q \rangle_s = \frac{\langle Q \Sigma \rangle}{\Sigma}$$

Diffusion (Gibson) velocity* | Normal vector | Surface-weighted average

Direct numerical simulation can be used to investigate iso-surface behavior

- 3D Incompressible Navier-Stokes equations
    - Fourier pseudospectral methods
    - Periodic boundary conditions
    - Adams-Bashforth time-stepping

- Advection-diffusion equation
    - Conserved passive scalar, Z

- Previously looked at a passive scalar in homogeneous, isotropic turbulence
    - B. C. Blakeley et al., JoT 2019

DNS of a turbulent, temporal jet is used to investigate passive scalar and T/NT interface

- $N = 512^3$ grid points (preliminary)
- $Re_{jet} = 3200, Sc = 0.7$
- Hyperbolic tangent profile for initial velocity and scalar fields
  - Homogeneous, isotropic background velocity perturbation

Spatial Jet

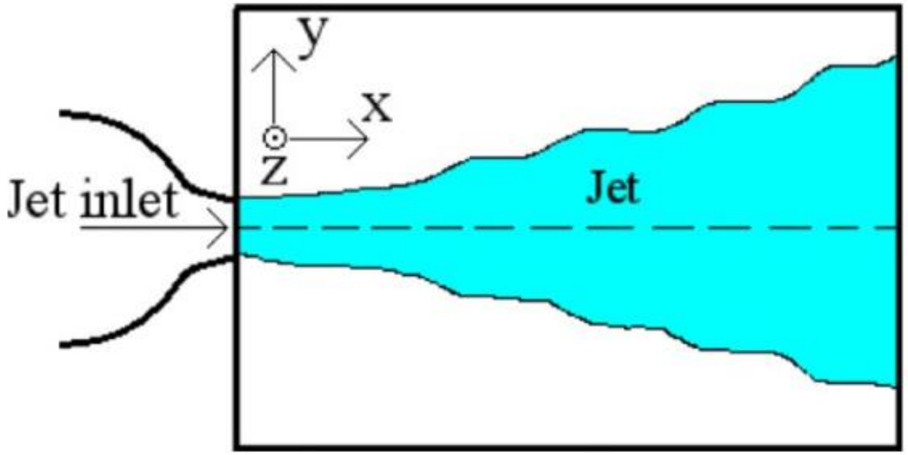

Temporal Jet

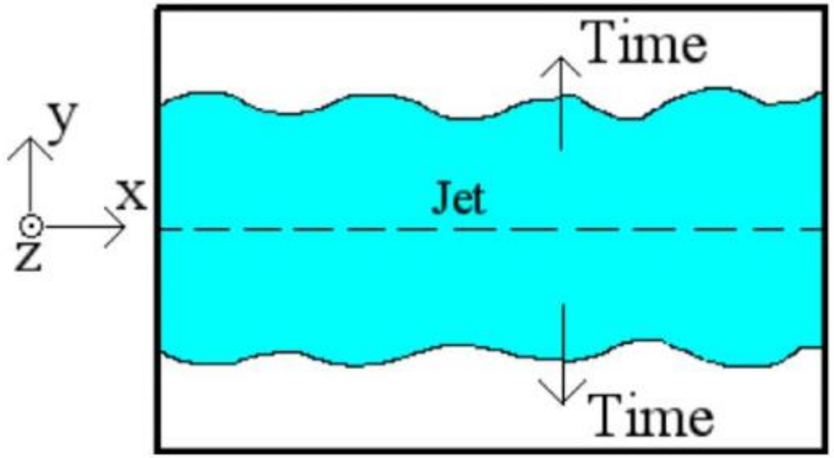

Da Silva and Pereira. PoF (2008)

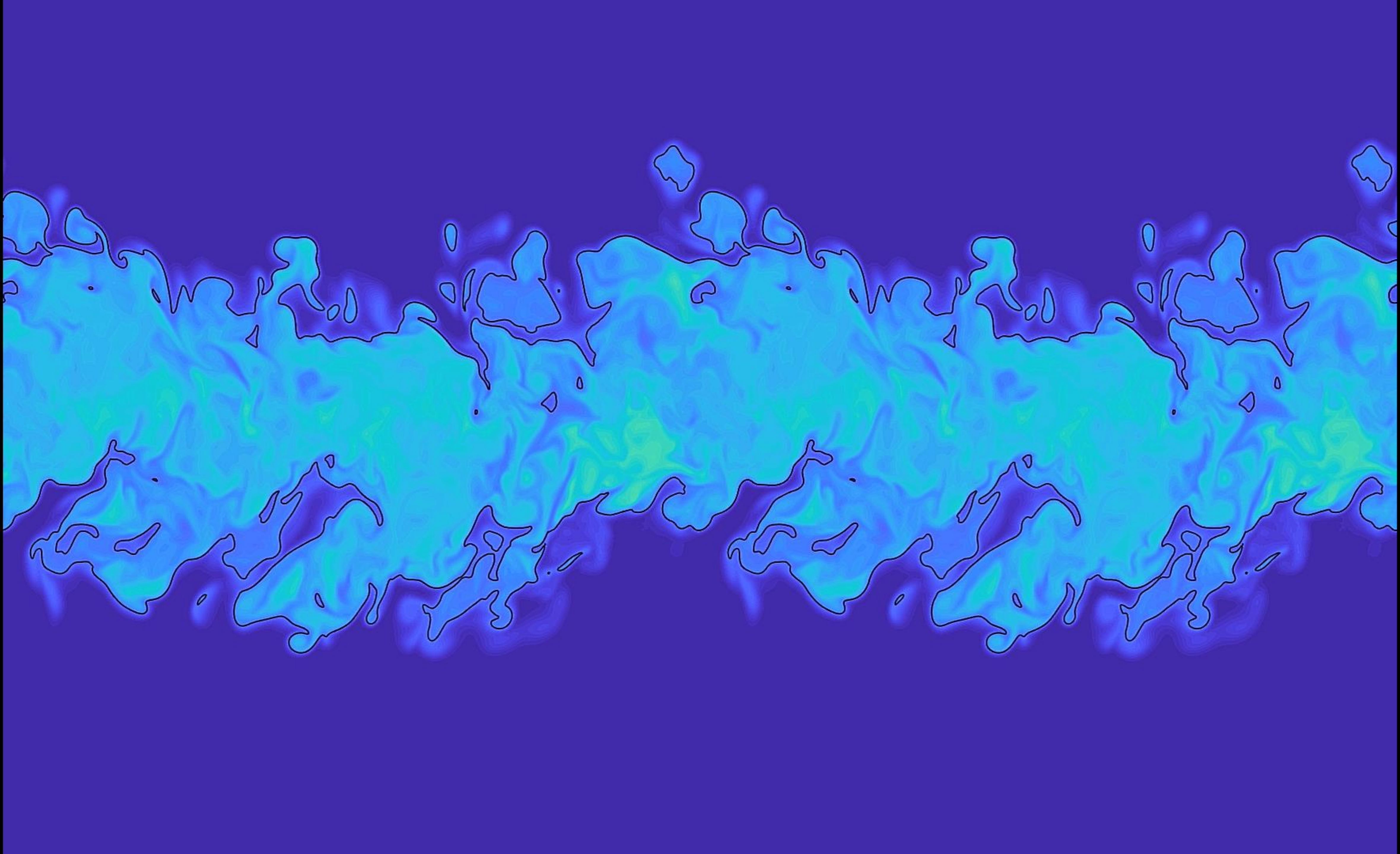

An integral approach for computing surface integrals is used for this study

- Direct surface integration
  - Uses scalar field data sampled on a discrete grid
  - Guaranteed convergence using Daubechies wavelets
  - Parallelizable algorithm

$$A = \iint_{\partial\Omega} ds = \iiint_{R^3} \nabla\mathcal{X} \cdot \boldsymbol{n}\, dV \approx -\Delta^3 \sum_{i,j,k=1}^{n_x,n_y,n_z} \left[\frac{\nabla\mathcal{X} \cdot \nabla Z}{|\nabla Z|}\right]_{i,j,k}$$

$$\mathcal{X} = \begin{cases} 1, & Z < Z_{iso} \\ 0, & Z > Z_{iso} \end{cases}$$

M. Yurtoglu, M. Carton, and D. Storti. JCISE (2018)

Surface area measurements demonstrate strong dependence on Z_{iso}

- Surfaces with 'large' values of Z_{iso} grow initially but disappear due to molecular diffusion
- Iso-surfaces with 'small' values of Z_{iso} level off and remain steady in self-similar region

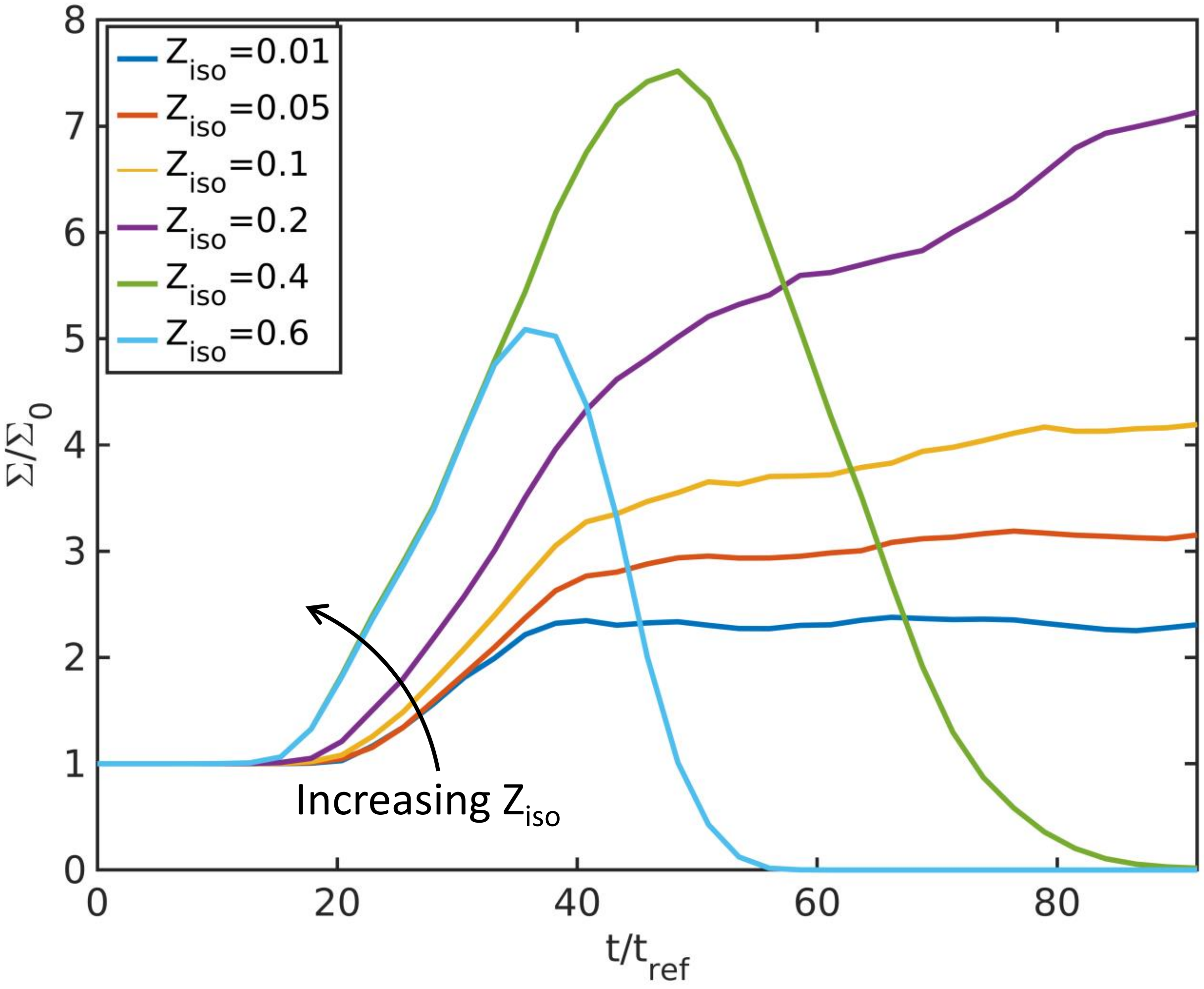

Surface area measurements demonstrate strong dependence on Z_{iso}

- Surfaces with 'large' values of Z_{iso} grow initially but disappear due to molecular diffusion
- Iso-surfaces with 'small' values of Z_{iso} level off and remain steady in self-similar region

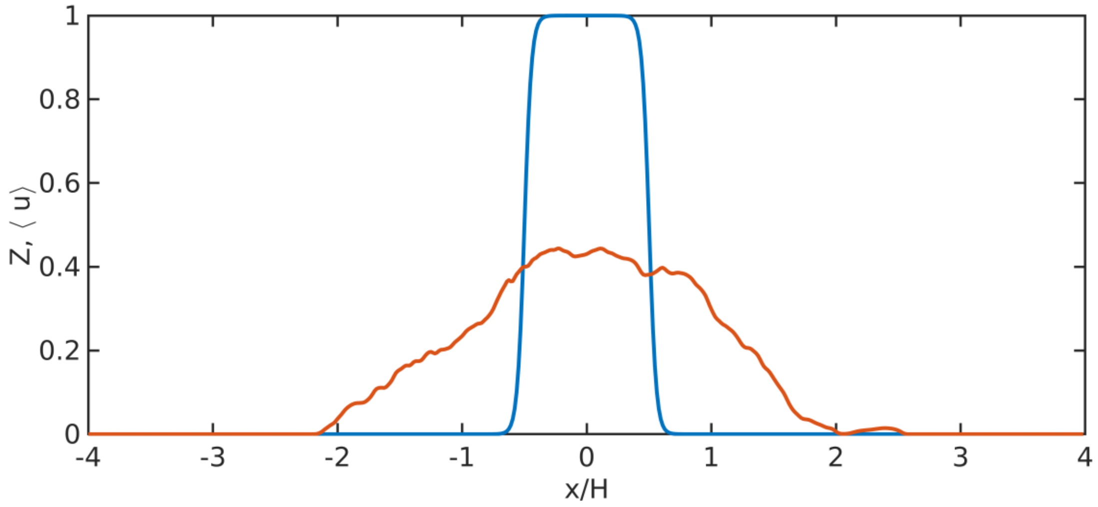

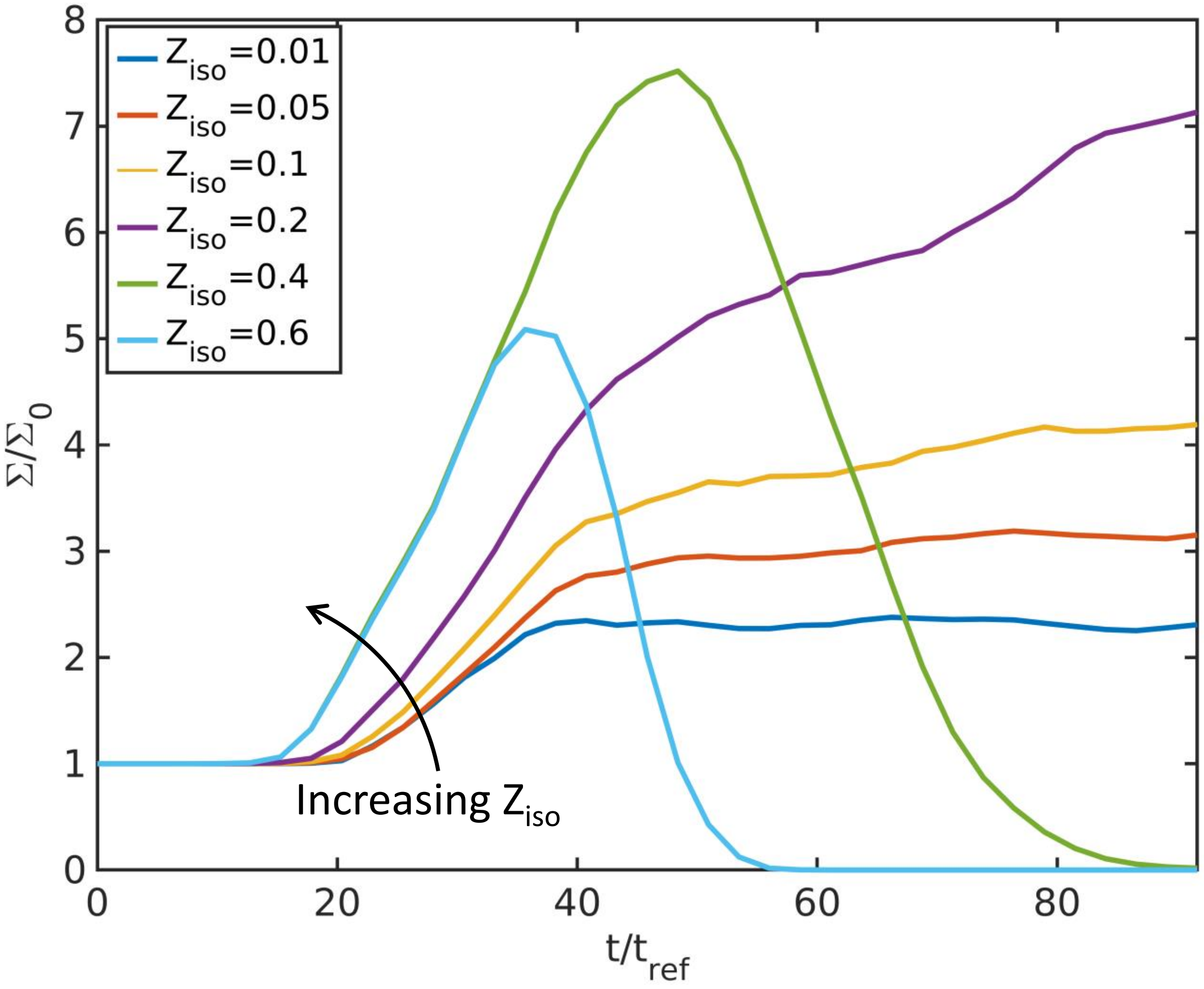

Surface area measurements demonstrate strong dependence on Z_{iso}

- Surfaces with 'large' values of Z_{iso} grow initially but disappear due to molecular diffusion
- Iso-surfaces with 'small' values of Z_{iso} level off and remain steady in self-similar region

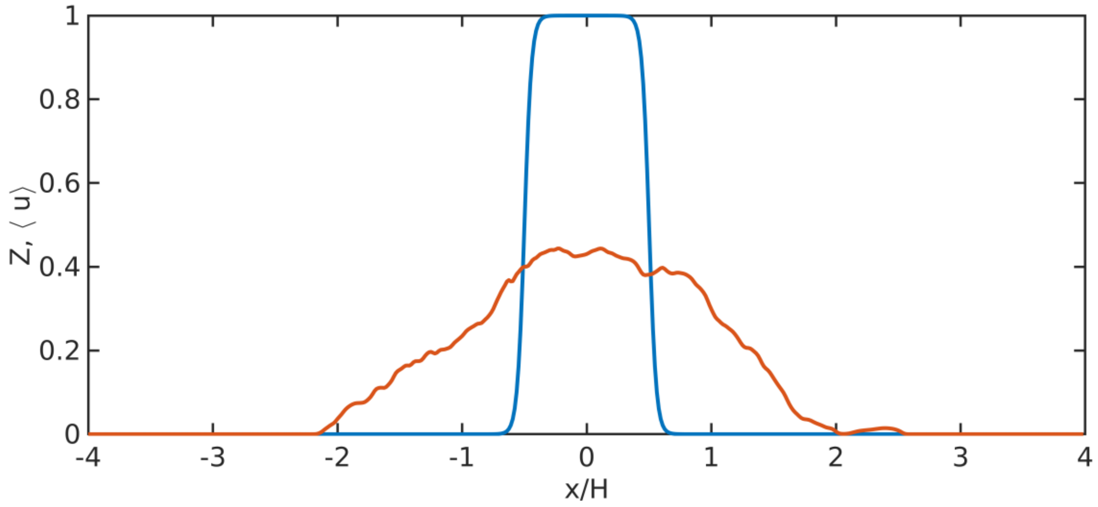

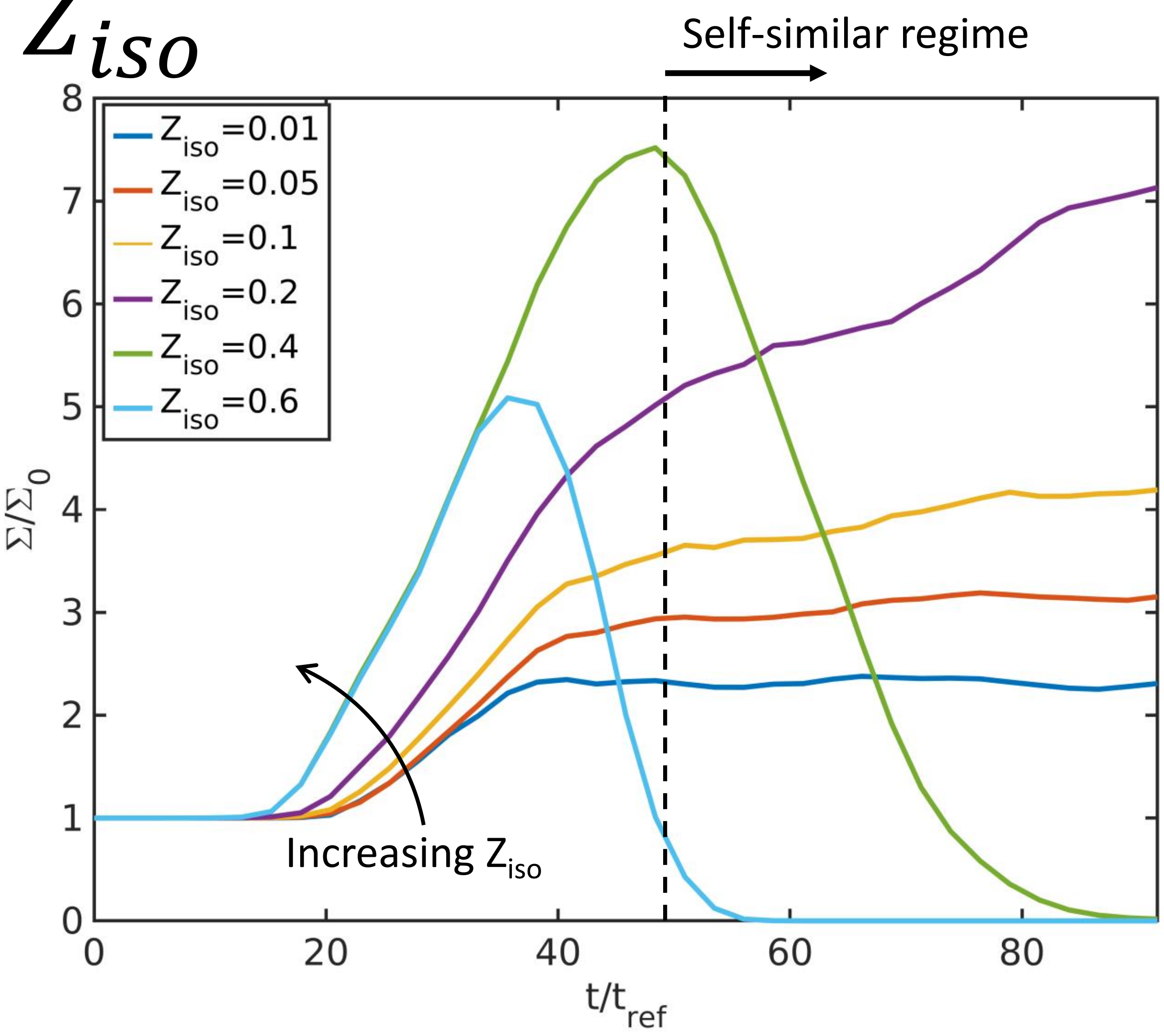

Evaluating terms in the Σ transport equation for volume averaged, incompressible flow

$$\overbrace{\frac{1}{\Sigma}\frac{\partial \Sigma}{\partial t}}^{\text{Term I: Time rate-of-change of } \Sigma} = \underbrace{-\langle \boldsymbol{nn} \colon S \rangle_s}_{\text{Term III: Production from strain-rate}} + \overbrace{\langle w(\nabla \cdot \boldsymbol{n}) \rangle_s}^{\text{Term V: Effects of curvature and molecular diffusion}}$$

$$S = \frac{1}{2}(\nabla \boldsymbol{u} + \nabla \boldsymbol{u}^T)$$

Strain-rate tensor

Surface area evolution is a balance of production and destruction

- Strain-rate term dominates at early times to produce area
- Strain-rate and diffusion terms balance in self-similar region
- Some numerical error during roll-up and onset of turbulence

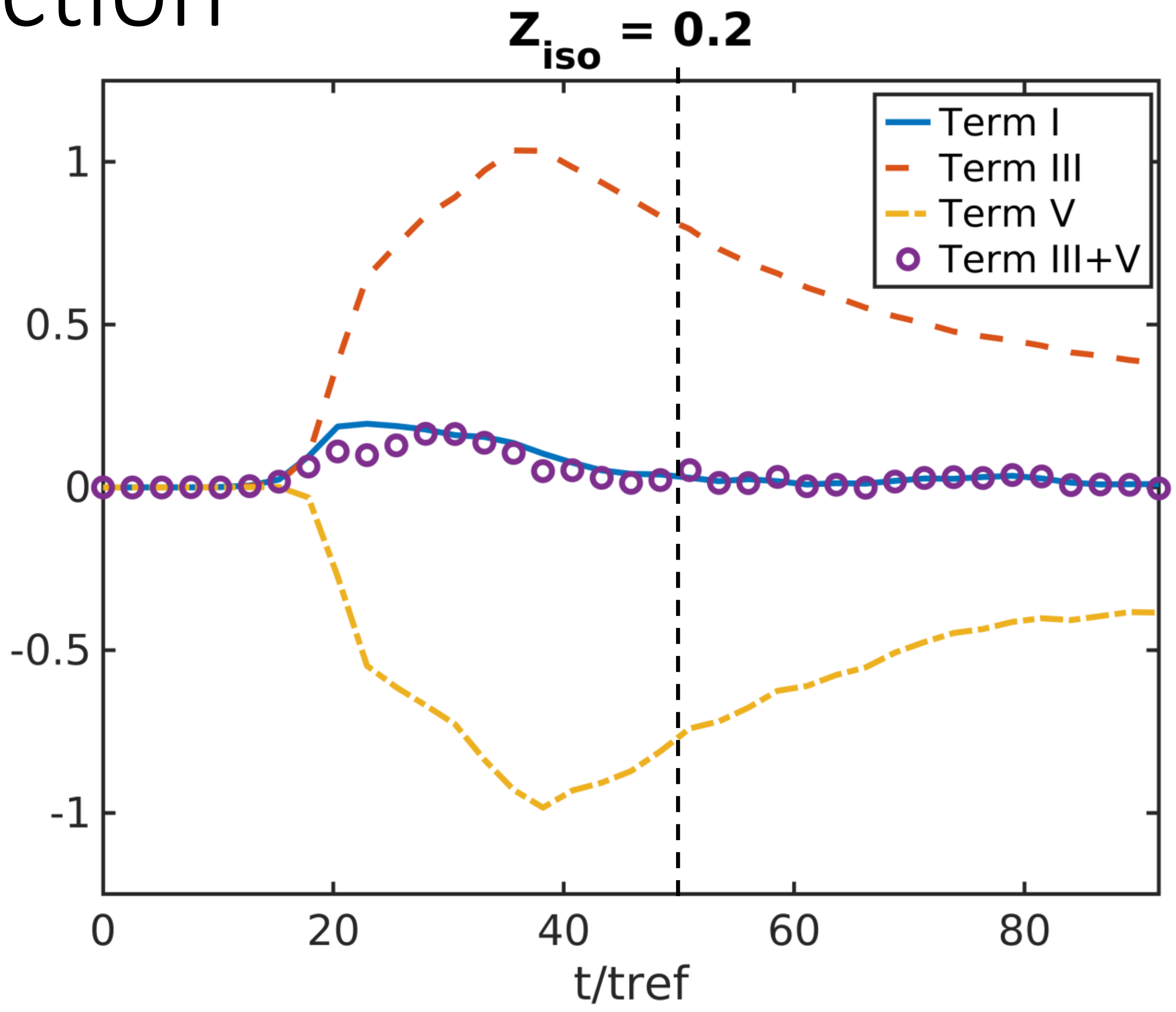

Conclusions and Future Work

- Looked at properties of various scalar iso-surfaces in a turbulent jet
  - Predict surface area growth based on balance of iso-surface transport equation
  - Other properties to investigate in the future, such as diffusion velocity, mass flux, curvature, etc.

- Would like to examine the turbulent/non-turbulent interface
  - Detection of T/NT interface using area is not trivial
  - Proper threshold value of $|\omega|_{iso}$ for the T/NT interface may vary with time

- Plan to increase resolution and Reynolds number

Thanks to:

- Amazon Web Services CCR
- Nvidia Corporation

Contact:

- bcb314@uw.edu
- During coffee break!

Questions?

Investigation of Two-Phase Supersonic Combustion in Hypersonic Flight

Foluso Ladeinde, Ph.D.

Department of Mechanical Engineering

Stony Brook University

Stony Brook, NY 11794-2300

APS/DFD 2019, November 23 – 26, 2019
Washington State Convention Center , Seattle, WA

Tribute to Ted O'Brien

Basic Research Issues

Simple-looking, technically quite complicated!

- **Inlet**
  - Mass capture contraction limit
  - BL transition
  - Cowl lip drag and heat transfer
- **Compressor**
  - Aero compression, shock waves, dual mode
- **Isolator**
  - Flow field dominated by shock/boundary layer interactions
  - Need an appropriate turbulence models
  - Unstart due to BL separation

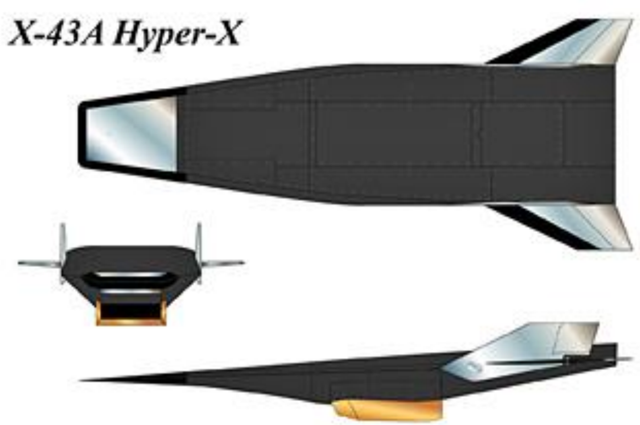

Engine/Airframe Balance

Nozzle Over-expansion at transonic Speeds

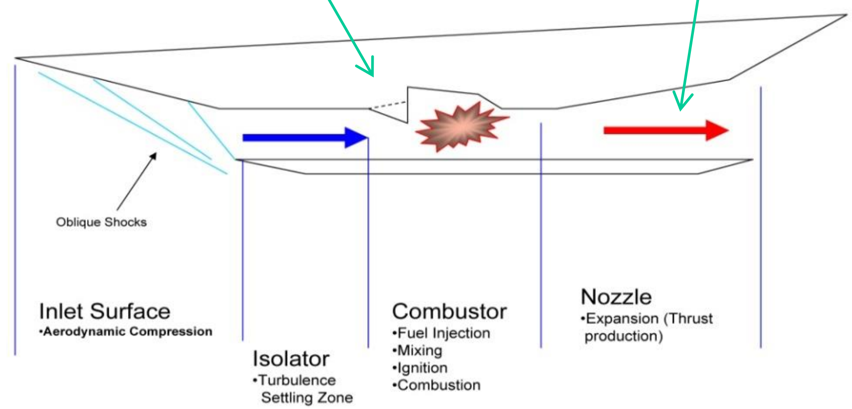

- **Combustor – Team Focus**
  - Fuel injection, Fuel Injection drag, Mixing, Ignition delay, flame stability and flame-holding, Dissociation due to high temperature, Aerodynamic heating, Unstart due to adverse pressure, turbulence-chemistry interaction, spray modeling
- **Nozzle**
  - Acceleration, heated exhaust

Some Background

Motivation for Hypersonic Systems

- War-fighting capabilities (rapid response; impact - scales as velocity-squared)
- Hypersonic ISR
- Commercial transport

Boeing

Why Now?

- International Competition Landscape
- Increasingly Better M&S Tools
- Encouraging Hypersonic Flight Demonstration Results

Army Wants Hypersonic Missile Unit by 2023

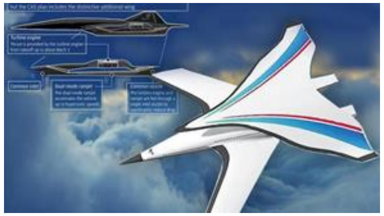

China's Hypersonic Plane

British 's Sabre Engine

Maiden Flight of Chinese HyperSonic Aircraft Flew Faster than US Blackbird

Motivation

- Advantages of Liquid Fuels
  - ✓ High heat release
  - ✓ Easy handling
  - ✓ Easy storage
  - ✓ Easy pumping
  - ✓ More quiet

- Better Understanding of High-speed Combustion of Liquid Fuels

Opportunities

- Hard Question: Several Complex Modeling Issues
  - ✓ Supersonic flow fields with shock waves
  - ✓ Turbulence
  - ✓ Two-Phase Flows
  - ✓ Combustion
  - ✓ Interactions
- Focus on Supersonic Combustion and Two-Phase (Liquid-Gas)

Ultimate Interest

- Understanding transition equivalence ratio (TER), thermal Choking
- Isolator length, inlet conditions, wall friction, backpressure, combustion efficiency
- Effect of barbotage aeration gas type on TER
- Effects of fuel type (hydrogen, methane, ethylene, and kerosene) on propulsive efficiency,…
- Identifying the main flame stabilization mechanisms in the presence of droplets
- Fragmentation and factors that drive droplet evaporation
- Differential roles of premixed combustion, non-premixed combustion, and partially-premixed combustion
- Two-phase correlations for the supersonic case

State-of-the-Art

- The low-speed problem – spherical particles and breakup – has received a lot of attention
  - ✓ Bravo and Kweon (2014), Pickett et al. (2012), Weber et al. (2005), Reitz (1978, 1996, 2013), Lin and Reitz (1998), Faeth et al. (1995), Meijer et al. (2012), Senecal (2003), Senecal et al. (2007), Senecal et al. (1999), Senecal et al. (2013), Iyengar et al. (2013), Ashgriz (2011), Williams (1958), Schmidt and Rutland (2000), Reitz and Diwakar (1986, 1987), Hwang et al. (1996), O'Rourke and Amsden (1987), Tanner (1997), Tanner and Weisser (1998), Beale (1999), som and Aggarwal (2010),Menard et al. (2006), Beau et al. (2006), DesJardin et al. (2007), Gorokhovski (2008), Demoulin et al. (2013),
  - ✓ Bilger (2011), Urzay et al (2011), Wang and Rutland (2007), Reveillon and Vervisch (2000), Balachandar and Eaton (2010), Li and Soteriou (2016), Martinez-Ruiz et al. (2013), Franzelli et al. (2013), De et al. (2011), Sirignano (1983, Sanchez et al. (2015)
    - Problem no longer considered urgent:
- Several papers with the objective of modeling supersonic spray combustion
  - ✓ Genin and Menon (2004), Chakraborty (2010), Balasubramayan et al. (2006), Menon et al. (2011)*
    - Based on spherical particles and monodisperse sprays
    - Conditions used do not consider the effects of shock waves on fluid dynamic sources, heat transfer, mass transfer
    - Incompressible drag laws used
    - Only contributions from the quasi-steady (Stokes) drags considered
    - No considerations for breakup and the role of shock waves, shock trains, and pseudo-shock

State-of-the-Art

More relevant work

- Schewer (2019)
  - Liquid fuel detonation , JP-10, Eulerian-Lagrangian PPM, Finite rate chemistry, mono- and poly-dispersed (log-normal) drops, and effects of ER studied. No breakup mechanism allowed.
  - Cellular structure confirmed for liquid sprays; regions of persistent fuel sprays after detonation wave has passed
  - Incompressible evaporation models, little consideration for BBO; no supersonic models for drag, Nu, Sh
- Watanabe et al (2019)
  - Gaseous detonation with dilute water spray – determine drop size for maximum quenching of detonation
  - Eulerian-Lagrangian PPM, Finite rate chemistry
  - Little consideration for BBO; no supersonic models for drag, Nu, Sh
- Ladeinde (2017, 2018, 2019a, 2019b)
  - Assembled model equations for supersonic drag, fluid dynamic forces, and Nusselt number
  - Studied the experimental literature on drop breakup by shock waves, to help develop breakup models, which will invariably be very different from those for low-speed spray combustion.
  - Proposed a model for the Sherwood number
  - Modified VULCAN to incorporate the supersonic versions of drag laws, fluid dynamic body forces, Nu, and Sh, within the framework of the Eulerian-Lagrangian PPM-based spray modeling of supersonic and finite rate combustion
  - Began evaluating the proposed models by modifying the low-speed Eulerian-Lagrangian procedures his team implemented in VULCAN
  - Transported species, fairly complex chemistry,; implementation for dual-mode scramjet, and RDE
  - Some details are given in the rest of the presentation

Basic Research Questions to Answer

- **How Should We Model Supersonic Spray Combustion?**
  - ✓ Which method should we use within the framework of Balachandar and Eaton (2010)?
  - ✓ Don't we need the drag forces that evolve from BBO?
    - ❖ $C_{Dstd}, C_{Dadd}, C_{Dfld}, C_{Dhis}, C_{Dini}, C_{Dgrv}$
  - ✓ Shouldn't high-speed models for particle momentum, mass transfer, and heat transfer be more appropriate within p-pm?
  - ✓ How relevant are those supersonic two-phase flow studies for rockets and explosions (Balachandar, Eaton, Jackson, Parmar, Sridhanara, Nagata,…)?
  - ✓ How do we handle the complexities of droplet breakup in shocked flows?
  - ✓ Can we really separate the modeling of the fragmentation process from that of thermal evaporation and combustion?

Which Method to Use?

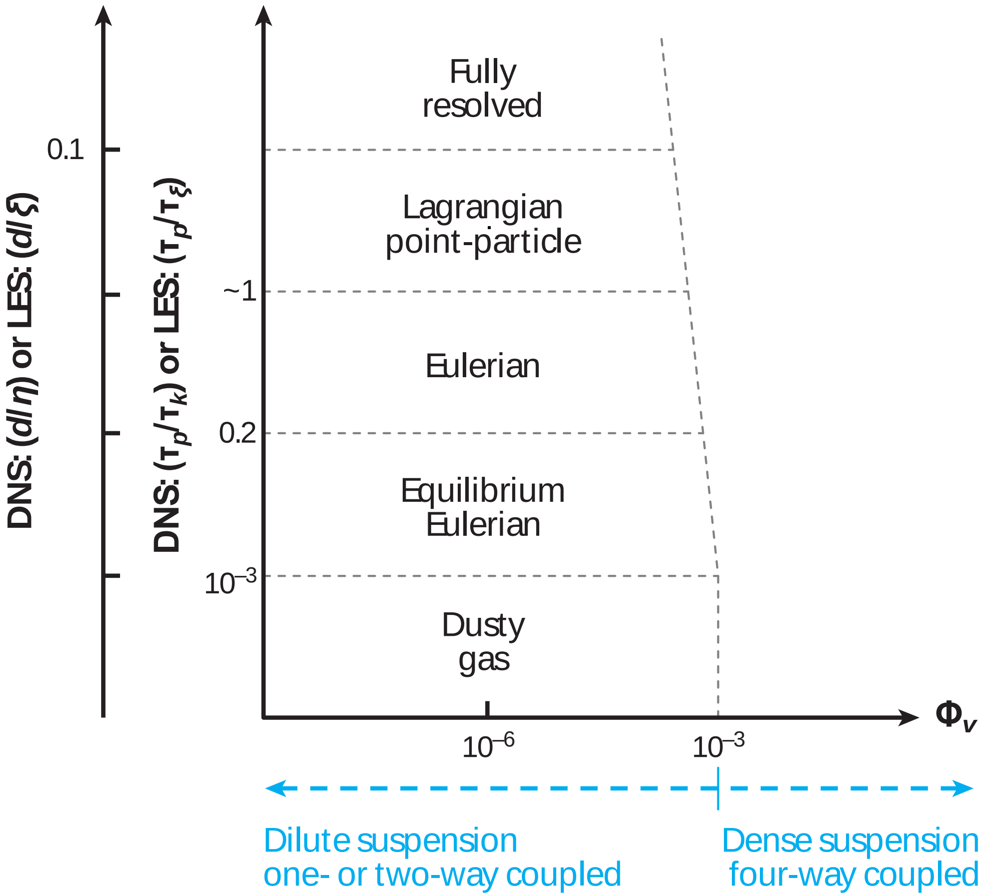

Eaton and Balachandar (2012)

FLUID DYNAMIC FORCES

Forces Acting on a Drop

$$m_d \frac{d\boldsymbol{u}_d}{dt} = \boldsymbol{F}_D + \boldsymbol{F}_C + \boldsymbol{F}_G \, ,$$

$(\boldsymbol{F}_D, \boldsymbol{F}_C, \boldsymbol{F}_G)$ = fluid dynamic forces, gravity, and con tact forces between droplets.

Fluid dynamic forces

$$\underbrace{\pi/8 \; C_D \rho_g d_d^2 \; |\boldsymbol{u} - \boldsymbol{u}_d|(\boldsymbol{u} - \boldsymbol{u}_d)}_{\text{drag in a steady,uniform flow}} \quad - \quad \underbrace{V_d \nabla p}_{\text{pressure gradient force}}$$

$$+ \quad \underbrace{V_d \nabla . \boldsymbol{\tau}}_{\text{shear stress gradient force}} \quad + \underbrace{\frac{1}{2} \rho_g \mathrm{V}_p \left(\frac{D\boldsymbol{u}}{Dt} - \frac{d\boldsymbol{u}_d}{dt} \right)}_{\text{Apparent mass force}} +$$

$$\underbrace{\frac{3}{2} d_p^2 \sqrt{\pi \rho_g \mu} \left\{ \int_{t_0}^{t} \left(\frac{1}{\sqrt{t-t'}} \left(\frac{D\boldsymbol{u}}{Dt} - \frac{d\boldsymbol{u}_d}{dt} \right) \right) dt' + \frac{1}{\sqrt{t}} (\boldsymbol{u} - \boldsymbol{u}_d)|_{t_0} \right\}}_{\text{Basset force}},$$

FLUID DYNAMIC FORCES

Pressure Gradient and Shear Stress Forces

$V_d \nabla p$ and $V_d \nabla . \boldsymbol{\tau}$ should ordinarily be negligible because of the small volume of droplet (V_d). However; there is the possibility of large gradients. Retain terms pending further analysis.

$$\nabla_d \rho_d \frac{\partial \boldsymbol{u}_d}{\partial t} = \underbrace{\pi/8\, C_D \rho_g d_d^2\, |\boldsymbol{u} - \boldsymbol{u}_d|(\boldsymbol{u} - \boldsymbol{u}_d)}_{\text{drag in a steady,uniform flow}} + \underbrace{\frac{1}{2}\rho_g V_p \left(\frac{D\boldsymbol{u}}{Dt} - \frac{d\boldsymbol{u}_d}{dt}\right)}_{\text{Apparent mass force}}$$

Added Mass Force

$$\frac{d\boldsymbol{u}_d^*}{dt^*} = \frac{Re}{24} C_D\, |\boldsymbol{u}^* - \boldsymbol{u}_d^*|(\boldsymbol{u}^* - \boldsymbol{u}_d^*) + \frac{\beta}{2}\left(\frac{D\boldsymbol{u}^*}{Dt} - \frac{d\boldsymbol{u}_d^*}{dt}\right);\ \beta = \frac{\rho_g}{\rho_d},$$

With $Re \sim 10^5$ or greater, $C_D \sim O(1)$, and $\beta \sim 0.001$, the added mass terms will ordinarily be negligibl y small compared to the drag terms, and possibly the other terms in the original expression above.

However, there are situations where the added mass terms could indeed be significant (Shimada et al. (2006).

In our case: Eye of the mixing layers formed by the interaction of gas and the fuel streams. . In fact, previous calculations of the PDF in reacting high-speed flows with shockwaves gave adv ective term magnitudes that are of $O(10^7)$.

Shimada, T., Daimon, Y., Sekino, N. ,Computational Fluid Dynamics of Multiphase Flows in Solid Rocket Motors, ISSN 1349-113X, JAXA-SP-05-035E, March 2006, Pub. Japan Aerospace Exploration Agency.

Gravitational Force Field

Velocity of a thermal, $V \sim \sqrt{gL_c}$,

L_c = Length of a scramjet combustor Along the gravitational force field,

g = Acceleration due to gravity,

$g = 9.81 \frac{m}{s^2}$,

$V = 2.8 \frac{\mathrm{m}}{\mathrm{s}} \ll 450 \frac{m}{s}$.

FLUID DYNAMIC FORCES

Evolution of Droplet Models for P-P

Basset (1888), Boussinesq (1903), and Oseen (1927) (BBO) - Creeping Flow (Unsteady Rectilinear motion of a sphere in a stagnant incompressible, viscous flow).

$$m_p \frac{dv}{dt} = -6\pi a \mu_f v - \frac{1}{2} m_f \frac{dv}{dt} - 6a^2 (\pi \mu_f \rho_f)^{\frac{1}{2}} \int_0^t \frac{dv/dt}{(t-\tau)^{\frac{1}{2}}} d\tau + (m_d - m_g) g$$

Maxey and Riley (1983): Non-uniform creeping flows:

$$m_p \frac{d\boldsymbol{v}}{dt} = -6\pi a \mu_f (\boldsymbol{u} - \boldsymbol{v}) + \frac{1}{2} m_f \frac{d(\boldsymbol{u} - \boldsymbol{v})}{dt} + m_f \frac{D\boldsymbol{u}}{Dt} + 6a^2 (\pi \mu_f \rho_f)^{\frac{1}{2}} \int_0^t \frac{d(\boldsymbol{u} - \boldsymbol{v})/d\tau}{(t-\tau)^{\frac{1}{2}}} d\tau + (m_d - m_g) \boldsymbol{g}$$

Berlemont, Desjongueres and Gouesbet (1990) – Simpler, non-creeping flows:

$$m_p \frac{d\boldsymbol{v}}{dt} = \frac{1}{2} C_{Dstd} \pi a^2 \mu_f |\boldsymbol{u} - \boldsymbol{v}| (\boldsymbol{u} - \boldsymbol{v}) + \frac{1}{2} m_f \frac{d(\boldsymbol{u} - \boldsymbol{v})}{dt} + m_f \frac{D\boldsymbol{u}}{Dt} + 6a^2 (\pi \mu_f \rho_f)^{\frac{1}{2}} \int_0^t \frac{d(\boldsymbol{u} - \boldsymbol{v})/d\tau}{(t-\tau)^{\frac{1}{2}}} d\tau + (m_d - m_g) \boldsymbol{g}$$

For practical engineering applications:

$$m_d \frac{d\boldsymbol{u}_d}{dt} = \underbrace{\pi/2 C_D \rho_g d_d^2 \, |\boldsymbol{u} - \boldsymbol{u}_d| (\boldsymbol{u} - \boldsymbol{u}_d)}_{\text{drag in a steady ,uniform flow}} + (m_d - m_g) \boldsymbol{g}$$

FLUID DYNAMIC FORCES

Evolution of Droplet Models for P-P...

Odar and Hamilton (1964) and Odar (1966) proposed a model for the motion of a sphere with finite Reynolds number:

$$m_p \frac{dv}{dt} = -\frac{1}{2} C_{Dstd} \pi a^2 \rho_f |\boldsymbol{v}| v - C_a \frac{1}{2} m_f \frac{dv}{dt} - C_h 6a^2 (\pi \mu_f \rho_f)^{\frac{1}{2}} \int_0^t \frac{dv/dt}{(t-\tau)^{\frac{1}{2}}} d\tau$$

$$C_a = 2.1 - 0.132 M_{A1}^2/(1 + 0.12 M_{A1}^2);$$
$$C_h = 0.48 + 0.52 M_{A1}^3/(1 + M_{A1}^3);$$

$M_{A1} = \frac{2a}{|\boldsymbol{u}-\boldsymbol{v}|^2} \left| \frac{d|\boldsymbol{u}-\boldsymbol{v}|}{dt} \right|$ (Acceleration parameter).

Note: $C_a \longrightarrow 1, C_h \longrightarrow 1$ as $A1 \longrightarrow \infty$.

Mei et al. (1991) Basset-force term must have a Kernel:

$$m_p \frac{dv}{dt} = \frac{1}{2} C_{Dstd} \pi a^2 \rho_f |u - v| (u - v) + \frac{1}{2} m_f \left(\frac{Du}{Dt} - \frac{Dv}{Dt} \right) + m_f \frac{Du}{Dt} + 6a\pi\mu_f \int_{-\infty}^{t} K(t-\tau,\tau) \frac{d(u-v)}{d\tau} d\tau + (m_d - m_g) g$$

$$K(t-\tau,\tau) = \left\{ \left[\frac{\pi (t-\tau) \nu_f}{a^2} \right]^{1/4} + \left[\frac{\pi}{2} \frac{|u(\tau) - v(\tau)|^3}{a \nu_f f_H^3(Re_t)} (t-\tau)^2 \right]^{1/2} \right\}^{-2}$$

$f_H(Re_t) = 0.75 + 0.105 Re_t(\tau)$;
$Re_t = 2a|u(\tau) - v(\tau)|/\nu_f$.

FLUID DYNAMIC FORCES

Evolution of Droplet Models for P-P…

Kim, Elghobashi and Sirignano (1998), Modified the history terms to allow for the effects of large relative acceleration or deceleration the particle and the initial relative velocity between the fluid and the particle:

$$m_p \frac{dv}{dt} = \frac{1}{2} C_{Dstd} \pi a^2 \rho_f |u-v|(u-v) + \frac{1}{2} m_f \left(\frac{Du}{Dt} - \frac{Dv}{Dt}\right) + m_f \frac{Du}{Dt} + 6a\pi\mu_f \int_{0^+}^{t} K(t-\tau,\tau) \frac{d(u-v)}{d\tau} d\tau + (m_d - m_g)g + 6a\pi\mu_f K_1(t)[u(0^+) - v(0^+) - u(0^-) + v(0^-)].$$

$$K(t-\tau,\tau) = \left\{ \left[\frac{\pi(t-\tau)\nu_f}{a^2}\right]^{1/(2c_1)} + G(\tau) \left[\frac{\pi}{2} \frac{|u(\tau)-v(\tau)|^3}{a\nu_f f_H^3(Re_t)} (t-\tau)^2\right]^{1/c_1} \right\}^{-c_1},$$

$$G(\tau) = \frac{1}{1+\beta\left(M_{A1}(\tau)\right)^{1/2}},$$

$$\beta = \frac{1}{1+\phi_r \phi_r^{c4}/[c_3(\phi_r+\phi_r^{c4})]},$$

$$f_H = 0.75 + c_5\, Re_t(\tau).$$

FLUID DYNAMIC FORCES

Evolution of Droplet Models for P-P…

Kim, Elghobashi and Sirignano (1998) Cont'd…

$$m_p \frac{dv}{dt} = \frac{1}{2}\pi a^2 \rho_f |u-v|(u-v) C_{Dtot}$$
$$= \frac{1}{2}\pi a^2 \rho_f |u-v|(u-v)\{C_{Dstd} + C_{Dadd} + C_{Dfld} + C_{Dhis} + C_{Dini} + C_{Dgrv}\}$$

Abbreviation	Definition	Approximation
C_{Dstd}	Quasi-steady drag coefficient from the (steady) standard drag curve	
C_{Dadd}	Drag coefficient due to added mass force	$\frac{2}{3} M_{A1}$
C_{Dfld}	Drag coefficient due to carrier fluid acceleration, or the gradient of the pressure and the shear stress at the position of sphere	$\frac{8}{3}\frac{Sl_\omega}{\lvert u^*-v^*\rvert(u^*-v^*)}\frac{\partial u^*}{\partial t'}$ t' is time normalize by frequencyω; u^*, v^* are velocities normalized by drop injection velocity; Sl =Strouhal number
C_{Dhis}	Drag due to the unsteady history force which is the integral of the past relative acceleration of the sphere weighted by the Kernel K	$\frac{6}{(\pi Re_R)^{1/2}}\int_0^{t^*} K^*(t^* - \tau^*, \tau^*) S\, M_{A1}(\tau^*) d\tau^*$
C_{Dini}	Drag coefficient due to the initial velocity difference between the carrier fluid and the sphere	$\frac{12}{(\pi Re_R)^{1/2}}\frac{K_1^*(t^*)}{\lvert u^*-v^*\rvert(u^*-v^*)}[u^*(0) - v^*(0)]$
C_{Dgrv}	Drag coefficient due to the net gravity force which	$\frac{8}{3}\frac{a(\rho_r - 1)g}{\lvert u-v\rvert(u-v)}$

$$K^*(t^*-\tau^*,\tau^*) = \left\{(t^*-\tau^*)^{1/5} + G(\tau)\left[\frac{\pi^{1/2}}{2} Re_R^{3/2} \frac{|u^*(\tau^*) - v^*(\tau^*)|^3}{a v_f f_H^3(Re_t)}(t^*-\tau^*)^2\right]^{2/5}\right\}^{-5/2}$$

FLUID DYNAMIC FORCES

A Few Point-Particle Models (Compressible)

Balachandar, Parmer, Jackson, Sridharan, …

Model for Pressure Gradient Force (Inviscid)

$$F_{pg}(t') = \overline{m_{f}\frac{Du_f}{Dt}}$$

$$= \frac{1}{V_p}\int_{V_p} m_{f}\frac{Du_f}{Dt} dV = \int_{V_p} \rho_{f}\frac{Du_f}{Dt} dV =$$

$$-\int_{V_p} \frac{\partial p_f}{\partial x}\, dV = (p_s - p_a)A_i(t')$$

$$\overline{(.)} = \frac{1}{V_p}\int_{V_p} (.)dV,$$

$$m_{f=}\rho_f V_p$$

$$(p_s, p_a) = (\text{pressure post} - \text{shock, pressure ahead of shock})$$

Mass-averaged Particle Pressure Model

$$\overline{p_p} = p_s + (p_{a-}p_s)\left[\frac{1+\frac{A\cos^2 Bt'}{\tau}}{1+A}\right]e^{-\frac{Ct'}{\tau}};$$

A, B, C are known constants that depend on p_s.

Net drag (Inviscid)

$$C_{D,\text{model}} = C_{D,pg} + C_{D,am}$$

$$C_D \equiv \frac{F}{\frac{1}{2}\rho_s u_s^2 A}$$

Added-Mass Force

$$F_{am}(t') = \overline{m_{f}\frac{Du_f}{Dt}} = V_p \int_0^\infty K(\bar{c}\chi/a)\left[\frac{d\overline{(\rho_f u_{fr})}}{dt} - \frac{d\overline{(\rho_f u_{pr})}}{dt}\right] d(\bar{c}\chi/a),$$

$$K(\bar{c}\chi/a) = e^{-\bar{c}\chi/a}\cos(\bar{c}\chi/a)$$

$$\left[\frac{d\overline{(\rho_f u_{fr})}}{dt} - \frac{d\overline{(\rho_f u_{pr})}}{dt}\right]$$

$$= d_p^{-3}\left[\rho_s\left(u_i - \overline{u_p}\right) + \rho_a \overline{u_p}\right]\left(x_i - \overline{x_p}\right)^2\left(u_i - \overline{u_p}\right)$$

COMPARISION OF SUPERSONIC FLOW MODELS

Drag Force for High-Speed Flows…

Model (a), Henderson [36]:

Case (a), $\boldsymbol{M \geq 1.75}$:

$$C_D = \left(1 + 1.86\left(\frac{M}{Re}\right)^{1/2}\right)^{-1}\left(0.9 + \frac{0.34}{M^2} + 1.86\left(\frac{M}{Re}\right)^{1/2}\left[2 + \frac{2}{S^2} + \frac{1.058}{s}\right]\left(\frac{T_p}{T_g}\right)^{1/2} - \frac{1}{S^4}\right)$$

Case (b), $\boldsymbol{M \leq 1}$:

$$C_D = 24\left[Re + S\left\{4.33 + A \times \exp\left(-0.247\frac{Re}{S}\right)\right\}\right]^{-1} +$$
$$\exp\left(-\frac{0.5M}{\sqrt{Re}}\right)\left[\frac{4.5+0.38\left(0.03Re+0.48\sqrt{Re}\right)}{1+0.03Re+0.48\sqrt{Re}} + 0.1M^2 + 0.2M^8\right] + \left[1 - \exp\left(-\frac{M}{Re}\right)\right]0.6S$$

$$A = \left(3.65 - 1.53\frac{T_p}{T_g}\right)\left(1 + 0.353\frac{T_p}{T_g}\right)^{-1}.$$

Case (c), $\boldsymbol{1 < Ma < 1.75}$:

Linear interpolation between Case (a) and Case (b) above:

$$C_D = C_D(M = 1, Re) + \frac{3}{4}(M - 1.0)[C_D(M = 1.75, Re) - C_D(M = 1, Re)]$$

SUPERSONIC FLOW MODELS

Drag Force for High-Speed Flows…

Model (b): Carlson and Hoglund [37]:

$$C_D = \frac{24}{Re}\left\{1 + \frac{M}{Re}\left[3.82 + 1.28\exp\left(-\frac{1.25Re}{M}\right)\right]\right\}^{-1}$$
$$\left\{(1 + 0.15Re^{0.087})\exp\left[-\left(\frac{0.427}{M^{4.63}}\right) - \left(\frac{3.0}{Re^{0.88}}\right)\right]\right\}$$

SUPERSONIC FLOW MODELS

Drag Force for High-Speed Flows

Model (c), Crowe [38]:

$$C_D = 2 + \left((C_{D_0} - 2)\exp\left(-3.07\sqrt{\gamma}\frac{M}{Re}F(Re)\right)\right) + \frac{G(M)}{\sqrt{\gamma}M}\exp\left(-\frac{Re}{2M}\right),$$

$$\log_{10}(F(Re)) = 1.25(1 + \tanh(0.77\log_{10}Re - 1.92)),$$

$$G(M) = \left\{2.3 + 1.7\sqrt{\frac{T_p}{T_g}}\right\} - 2.3 tanh(1.17\log_{10}M)$$

Model (d), Hermsen [39]:

$$C_D = 2 + \left((C_{D_0} - 2)\exp\left(-3.07\sqrt{\gamma}\frac{M}{Re}F(Re)\right)\right) + \frac{G(M)}{\sqrt{\gamma}M}\exp\left(-\frac{Re}{2M}\right),$$

$$\log_{10}(F(Re)) = (1 + 11.278\ Re)^{-1}\{1 + Re(12.278 + 0.548\ Re)\},$$

$$G(M) = \frac{5.6}{1 + M} + 1.7\sqrt{\frac{T_p}{T_g}}$$

SUPERSONIC FLOW MODELS

Comparison of Drag Force Models for Low-Speed/Supersonic Flows

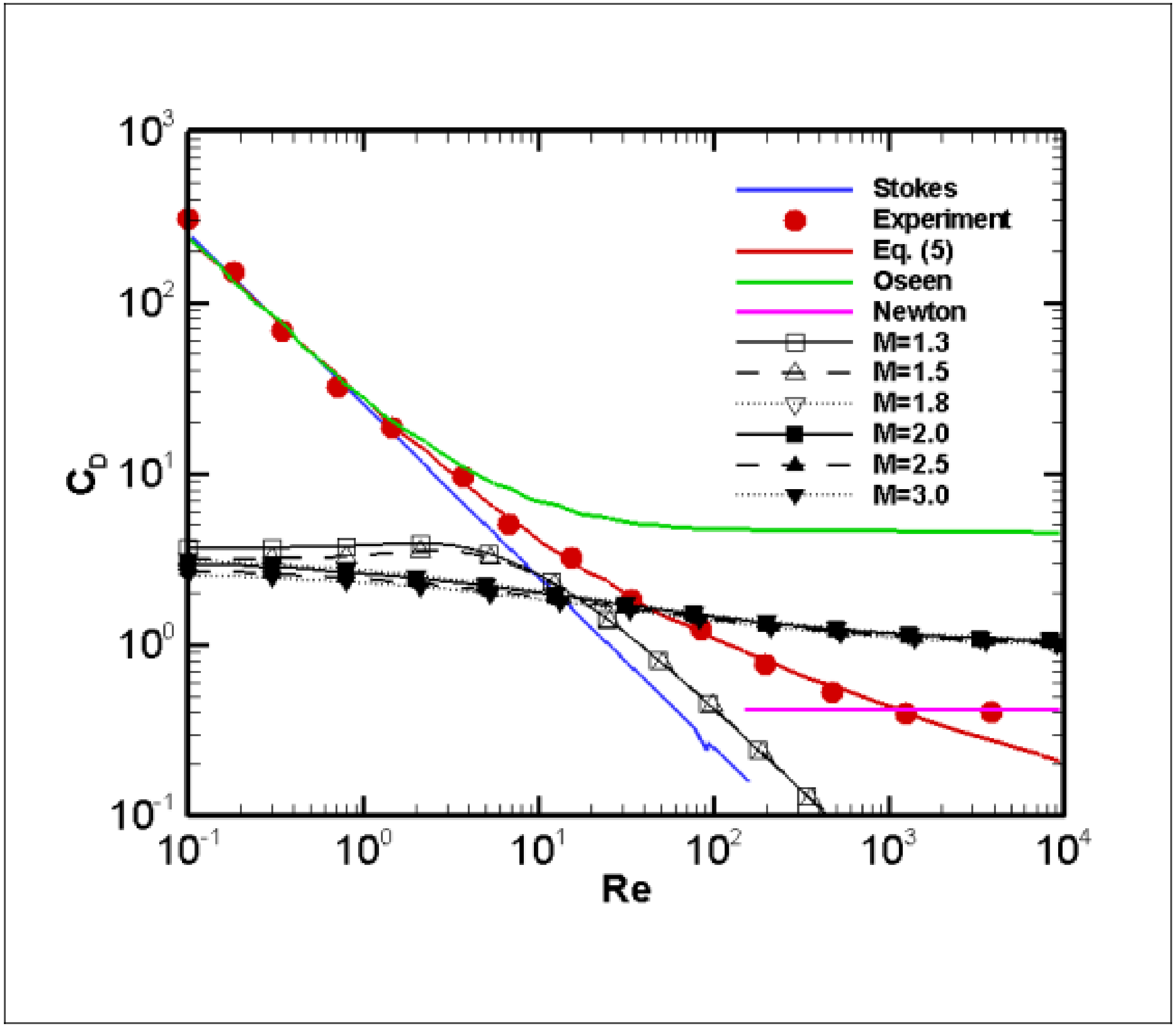

SUPERSONIC FLOW MODELS

Comparison of Drag Force Models for Supersonic Flows

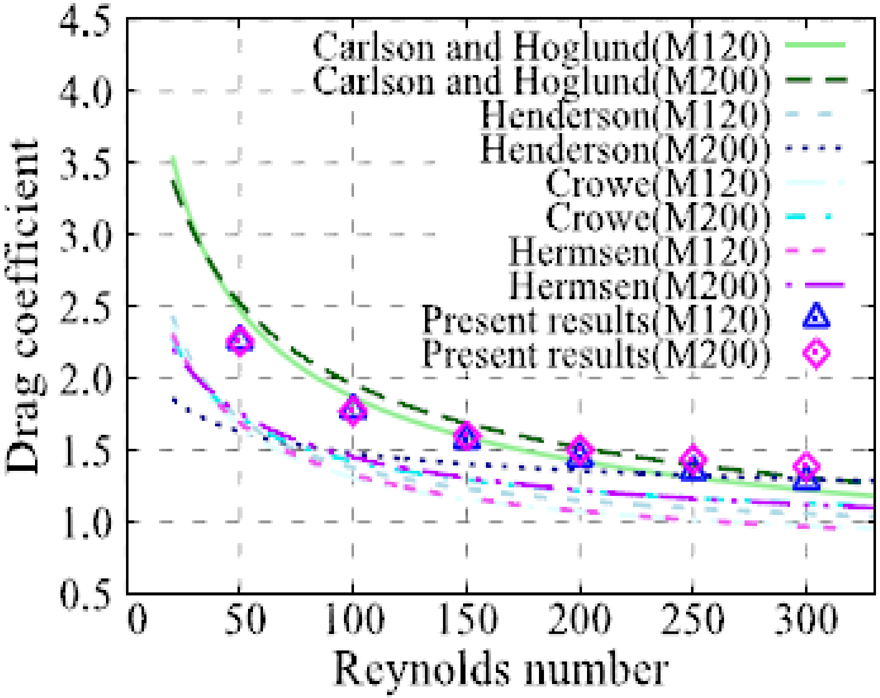

SUPERSONIC FLOW MODELS

Nusselt Number Relations in High-Speed Flows

Incompressible Flows

$$m_d C_{p,d} \frac{dT_d}{dt} = h_d \pi d_d^2 \left(\tilde{T}_g - T_d\right) - \dot{m}_d \Delta h_v$$

Supersonic flows

$$m_d \frac{d}{dt}\left(C_{p,d} T_d\right) = h_d \pi d_d^2 \left(\tilde{T}_g - T_d\right) - \dot{m}_d \Delta h_v + \frac{\pi d_d^3 \lambda}{12} \nabla^2 T_g$$

$$+ \pi d_d^2 \lambda \left\{ \int_{t_0}^{t} \left(\frac{1}{\sqrt{\pi \alpha_g (t - t')}} \left(\frac{DT_g}{Dt} - \frac{dT_p}{dt} \right) \right) dt' + \frac{1}{\sqrt{t}} \left(u - u_p\right)\Big|_{t_n} \right\}$$

A radiative component Q_R may also need to be added to the foregoing heat transfer relation, where

$$Q_R = \varepsilon\sigma\, \pi d_d^2 \left(T_g^4 - T_d^4\right),$$

and (ε, σ) are respectively the emissivity of the droplet and the Stefan-Boltzmann constant, $\sigma = 5.670 \times 10^{-8} \frac{W}{m^2}.K^4$.

SUPERSONIC FLOW MODELS

Nusselt Number Relations in High-Speed Flows

High-speed Nusselt number correlations include the two below:

Kavanu and Drake:

$$Nu = \left\{1 + 3.42\left(\frac{M}{RePr}\right)(2 + 0.459Re^{0.55}Pr^{0.33})\right\}^{-1}(2 + 0.459Re^{0.55}Pr^{0.33}).$$

NASA:

$$Nu = \left\{\left(2 + 0.654Re^{1/2}Pr^{1/3}\right)^{-1} + 3.42\frac{M}{RePr}\right\}^{-1}$$

SUPERSONIC FLOW MODELS

Comparison of Nusselt Number Models

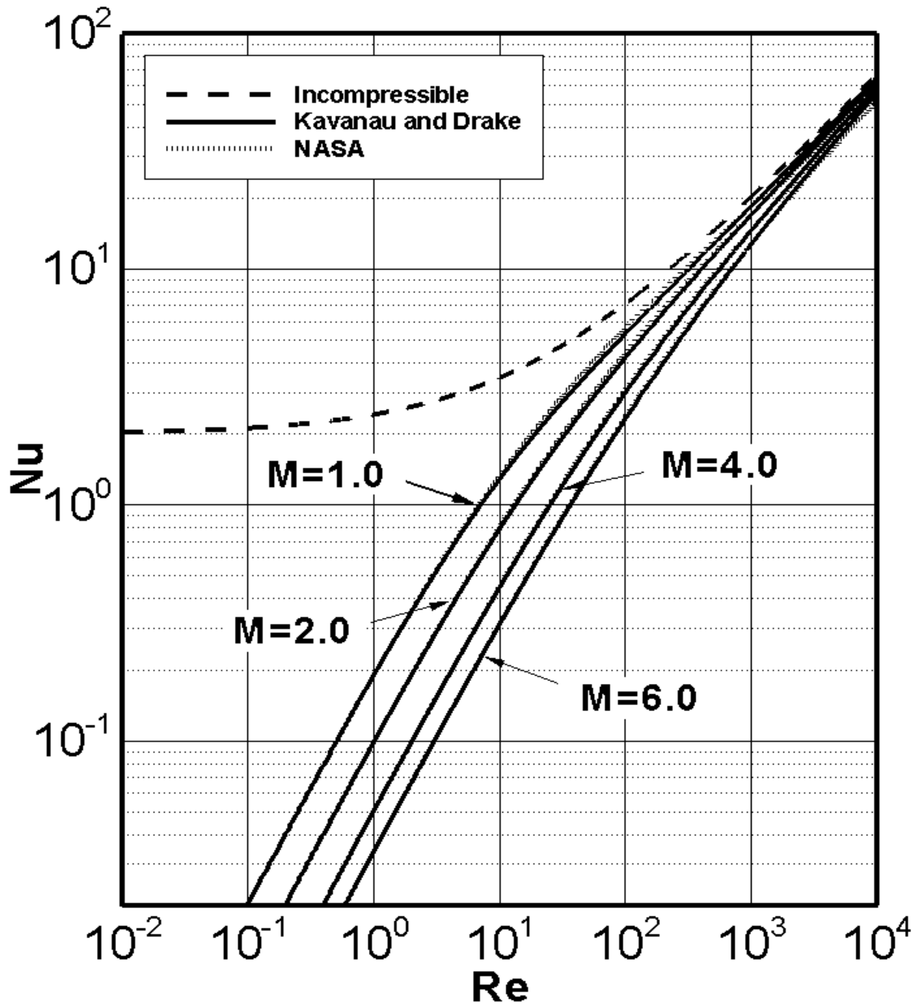

SUPERSONIC FLOW MODELS

Sherwood Number Relations in High-Speed Flows

None Available, Adopt Nu Correlations

Modified Kavanu and Drake:

$$Sh = \left\{1 + 3.42\left(\frac{M}{ReSc}\right)(2 + 0.459Re^{0.55}Sc^{0.33})\right\}^{-1}(2 + 0.459Re^{0.55}Sc^{0.33}).$$

Modified NASA:

$$Sh = \left\{(2 + 0.654Re^{1/2}Sc^{1/3})^{-1} + 3.42\frac{M}{ReSc}\right\}^{-1}$$

RESULTS FROM EXPERIMENTAL WORK BY OTHERS

Air-Shock-Droplet Interaction, Which Way?

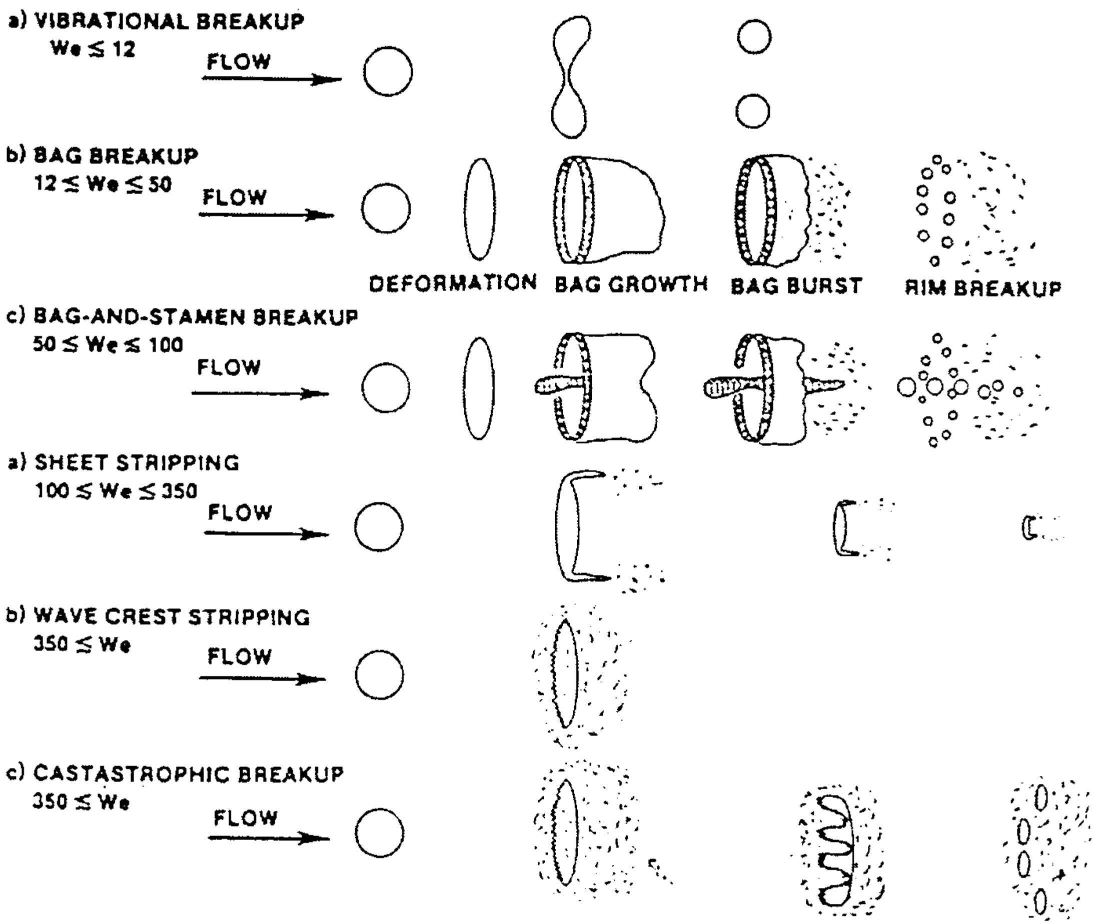

Pilch and Erdman (1987)

EXPERIMENTS BY OTHERS

Air-Shock-Droplet Interaction

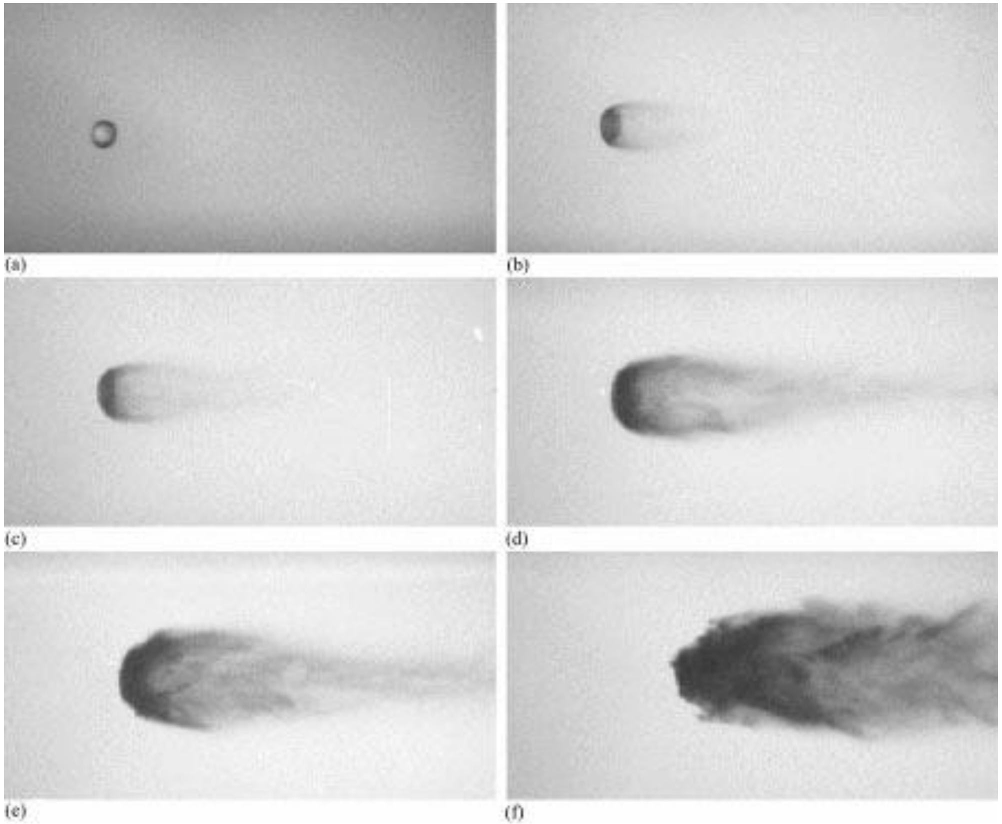

Fig. 1. Stages in the breakup of a water drop (diameter = 2.6 mm) in the flow behind a Mach 2 shock wave. Air velocity = 432 m/s; dynamic pressure = 158.0 kPa; Weber No. = 11,700. Time (J.s): (a) 0, (b) 45, (c) 70, (d) 135, (e) 170, (f) 290.

Joseph, Belanger, and Beavers (1999)

EXPERIMENTS BY OTHERS

Air-Shock-Droplet Interaction

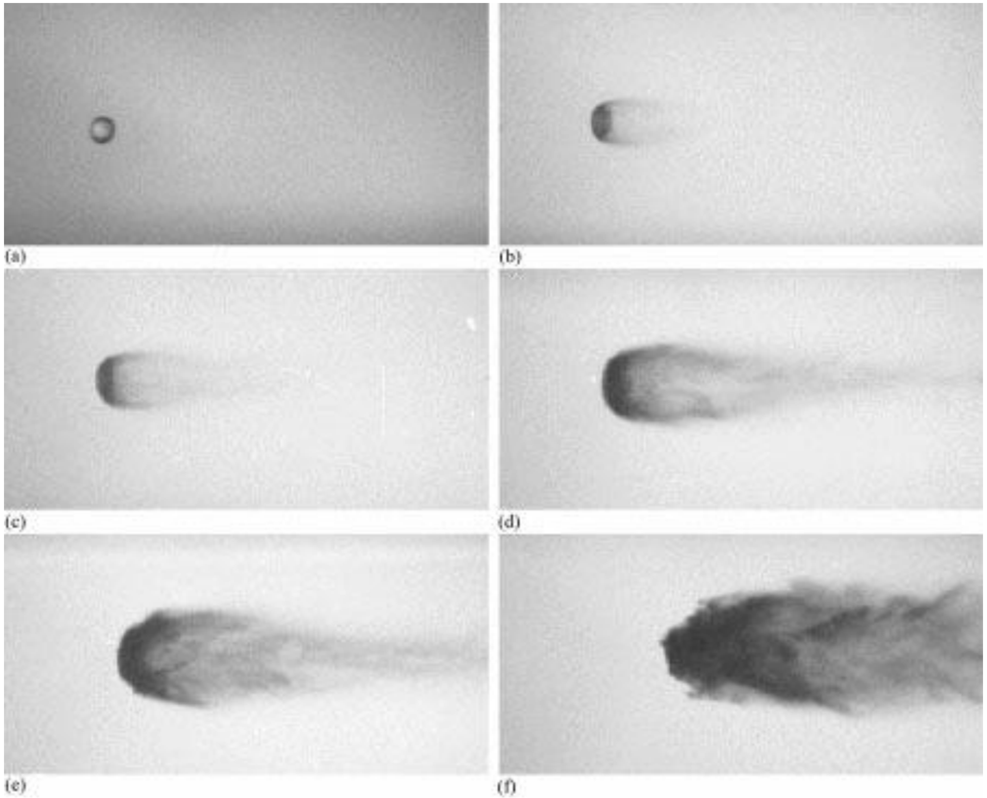

Fig. 1. Stages in the breakup of a water drop (diameter = 2.6 mm) in the flow behind a Mach 2 shock wave. Air velocity = 432 m/s; dynamic pressure = 158.0 kPa; Weber No. = 11,700. Time (J.s): (a) 0, (b) 45, (c) 70, (d) 135, (e) 170, (f) 290.

Joseph, Belanger, and Beavers (1999)

EXPERIMENTS BY OTHERS

Air-Shock-Droplet Interaction

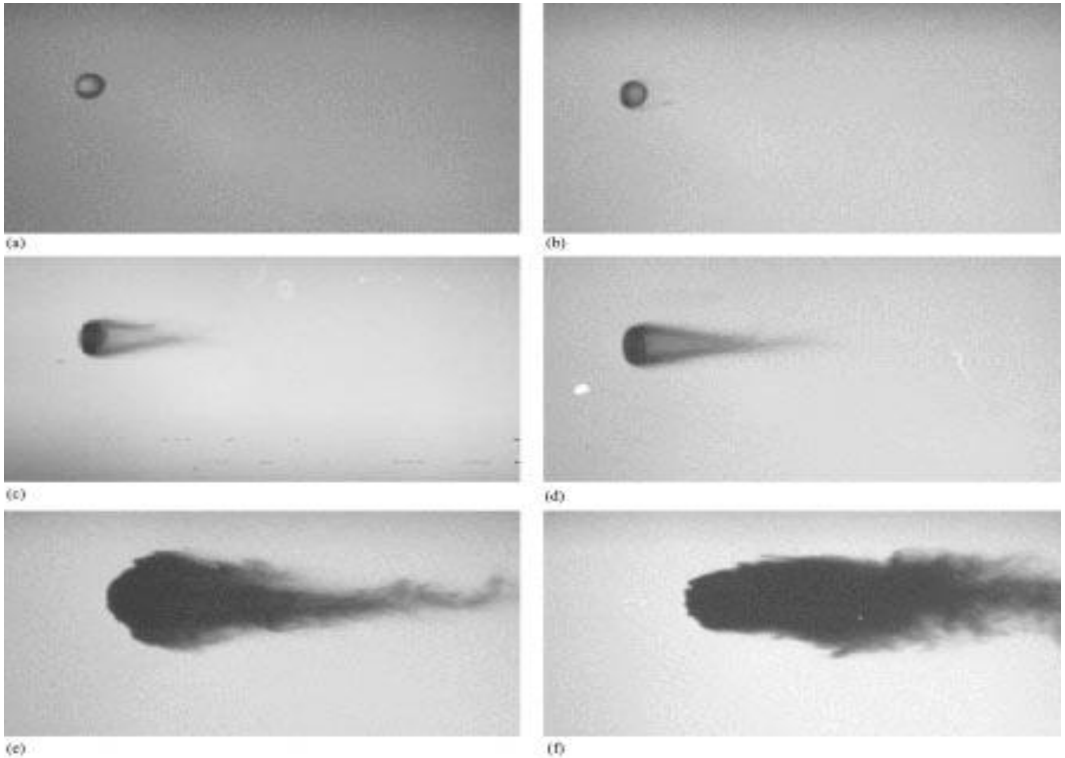

Fig. 2. Stages in the breakup of a water drop (diameter = 2.5 mm) in the flow behind a Mach 3 shock wave. Air Velocity = 764 mfs; dynamic pressure = 606.4 kPa; Weber No. = 43,330. Time =s): (a) 0, (b) 15, (c) 30, (d) 40, (e) 95, (f) 135.

Joseph, Belanger, and Beavers (1999)

EXPERIMENTS BY OTHERS

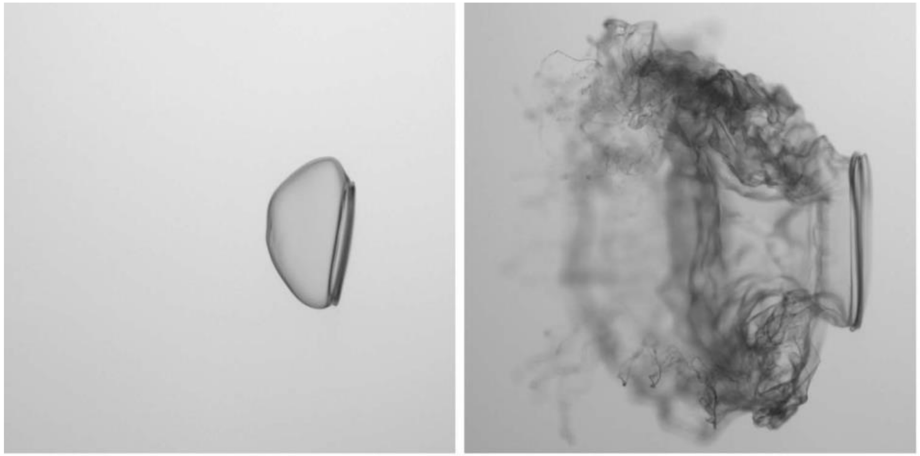

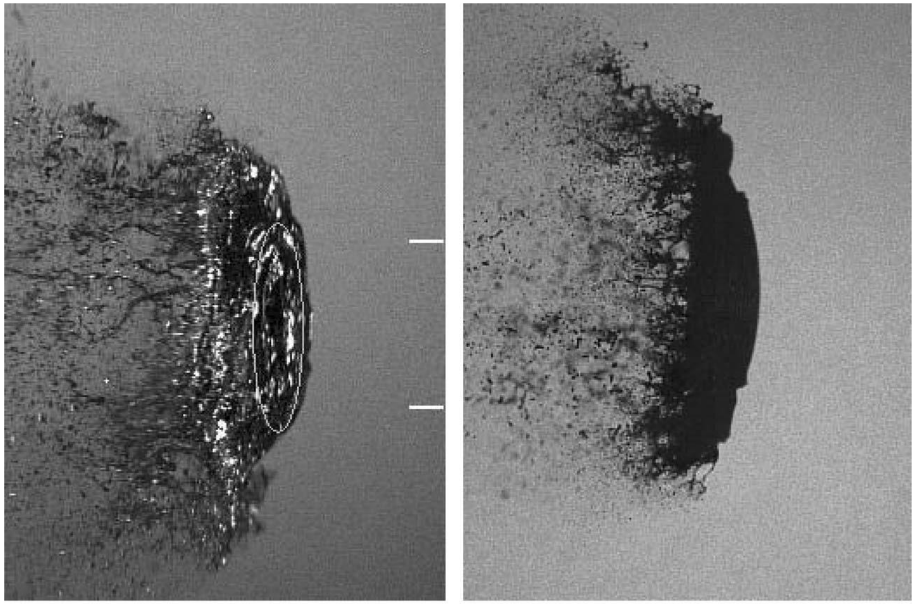

(a) (b)

EXPERIMENTS BY OTHERS

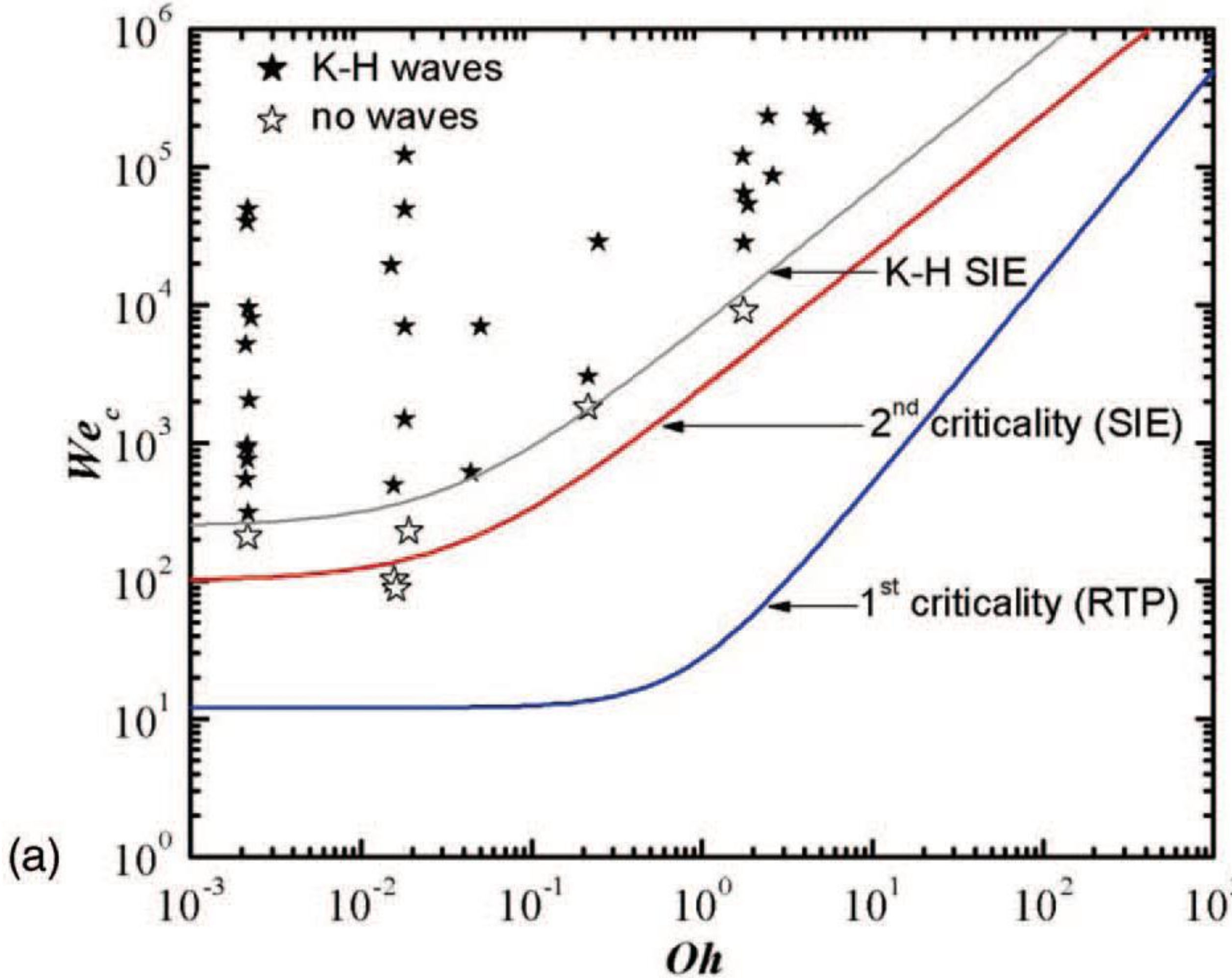

EXPERIMENTS BY OTHERS

Deformation in Time

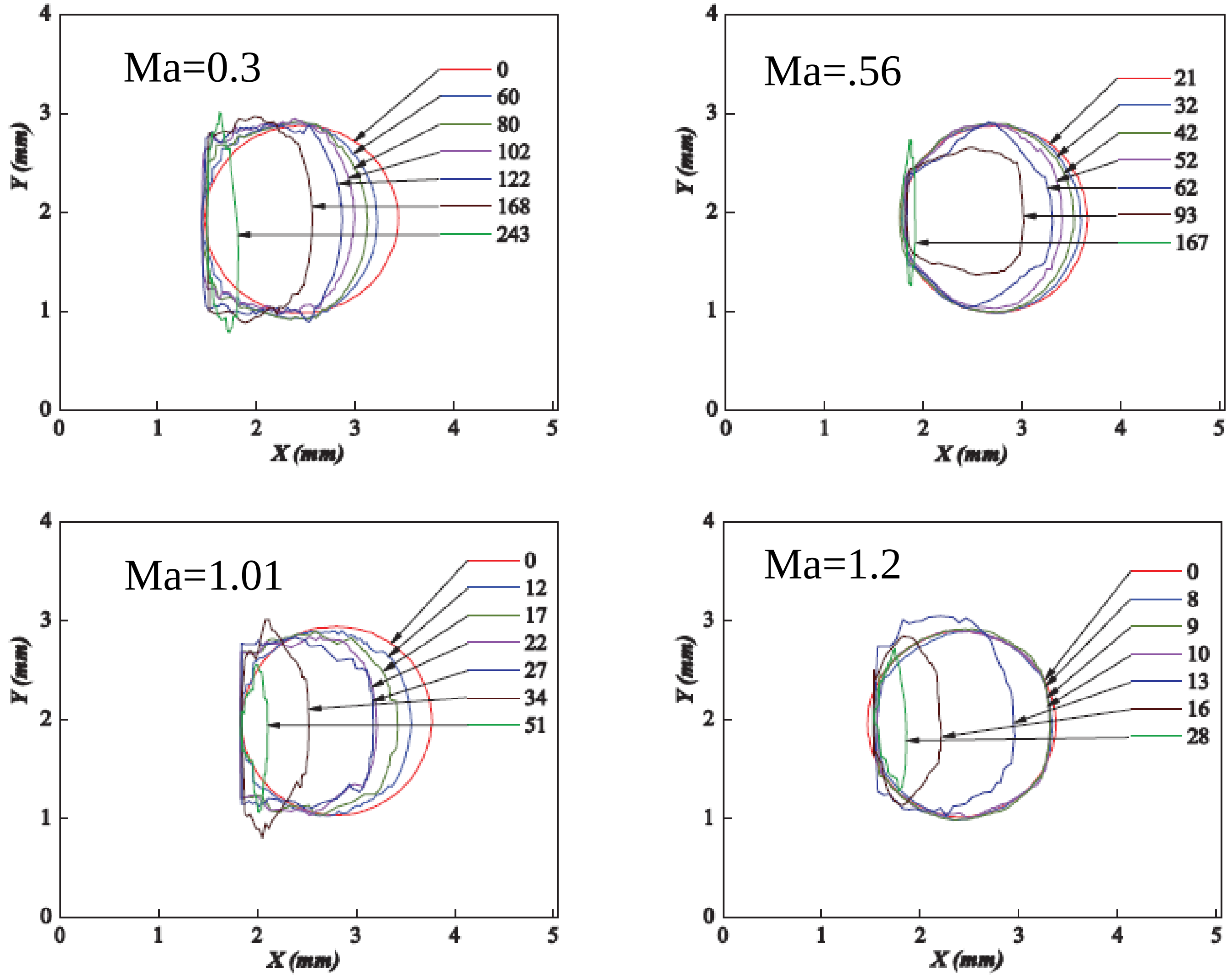

WHAT WE KNOW ABOUT FRAGMENTATION FROM EXPERIMENTS

- **The high momentum of the flow from the isolator doesn't just carry the drop about!!!**
- **Drop acceleration of the order of 10^4 or greater compared to g**
- **Rayleigh-Taylor instability most likely. Acceleration directed from lighter to heavier fluid**
- **Boundary layers originate from the poles of the drop and end at the equator**
- **Can estimate critical diameter of the drop that cannot be fragmented**
- **Can correct the estimate of the growth rate of the most dangerous waves for viscous effects**
- **Acceleration doesn't translate to a force that crushes the drop but causes waves in windward face and mist in the leeward face**
- **There is some latency before the drop feels the presence of the high-speed air**
- **For scramjet combustion flows, drop acceleration is very large**
- **Breakup happens before drift velocity becomes flow velocity**
- **For the analysis of SCSJ, can think of an imaginary shock wave, such that the local conditions where drop finds itself is equivalent to the conditions behind a shock wave**
- **The shock wave is only as important as the conditions behind. It does not have an intrinsic effect on drop fragmentation!!!**
- **Fragmentation theories: Mechanical vaporization, Sound waves as a source of mist, Surface waves as a source of mist, Turbulence (vortices, swirls) as a source of mist, Taylor's unstable waves, Airflow stripping of surface layer.**

EVALUATION OF THE HIGH-SPEED MODELS

The Hyshot Scramjet Engine

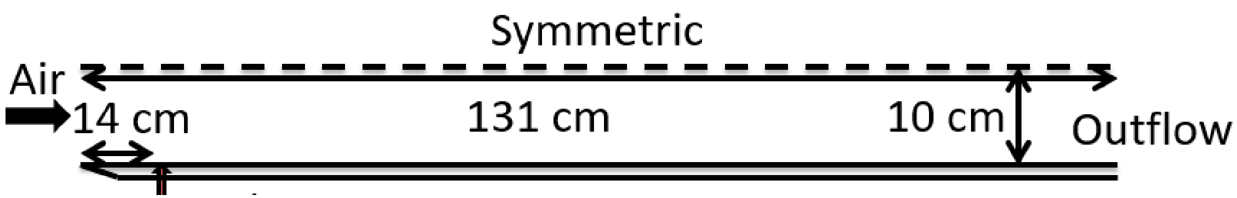

Variables	Definition	Air Inlet
Ma	Mach Number	3.0
M [g/mol]	Molecular Weight	28.8558
T [K]	Static Temperature	600
P [dyne/cm 2]	Static Pressure	1 0 6
P *	Non-dimensional Press ure	0.08075
ρ [g/cm 3]	Density	0.000581
ρ *	Non-dimensional Densi ty	1.0
u [cm/s]	Velocity	146057.6
u *	Non-dimensional Veloc ity	1.0
φ	Equivalence Ratio	

$$C_D = \begin{cases} \dfrac{24}{\mathrm{Re}_k}\left(1+\dfrac{1}{6}\mathrm{Re}_k^{2/3}\right), & \mathrm{Re}_k \le 1000 \\ 0.424 & \mathrm{Re}_k > 1000 \end{cases}$$

Putnam

$$C_D = \left(1 + 1.86\left(\frac{M}{Re}\right)^{1/2}\right)^{-1}\left(0.9 + \frac{0.34}{M^2} + 1.86\left(\frac{M}{Re}\right)^{1/2}\left[2 + \frac{2}{S^2} + \frac{1.058}{s}\right]\left(\frac{T_p}{T_g}\right)^{1/2} - \frac{1}{S^4}\right)$$

Henderson, Ma> 1.75

SPHERICAL PARTICLES: LOW MACH NUMBER

Baseline Two-Phase Models (Point-Particle Method)

Continuous-Phase Equations

Overall Mass Conservation

$$\frac{\partial \bar{\rho}}{\partial t} + \frac{\partial}{\partial x_j}\left(\bar{\rho} u_j\right) = \dot{M}$$

Overall Momentum Equation

$$\frac{\partial}{\partial t}\left(\bar{\rho} u_i\right) + \frac{\partial}{\partial x_j}\left(\bar{\rho} u_j u_i\right) + \theta \frac{\partial p}{\partial x_i} - \frac{\partial}{\partial x_j}\left(\tau_{ij}\right)$$
$$= \sum_k n^{(k)} \dot{m}^{(k)} u_{li}^{(k)} - F_{Di} + \bar{\rho} g_i$$

Overall Enthalpy Equation

$$\frac{\partial}{\partial t}\left(\bar{\rho} h\right) + \frac{\partial}{\partial x_j}\left(\bar{\rho} u_j h\right) - \theta \frac{\partial}{\partial x_j}\left(\lambda \frac{\partial}{\partial x_j} T\right) - \theta \frac{\partial}{\partial x_j}\left(\rho D \sum_m h_m \frac{\partial Y_m}{\partial x_j}\right)$$
$$= \frac{d}{dt}\left(\theta p\right) + \bar{\rho} \sum_m \dot{\omega}_m Q_m - \sum_k n^{(k)} \dot{m}^{(k)} L_{eff}^{(k)} + \sum_k n^{(k)} \dot{m}^{(k)} h_s^{(k)}$$

Species Transport Equation

$$\frac{\partial}{\partial t}\left(\bar{\rho} Y_m\right) + \frac{\partial}{\partial x_j}\left(\bar{\rho} u_j Y_m\right) - \theta \frac{\partial}{\partial x_j}\left(\rho D \frac{\partial}{\partial x_j} Y_m\right)$$
$$= \dot{M}_m + \bar{\rho} \dot{\omega}_m = \sum_k n^{(k)} \dot{m}_m^{(k)} + \bar{\rho} \dot{\omega}_m$$

Droplet Equations

Mass Conservation

$$\frac{dR}{dt} = -\frac{\dot{m}}{4\pi \rho_l R^2}$$

Kinematics

$$\frac{dx_i}{dt} = u_{li}$$

Momentum

$$\frac{du_{li}}{dt} = \frac{3F_{Di}}{4\pi \rho_l R^3} + g_i\left(1 - \frac{\rho}{\rho_l}\right) + \frac{\rho}{\rho_l}\frac{du_i}{dt}$$

Energy

$$\frac{de_l}{dt} = \frac{3\dot{m}}{4\pi \rho_l R^3}\left(e_l - e_{ls} + \frac{\dot{q}_l}{\dot{m}}\right) + \frac{\sum_k B^{(k)}}{\rho_l\left(1-\theta\right)}$$

SUPERSONIC FLOW MODEL EVALUATION

QL chemistry model calculates $\overline{\dot{\omega}_k}$ directly from the detailed chemical mechanism by using large-scale turbulence field quantities and neglecting the effects of the sub-grid turbulence-chemistry interactions.

$$\overline{\dot{\omega}_i\ (\rho, T, Y_k)} \approx \dot{\omega}_i\left(\bar{\rho}, \tilde{T}, \widetilde{Y_k}\right)$$

$\dot{\omega}_i$ is modeled by the Arrhenius equation

Two-Phase Boundary Conditions

Liquid Boundary Conditions in VULCAN

Two-phase Boundary Condition	Boundary Treatment
1. Outflow boundary	Liquid particle gets destroyed on crossing this boundary
2. Wall boundary	Liquid particle is reflected
3. Inter-grid boundary	Particle block flag is changed and/or it gets passed to a different processor
4. Liquid injection	Liquid particles are introduced according to a specified volume flow rate and size distribution (PDF)

LOW-LEVEL VALIDATION

- Conservation
  - All liquid added in *fuel_inject* is integrated
  - All liquid that is being destroyed or added as source term is also added up
  - Total liquid at selected time step is computed
- Mass fraction test
- Boundary condition test
  - Wall reflection
  - Outflow
  - Interblock (cut conditions)
- Multi-block parallel integrity test (MPI)
- Reasonableness tests
  - Response to changes in flow rate, inlet temperature, inlet velocity

TWO-PHASE RESULTS

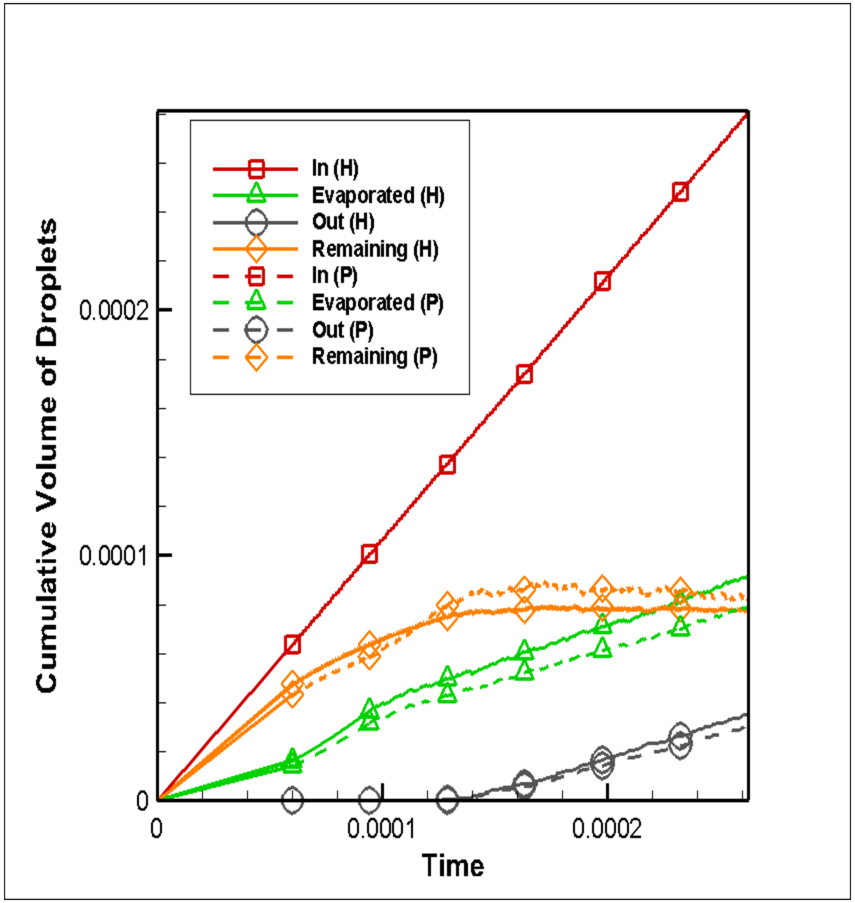

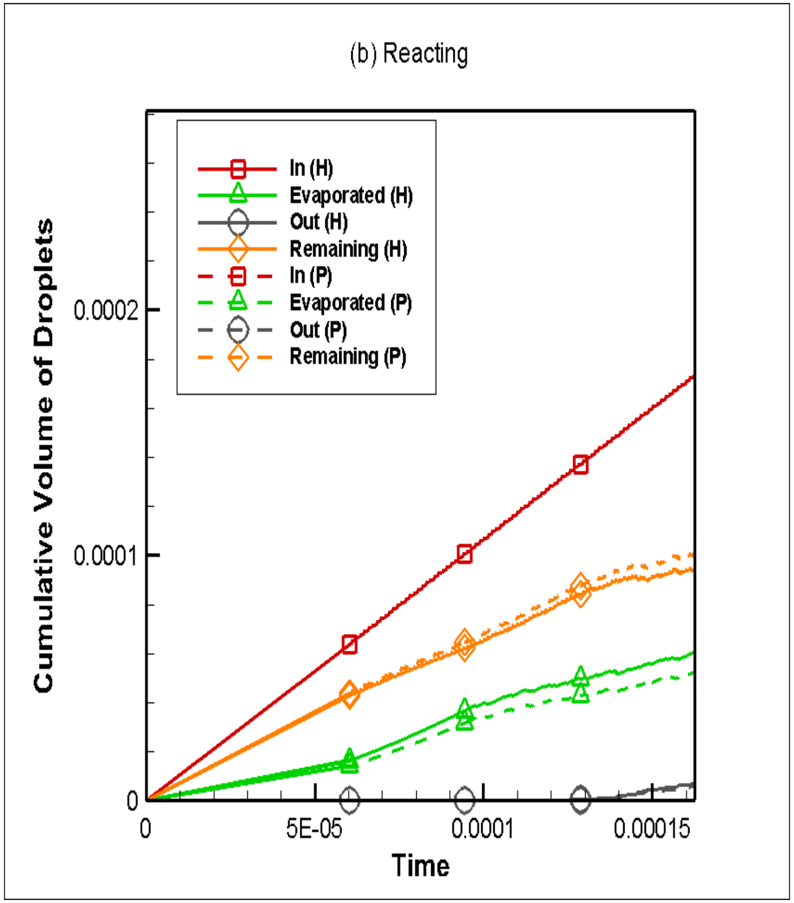

Non-Reacting

Reacting

Comparison of the effects of subsonic (Putnam, or P) and supersonic (Henderson, H) drag models on drople t mass transfer, showing droplet mass balance: inflow, evaporation, outflow, and accumulation (“Remaining”).

Conclusions

- **Work-in-Progress; Will take time to fully answer questions raised:**
  - ✓ Which method should we use within the framework of Balachandar and Eaton (2010)?
  - ✓ Don't we need the drag forces that evolved from BBO?
    - $C_{Dstd}, C_{Dadd}, C_{Dfld}, C_{Dhis}, C_{Dini}, C_{Dgrv}$
  - ✓ Shouldn't high-speed models for particle momentum, mass transfer, and heat transfer be more appropriate within p-pm?
  - ✓ How relevant are those supersonic two-phase flow studies for rockets (Balachandar, Eaton, Jackson, Parmar, Sridhanara, Nagata,…)?
  - ✓ How do we handle the complexities of droplet breakup in shocked flows?
  - ✓ Can we separate the modeling of the fragmentation process from that of thermal evaporation and combustion?

THE END

THANK YOU!

Foluso.Ladeinde@stonybrook.edu

Evaluation of Entropy Transport Equation in Turbulent Jet Flames using Filtered Density Function

Mehdi Safari

Department of Mechanical Engineering
Fairfield University, Fairfield, CT 06824

Reza Sheikhi

Department of Mechanical Engineering
University of Connecticut, Storrs, CT 06269

Objective

Looking at Efficiency in Turbulent Combustion via 2nd law of thermodynamics

- "Quality" of energy
- Max. *work-producing* capacity of combustion

$$\dot{E}_{x_D} = T_0 \dot{S}_g$$

Irreversibilities:

- Viscous Dissipation
- Heat Conduction
- Mass Diffusion
- Chemical Reaction

$$\left.\begin{array}{l}\langle p\rangle \\ \langle T\rangle_L \\ \langle Y_\alpha\rangle_L\end{array}\right\} \nRightarrow \left\langle \dot{S}_g \right\rangle_L$$

Entropy Transport

Gibb's Relation

$$T\,ds = de + pdv - \sum_{\alpha=1}^{N_s} \mu_\alpha\, d\phi_\alpha$$

$$T\,\rho\frac{Ds}{Dt} = \rho\frac{De}{Dt} + p\,\rho\frac{Dv}{Dt} - \sum_{\alpha=1}^{N_s} \mu_\alpha\,\rho\frac{D\phi_\alpha}{Dt}$$

Entropy Transport

Viscous Dissipation

Heat Conduction

$$\frac{\partial \rho s}{\partial t} + \frac{\partial \rho\, u_i s}{\partial x_i} = \frac{\partial}{\partial x_i}\left(\gamma \frac{\partial s}{\partial x_i}\right) + \frac{1}{T}\tau_{ij}\frac{\partial u_i}{\partial x_j} + \frac{\gamma c_p}{T^2}\frac{\partial T}{\partial x_i}\frac{\partial T}{\partial x_i}$$

$$+ \sum_{\alpha=1}^{N_s} \frac{\gamma R_\alpha}{X_\alpha}\frac{\partial \phi_\alpha}{\partial x_i}\frac{\partial X_\alpha}{\partial x_i} - \frac{\rho}{T}\sum_{\alpha=1}^{N_s} \mu_\alpha S_\alpha$$

Mass Diffusion

Chemical Reaction

Governing Equations

$$\frac{\partial\langle\rho\rangle}{\partial t} + \frac{\partial\left\langle\rho\right\rangle\left\langle u_i\right\rangle_L}{\partial x_i} = 0$$

$$\frac{\partial\left\langle\rho\right\rangle\left\langle u_i\right\rangle_L}{\partial t} + \frac{\partial\left\langle\rho\right\rangle\left\langle u_j\right\rangle_L\left\langle u_i\right\rangle_L}{\partial x_j} = -\frac{\partial\left\langle p\right\rangle}{\partial x_i} + \frac{\partial\left\langle\tau_{ij}\right\rangle}{\partial x_j} - \frac{\partial\left\langle\rho\right\rangle\tau(u_i,u_j)}{\partial x_j}$$

$$\frac{\partial\left\langle\rho\right\rangle\left\langle\phi_\alpha\right\rangle_L}{\partial t} + \frac{\partial\left\langle\rho\right\rangle\left\langle u_i\right\rangle_L\left\langle\phi_\alpha\right\rangle_L}{\partial x_i} = \frac{\partial\left\langle J_i^\alpha\right\rangle}{\partial x_i} - \frac{\partial\left\langle\rho\right\rangle\tau(u_i,\phi_\alpha)}{\partial x_i} + \left\langle\rho S_\alpha\right\rangle \qquad \alpha = 1,\ldots,N_s+1$$

$$\frac{\partial\left\langle\rho\right\rangle\left\langle s\right\rangle_L}{\partial t} + \frac{\partial\left\langle\rho\right\rangle\left\langle u_i\right\rangle_L\left\langle s\right\rangle_L}{\partial x_i} = \frac{\partial}{\partial x_i}\left(\gamma\frac{\partial\langle s\rangle_L}{\partial x_i}\right) - \frac{\left\langle\rho\right\rangle\tau(u_i,s)}{\partial x_i}$$
$$+\underbrace{\left\langle\frac{1}{T}\tau_{ij}\frac{\partial u_i}{\partial x_j}\right\rangle}_{\text{Viscous Dissipation}} + \underbrace{\left\langle\gamma\frac{c_p}{T^2}\frac{\partial T}{\partial x_i}\frac{\partial T}{\partial x_i}\right\rangle}_{\text{Heat Conduction}} + \underbrace{\left\langle\gamma\sum_{\alpha=1}^{N_s}\frac{R_\alpha}{X_\alpha}\frac{\partial\phi_\alpha}{\partial x_i}\frac{\partial X_\alpha}{\partial x_i}\right\rangle}_{\text{Mass Diffusion}} - \underbrace{\left\langle\frac{\rho}{T}\sum_{\alpha=1}^{N_s}\mu_\alpha S_\alpha\right\rangle}_{\text{Chemical Reaction}}$$

Entropy-FDF (En-FDF)

$$\mathcal{F}_{en}\left(\hat{\boldsymbol{\phi}}, \hat{s}, \mathbf{x}; t\right) = \int_{-\infty}^{+\infty} \rho(\mathbf{x}', t)\xi\left(\hat{\boldsymbol{\phi}}, \hat{s}\,; \boldsymbol{\phi}(\mathbf{x}', t), s(\mathbf{x}', t)\right)\mathcal{G}(\mathbf{x}' - \mathbf{x})d\mathbf{x}'$$

Fine-Grained Density

$$\xi\left[\hat{\boldsymbol{\phi}}, \hat{s}\,; \boldsymbol{\phi}(\mathbf{x}, t), s(\mathbf{x}, t)\right] = \delta\left(\hat{s} - s(\mathbf{x}, t)\right) \times \prod_{\alpha=1}^{N_s+1} \delta\left(\hat{\phi}_\alpha - \phi_\alpha(\mathbf{x}, t)\right)$$

Exact Entropy FDF

$$\frac{\partial \mathcal{F}_{en}}{\partial t} + \frac{\partial\left[\left\langle u_i \middle| \hat{\boldsymbol{\phi}}, \hat{s}\right\rangle \mathcal{F}_{en}\right]}{\partial x_i} = -\sum_{\alpha=1}^{N_s} \frac{\partial}{\partial \hat{\phi}_\alpha}\left[S_\alpha(\hat{\boldsymbol{\phi}})\mathcal{F}_{en}\right] + \frac{\partial}{\partial \hat{s}}\left[\frac{1}{T}\sum_{\alpha=1}^{N_s} \mu_\alpha S_\alpha(\hat{\boldsymbol{\phi}})\mathcal{F}_{en}\right] + [\textit{unclosed terms}]$$

Modeled En-FDF Transport

$$dX_i^{+} = \left(\langle u_i\rangle_L + \frac{1}{\langle\rho\rangle}\frac{\partial(\gamma+\gamma_t)}{\partial x_i}\right)dt + \left(\sqrt{\frac{2(\gamma+\gamma_t)}{\langle\rho\rangle}}\right)dW_i$$

$$d\,\phi_\alpha^{+} = -\,C_\phi\,\Omega\left(\phi_\alpha^{+} - \langle\phi_\alpha\rangle_L\right)dt + S_\alpha(\boldsymbol{\phi}^{+})\,dt$$

$$\boxed{\begin{aligned} ds^{+} &= \frac{\epsilon_t}{T^{+}}\,dt + \frac{1}{T^{+}}\sum_{\alpha=1}^{N_s}\frac{\mu_\alpha^{+}}{M_\alpha}C_\phi\Omega(\phi_\alpha^{+} - \langle\phi_\alpha\rangle_L)\,dt \\ &\quad - \frac{1}{T^{+}}C_\phi\Omega(h^{+} - \langle h\rangle_L)\,dt - \frac{1}{T^{+}}\sum_{\alpha=1}^{N_s}\mu_\alpha^{+}(\boldsymbol{\phi}^{+})S_\alpha(\boldsymbol{\phi}^{+})\,dt \end{aligned}}$$

where:

$$\epsilon_t = k\,\Omega + \frac{1}{\langle\rho\rangle}\langle\tau_{ij}\rangle\frac{\partial\langle u_i\rangle_L}{\partial x_j} \qquad \Omega = \frac{\gamma+\gamma_t}{\langle\rho\rangle\,\Delta^2}$$

Filtered Entropy Closure

$$\left\langle \frac{1}{T}\tau_{ij}\frac{\partial u_i}{\partial x_j}\right\rangle \approx \left\langle \frac{1}{T}\right\rangle_L \langle\rho\rangle \epsilon_t = \left\langle \frac{1}{T}\right\rangle_L \left(\langle\rho\rangle k\,\Omega + \langle\tau_{ij}\rangle \frac{\partial \langle u_i\rangle_L}{\partial x_j}\right)$$

$$\left\langle \gamma\frac{c_p}{T^2}\frac{\partial T}{\partial x_i}\frac{\partial T}{\partial x_i}\right\rangle \approx \langle\rho\rangle C_\phi \Omega \left[\sum_{\alpha=1}^{N_s} \tau\left(\phi_\alpha, \frac{g_\alpha}{T}\right) - \tau\left(h, \frac{1}{T}\right)\right]$$

$$\left\langle \sum_{\alpha=1}^{N_s} \gamma R_\alpha \frac{1}{X_\alpha}\frac{\partial \phi_\alpha}{\partial x_i}\frac{\partial X_\alpha}{\partial x_i}\right\rangle \approx \langle\rho\rangle C_\phi \Omega \sum_{\alpha=1}^{N_s} R_\alpha \tau\left(\phi_\alpha, lnX_\alpha\right)$$

Entropy Statistics

x=15D

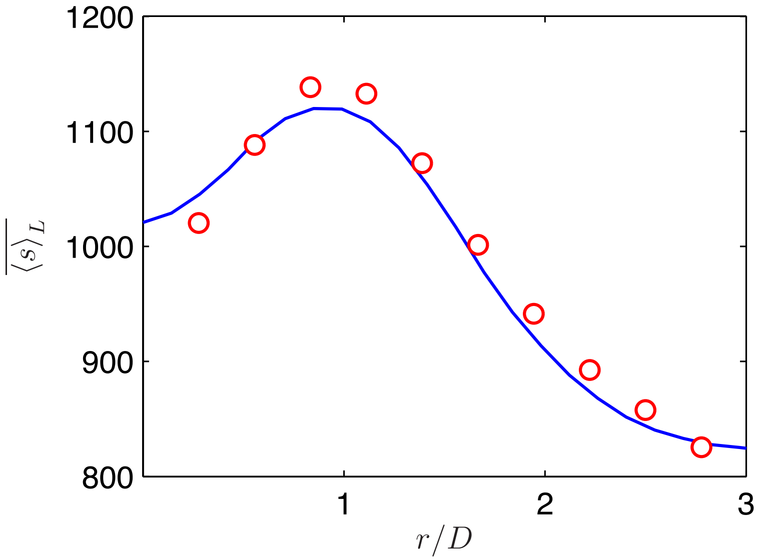

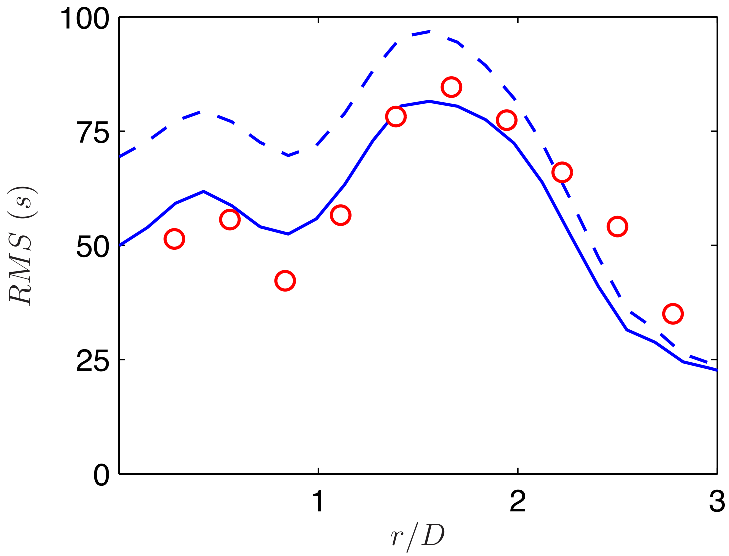

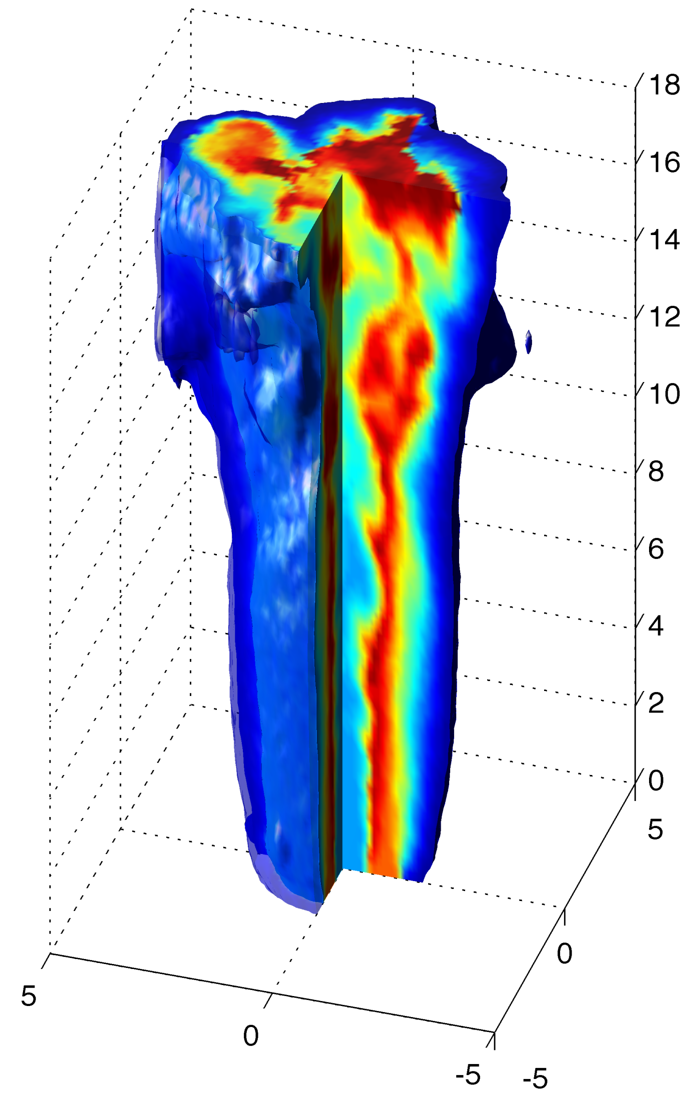

Entropy Generation

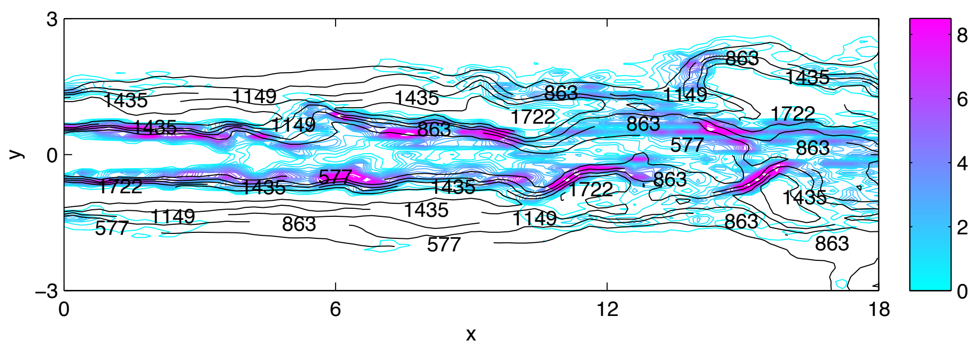

$$\langle S_{g_H} \rangle = \left\langle \gamma \frac{c_p}{T^2} \frac{\partial T}{\partial x_i} \frac{\partial T}{\partial x_i} \right\rangle$$

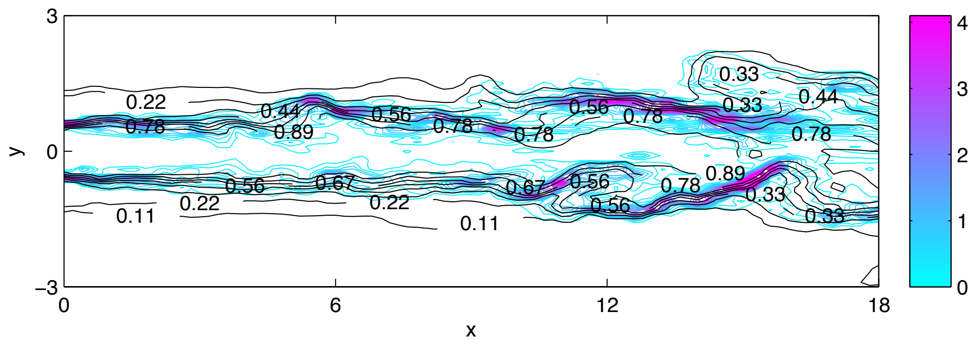

$$\langle S_{g_M} \rangle = \left\langle \sum_{\alpha=1}^{N_s} \gamma R_\alpha \frac{1}{X_\alpha} \frac{\partial \phi_\alpha}{\partial x_i} \frac{\partial X_\alpha}{\partial x_i} \right\rangle$$

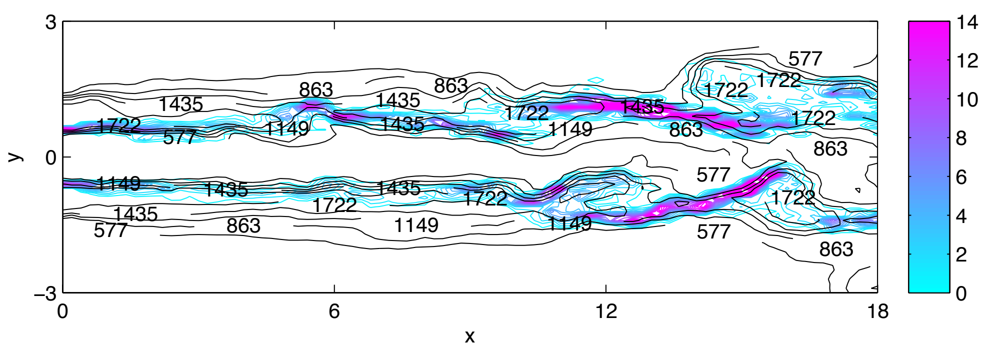

$$\langle S_{g_C} \rangle = \left\langle \frac{\rho}{T} \sum_{\alpha=1}^{N_s} \mu_\alpha S_\alpha \right\rangle$$

Chemical Reaction Source

$$\langle\rho\rangle\left\langle\frac{1}{T}\sum_{\alpha=1}^{N_s}\mu_\alpha S_\alpha\right\rangle=\langle\rho\rangle^2 C_\phi\Omega\sum_{\alpha=1}^{N_s}\tau\left(\frac{\mu_\alpha}{T},\phi_\alpha\right)-\langle\rho\rangle^2 C_\phi\Omega\sum_{\alpha=1}^{N_s}\tau\left(\frac{\mu_\alpha}{T}\frac{d\phi_\alpha}{d\xi},\xi\right)$$

Flamelet

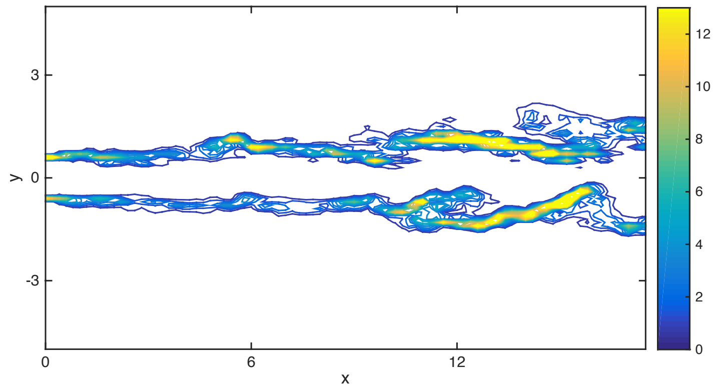

ARM

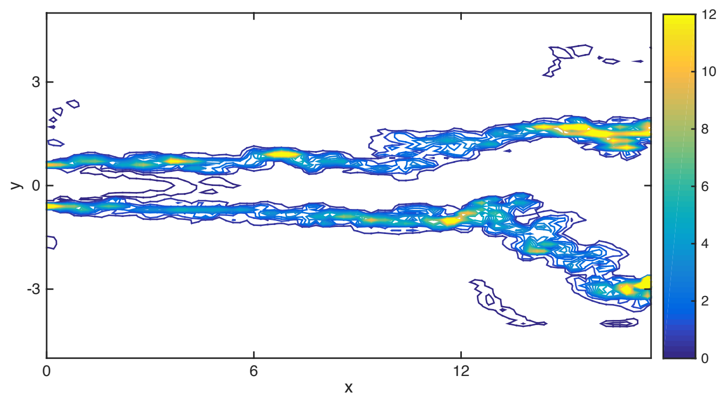

x/D=15

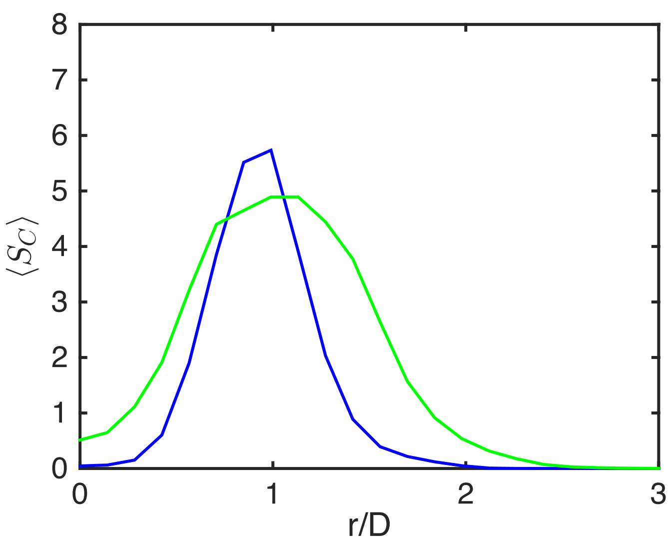

Concluding Remarks

- En-FDF prediction of entropy statistics compare favorably with the experimental data.
- En-FDF is an effective means of irreversibility analysis of turbulent reacting flows. Simple change in flow condition can change exergy loss due to entropy production up to 20% of total exergy of flow.
- Further analysis and optimization of turbulent flames is underway.

Acknowledgments:

TACC TEXAS ADVANCED COMPUTING CENTER

Powering Discoveries That Change The World

72nd Annual Meeting of the APS Division of Fluid Dynamics

Volume 64, Number 13

Saturday–Tuesday, November 23–26, 2019; Seattle, Washington

Session Index

Sh

Session C01: Turbulent and Chemically-reacting Flow Modeling I

Chair: Peyman Givi, University of Pittsburgh
Room: *2A*

Abstract: C01.00001: Edward E. O'Brien's Seminal Contributions to Turbulence Theory

8:00 AM–8:13 AM

Authors:
Foluso Ladeinde
(Stony Brook University)

Cesar Dopazo
(Universidad Zaragoza)

Peyman Givi
(University of Pittsburgh)

A brief overview will be presented of the influential contributions of Edward E. (Ted) O'Brien to the theory of turbulence, with an emphasis on scalar mixing and reaction. While perhaps best known for his work on the transported PDF methods, Ted's contributions are very diverse and consider a broad range of theoretical and computational approaches. In the 1960s, he made some very fundamental contributions to the spectral theory of reactive scalars, analyzed the consequences of passive scalar tagging using Corsin's ``backward Lagrangian diffusion'' concept, and contributed to the interpretation of Kraichnan's ``direct interaction approximation'' (DIA) for turbulent mixing. In the 1970s-1980s, he focused on scalar PD Functional and Function methods. In fact, he is widely recognized for introducing and popularizing single- and multi-point PDF closures, as well as the scalar-gradient PDF within the reactive turbulent flow community. In the 1990s, he focused on applying the EDQNM and the ``amplitude mapping closure'' (AMC) models, respectively to reactive turbulent scalars and mixing. With wider availability of supercomputers in the late 1990's-2000's, Ted utilized DNS for the development and appraisal of modern turbulence closures. He is also credited with introducing the ``filtered density function'' (FDF) transport equation for LES of turbulent reactive flows. In fact, he is the first to develop a transported scalar-FDF equation for multi-species turbulent reactive flows. Professor O'Brien's publications continue to be highly cited within the turbulence research community.

Abstract: C01.00002: Numerical Simulation of Colorless Distributed Combustion with LES/FMDF

8:13 AM–8:26 AM

Authors:

Husam Abdulrahman
(Michigan State University)

Farhad Jaberi
(Michigan State University)

Abdoulahad Validi
(ANSYS Inc.)

Ashwani Gupta
(University Of Maryland)

\textbf{Honoring Ted O'Brien. }Turbulent mixing and combustion in non-premixed and premixed Colorless Distributed Combustion (CDC) systems are studied with the hybrid large eddy simulation/filtered mass density function (LES/FMDF) methodology and its Eulerian--Lagrangian computational solver. The CDC has shown to significantly reduce NOx and hydrocarbon emissions while improving the reaction pattern factor and stability with low pressure drop and noise. The combustion in CDC is distributed and is characterized by wide fluctuations in flow variables. In addition to non-conventional distributed turbulent reaction, mixing between fuel, oxidizer, and combustion products in CDC is unique and complex. The LES/FMDF model is shown to be able to capture all the unique features of turbulent mixing and combustion in CDC. The consistency of the Eulerian and Lagrangian parts of LES/FMDF is established for both non-reacting and reacting conditions. The LES/FMDF results are shown to be in good agreement with the available experimental data. The numerical results indicate that the variations in the inflow air temperature, jet velocity and composition and premixing have a significant effect on the flow, mixing and combustion in the CDC. They also indicate the importance of jets setup in the combustor.

Abstract: C01.00003: Filtered Mass Density Function for Large-Eddy Simulations of Multiphase Turbulent Reacting Flows

8:26 AM–8:39 AM

Authors:
Farhad Jaberi
(Michigan State University)

Zhaorui Li
(Texas A\&M University-Corpus Christi)

Araz Banaeizadeh
(Altair Engineering Inc.)

Abolfazl Irannejad
(Alcon-Novartis Inc.)

Honoring Ted O'Brien. The filtered mass density function (FMDF) methodology is further extended and employed for large-eddy simulations (LES) of multiphase turbulent reacting flows. The two-phase LES/FMDF model is implemented with a unique Lagrangian-Eulerian-Lagrangian mathematical/computational methodology. In this methodology, the filtered carrier gas velocity field is obtained by solving the filtered form of the compressible Navier-Stokes equations while the gas scalar (e.g. temperature and species mass fractions) field and the liquid (spray) phase are obtained by solving two different sets of Lagrangian equations. The two-way interactions between the phases and all the Eulerian and Lagrangian fields are included in the two-phase LES/FMDF methodology. The accuracy and reliability of the model is demonstrated by comparing the two-phase LES/FMDF results with those obtained from the direct numerical simulation (DNS) and experimental data for a range of fundamental and practical

multiphase flows including a spatially developing turbulent mixing layer with evaporating and reacting droplets and spray combustion in a preheated high-pressure closed chamber, a dump combustor, a double-swirl burner, and an internal combustion engine.

Abstract: C01.00004: A High-Order FDF Large Eddy Simulator of Complex Flows

8:39 AM–8:52 AM

Authors:
Shervin Sammak
(Center for Research Computing, University of Pittsburgh)

Aidyn Aitzhan
(Department of Mechanical Engineering and Materials Science, University of Pittsburgh)

Arash Nouri
(Department of Mechanical Engineering and Materials Science, University of Pittsburgh)

Peyman Givi
(Department of Mechanical Engineering and Materials Science, University of Pittsburgh)

Honoring Ted O'Brien. The flow solvers in most previous LES-FDF are based either on high-order discretization schemes in simple flows, or low-order (finite-volume) methods in complex flows. In this work, we develop a new computational methodology which allows LES of complex flows via the use of a high-order spectral-hp element scheme. The high order accuracy of the spectral discretization and the versatility of the finite element domain decomposition, facilitate high-fidelity simulation of flows within complex geometries. This CFD solver is combined with a Lagrangian Monte Carlo scheme for LES of a bluff-body reacting flow via the FDF subgrid scale closure [1]. Demonstrations are made of the consistency and the overall superior performance of this high order hybrid scheme. [1] Gao, F. and O'Brien, E. E., ``A Large-Eddy Simulation Scheme for Turbulent Reacting Flows,'' Phys. Fluids A, vol. 5(6), pp. 1282-1284 (1993).

Abstract: C01.00005: On Large Eddy Simulation/Filtered Density Function based Modeling of Circular Bluff Body Configurations.

8:52 AM–9:05 AM

Authors:
Cesar Celis
(Pontificia Universidad Catolica del Peru (PUCP))

Ricardo Franco
(Pontificia Universidad Catolica del Peru (PUCP))

Honoring Ted O'Brien. Large eddy simulation/filtered density function (LES/FDF) numerical results of inert and reacting flows characterizing the near wake of bluff body configurations are discussed in this work. Circular bluff body configurations are studied because they feature strong interactions between turbulence and chemical reaction, as well as pollutants formation. All numerical results obtained here are compared to experimental data gathered previously. Parameters particularly analyzed include velocity profiles, turbulent kinetic energy, Reynolds stress and strain rate tensors. A strong anisotropic flow is observed from the obtained results along with a flow recirculation zone consisting of a toroidal vortex. At inert conditions, large turbulent fluctuations are found at the stagnation point region. The observed flow anisotropy is associated with the stagnation point flow. The results discussed here correspond to on-going work involving both bluff body burner configurations and numerical predictions of rather complex phenomena such as soot formation.

Abstract: C01.00006: Molecular mixing in highly turbulent premixed flames*

9:05 AM–9:18 AM

Authors:
Xinyu Zhao
(University of Connecticut)

Patrick Meagher
(University of Connecticut)

Honoring Ted O’Brien: The molecular mixing rules and rates in premixed flames subject to intense turbulence are investigated in this study. Direct numerical simulation (DNS) of a spherical product kernel is conducted in a homogeneous isotropic turbulence box. The triply periodic computational domain outside the product kernel is comprised of fresh mixtures. The transient flame kernel undergoes flame propagation, local extinction, and eventually global extinction. During the transition, the compositional space evolves from a low-dimensional manifold to increasingly higher dimensions. The DNS data are subsequently explicitly filtered to study the subgrid-scale behavior of the scalars. The Euclidean minimum spanning trees are constructed to understand the change of localness during the extinction process. Conditional statistics of major and minor species are collected, according to the mixing rules of various mixing models. A scalar gradient based mixing frequency model is constructed and assessed for its suitability to represent the mixing rates of critical species during all phases of the flame kernel evolution.

*The work was supported by the Air Force Office of Scientific Research under the grant number FA9550-18-1-0173 (Dr. Chiping Li).

Abstract: C01.00007: Uniform mean scalar gradient in grid turbulence: Asymptotic probability distribution of a paasive scalar

9:18 AM–9:31 AM

Author:
Xiaodan Cai
(United Technologies Research Center)

Honoring Ted O'Brien. Dr. Edward E. O'Brien was my Ph.D advisor in mechanical engineering at Stony Brook University. It was he who introduced me to study flow turbulence in the United States after we met at a Fluid Dynamics confererence in Beijing. He was an extremely humble, patient and optimistic person, and was an inspiration to all. Dr. O'Brien stressed the importance of understanding the fundamentals and was rigorous in applying them to solve important problems. I am one of Professor O'Brien's students who has benifited immensely from his approaches and values. I will now present our work on asymptotic behaviors of probability distribution function for a passive scale in grid turbulence, which highlights Professor O'Brien's legacy.

Abstract: C01.00008: Modeling Radiative Heat Transfer and Turbulence-Radiation Interactions Using PDF and FDF Methods

9:31 AM–9:44 AM

Author:

Daniel Haworth
(The Pennsylvania State University)

Honoring Ted O'Brien. In 1974, Dopazo and O'Brien proposed using a modeled equation for the probability density function of a set of scalar variables that describe the thermochemical state of a reacting medium (a transported composition joint PDF) to model mixing and reaction in chemically reacting turbulent flows. Since then, the benefits of PDF methods, including subsequent extension to large-eddy simulations (filtered density function -- FDF) methods, for modeling turbulence-chemistry interactions have been well established. Those benefits are a consequence of the ability of PDF/FDF methods to represent the influences of unresolved turbulent fluctuations on one-point physical processes (such as chemical reactions) in a natural way. For the same reason, PDF/FDF methods have an advantage in dealing with the influences of unresolved turbulent fluctuations on radiative emission. And when coupled with a stochastic radiation solver, the benefits can be extended to radiative absorption, thereby capturing both emission and absorption turbulence-radiation interactions. A model that combines stochastic Lagrangian particle PDF/FDF methods and a photon Monte Carlo method for radiative transfer is presented. Results are presented for laboratory flames and high-pressure combustion systems.

Abstract: C01.00009: Deep Learning of Single-Point PDF Closure for Turbulent Scalar Mixing

9:44 AM–9:57 AM

Authors:
Peyman Givi
(University of Pittsburgh)

Hessam Babaee
(University of Pittsburgh)

Maziar Raissi
(Nvidia Corp., and Brown University)

Honoring Ted O'Brien. O'Brien and Jiang [1] have shown that a useful means of characterizing the single-point PDF of a scalar field, is to consider its corresponding rate of the conditional expected dissipation. They demonstrate it by implementing the amplitude mapping closure (AMC) as applied to the classical problem of the binary scalar mixing. Based on recent developments in physics-informed deep learning and deep hidden physics models, we put forth a framework for discovering turbulent scalar mixing models from scattered and potentially noisy spatio-temporal measurements of the PDF. Our discovered model is appraised via comparison with the exact solution obtained by O'Brien and Jiang [1]. [1] O'Brien, E. E. and Jiang, T.-L., ``The Conditional Dissipation Rate of an Initially Binary Scalar in Homogeneous Turbulence,'' Phys. Fluids A, vol. 3(12), pp. 3121-3123 (1991).

Abstract: C01.00010: Investigation of scalar-scalar-gradient filtered joint density function for large eddy simulation of turbulent combustion*

9:57 AM–10:10 AM

Author:
Chenning Tong
(Clemson University)

Honoring Ted O'Brien. The scalar-scalar-gradient filtered joint density function (FJDF) is studied experimentally. Measurements are made in the fully developed region of an axisymmetric turbulent jet (with a jet Reynolds number of 40000) using an array consisting of three X-wires and three resistance-wire

temperature probes. Filtering in the cross-stream and streamwise directions are realized by using the array and by invoking Taylor's hypothesis, respectively. The measured mean FJDF conditional on the (subgrid-scale) SGS scalar variance is unimodal when the SGS scalar variance is small compared to its mean. The scalar gradient depends weakly on the SGS scalar. For large SGS variance the FJDF is bimodal and the gradient depends strongly on the SGS scalar. The SGS scalar under such a condition contains diffusion layer structures and the SGS mixing is similar to the early stages of binary mixing. The iso-scalar surface in the diffusion layer has a lower surface-to-volume ratio than those in a well mixed scalar. The conditionally filtered diffusion of the scalar gradient has a S-shaped dependence on the scalar gradient, which is expected to be qualitatively different from that of a reacting scalar under fast chemistry conditions. However, because modeling is performed at a higher level and because the scalar-scalar-gradient FJDF contains the information about the scalar dissipation and the surface-to-volume ratio, the FJDF approach is expected to be more accurate than scalar filtered density function approaches and has the potential to model turbulent combustion over a wide range of Damkohler numbers.

*Supported by NSF

Saturday–Tuesday, November 23–26, 2019; Seattle, Washington

Session G12: Turbulent and Chemically-reacting Flow Modeling II

3:48 PM–5:32 PM, Sunday, November 24, 2019
Room: 303

Chair: William Jones, Imperial College London

Abstract: G12.00001: Honoring Ted O’Brien: High order methods for filtered and probability density function models

3:48 PM–4:01 PM

Author:
Gustaaf Jacobs
(San Diego State University)

The systems of partial differential equations that govern probability and filtered density function models can be solved directly using numerical methods. Oftentimes, this type of system is also solved using a combination of Monte-Carlo and stochastic differential equations. If the density function model is coupled with another model that has feedback, as can occur in multi-physics or multi-phase environments, then the numerical coupling must be consistent for both approaches to obtain an accurate numerical solution. In this talk, I will discuss recent progress in the development of high order accuracy methods for models governing, chemically reaction and/or particle-laden, high-speed flows with shocks. High order distribution functions and weighted interpolations combined with spectral elements methods are presented and are shown to give accurate results for time-dependent problems that require long time integration.

Abstract: G12.00002: Combustion LES and the stochastic fields method

4:01 PM–4:14 PM

Author:
William Jones
(Imperial College London)

Honoring Ted O’Brien. The large eddy pdf equation formulated by Gao and O'Brien is a powerful method for simulating turbulent combustion. No assumptions are required regarding specific modes of burning so

the method is applicable to non-premixed and partially and perfectly premixed flames including ignition and extinction. The large eddy pdf equation involves a large number of independent variables so that stochastic methods are required for its solution; in the present work the stochastic fields method is utilised. It has been applied to simulate the evolution of self-excited thermo-acoustic instabilities in a gas turbine model combustor, using a fully compressible formulation. An unstable operating condition in the PRECCINSTA combustor, involving flame oscillation driven by thermo-acoustic instabilities, is the chosen target configuration. The flame's self-excited oscillatory behaviour is successfully captured without any external forcing being involved. Power spectral density analysis of the oscillation reveals a dominant thermo-acoustic mode at a frequency of 300~Hz providing remarkably good agreement with experimental observations. Moreover, the predicted limit-cycle amplitude closely matches the experimental value obtained with rigid metal combustor side walls.

Abstract: G12.00003: Physics-Based vs. Data-Driven Modeling for Turbulence and Combustion

4:14 PM–4:27 PM

Author:
Sharath Girimaji
(Ocean and Aerospace Engineering, Texas A&M University)

Honoring Ted O'Brien: Ted O'Brien had a long and distinguished career in modeling and computing chemically reacting turbulent flows. He made important contributions toward modeling/computation of auto-ignition in turbulent mixtures, conditional scalar dissipation, PDF (probability density function) methods and mapping closure methods. Currently, drive toward use of data-driven models is pervasive in nearly all fields involving complex phenomena including turbulent combustion. This presentation will discuss some of the benefits and challenges of using data-driven models for prediction of reacting turbulent flows. For a variety of turbulence and combustion features, we will compare the strengths and weaknesses of data-driven modeling against that of physics-based modeling. Specifically we will examine the general capabilities of data-driven approaches for handling (i) distant interactions - specifically non-local effects due to the elliptic nature of pressure and (ii) purely local process of chemical reactions. The talk will conclude with some recommendations on synergistically combining physics-based and data-driven approaches for developing predictive tools for turbulence and combustion.

Abstract: G12.00004: Differential diffusion modelling in transported PDF simulations of turbulent flames*

4:27 PM–4:40 PM

Authors:
Zhuyin Ren
(Tsinghua University)

Hua Zhou
(University of New South Wales)

Tianwei Yang
(Tsinghua University)

Honoring Ted O'Brien. The modelling strategy to incorporate differential diffusion effects in transported density function method (PDF), particularly in the context of large eddy simulation (LES) is proposed. Differential diffusion at the filter scale is resolved by the mean drift term in composition equations, while subgrid differential diffusion is modelled by the augmented mixing models that can account for differential mixing rates for each individual species. Both RANS/PDF and LES/FDF simulations of a jet-in-hot-coflow methane-hydrogen flame have been performed to investigate the effects of differential diffusion on flame characteristics.

*This work is supported by National Natural Science Foundation of China 91841302 and 91441202.

Abstract: G12.00005: Mathematical Models For Eulerian Conditional Statistics in a Complex Turbulent Flow

4:40 PM–4:53 PM

Authors:
James Hill
(Iowa State University (Retired))

Emmanuel Hitimana
(Iowa State University)

Michael Olsen
(Iowa State University)

Rodney Fox
(Iowa State University)

Honoring Ted O'Brien. Conditional moment closure (CMC) methods were developed for predicting turbulent reacting flows. However, conditional averages appear as unclosed terms that need to be modeled. In the present work the linear approximation and PDF gradient models were used to predict the conditional mean velocity and mixture fraction and compare with experimental data obtained for a macroscale multi-inlet vortex chemical reactor (macro-MIVR) using laser diagnostic techniques. The results for velocity conditioned on mixture fraction show that the linear model works well in a low turbulence region away from the reactor center. The PDF model with an isotropic turbulent diffusivity performs poorly for the tangential and axial conditional velocities, but a modified version that considers three components of turbulent diffusivity is better. Furthermore, the mixture fraction conditioned on the velocity vector components has a more linear behavior near the reactor center, where the probability density function (PDF) of the mixture fraction is close to a Gaussian distribution.

Abstract: G12.00006: On the kinematics of scalar iso-surfaces in a turbulent, temporally developing jet

4:53 PM–5:06 PM

Authors:
Brandon Blakeley
(University of Washington)

Weirong Wang
(University of Washington)

Duane Storti
(University of Washington)

James Riley
(University of Washington)

The kinematics and dynamics of scalar iso-surfaces in turbulent flows is of fundamental importance for a number of problems, e.g., the stoichiometric flame surface in non-premixed combustion or the turbulent/non-turbulent interface in turbulent shear flows. We investigate the effects of turbulence on iso-surfaces by examining the surface area density, Σ, and its evolution. Using direct numerical simulation of a temporally developing jet and a novel algorithm for evaluating iso-surface properties, we report on the direct computation of Σ and the terms in its transport equation. Iso-surface properties, such as the surface area, are evaluated by converting the surface integrals to volume integrals on a regularly-sampled grid. In particular, we analyze the behavior of two different scalar iso-surfaces: the vorticity magnitude, which represents the T/NT interface in a turbulent free shear flow, and a passive scalar field which represents an inert tracer such as dye concentration or the mixture fraction. Differences between the evolution of the two iso-surfaces will be addressed, such as the production of iso-surface area due to the turbulent strain-rate and the destruction of iso-surface area due to the combined effects of diffusion and surface curvature.

Abstract: G12.00007: Investigation of Two-Phase Supersonic Combustion in Hypersonic Flight

5:06 PM–5:19 PM

Author:
Foluso Ladeinde
(Stony Brook University)

The author's initial studies on compressible turbulence and combustion in high-speed flows were done via DNS in collaboration with the Late Professor Edward E. O'Brien in several joint publications on the topic. However, the author's focus has evolved, and the transport of momentum, energy, and chemical species in supersonic spray combustion for systems that approximate the scramjet engine in hypersonic flight is of current interest. Many advantages can be derived from the use of liquid fuels, such as the higher heat release and ease of storage and handling. The system in question is complicated by the interaction of many effects, including those due to combustion, evaporation, turbulence, shock waves, and their interactions. Consequently, not many studies have addressed the issues. Based on the parameters for the application of interest, the point-particle approach via the Eulerian-Lagrangian formulation is followed in the present endeavor. This approach introduces explicit force and energy sources, some of which involve history integrals. The significance of these sources is investigated in terms of their roles in the rather complex drop breakup mechanism in the presence of shockwaves, and the eventual evaporation and combustion to provide the needed propulsive force. The progress made by the author will be reported.

Abstract: G12.00008: Evaluation of Entropy Transport Equation in Turbulent Jet Flames using Filtered Density Function

5:19 PM–5:32 PM

Authors:
Mehdi Safari
(Assistant Professor)

Reza Sheikhi
(Professor)

Evaluation of entropy provides a tool to optimize performance of combustion systems through the second law of thermodynamics. In turbulent reacting flows, entropy is generated due to viscous dissipation, heat conduction, mass diffusion and chemical reaction. In large eddy simulation (LES), all of these effects along with subgrid scale (SGS) entropy flux, appear as unclosed terms. The closure is provided by utilizing a special form of filtered density function (FDF) called entropy FDF (En-FDF). The prime advantage of using the En-FDF is that it provides closure for all individual entropy generation effects as well as scalar-entropy statistics. It also includes the effect of chemical reaction in a closed form. The En-FDF transport is modeled by a set of stochastic differential equations. The numerical solution procedure is based on a hybrid form of finite difference and Monte Carlo solvers in which the filtered transport equations are solved by the finite difference solver and the stochastic differential equations are solved by a Lagrangian Monte Carlo procedure. This methodology is applied to a turbulent nonpremixed jet flame and sources of irreversibilities are predicted and analyzed.